School of Civil and Mechanical Engineering
Department of Civil Engineering

Assessment of seismic performance of reinforced concrete frame buildings with or without infill wall in Bhutan

Kinzang Thinley

This thesis is presented for the Degree of
Doctor of Philosophy
of
Curtin University

January 2017

Declaration

To the best of my knowledge and belief this thesis contains no material previously published by any other person except where due acknowledgment has been made.

This thesis contains no material which has been accepted for the award of any other degree or diploma in any university.

Signature:

Date: 10/05/2017

ABSTRACT

Reinforced concrete (RC) frame buildings with or without masonry infill are the most common building structures in all parts of the world. All classes of buildings namely residential, commercial, educational and even the lifeline buildings such as hospitals are built of RC frames with or without masonry infill walls. Earthquakes in the past have proved that these buildings are very vulnerable and pose a significant risk to lives and properties. Although the improved knowledge on earthquakes and seismic response analysis had led to the design of these buildings for seismic actions in the recent past, yet many newly built RC frame buildings were still damaged in recent earthquakes. It is hence necessary to assess the seismic performance of existing masonry infilled RC buildings so as to mitigate the loss of lives and properties.

The primary objective of this thesis is to assess the seismic performance of low-rise RC frame buildings with or without masonry infill walls in general and those buildings in Bhutan in particular. Being located in one of the most active seismic regions in the Himalaya where the Indo-Australian Plate is continuously being sub ducted under the Eurasian Plate, a number of earthquakes of various sizes have occurred in Bhutan inflicting huge loss of lives and properties. In spite of this, Bhutan has no seismic design code of its own even to this day. The masonry infilled RC buildings constitute more than 70 percent of the building structures in the urban areas of Bhutan. Many of them were built since the 1970s without considering the seismic action. Only the buildings constructed after 1997 were designed for seismic load according to Indian Seismic Code while the applicability of the code to the site conditions in Bhutan has not been examined. As a result, the performance of building structures in the high seismicity country subjected to earthquake loadings is not known. This makes it not possible to prepare an effective emergency plan should such an event like the one in Nepal in 2015 occur in Bhutan, and not possible to design the effective and economic strengthening scheme of building structures to resist seismic loadings.

Realising the outmost importance of mitigating the seismic risk in Bhutan, Probabilistic Seismic Hazard Analysis (PSHA) is first carried out to predict ground motions at the generic soil sites in Thimphu, Bhutan for both the 475 and 2475 year return periods. Using the predicted ground motions, extensive numerical investigations are carried out to study the seismic response and seismic performance of RC buildings without and with masonry infill considering soil-structure interaction (SSI). In addition, seismic performance of the masonry infilled RC buildings with the open ground floor and with partial infill wall and openings are

also investigated. The nonlinear dynamic analysis and performance assessment program, Perform 3D is used for the dynamic nonlinear analysis of the buildings. The numerical models of bare, masonry infilled and soft storey RC frames are calibrated with the experimental test results to ascertain the accuracy of the numerical results. The three typical existing masonry infilled RC buildings in Bhutan which were built prior to and after the adoption of Indian Seismic Code are considered for the seismic risk assessment. The performance of the buildings is comprehensively assessed considering the randomness in the material and geometrical parameters and fuzziness in the damage criteria. In absence of the damage criteria specific to the RC buildings in Bhutan, the damage states defined by other researchers are used. The fragility analysis of the masonry infilled RC buildings is also carried out considering both the material and ground motion uncertainties. In addition, the adequacy of using Indian Seismic Code in Bhutan and the adequacy of design provision recommended by the Indian Seismic Code for the soft storey buildings are also investigated.

It is observed that RC buildings built prior to the adoption of Indian Seismic Code have the high probability of undergoing repairable to irreparable damages under the 475 return period ground motion and severe damage to complete collapse under the 2475 return period ground motion. On the other hand, RC buildings built after the adoption of Indian Seismic Code have the high probability of experiencing repairable and irreparable damages under the 475 and 2475 year return period ground motions, respectively. Soft storey buildings built prior to the adoption of Indian Seismic Code are found to be highly vulnerable to earthquakes. The soft storey buildings, in general, are observed to be more vulnerable than the masonry infilled RC buildings. The effect of soil-structure interaction is observed to be significant at the soft soil sites, while it is found to be less significant at the other soil sites. The use of Indian Seismic Code for the design of buildings in Bhutan needs to be further investigated. The incorporation of design provision of Indian Seismic Code for soft storey buildings slightly improves the performance, but the alternative approach of strengthening only the columns has the same effect with more advantages.

The findings in this study of the seismic performance of the typical RC buildings with or without masonry infill wall in Bhutan are useful in preparing the seismic risk response plan, retrofitting options and loss estimations in the country. The study could also be useful in the other regions with the similar seismicity and construction types such as Nepal and India.

ACKNOWLEDGEMENT

This PhD study has been a long and wonderful journey compounded with both exciting and testing moments. Without the contribution of so many people along the way, the completion of this thesis would not have been possible.

First and foremost, I would like to sincerely thank my supervisor Prof. Hong Hao for his excellent guidance, patience, encouragement and amongst all his unwavering support throughout this PhD journey. Coming from a non-academic background, it was a bit tough in the beginning getting adjusted to the academic world. The constant encouragement and special attention of Prof. Hong Hao made it much easier for me to smoothly squeeze into the academic world. I cannot describe in words how deeply grateful I am for all he had done for the successful completion of this thesis. I learnt a lot from him and he easily is the greatest human being I have ever come across in my life. I am also thankful to my second supervisor, Dr. Kaiming Bi whose invaluable comments helped me to improve and shape this thesis. I would also like gratefully acknowledge my other co-author, Mr. Choki Tashi whose contribution in one of the papers form the part of this thesis.

Secondly, I would like to thank the Government of Australia for providing me with the Endeavour Postgraduate Award to undertake this PhD study. Without this, it would not have been possible for me to set my feet in Australia. I am highly indebted and would remain ever grateful for the scholarship. I am also grateful to the University of Western Australia and Curtin University for topping up the tuition fees on the fixed amount covered by the scholarship. Further, I am grateful to the Ministry of Works and Human Settlement, Royal Government of Bhutan for approving my study leave to study in Australia for four long years.

Thirdly, my sincere thanks go to Dr Andrew Whyte, the head of the Civil Engineering Department, Curtin University for providing me opportunities to attend and present papers at the national and international conferences. I am also thankful to Mrs Sucy Leong, Mr Frankie Sia, Ms Ying Hong Lin and Ms Cheryl Cheng for assisting me in all administrative works. Similarly, I am thankful to the staff of the administrative section at the University of Western Australia for assisting me during my stay at the University for little more than a year. I also acknowledge the IT and library supports provided by both the Universities.

Fourthly, I would like to thank all the members of Prof. Hao's research group for their invaluable comments and feedbacks during the weekly Friday group meetings. I would like to especially thank Dr Bepin Shrestha with whom I discussed a number of topics related to my research and Mr Musaad Khan for the wonderful friendship.

Furthermore, I would like to gratefully acknowledge Dr Paolo Negro of Joint Research Centre, European Commission for generously sharing the experimental test results. This enabled me to calibrate numerical models for further analyses.

Last but not the least, my special thanks go to my late mum and dad without whose sacrifices and never ending encouragement, I would not have been here writing this thesis. My heartfelt thanks also go to my wife Yeshi Yangki for her selfless love, understanding and continuous support and my dear son Pema Choejur Dorji for bearing with me for the limited time I spent with him throughout this strenuous journey. Many thanks are due to my brothers, sisters and in-laws for their constant encouragement and support without which this PhD journey would have become even more challenging.

LIST OF PUBLISHED WORK AND WORK PREPARED FOR PUBLICATIONS

The list of published paper and work prepared for publications, with the full bibliographic citations in the order they appear in the thesis, are listed below.

Chapter 2

Thinley, K., Hao, H., & Tashi, C. (2017). Seismic performance of reinforced concrete buildings in Thimphu, Bhutan. *International Journal of Structural Stability and Dynamics*, DOI: http://dx.doi.org/10.1142/S0219455417500742.

Chapter 3

Thinley, K., & Hao, H. (2017). Seismic performance of reinforced concrete frame buildings in Bhutan based on fuzzy probability analysis. *Soil Dynamics and Earthquake Engineering*, 92, 604-620.

Chapter 4

Thinley, K., & Hao, H. (2016). Seismic response analysis and performance assessment of masonry infilled RC buildings in Bhutan with and without soft storey. *Advances in Structural Engineering*, DOI: 10.1177/1369433216661336.

Chapter 5

Thinley, K., & Hao, H. (2016). Seismic damage prediction of masonry infilled RC buildings without and with soft storey in Bhutan based on fuzzy probability analysis. *Earthquakes and Structures*, (Under review)

Chapter 6

Thinley, K., & Hao, H. (2016). Seismic fragility analysis of masonry infilled reinforced concrete frame buildings in Bhutan. *Bulletin of Earthquake Engineering*, (Under review)

Chapter 7

Thinley, K., & Hao, H. (2017). Effect of partial infill wall on the seismic behavior of RC frame buildings. (To be submitted to Advances in Structural Engineering)

LIST OF RELEVANT ADDITIONAL PUBLICATIONS

The list of additional publications relevant to the thesis, with the full bibliographic citations, is given below.

1. **Thinley, K**., Hao, H., & Tashi, C. (2014). *Seismic performance of reinforced concrete buildings in Bhutan*. Proceeding of Australian Earthquake Engineering Society annual conference 2014, Lorne, Victoria, Australia.

2. **Thinley, K**., & Hao, H. (2015). *Fuzzy probability analysis of the performance of reinforced concrete frame buildings in Bhutan.* Proceeding of the 10th Pacific Conference on Earthquake Engineering, Sydney, Australia.

3. **Thinley, K**., & Hao, H., (2015). *Seismic assessment of masonry infilled reinforced concrete frame buildings in Bhutan.* Proceeding of the 10th Pacific Conference on Earthquake Engineering, Sydney, Australia.

4. **Thinley, K**., & Hao, H., (2016). *Effect of partially infill wall on the seismic behavior of RC frame buildings*. Proceedings of the 24th Australasian Conference on the Mechanics of Structures and Materials, Perth, Australia.

5. **Thinley, K**., & Hao, H. (2017). *Seismic damage prediction of the masonry infilled RC frame buildings in Bhutan based on fuzzy probability analysis.* Proceedings of the 16th World Conference on Earthquake Engineering, Santiago, Chile.

STATEMENT OF CONTRIBUTION OF OTHERS

The works presented in this thesis were primarily carried out by the first author, which mainly include but not limited to reviewing literatures, developing numerical models, conducting numerical analyses, interpreting numerical results and writing manuscripts. Contributions of the co-authors are described below.

Chapter 2

Prof. Hong Hao helped in defining the overall scope and objectives of the work, suggesting research methodologies and approaches, and procuring the nonlinear analysis and performance assessment software, Perform 3D used for the research. In addition, Prof. Hong Hao had thoroughly revised and edited draft manuscript prepared by the first author. Mr Choki Tashi provided a significant support in carrying out the Probabilistic Seismic Hazard Analysis in Thimphu, Bhutan.

Chapter 3 to Chapter 7

As in chapter 2, Prof. Hong Hao made a significant contribution in defining the scope of the work and providing uninterrupted intellectual support to all works in chapters 3 to 7. The manuscripts written by the first author were similarly revised and edited by Prof. Hong Hao before the onward submission to the respective journals.

TABLE OF CONTENTS

ABSTRACT… iii

ACKNOWLEDGEMENT v

LIST OF PUBLISHED WORK AND WORK PREPARED FOR PUBLICATIONS vii

LIST OF RELEVANT ADDITIONAL PUBLICATIONS viii

STATEMENT OF CONTRIBUTION OF OTHERS ix

TABLE OF CONTENTS x

LIST OF FIGURES xiv

LIST OF TABLES xviii

NOTATION… xx

CHAPTER 1 INTRODUCTION 1

1.1 Background 1

1.2 Research Objectives 5

1.3 Research Outline 6

1.4 References 7

CHAPTER 2 SEISMIC PERFORMANCE OF REINFORCED CONCRETE BUILDINGS IN THIMPHU, BHUTAN 11

2.1 Abstract 11

2.2 Introduction 11

2.3 Prediction of Design Ground Motion in Thimphu 14

2.3.1 Probabilistic Seismic Hazard Analysis 14

2.3.2 Spectral Matching 16

2.3.3 Site response analysis 17

2.4 Ground Motion from Indian Seismic Code 20

2.5 Model Calibration 22

2.5.1 Modelling of stiffness parameters 23

2.5.2 Modelling of strength parameters 24

2.5.3 Modelling of deformation parameters 25

2.5.4 Modelling of viscous damping 25

2.5.5 Shear strength of RC members 26

2.6 Typical Buildings in Thimphu 27

2.7 Structural Response of Typical Buildings 30

2.8 Performance Evaluation of Typical Buildings and Discussion 33

2.9 Adequacy of using Indian Seismic Code 37

2.10 Conclusions 39

2.11 References 41

CHAPTER 3 SEISMIC PERFORMANCE OF REINFORCED CONCRETE FRAME BUILDINGS IN BHUTAN BASED ON FUZZY PROBABILITY ANALYSIS 44

3.1 Abstract 44

3.2 Introduction 44

3.3 Ground Motion Time Histories 47

3.4 Structural model for performance assessment 48
3.4.1 Case study buildings 48
3.4.2 Numerical model 52

3.5 Modelling of uncertainties 55
3.5.1 Compressive strength of concrete, f_c 55
3.5.2 Modulus of elasticity of concrete, E_c 56
3.5.3 Yield strength of steel, f_y 56
3.5.4 Member Dimensions, M 57

3.6 Probabilistic Structural Response Estimation 57
3.6.1 Rosenbluth Point Estimate Method 58
3.6.2 Monte Carlo Simulation Method 59
3.6.3 Validation of Rosenbluth Point Estimate Method 61
3.6.4 Determination of statistical distribution of structural responses 63

3.7 Fuzzy failure probability analysis 64

3.8 Numerical results and discussion 66

3.9 Conclusion 77

3.10 References 78

CHAPTER 4 SEISMIC RESPONSE ANALYSIS AND PERFORMANCE ASSESSMENT OF MASONRY INFILLED RC BUILDINGS IN BHUTAN WITHOUT AND WITH SOFT STOREY 82

4.1 Abstract 82

4.2 Introduction 82

4.3 Ground motions 84

4.4 Typical buildings considered for study 85

4.5 Numerical modelling and model calibration 87
4.5.1 Modelling of RC members 87
4.5.2 Modelling of masonry infill wall 89
4.5.3 Calibration of the model 90

4.6 Incorporation of opening and soil-structure interaction 91
4.6.1 Incorporation of opening 91
4.6.2 Incorporation of soil-structure interaction (SSI) 92

4.7 Structural response of masonry infilled RC buildings 93

4.8 Response of soft storey buildings designed according to Indian Seismic Code 97

4.9 Performance of masonry infilled and soft storey buildings 100

4.10 Summary and conclusion 104

4.11 References 105

CHAPTER 5 SEISMIC DAMAGE PREDICTION OF MASONRY INFILLED RC BUILDINGS WITHOUT AND WITH SOFT STOREY IN BHUTAN BASED ON FUZZY PROBABILITY ANALYSIS 109

5.1 Abstract 109

5.2 Introduction 109

5.3 Description of Buildings considered for the Study 112

5.4 Ground Motions 114

5.5 Numerical Modelling 115
5.5.1 Modelling of RC members 116
5.5.2 Modelling of masonry infill wall 117
5.5.3 Incorporation of opening and soil structure interaction (SSI) in the model 118

5.6 Estimation of Probabilistic Structural Responses 119
5.6.1 Consideration of uncertainties 119
5.6.1.1 Compressive strength of masonry wall (f_m) 120
5.6.1.2 Compressive strength of concrete (f_c) 121
5.6.1.3 Yield strength of steel (f_y) 121
5.6.1.4 Member dimension (M_d) 121
5.6.2 Estimation of structural responses 122
5.6.2.1 Rosenbluth Point Estimate Method (RPEM) 122
5.6.2.2 Monte Carlo Simulation Method (MCSM) 123
5.6.3 Probabilistic results and discussion 126

5.7 Fuzzy Failure Probability analyses and Prediction of Damages 131

5.8 Summary and Conclusion 139

5.9 References 140

CHAPTER 6 SEISMIC FRAGILITY ANALYSIS OF MASONRY INFILLED REINFORCED CONCRETE FRAME BUILDINGS IN BHUTAN 144

6.1 Abstract 144

6.2 Introduction 144

6.3 Development of fragility curves 148
6.3.1 Selection of Ground Motion 149
6.3.2 Selection of Masonry infilled RC buildings 152
6.3.3 Numerical Modelling of buildings for nonlinear analysis 154
6.3.4 Consideration of uncertainties 156
6.3.4.1 Material uncertainty 157
6.3.5 Selection of Damage States 158
6.3.6 Incremental Dynamic Analysis (IDA) 159

6.4 Effect of material uncertainties 160

6.5 Fragility curves for typical masonry infilled RC buildings 164

6.6 Fragility curves of soft storey buildings 170

6.7 Comparison of Fragility Curves for masonry infilled and soft storey buildings 174

6.8 Summary and conclusion 175

6.9 References 176

CHAPTER 7 EFFECT OF PARTIALLY INFILLED WALL ON THE SEISMIC BEHAVIOR OF REINFORCED CONCRETE FRAME BUILDINGS 180

7.1 Abstract 180

7.2 Introduction 180

7.3 Description of an example building 183

7.4 Ground motions 185

7.5 Numerical modelling of partially infilled RC frame 186

7.5.1 Modelling of partial infill wall 186

7.5.2 Modelling of surrounding RC frame 188

7.6 Numerical results and discussion 190

7.7 Conclusion 194

7.8 References 195

CHAPTER 8 CONCLUSION AND RECOMMENDATIONS 197

8.1 Main Contributions 197

8.2 Recommendations for future works 200

LIST OF FIGURES

Figure 2-1(a) Seismic hazard map of Bhutan (GSHAP, 1992); (b) Earthquakes in and around Bhutan (Motegi, 2001). 12
Figure 2-2 (a) Hazard curve for 8.CH.227 source zone in log scale; (b) Total hazard curve and hazard curves from all other sources in log scale. 16
Figure 2-3 Probabilistic spectra for bedrock motion. 16
Figure 2-4 Output acceleration time histories at bedrock obtained from spectral matching. 17
Figure 2-5 Spectral acceleration for four site classes with 5% damping, (a) 475 and (b) 2475 year return periods 18
Figure 2-6 Ground motion time histories at generic soil sites for the 475 year return period (RP). 19
Figure 2-7 Ground motion time histories at generic soil sites for the 2475 year return period (RP). 19
Figure 2-8 (a) Normalised response spectra with 5% damping defined in Indian Seismic Code and (b) comparison of response spectra at soft soil site obtained from PSHA for 2475 year return period and Indian Seismic Code for MCE with 5% damping. 21
Figure 2-9 (a) Acceleration response spectrum matched to response spectrum of Indian Code at soft soil site for 5% damping and MCE and (b) horizontal ground motion time history derived from the matched spectrum. 21
Figure 2-10 Accelerograms from 1976 Friuli Earthquake used in the tests. 22
Figure 2-11 Experimental building, (a) beam column layout plan and (b) sectional elevation. 22
Figure 2-12 (a) General F-D relationship of Perform 3D (CSI, 2006) and (b) F-D relationship used in this study. 23
Figure 2-13 Comparison of storey displacements obtained from numerical analyses and test results for low-level test. 26
Figure 2-14 Comparison of storey displacements obtained from numerical analysis and test results for high-level test. 27
Figure 2-15 Structural details of 6 storey building. 28
Figure 2-16 Structural details of 3 storey buildings. 28
Figure 2-17 Displacement profiles of typical buildings under 475 year return period ground motion, (a) rock; (b) shallow stiff soil; (c) soft rock and (d) soft soil sites. 32
Figure 2-18 Displacement profiles of typical buildings under the 2475 year return period ground motion, (a) rock; (b) shallow stiff soil; (c) soft rock and (d) soft soil sites. 32
Figure 2-19 Inerstorey drift profiles and performance levels of typical buildings under the 475 return period ground motion, (a) rock; (b) shallow stiff soil; (c) soft rock and (d) soft soil sites. 34
Figure 2-20 Interstorey drift profiles and performance levels of typical buildings under the 2475 return period ground motion, (a) rock; (b) shallow stiff soil; (c) soft rock and (d) soft soil sites. 36
Figure 2-21 Comparison of interstorey drift at the soft soil site estimated from PSHA and Indian Code response spectrum matched ground motion, (a) with fixed support and (b) with SSI. 38
Figure 2-22 (a) The plot of Indian Seismic Code and PSHA response spectra at the soft soil site with 5% damping and (b) comparison of velocity time histories. 39
Figure 3-1 Ground motion time histories at generic soil sites in Thimphu for 475 year return periods. 47
Figure 3-2 Ground motion time histories at generic soil sites in Thimphu for 2475 year return periods. 48

Figure 3-3 Ground motion response spectra at different sites for (a) 475 and (b) 2475 year return periods. 48
Figure 3-4 (a) Beam and column layout plan and (b) sectional elevation of 6 storey building. 49
Figure 3-5 (a) Beam and column layout plan and (b) sectional elevation of 3 storey buildings..... 50
Figure 3-6 (a) Typical beam cross section showing top and bottom reinforcement of beam and (b) column cross sections with a different number of reinforcement bars. 51
Figure 3-7 (a) Implementation of chord rotation model of Perform 3D (CSI, 2006) and (b) F-D relationship used for numerical model. 52
Figure 3-8 (a) Provision of translational and rotational springs in the three mutually perpendicular directions and (b) section of typical square column footing. 54
Figure 3-9 The convergence of mean interstorey drift obtained from Monte Carlo Simulation method at (a) rock; (b) shallow stiff soil; (c) soft rock and (d) soft soil sites. 60
Figure 3-10 Convergence of standard deviation of interstorey drift obtained from Monte Carlo Simulation Method at (a) rock; (b) shallow stiff soil; (c) soft rock and (d) soft soil sites. 61
Figure 3-11 Comparison of mean interstorey drift obtained from RPEM and MCSM at (a) rock; (b) shallow stiff soil; (c) soft rock and (d) soft soil sites. 62
Figure 3-12 Comparison of interstorey drift standard deviation obtained from RPEM and MCSM at (a) rock; (b) shallow stiff soil; (c) soft rock and (d) soft soil sites. 63
Figure 3-13 Comparison of actual and fitted CDF at (a) rock; (b) shallow stiff soil; (c) soft rock and (d) soft soil sites. 64
Figure 3-14 Triangular membership function adopted in this study. 66
Figure 3-15 Mean interstorey drift profiles for typical buildings subjected to 475 year return period ground motions at (a) rock; (b) shallow stiff soil; (c) soft rock and (d) soft soil sites. 69
Figure 3-16 Mean interstorey drift profiles for typical buildings subjected to 2475 year return period ground motions at (a) rock; (b) shallow stiff soil; (c) soft rock and (d) soft soil sites. 69
Figure 4-1 Acceleration response spectra at generic soil sites for 475 and 2475 year return period (RP) ground motions at 5% damping. 85
Figure 4-2 Masonry wall and column layout plan for (a) 6 storey; (b) 3 storey; (c) typical column cross section and (d) typical beam cross section. 86
Figure 4-3 (a) Chord rotation model; (b) F-D relationship of RC members; (c) masonry infilled wall representation by equivalent strut and (d) F-D relationship of equivalent strut model. 88
Figure 4-4 Comparisons of displacement time histories obtained from numerical analyses and experimental tests for (a) infilled frame building and (b) soft storey building. 91
Figure 4-5 Column footing details showing various notations and axes. 93
Figure 4-6 Interstorey drift profiles of '6 storey' infilled, bare and soft storey frame buildings subjected to the 475 and 2475 year return period ground motions at (a) rock; (b) shallow stiff soil; (c) soft rock and (d) soft soil sites. 95
Figure 4-7 Interstorey drift profiles of '3 storey new' infilled, bare and soft storey frame buildings subjected to the 475 and 2475 year return period ground motions at (a) rock; (b) shallow stiff soil; (c) soft rock and (d) soft soil sites. 95
Figure 4-8 Interstorey drift profiles of '3 storey old' infilled, bare and soft storey frame buildings subjected to the 475 and 2475 year return period ground motions at (a) rock; (b) shallow stiff soil; (c) soft rock and (d) soft soil sites. 96
Figure 4-9 Pushover curves for bare, infilled and soft storey frames for (a) 6 storey; (b) 3 storey new and (c) 3 storey old buildings. 96

Figure 4-10 Interstorey drift profiles of soft storey frames strengthened with different options (a) 6 storey; (b) 3 storey new and (c) 3 storey old buildings at shallow stiff soil site subjected to the 475 return period ground motion. 99
Figure 4-11 Performance levels and interstorey drift profiles of masonry infilled RC buildings subjected to the 475 year return period ground motions at (a) rock; (b) shallow stiff soil; (c) soft rock and (d) soft soil sites with fixed support (FS) and with SSI. 102
Figure 4-12 Performance levels and interstorey drift profiles of masonry infilled RC buildings subjected to the 2475 year return period ground motions at (a) rock; (b) shallow stiff soil; (c) soft rock and (d) soft soil sites with fixed support (FS) and with SSI. 102
Figure 4-13 Performance levels and interstorey drift profiles of soft storey buildings subjected to the 475 year return period ground motions at (a) rock; (b) shallow stiff soil; (c) soft rock and (d) soft soil sites. 103
Figure 4-14 Performance levels and interstorey drift profiles of soft storey buildings subjected to the 2475 year return period ground motions at (a) rock; (b) shallow stiff soil; (c) soft rock and (d) soft soil sites. 104
Figure 5-1 Plan and sectional elevation of typical buildings, (a) 6 storey and (b) 3 storey buildings. 113
Figure 5-2 Acceleration time histories of ground motions at rock, shallow stiff soil, soft rock and soft soil sites for (a) 475 and (b) 2475 year Return Periods(RP). 115
Figure 5-3 Numerical modelling of masonry infilled RC frame, (a) chord rotation model; (b) F-D relationship of RC members; (c) masonry infill wall representation by equivalent strut; (d) F-D relationship of the equivalent strut model and (e) comparison of reduction factors. 117
Figure 5-4 The convergence of mean interstorey drift obtained from Monte Carlo Simulation Method, (a) rock; (b) shallow stiff soil; (c) soft rock and (d) soft soil sites. 124
Figure 5-5 The convergence of standard deviation obtained from Monte Carlo Simulation Method, (a) rock; (b) shallow stiff soil; (c) soft rock and (d) soft soil sites. 124
Figure 5-6 Comparison of actual and fitted CDF, (a) rock; (b) shallow stiff soil; (c) soft rock and (d) soft soil sites. 125
Figure 5-7 Mean interstorey drift profiles of masonry infilled RC buildings without soft storey under the 475 and 2475 return period ground motions with fixed support, (a) rock; (b) shallow stiff soil; (c) soft rock and (d) soft soil sites. 129
Figure 5-8 Mean interstorey drift profiles for masonry infilled RC buildings with soft storey subjected to the 475 and 2475 return period ground motions, (a) rock; (b) shallow stiff soil; (c) soft rock and (d) soft soil sites. 129
Figure 5-9 Comparison of mean interstorey drift profiles of masonry infilled RC buildings without soft storey at the soft soil site with and without considering SSI, (a) 475 and (b) 2475 year return period ground motion. 130
Figure 5-10 Triangular membership function used for the estimation of the fuzzy failure probabilities of the masonry infilled RC buildings, (a) without and (b) with soft storey. ... 133
Figure 6-1 Typical masonry infilled RC buildings in Thimphu, Bhutan. 145
Figure 6-2 Approximate location of the big Himalayan earthquakes in and around Bhutan as indicated by the red star. 146
Figure 6-3 Selected ground motion spectra with their geometric mean and target spectrum 151
Figure 6-4 Column and masonry wall layout plan of (a) 6 storey and (b) 3 storey buildings. Reinforcement arrangement details of (c) beams and (d) columns. 153
Figure 6-5 (a) F-D relationship of RC member; (b) equivalent strut representation of masonry wall and (c) F-D relationship of the equivalent strut. 155
Figure 6-6 Comparison of fragility curves for Case I and Case II in terms of S_a (T_1, 5%) for (a) no damage; (b) repairable; (c) irreparable and (d) severe damages. 162

Figure 6-7 Comparison of fragility curves for Case I and Case II in terms of PGA for (a) no damage; (b) repairable; (c) irreparable and (d) severe damages. 163
Figure 6-8 IDA curves for (a) 6 storey; (b) 3 storey new and (c) 3 storey old masonry infilled RC buildings. 166
Figure 6-9 Fragility curves for (a) 6 storey; (b) 3 storey new and (c) 3 storey old masonry infilled RC buildings derived in terms of S_a (T_1, 5%) for various damage states. 167
Figure 6-10 Fragility curves for (a) 6 storey; (b) 3 storey new and (c) 3 storey old masonry infilled RC buildings derived in terms of PGA for various damage states. 168
Figure 6-11 Comparison of fragility curves for (a) no damage; (b) repairable; (c) irreparable; (d) severe and (e) collapse-IDA damage states for masonry infilled RC buildings. 169
Figure 6-12 Fragility curves for (a) 6 storey; (b) 3 storey new and (c) 3 storey old soft storey buildings derived in terms of S_a (T_1, 5%) for various damages. 172
Figure 6-13 Fragility curves for (a) 6 storey; (b) 3 storey new and (c) 3 storey old soft storey buildings derived in terms of PGA for various damage states. 172
Figure 6-14 Comparison of fragility curves for (a) no damage; (b) repairable; (c) severe and (d) collapse-IDA damage states of soft storey buildings. 174
Figure 6-15 Comparison of fragility curves for collapse-IDA damage state for (a) 6 storey; (b) 3 storey new and (d) 3 storey old soft storey buildings. 175
Figure 7-1 Captive column effect induced by the partially infill wall. 181
Figure 7-2 (a) Masonry infill wall layout plan of 3 storey building and (b) various heights of infill wall considered for analyses. 184
Figure 7-3 Acceleration time histories of ground motions at the generic soil sites for 475 year return period. 186
Figure 7-4 (a) Representation of partial infill wall by an equivalent strut and (b) F-D relationship of an equivalent strut. 188
Figure 7-5 Numerical modelling of column with partial infill wall, (a) column with partial infill wall, (b) chord rotation model with shear hinge, (c) F-D relationship of shear hinge for shear failure and (d) F-D relationship of shear hinge for flexure-shear failure. 189
Figure 7-6 Column shear force corresponding to the various heights of infill wall at (a) rock; (b) shallow stiff soil; (c) soft rock and (d) soft soil sites under the 475 year return period ground motion. 192
Figure 7-7 Interstorey drift of building with increased strength of ground floor columns at shallow stiff soil under the 475 year return period ground motion for infill wall height of (a) 0.0H; (b) 0.25H; (c) 0.5H; (d) 0.75H and (e) 1.0H. 192

LIST OF TABLES

Table 2-1 Generic soil sites in Thimphu 18
Table 2-2 Loading details of typical buildings 29
Table 2-3 Reinforcement details of 6 storey building 29
Table 2-4 Reinforcement details of '3 storey new' and '3 storey old' buildings 30
Table 2-5 Fundamental periods of typical buildings in seconds for different site classes for the 475 and 2475 year return period (RP) 31
Table 2-6 Performance levels, damage states and interstorey drift limits from Vision 2000 33
Table 3-1 Dimension and reinforcement details for RC members for '6 storey' building 51
Table 3-2 Dimension and reinforcement details of RC members for '3 storey new' and '3 storey old' buildings 52
Table 3-3 The stiffness of springs for various degrees of freedom. 55
Table 3-4 Mean, CoV and distribution type of the material and geometrical parameters 57
Table 3-5 Possible combination of four parameters using RPEM for '3 storey new' building. 59
Table 3-6 Comparison of interstorey drift and standard deviation obtained from RPEM and MCSM 62
Table 3-7 K-S test statistic values of interstorey drift at the second floor. 64
Table 3-8 Performance levels, damage states and interstorey drift limits from Vision 2000 65
Table 3-9 Fundamental period of typical buildings for uncracked and cracked concrete 67
Table 3-10 Mean maximum interstorey drift and corresponding standard deviation of '6 storey' building 68
Table 3-11 Mean maximum interstorey drift and corresponding standard deviation of '3 storey new' building 68
Table 3-12 Mean maximum interstorey drift and corresponding standard deviation of '3 storey old' building 68
Table 3-13 Failure probabilities of '6 storey' building with fixed support. 73
Table 3-14 Failure probabilities of '3 storey new' building with fixed support. 74
Table 3-15 Failure probabilities of '3 storey old' building with fixed support. 75
Table 3-16 Probabilities of '6 storey' and '3 storey new' buildings at soft soil site incorporating SSI. 75
Table 4-1 Reinforcement and member dimensions of typical buildings 87
Table 4-2 Proportion of energy dissipated by different components of buildings at soft soil site under the 475 and 2475 year return period ground motions 97
Table 4-3 Interstorey drift limits and corresponding performance levels and damage states of masonry infilled and general RC frame buildings. 100
Table 5-1 Reinforcement and member dimension details of the typical buildings 114
Table 5-2 Mean and coefficient of variation of material and geometrical parameters 120
Table 5-3 Mean interstorey drift and standard deviation obtained from RPEM and MCSM under the 475 year return period ground motions 126
Table 5-4 K-S statistic values of interstorey drift and critical values 126
Table 5-5 Mean maximum interstorey drift and corresponding standard deviation for typical masonry infilled RC buildings in Bhutan 127
Table 5-6 Mean maximum interstorey drift and corresponding standard deviation for typical soft storey buildings in Bhutan 128
Table 5-7 Fundamental period of typical buildings using scant stiffness to yield 128
Table 5-8 Damage states and corresponding interstorey drift limits 132

Table 5-9 Comparison of failure probabilities obtained from fuzzy and conventional probability analyses at shallow stiff soil site under the 475 year return period ground motion 134
Table 5-10 Fuzzy failure probabilities of '6 storey' masonry infilled RC buildings with and without soft storey..... 135
Table 5-11 Fuzzy failure probabilities of '3 storey new' masonry infilled RC building with and without soft storey..... 136
Table 5-12 Fuzzy failure probabilities of '3 storey old' masonry infilled RC building with and without soft storey..... 137
Table 6-1 Reinforcement and member dimension details of the typical buildings..... 153
Table 6-2 Damage states correlated to interstorey drift of building 158
Table 6-3 Application of Rosenbluth Point Estimate Method..... 161
Table 6-4 Lognormal mean and standard deviation with and without consideration of random variation of material parameters 162
Table 6-5 Lognormal mean and standard deviation of IM obtained for 3 typical masonry infilled RC buildings..... 164
Table 6-6 Lognormal mean and standard deviation estimated for soft storey buildings at various damage states 171
Table 7-1 Reinforcement and member dimension details of the example building..... 185
Table 7-2 Periods of building with various wall heights 191

NOTATION

a = Shear span of column, m

A_g = Gross cross sectional area of column, mm^2

A_{st} = Area of transverse reinforcement parallel to applied shear, mm^2

A_v = Area of transverse steel reinforcement, mm^2

b = Width of reinforced concrete member, m

B = Width of square footing, m

D = Depth of reinforced concrete member, m

d = Effective depth of column cross section, m

d_b = Diameter of longitudinal reinforcement bar, mm

d_c = Depth of column core parallel to applied shear, mm

D_f = Depth of foundation from ground level, m

D_L = Lower fuzzy limit

D_m = Maximum interstorey drift of building

D_{max} = Maximum displacement of infill wall, m

DM^{DS} = Specified damage state

d_o = Diagonal length of opening, m

D_r = Displacement of infill wall corresponding to its residual strength, m

D_u = Displacement of infill wall at collapse, m

D_U = Upper fuzzy limit

D_y = Displacement of infill wall at yield point, m

E_c = Modulus of elasticity of concrete, MPa

E_w = Modulus of elasticity of masonry wall, MPa

f_c = Compressive strength of concrete, MPa

$f_D\ (D)$ = Probability density function

f_m= Compressive strength of masonry wall, MPa

F_{max} = Maximum strength of infill wall, kN

F_r = Residual strength of infill wall, kN

f_{tp}= cracking strength of the infill wall, kN

Fy = Yield strength of infill wall, kN

f_y = Yield strength of reinforcement bars, MPa

f_{yt} = Yield strength of transverse reinforcement, MPa

G = Shear modulus of soil, MPa

G_w = Shear modulus of infill wall, MPa

H = Depth of bedrock, m

h = Effective depth of foundation, m

h_c = Centre to centre height of the column, m

h_o = Height of opening, m

H_w = Height of infill wall, m

I_c = Moment of inertia of column, mm^4

I_g = Moment of inertia of gross section, mm^4

k = Coefficient of shear strength degradation with increasing displacement ductility

K_e = Effective stiffness, kN/m

K_i = Initial stiffness of infill wall, kN/m

K_{pc} = Effective post capping stiffness, kN/m

K_{rx} = Rocking stiffness along x–direction, kN/m

K_{ry} = Rocking spring stiffness along y-directions, kN/m

K_s = Strain hardening or post yield stiffness, kN/m

K_{so} = Negative stiffness of the softening branch, kN/m

K_{tz} = Torsional stiffness along the z-direction, kN/m

K_x = Translational spring stiffness along x–direction, kN/m

K_y = Translational spring stiffness along y–direction, kN/m

K_z = Translational spring stiffness along z–direction, kN/m

L = Clear height of column, m

l_o = Length of opening, m

L_w = Length of infill wall, m

M_c = Capping moment or maximum moment, kN-m

M_d = Member dimension

M_r = Residual moment, kN-m

M_y = Yield moment, kN-m

P = Axial load on column, kN

P[.] = Probability of damage measure

P_f = Failure/damage probability

P_{ff} = Fuzzy failure probability

q = Behaviour factor

R_f = Reduction factor

s = Spacing of column ties, mm

S_a (T_1, 5%) = spectral acceleration at the first mode period with 5% damping, g

t = Exposure time, Sec

T_1 = First mode period, Sec

t_m = Thickness of main infill wall, m

T_n = Site natural period of soil, Sec

t_p = Thickness of partition wall, m

t_w = Thickness of infill wall, m

v = Poisson's ratio

V_n = Nominal shear strength of the column, kN

V_p = Plastic shear capacity of column, kN

V_s = Shear wave velocity of soil, m/sec

w = Equivalent strut width, m

α = Factor by which member forces of the soft storey beams and columns is increased

γ = Annual exceedance frequency

δ_a = Drift ratio at axial load failure

δ_{flex} = Drift due to flexure

δ_s = Drift ratio at shear failure

δ_{shear} = Drift ratio due to shear

δ_{slip} = Drift due to bar slip

δ_y = Drift ratio at yield

θ = Critical crack angle, deg

θ_o = Angle made by diagonal length of opening with horizontal length, deg

θ_p = Pre-capping rotation, rad

θ_{pc} = Post-capping rotation, rad

θ_w = Angle made by diagonal length of infill wall with horizontal length, deg

θ_y = Yield rotation, rad

$\mu\ (D)$ = membership function

μ_{ln} = lognormal mean

ρ'' = Transverse steel ratio

σ_{ln} = Lognormal standard deviation

Φ = Standard cumulative probability function

ϕ_y = Yield curvature, rad/m

CHAPTER 1 INTRODUCTION

1.1 Background

Reinforced concrete (RC) frames with or without masonry infill walls are the most common building structural systems in the world. Due to its simple construction techniques and readily available infill materials such as bricks and concrete hollow blocks, RC frames with and without infill walls were predominately constructed in the past and are still being constructed throughout the world. However, infilled frames are reported to be more vulnerable to earthquakes and are generally termed as Earthquake Risk buildings (Bell and Davidson, 2001). In many of the earthquakes in the past such as the 1999 Izmit earthquake in Turkey, 2001 Bhuj earthquake in India, 2008 Sichuan earthquake in China and 2010 Haiti earthquake, a lot of masonry infilled RC frame buildings suffered extensive damages (Haldar et al., 2012). The wide spread damages of masonry infilled RC buildings during the recent earthquake in Nepal in May 2015 also demonstrated the high vulnerability of these buildings. This clearly shows that in spite of the number of analytical and experimental studies conducted on the masonry infilled RC frames for more than 60 years, their behavior under the seismic action is still not well understood. This is the primary reason why infilled frame buildings are still being designed by grossly neglecting the strength and stiffness of the infill walls, despite the fact that it leads to substantial inaccuracy in predicting the lateral stiffness, strength and ductility (Asteris et al., 2011; Crisafulli et al., 2000; Sattar and Liel, 2010). The complexity in understanding the seismic behavior of infilled frames is also reflected in many seismic design codes wherein the influence of the masonry infill wall to the reinforced concrete frames has not been adequately covered. For instance, Euro Code 8 (2000) and Indian Seismic Code, IS 1893 (2002) just specify the modification of the building period with infill walls. Kaushik et al. (2006) made a detailed comparison of various seismic codes and found many inconsistencies among the seismic codes. Some codes are in favour of separating infill wall from the RC frame to maintain the regular structural characteristics while some other codes consider the behavior of both the components (Kappos and Ellul, 2000). These researches demonstrate that studies on the seismic behavior and performance of RC frames with infill walls remain a challenge and are the subject of interest for many researchers throughout the world.

In general, the addition of infill wall drastically changes the load transfer mechanism from frame action to more of a truss action resulting in an increase in axial forces and a decrease in bending moments in the columns (Murthy & Jain, 2000). The seismic demand of infilled frame buildings also changes due to the sizeable reduction of the natural period as compared to that

of bare frame buildings (Aseris et al., 2011). Globally, researchers have come to the consensus that infill wall increases the global strength, stiffness, damping and energy dissipation capacity of the structures which are desirable for the better performance of the buildings. However, it is also reported that increase in strength is accompanied by an increase in lateral stiffness which in turn adversely increases the inertia force (Negro & Verzeletti, 1996; Lee and Woo, 2002). In reality, the addition of infill walls on the RC frames is said to have both beneficial and detrimental effects depending on the arrangement of the infill walls in plan and elevation (Dolsek & Fajfar, 2008). The regular arrangement of infill walls in both plan and elevation is found to have beneficial effect resulting in an increase in strength, stiffness and energy dissipation capacity on the one hand and reduction of interstorey drift on the other hand. The vulnerability of masonry infilled RC buildings is mainly due to the irregular arrangement of infill walls in plan and elevation which respectively give rise to torsional and soft storey effects (Murthy & Jain, 2000). The brittle failure of infill walls during earthquakes also results in the irregularity of strength and stiffness and usually gives rise to the formation of soft storey building (Fardis & Panagiotakos, 1997; Fiore et al., 2012). The soft storey buildings especially with the open ground floors are highly vulnerable and have been the major victims of the earthquakes in the past. In addition, the presence of openings in the infill wall introduces a wide variability of structural responses depending on their geometry, size and location (Decanini et al., 2004). The provision of opening normally gives rise to captive column effect as a result of partially infilling the wall in the RC frames for openings. The infilled frame buildings with captive columns were also reported to be the victims of earthquakes in the past (Guevara & Garcia, 2005).

However, in spite of the variability of structural responses induced by the addition of infill wall, there are limited studies conducted on the desirable and undesirable effects of the infill wall. Most studies have not considered the presence of openings and the few studies that incorporated openings had done by means of reduction factor to account for the reduction of strength and stiffness of the wall due to opening (Smyrou et al., 2011; Decanini et al., 2012). However, the reduction factors proposed by different studies vary to a great extent, which in turn lead to different predictions of structural responses. As such, seismic performance of the masonry infilled RC frame buildings is mostly assessed using the bare frame models or by considering the solid infilled walls. The study on the captive column effect is even more limited wherein even the seismic codes such as Euro Code 8 (2002) and Indian Seismic Code IS 1893 (2002) simply recommend the confinement of ties in columns with the partial infill wall. Soft storey effect is reasonably studied in detail, but there is still no well-developed design guideline that can be used to offset the soft storey effect. Hence, an extensive study on the seismic response and performance of masonry infilled RC frame buildings considering

both desirable effect and undesirable effects of the infill wall such as soft storey effect, torsional effect and captive column effect is still very much needed. This study is in fact rightly geared towards this very direction.

From the modelling perspective, infill walls are generally modelled based on either micro or macro models. Since micro models are computationally expensive, the macro model in the form of the equivalent diagonal strut is commonly employed in practice. Although the single equivalent strut is capable of capturing the global response of the infilled frame, multiple struts are also used by some researchers to help capture local effects. Determining the width of the equivalent strut has been the main focus of many researchers since it is central to the estimation of equivalent strength and stiffness of the infill wall. However, there are various equations proposed by different researchers in estimating the strut width. Some researchers such as Holmes (1961), Pauley and Priestly (1992) and Penelis and Kappos (1997) simply estimate the width of the strut as a fraction of the diagonal length of the wall. Other researchers such as Mainstone (1974) Liauw and Kwan (1984) and Durrani and Luo (1994) estimate the width based on the relative stiffness of the wall and frame. The equivalent width of the strut proposed by these researchers varies to a great extent and hence results in the variation of structural response predictions of the infilled frame buildings.

On the other hand, buildings are founded on various classes of soils and their response to earthquake action is hugely influenced by the soil-structure interaction (SSI). The soil located in the vicinity of structure undergoes nonlinear behavior with permanent deformation under strong shaking causing the change in natural period (Bhattacharya et al., 2004, Avilés & Suárez, 2002, Dutta et al., 2004). The effects of SSI on the dynamic response of structure have been studied by many researchers for more than thirty years. However, most of the studies were focused on the linear elastic behavior of structure and soil, while the real structures invariably undergo nonlinear behavior under the seismic action (Bielak, 1978). Owing to the complexity in understanding SSI, many seismic design codes either ignore the effects of SSI altogether or consider it as beneficial in the seismic analysis of buildings (Moghaddasi et al., 2011, Jarernprasert et al., 2012). As a result, many buildings were designed and built without considering the effect of SSI and in turn compromising the safety of the buildings. It is commonly known that the destructive nature of the 1985 Mexico earthquake was particularly due to the effects of soil-structure interaction. The Mexico City is located on an old lake bed with soft soil deposits of 38 - 50m in depth and with a site natural period of 1.6 - 2.8 seconds as pointed out by Gullu and Pala, (2014). The maximum damage of mid-rise buildings was mainly due to the resonance condition which was resulted from the comparatively similar vibration frequencies of mid-rise buildings and the soil deposits. It was also argued by

Mylonakis and Gazetas (2000) that beneficial effect of SSI is an oversimplification and that SSI is detrimental in some cases such as forward fault rupture and soil resonance. Hence, consideration of SSI in the study of the seismic response of masonry infilled RC frames deserves special attention.

From the number of issues discussed above, it can be confirmed that the safety of existing masonry infilled RC buildings under the seismic action is highly questionable. Extensive damages of these buildings during the recent earthquakes such as the one in Nepal in 2015 further question the seismic safety of both designed and un-designed infilled frame buildings. It is therefore very important to assess the seismic performance of existing masonry infilled RC buildings so as to mitigate the loss of lives and properties during earthquakes. It is generally said that earthquakes do not kill people but unsafe buildings do. Realizing the importance, various researchers have carried out the seismic performance assessment of masonry infilled RC buildings in various parts of the world using various approaches. Lynch et al. (2011), Duan and Hueste (2012) and Rezaei and Massumi (2014) studied the seismic performance of existing RC buildings in Southern California, China and Iran respectively. Sadjadi et al. (2007), Kueht and Hueste (2009) and Chaulagain et al. (2015) conducted the seismic assessment of existing RC buildings in Canada, central United States and Nepal respectively. Similarly, many other researchers have carried out the seismic assessment of masonry infilled RC buildings in the various parts of the world. However, most of these studies are deterministic in nature and are based on the distinct interstorey drift limits in defining the damage boundaries. Some of the studies have not incorporated openings in the infill wall while others are based on the linear structural analysis. The soft storey, captive column and SSI effects are not adequately considered in many studies. Hence, the comprehensive and realistic seismic assessment of masonry infilled RC buildings considering openings, soft storey, captive column and SSI and using the correct modelling approaches is paramount in mitigating the seismic risk of the existing buildings.

The masonry infilled RC buildings are also the most dominant building structures in Bhutan wherein they constitute more than 70% of the buildings in the urban centres. However, they are no different from the masonry infilled RC buildings in other parts of the world. All the issues discussed above in regard to the masonry infilled RC buildings are very much applicable to the buildings in Bhutan. In fact, they are more vulnerable than those in other regions, since all buildings built in Bhutan prior to 1997 were not designed to any standard. It was only from 1997 that the country has started following Indian Seismic Code for the design of buildings. Bhutan still has no seismic design code of its own and moreover, the applicability of using Indian Seismic Code for the conditions in Bhutan has never been studied. On the

other hand, the country is located right on the interplate boundary where the Indo-Australian plate is continuously being sub ducted under the Eurasian plate. A number of destructive earthquakes had occurred in and around Bhutan causing huge loss to lives and properties (Walling and Mohanty, 2009). Excluding the recent M_w=5.5 and M_w=6.1 earthquakes that occurred in 2009, it was reported that a total of 30 earthquakes in the magnitude range of 4.2-6.75 had occurred in Bhutan since 1937 (Drukpa et al., 2006). Moreover, based on the seismic gap hypothesis and other evidence, Bilham et al. (2001) and Banerjee and Bürgmann (2002) reported an overdue of one or more large earthquakes in the Himalaya. However, regardless of these risks, only a couple of studies had attempted to assess the seismic performance of building structures in Bhutan. The first study was initiated by the Government of Bhutan wherein 15 masonry infilled RC buildings were assessed by employing consultants from Nepal. This study was very preliminary and mostly based on the visual judgement of the consultant and on some linear analyses (UNDP report, 2006). The other study was conducted by Dorji (2009) using the two-dimensional building frame and three ground motions from other regions. This study is also not realistic owing to the simplified model and the arbitrary use of ground motions. As such, assessing the realistic seismic performance of the existing masonry infilled RC buildings in Bhutan has become the most pressing need at this juncture.

1.2 Research Objectives

The primary objective of this study is to realistically assess the seismic performance of existing RC buildings with or without infill walls in general and more specifically in Bhutan. The other objective is to address the issues related to openings in the infill wall, soft storey frame and partially infilled frame. The three typical existing masonry infilled RC buildings built in different eras with different designs and with varying heights in Bhutan are considered for the study. The nonlinear analysis and performance assessment software, Perform 3D (CSI, 2006) is used for carrying out the nonlinear analyses of the building models to help achieve the objectives. The specific objectives of this research are:

- To predict the earthquake ground motions at the generic soil sites in Bhutan to be used for the realistic seismic response analysis and performance assessment of the RC building structures with or without infill walls in Bhutan.

- To assess the seismic performance of the typical RC buildings with or without infill walls and the buildings with open ground floor both deterministically and probabilistically considering the randomness in material and geometrical parameters and fuzziness in the damage criteria using the predicted ground motions in Bhutan.

- To investigate the effects of openings in the infill wall on the seismic behaviour of the buildings.

- To investigate the beneficial and detrimental effect of soil structure interaction on the seismic performance of the typical RC buildings with or without infill walls in Bhutan.

- To study the adequacy of using Indian Seismic Code for seismic resistance design of building structures in Bhutan in general and to investigate the adequacy of its design provision for soft storey buildings in particular.

- To carry out the fragility analysis of RC buildings with and without infill walls and the buildings with open ground floor considering both material and ground motion uncertainties.

- To study the effect of partial infill walls and strengthening options of the columns in frames with partial infill walls on the seismic behaviour of buildings.

1.3 Research Outline

This thesis is produced by combining the journal papers that are either published, accepted, under review or under preparation which form the individual chapters. The contents of each chapter are briefly and subsequently described below:

Chapter 2 presents the prediction of earthquake ground motions at generic soil sites in Bhutan from the probabilistic seismic hazard analysis. A numerical model for RC member is developed and calibrated with the experimental results. The model is then used to carry out the dynamic nonlinear analysis of typical RC buildings without infill wall in Bhutan using the predicted ground motions as input. Seismic assessment of the buildings is evaluated deterministically incorporating the soil structure interaction. The adequacy of using Indian Seismic Code for the building structures in Bhutan is also investigated.

Chapter 3 describes the probabilistic seismic performance assessment of typical RC buildings without infill wall in Bhutan considering the randomness in material and geometrical parameters and fuzziness in the damage criteria. The effect of soil-structure interaction is considered for the assessment.

Chapter 4 develops and calibrates numerical models for masonry infilled RC frame buildings with and without soft storey. Seismic response and performance of masonry infilled RC buildings with and without soft storey are evaluated. The effect of opening and soil-structure

interaction are duly considered in this chapter. The adequacy of design provision provided by the Indian Seismic Code, IS 1893 (2002) for the soft storey buildings are investigated.

Chapter 5 deals with the probabilistic seismic performance assessment of masonry infilled RC buildings with and without soft storey. Rosenbluth Point Estimate and Monte Carlo Simulation methods are employed for modelling the statistical variations of geometrical and material parameters. The fuzzy probability analysis is used to model the fuzziness in the damage boundaries. Soil-structure interaction is similarly incorporated as in the previous chapters.

Chapter 6 presents the fragility analysis of the typical masonry infilled RC frame buildings with and without soft storey in Bhutan considering both material and ground motion uncertainties. A total of 21 ground motions selected from the PEER ground motion database are used for the analysis. Fragility curves for the buildings are provided and discussed.

Chapter 7 investigates the effect of the partially infilled frame on the seismic behavior of the masonry infilled RC buildings. The infill wall height is varied along the column height and its influences on the seismic responses of buildings are studied in terms of the shear demand and interstorey drift. The effect of increasing the strength and stiffness of the columns with partial infill wall is also investigated.

Chapter 8 concludes the contributions of the current study and recommendations for the future research.

1.4 References

Asteris, P. G, Antoniou, S., Sophianopoulos, D., & Chrysostomou, C. Z. (2011). Mathematical macromodeling of infilled frames: State of the art. *Journal of Structural Engineering, 137* (12), 1508-1517.

Aviles, J., & Suarez, M. (2002). Effective periods and damping of building foundation systems including seismic wave effects. *Engineering Structures, 24*, 553-562.

Banerjee, P., & Bürgmann, R. (2002). Convergence across the northwest Himalaya from gap measurements. *Geophysical Research Letters, 29* (13), 30-1-30-4.

Bell, D., & Davidson, B. (2001). Evaluation of earthquake risk buildings with masonry infill panels. In: *New Zealand Society for Earthquake Engineering Conference*, Taupo, New Zealand.

Bhattacharya, K., Dutta, S. C., & Dasgupta, S. (2004). Effect of soil-flexibility on dynamic behaviour of building frames on raft foundation. *Journal of Sound and Vibration, 274*, 111-135.

Bielak, J. (1978). Dynamic response of non-linear building foundation systems. *Earthquake Engineering and Structural Dynamics, 6*, 17-30.

Bilham, R., Gaur, V. K., & Molnar, P. (2001). Himalayan seismic hazard. *Science (Washington), 293* (5534), 1442-1444.

Chaulagain, H., Rodrigues, H., Spacone, E., & Varum, H. (2015). Seismic response of current RC buildings in Kathmandu Valley. *Structural Engineering and Mechanics, 53* (4), 791-818.

Crisafulli FJ, Carr AJ and Park R (2000) Analytical modelling of infilled frame structures-a general review. *Bulletin-New Zealand Society for Earthquake Engineering*. 33(1): 30-47.

CSI (2006). *Nonlinear analysis and performance assessment for 3D structures*. Computers & Structures Inc., Berkeley.

Decanini, L., Liberatore, L., & Mollaioli, F. (2012). The influence of openings on the seismic behaviour of infilled framed structures. In: *15th World Conference on Earthquake Engineering*, Lisbon, Portugal.

Dolšek, M., & Fajfar, P. (2008). The effect of masonry infills on the seismic response of a four-storey reinforced concrete frame—a deterministic assessment. *Engineering Structures, 30* (7), 1991-2001.

Dorji, J. (2009). *Seismic performance of brick infilled RC frame structures in low and medium rise buildings in Bhutan.* Master's degree Thesis, Queensland University of Technology, Australia.

Drukpa, D., Velasco, A. A., & Doser, D. I. (2006). Seismicity in the Kingdom of Bhutan (1937-2003): Evidence for crustal transcurrent deformation. *Journal of Geophysical Research (Solid Earth), 111***,** 6301.

Duan, H., & Hueste, M. B. D. (2012). Seismic performance of a reinforced concrete frame building in China. *Engineering Structures*, 41, 77-89

Dunand, F., Guéguen, P., Bard, P. Y., Rodgers, J., & Celebi, M. (2006). Comparison of the dynamic parameters extracted from weak, moderate and strong building motion. In: *Proceedings of the 1st European Conference of Earthquake Engineering and Seismology*, Geneva, Switzerland, 1021.

Durrani, A. J., & Luo, Y. (1994). *Seismic retrofit of flat-slab buildings with masonry infills.* Technical report, National Centre for Earthquake Engineering Research, pp. 1-8.

Dutta, S. C., Bhattacharya, K., & Roy, R. (2004). Response of low-rise buildings under seismic ground excitation incorporating soil-structure interaction. *Soil Dynamics and Earthquake Engineering, 24*, 893-914.

Eurocode 8 (2002). *Design of Structures for earthquake resistance–Part 1: General rules, seismic actions and rules for buildings*. European Standard, NF EN, 1.

Fardis, M., & Panagiotakos, T. (1997). Seismic design and response of bare and masonry-infilled reinforced concrete buildings part ii: Infilled structures. *Journal of Earthquake Engineering, 1* (3): 475-503.

Fiore, A., Netti, A., & Monaco, P. (2012). The influence of masonry infill on the seismic behaviour of RC frame buildings. *Engineering Structures, 44*, 133-145.

Guevra, L. T., & Garcia, L. E. (2005). The captive-and short-column effects. *Earthquake Spectra, 21*, 141-160.

Gullu, H., & Pala, M. (2014). On the resonance effect by dynamic soil-structure interaction: a revelation study. *Natural Hazards, 72*, 827-847.

Haldar, P., Singh, Y., & Paul, D. (2012). New lateral force distribution for seismic design of structures. *Journal of structural Engineering, 135*, 906-915.

Holmes, M. (1961). Steel frames with brickwork and concrete infilling. *Proceedings of the Institution of Civil Engineers* 19(4): 473-478.

IS-1893 (2002). *Criteria for Earthquake Resistant Design of Structures –Part I: General provisions and buildings*, Bureau of Indian Standards, New Delhi, India.

Jaremprasert, S., Bazan-Zurita, E., & Bielak, J. (2013). Seismic soil-structure interaction response of inelastic structures. *Soil Dynamics and Earthquake Engineering, 47*, 132-143.

Kappos, A. J., & Ellul, F. (2000). Seismic design and performance assessment of masonry infilled RC frames. In: *12th World Conference on Earthquake Engineering*, Auckland, New Zealand.

Kaushik, H. B., Rai, D. C., & Jain, S. K. (2006). Code approaches to seismic design of masonry infilled reinforced concrete frames: A state of the art review. *Earthquake Spectra, 22*, 961-983.

Kueht, E., & Hueste, M. B. (2009). Impact of code requirements in the central United States: Seismic performance assessment of a reinforced concrete building. *Journal of Structural Engineering, 135* (4), 404-413.

Lee, H. S., & Woo, S. W. (2002). Effect of masonry infills on seismic performance of a 3 storey R/C frame with non-seismic detailing. *Earthquake Engineering and Structural Dynamics, 31*, 353-378.

Liauw, T., & Kwan, K. (1984). New development in research of infilled frames. In: *8th World Conference on Earthquake Engineering*, San Francisco, California, USA.

Lynch, K. P., Rowe, K. L., & Liel, A. B. (2011). Seismic performance of reinforced concrete frame buildings in Southern California. *Earthquake Spectra*, *27* (2), 399-418.

Mainstone, R. (1974). *Supplementary note on the stiffness and strength of infilled frames.* 2ed edition, Institution of Civil Engineers, London, UK, pp. 57-90.

Moghaddasi, M., Cubrinovski, M., Chase, J. G., Pampanin, S., & Carr, A. (2011). Probabilistic evaluation of soil foundation structure interaction effects on seismic structural response. *Earthquake Engineering and Structural Dynamics*, *40*, 135-154.

Mondal, G., & Jain, S. K. (2008). Lateral stiffness of masonry infilled reinforced concrete (RC) frames with central opening. *Earthquake Spectra, 24* (3), 701-723.

Murty, C., & Jain, S. K. (2000). Beneficial influence of masonry infill walls on seismic performance of RC frame buildings. In: *12th World Conference on Earthquake Engineering*, Auckland, New Zealand.

Mylonakis, G., & Gazetas, G. (2000). Seismic soil-structure interaction on damage index of buildings. *Engineering Structures, 30*, 1491-1499.

Negro, P., & Verzeletti, G. (1996). Effect of infills on the global behaviour of RC frames: Energy considerations from pseudo dynamic tests. *Earthquake engineering & structural dynamics*, *25* (8), 753-773.

Paulay, T., & Priestley, M. (1992). *Seismic design of reinforced concrete and masonry buildings*. New York: John Wily and Sons Inc.

Penelis, G., & Kappos, A. (1997). *Earthquake resistant concrete structures*. London: EP & FN SPON, London.

Rezaei, E., & Massumi, A. (2014). Seismic performance of reinforced concrete frame buildings designed by Iranian seismic code. *Journal of Seismology and Earthquake Engineering*, *16* (3), 209-217.

Sadjadi, R., Kianoush, M. R., & Talebi, S. (2007). Seismic performance of reinforced concrete moment resisting frames. *Engineering Structures*, *29* (9), 2365-2380.

Sattar, S., & Liel, A. B. (2010). Seismic performance of reinforced concrete frame structures with and without masonry infill walls. In: *9th US National and 10th Canadian conference on earthquake engineering*, Toronto, Canada.

Smyrou, E., Blandon, C., Antoniou, S., Pinho, R., & Crisafulli, F. (2011). Implementation and verification of a masonry panel model for nonlinear dynamic analysis of infilled RC frames. *Bulletin of Earthquake Engineering, 9* (5), 1519-1534.

UNDP (2006). *Report on Thimphu valley earthquake risk management program.* Standards and Quality Control Authority, Ministry of Works and Human Settlement, Thimphu, Bhutan.

Walling, M. Y., & Mohanty, W. K. (2009). An overview on the seismic zonation and micro zonation studies in India. *Earth-Science Reviews, 96* (1), 67-91.

CHAPTER 2 SEISMIC PERFORMANCE OF REINFORCED CONCRETE BUILDINGS IN THIMPHU, BHUTAN

2.1 Abstract

In spite of its location in one of the most active seismic zones in the world, Bhutan has no seismic design code of its own and no detailed study on the performance of buildings under expected earthquake ground excitation has been carried out. In this study, probabilistic seismic hazard analysis is first carried out to predict the design ground motions in Thimphu, Bhutan for the return periods of 475 and 2475 years. These ground motions are then used to assess the performance of three typical RC buildings in the capital city, Thimphu. Soil Structure Interaction (SSI) is incorporated at different soil sites and the effects of SSI are discussed. Adequacy of using Indian Seismic Code in Bhutan is also studied and discussed. The study suggests that the typical buildings in Bhutan could undergo moderate to severe damages under the 475 year return period and could even collapse under the 2475 year return period ground motions. This study is the first such effort in predicting the design ground motions and then assessing the performance of the general building stocks in Bhutan. The result can guide the seismic preparedness of the country through proper design and mitigation measures.

2.2 Introduction

Bhutan, by its geographical position, is located in one of the high seismic regions in the world. Earthquakes of various sizes have occurred in the past and inflicted heavy casualties and damages for centuries. The high seismicity of Bhutan is due to its location on the Himalayan mountain belt which is one of the most earthquake-prone areas in the world. Himalaya was actually formed as a result of the continental collision between the Indian and Eurasian plates initiated more than 60 million years ago (Walling and Mohanty, 2009; Bilham et al., 1997). The subduction of Indian plate into the Eurasian plate is a continuous process and is reported to be taking place at an average of 20.5±2mm per year as per the Global Positioning System (GPS) measurement (Bilham et al., 1997; Bilham et al., 2001). A similar measurement was made at the north-west Himalaya by Banerjee and Bürgmann (2002) and found the convergence of these plates at an average of 14±1mm per year. Figure 2-1 (a) shows the seismic hazard map of Bhutan prepared by Global Seismic Hazard Assessment Program (GSHAP, 1992). The occurrence of earthquakes in and around Bhutan is depicted in Figure 2-1 (b) as given in Motegi (2001).

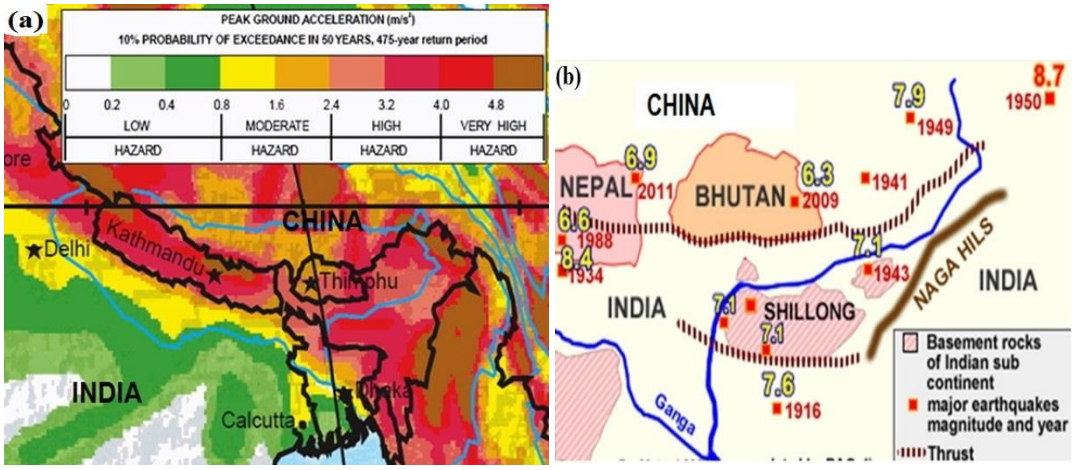

Figure 2-1(a) Seismic hazard map of Bhutan (GSHAP, 1992); (b) Earthquakes in and around Bhutan (Motegi, 2001).

Although not all earthquakes are reflected in Figure 2-1 (b), yet there were 32 earthquakes of engineering significance occurred in Bhutan in the last seven and half decades (Dorji, 2009). The first severe earthquake reported in the literature was 1713 earthquake which was believed to have occurred in eastern Bhutan near the Indian state of Arunachal Pradesh (Ambraseys and Jackson, 2003; Bilham, 2004). The most recent earthquake that rocked Bhutan was in 2009 which had a moment magnitude of 6.1. As per the joint report, this earthquake claimed 13 lives and damaged hundreds of buildings including rural and urban residential houses, schools and monasteries (Report, 2006). In addition, there were a lot of earthquakes occurred around Bhutan as shown in Figure 2-1 (b). Although these great earthquakes had occurred some epicentral distance away from Bhutan, their effects had been greatly felt in Bhutan. A very recent M_w 7.9 Nepal earthquake on 25th April 2015 was greatly felt in Thimphu which led people to rush out of the buildings in chaos and panic. There were also some damages reported in some of the old RC buildings from this earthquake. M_w 6.9 Sikkim earthquake in 2011 had killed one person, injured 16 others and damaged around 6000 buildings including rural houses, school buildings and monasteries in western Bhutan. It can be inferred from these earthquakes that Bhutan indeed is located in one of the most active seismic zones in the world.

In spite of being the victim of several past earthquakes, Bhutan is least prepared for the next such earthquake. Currently, Bhutan does not have a Seismic Code of its own and buildings are designed and constructed following the Indian Seismic Code, IS 1893 (2002). The seismicity of Bhutan is simply assumed to be the same as that of the north eastern states of India which is designated zone V in the Indian Seismic Code. However, the applicability of using Indian Seismic Code to site conditions in Bhutan is still a mystery today since no proper study has been done until now. Moreover, the use of Indian Seismic Code has begun only from 1997 in the urban areas. Prior to 1997, all buildings were either built based on some

thumb rules or designed only for gravity load. Although the RC buildings built after 1997 were designed based on the Indian Seismic Code, constructions were carried out with limited or no supervision from the technical personnel. Most of the constructions even to this day are carried out by building owners with the use of unskilled and semi-skilled labourers. Despite all these issues in regard to the safety of buildings, seismic performance of these buildings has not been properly assessed until now.

The first ever assessment of RC buildings in Bhutan was done in Thimphu under the initiation of Thimphu Valley Earthquake Risk Project (TVERMP) in 2005 (UNDP Report, 2006). Out of 15 RC buildings assessed in Thimphu under the project, 14 were found to be seismically unsafe. However, this assessment was very preliminary and was based on the linear elastic analyses according to the Indian Seismic Code. Since structures invariably exhibit non-linear behaviour under seismic action, response prediction made by this study is questionable. Dorji (2009) studied seismic performance of buildings in Bhutan considering a typical 2D RC frame subjected to El Centro, Kobe and Northridge earthquakes. Response prediction made by this study is also questionable since ground motions obtained from other sites were used, which do not necessarily represent the seismic ground motions in Bhutan. There is in fact not a single study done on the seismic performance of buildings purely based on the actual site conditions in Bhutan yet. On the other hand, there are thousands of buildings in both rural and urban areas built both prior to and after 1997. It is paramount to know the likely performance of these buildings beforehand so that mitigation measures can be addressed and be prepared for the future events.

Based on the seismic gap hypothesis and other evidence, Bilham et al. (2001) and Banerjee and Bürgmann (2002) reported a very likely occurrence of one or more large earthquakes in the Himalayan mountain belt on which Bhutan is located. Walling and Mohanty (2009) reported three seismic gaps in Himalayan mountain range namely Kashmir Seismic Gap, Central Seismic Gap and Assam Seismic Gap where earthquakes of magnitudes of 8 or more are expected at any time. Many experts gathered in Nepal after 25th April 2015 earthquake believed this earthquake to be the recurrence of M_w 8.3 1934 Nepal-Bihar earthquake which occurred in the Central Seismic Gap. If such earthquake occurred in the Assam Seismic Gap, Bhutan would have been greatly affected since it lies just along the southern border of Bhutan. As such, seismic performance assessment of buildings especially in the capital city, Thimphu has become the pressing need of the time. With more than 75% of the country's RC buildings and with highest population density, Thimphu is the nerve centre of Bhutan. In the event of a mishap during the earthquake, Bhutan would suffer immeasurably and would eventually take a very long time to recover.

This paper presents a comprehensive seismic performance assessment carried out for three typical RC buildings in Thimphu. Probabilistic seismic hazard analysis is first carried out to predict ground motions at generic soil sites in Thimphu to be used for the response analysis. Dynamic nonlinear analysis and performance assessment software, Perform 3D (CSI, 2006) is employed for the study. Soil-structure interaction is incorporated as per the provision in ASCE/SEI 41-13 (2014) for different soil sites. The performances of the typical buildings in terms of interstorey drift and displacements are predicted for the 475 and 2475 years return period earthquakes and compared with the provision in Vision 2000 document of Structural Engineers Association of California (SEAOC). The buildings are also analysed and assessed using ground motions matched to Indian Seismic Code response spectrum to check the adequacy of using Indian Seismic Code in Bhutan. The effects of soil structure interaction are also discussed. It is found that the buildings built after the adoption of Indian Seismic Code could suffer moderate to severe damages under the 475 return period and could suffer severe damages and even collapse under the 2475 year return period ground motion. The buildings built before the adoption of the Indian Seismic Code could suffer severe damages and even collapse under the 475 year return period and could collapse under the 2475 year return period ground motions. Except at the soft soil site, SSI is found to be insignificant. The use of Indian Seismic Code underestimates structural responses and hence its applicability in Bhutan needs to be further studied.

2.3 Prediction of Design Ground Motion in Thimphu

One of the objectives of this paper is to predict design ground motions in Thimphu and compare with the prediction made by Indian Seismic Code which is currently being used in Bhutan. To achieve this objective, a computer code EZ-FRISK (Risk Engineering Inc.) is used to carry out probabilistic seismic hazard analysis (PSHA), spectral matching and site response analysis in Thimphu.

2.3.1 Probabilistic Seismic Hazard Analysis

PSHA is conducted for Thimphu, Bhutan by defining its geographical location through the specification of latitude (27.4667 N) and longitude (89.6417 E) in the EZ-FRISK program. The seismic source of South Asia region that constitutes the countries of Bhutan, India, Nepal and Bangladesh is selected in the program. Since fault sources are not defined in the program for the South Asia region, only area sources within a distance of 400 km from Thimphu are considered for the analysis. The area sources are based on the historical seismicity of the region and are generated by the program based on the defined seismic source of the region. In this study, 18 seismic source zones were generated from the definitions of the seismic source

of South Asia and radial distance of 400 km from Thimphu in the program. Having defined the area source zones, the ground motion attenuation equations are selected to predict the ground motion of the future earthquake based on the magnitude of the earthquake, source to site distance, focal depth and other geological and uncertainty parameters. In this study, the Next Generation Attenuation (NGA) models proposed by Boore and Atkinson (2008), Chiou and Young (2008) and Idriss (2008) are used in the analyses since no earthquake ground motion attenuation model is available for Bhutan. These NGA models are assumed to be applicable in Bhutan as they were developed from a large number of earthquake recordings that occurred in the tectonically active shallow crustal regions in all parts of the world. They provide very good references for the regions where the attenuation model is not available such as Bhutan. The applicability of NGA models in the tectonically active regions of Europe and other similar regions was also reported by Campbell and Bozorgnia (2006).

Based on the seismic source zones and attenuation models, hazard curves and probabilistic seismic hazard spectra are generated for different return periods at the bedrock. Hazard curves are obtained in terms of peak ground acceleration (PGA) with respect to annual exceedance frequency. Figure 2-2 (a) shows the hazard curve for the source zone 8.CH.227 obtained from the three attenuation models. From the figure, it is evident that the smallest PGA is predicted from Boore and Atkinson model while highest PGA is predicted from Idriss model. The weighted average relation is used in this study. Figure 2-2 (b) shows the total hazard curve and the assembly of hazard curves obtained from all seismic source zones. As indicated in the figure, the direction of arrows shows the matching of source name with the respective curve. As the source name runs from top to bottom, the respective curve runs from right to left. The total hazard curve is obtained from the sum of the contributions from all source zones at different return periods. From the total hazard curve and using the relationship given by McGuire (2004), the annual exceedance frequency γ can be estimated for the probability of an event P and exposure time t by

$$\gamma = -\frac{\ln(1-P)}{t} \tag{2.1}$$

For 10% probability of exceedance in 50 years, the annual exceedance frequency is estimated to be 0.002107 or a return period of 475 years. This corresponds to PGA of 0.21 g in Thimphu. Similarly, PGA for different return periods can be obtained from the total hazard curve. Figure 2-3 shows the derived probabilistic curves for the bed rock motion under the return periods of 475 and 2475 years at 5% damping. The probabilistic hazard spectrum which is also known as the uniform hazard spectrum represents the horizontal acceleration of ground motion at 5% damping with respect to spectral time period. The effects of near and distant sources can be

observed from the figure in the form of two peaks at the shorter and longer periods respectively. These curves are used as the target spectra in the spectral matching process to generate the acceleration time histories for the bed rock motions under the 475 and 2475 year return periods.

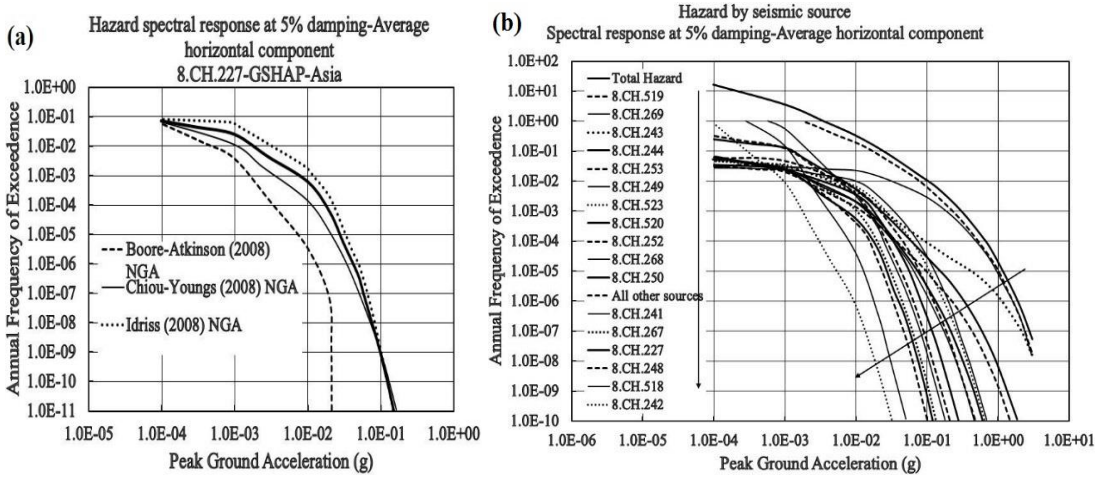

Figure 2-2 (a) Hazard curve for 8.CH.227 source zone in log scale; (b) Total hazard curve and hazard curves from all other sources in log scale.

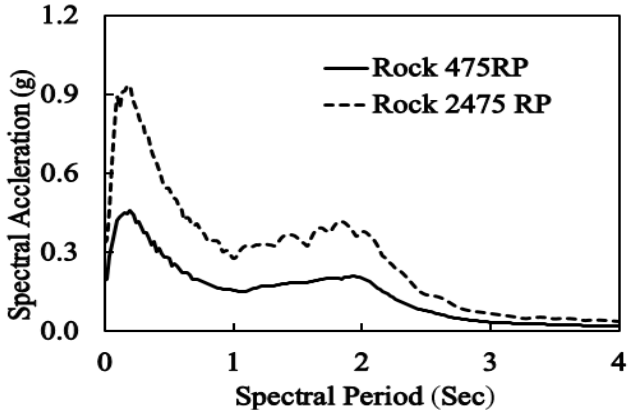

Figure 2-3 Probabilistic spectra for bedrock motion.

2.3.2 Spectral Matching

Spectral matching is the process wherein the response of an input accelerogram is matched to the target spectrum while keeping the realistic time-dependent characteristics of ground motion. The choice of input accelerogram to be matched with the target spectrum is governed by many factors such as the magnitude of earthquakes, site to source distance, deviation from target spectrum, site class and faulting mechanism. Pagliaroni and Lanzo (2008) reported that it is ideal to use accelerograms obtained from the earthquakes that have occurred near the site

of study so that more realistic future earthquakes can be represented. Since recorded ground motion is not available in Bhutan, accelerograms from 1999 Chi-Chi, 1994 Northridge, 1989 Loma Prieta and 1983 Coalinga earthquakes are considered for the spectral matching. Based on the scoring analysis of the software, accelerograms from 1983 Coalinga and 1999 Chi-Chi earthquakes are respectively selected to match with the target spectra obtained from PSHA in Figure 2-3 for the return periods of 475 and 2475 years. These two accelerograms are selected since they resulted in the lowest root mean square of deviation and a scale to match with the target spectrum closer to unity amongst other accelerograms. The output adjusted acceleration time histories obtained from the spectral matching for 475 and 2475 year return periods are shown in Figure 2-4. The spectra are found to be well matched with maximum and average misfits below 8% and 5% respectively, which are within the acceptable range from the engineering point of view. These output acceleration time histories are used for the site response analysis to derive the design response spectrum at various soil sites.

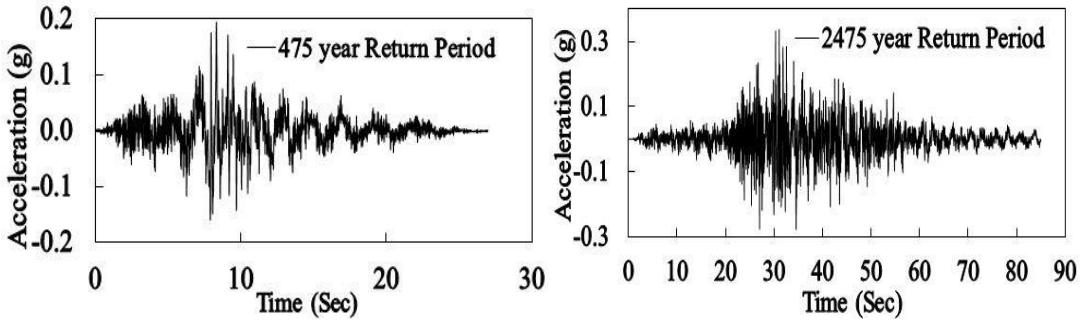

Figure 2-4 Output acceleration time histories at bedrock obtained from spectral matching.

2.3.3 Site response analysis

The ground motion gets amplified or de-amplified when travelling through different soil media. Significant damages have been reported during the past earthquakes such as 1985 Mexico City, 1989 Loma Prieta, 1994 Northridge and 1995 Kobe earthquakes due to soil amplification effects (Chang et al., 1996). Site response analysis is carried out to study soil amplification using the bedrock motion acceleration time histories in Figure 2-4. The site response analysis requires the soil profiles to be defined. Due to the absence of data on soil profiles in Thimphu, four generic soil classes are considered as per the site categorization method of Rodriguez-Marek et al. (1999). The soil classes and their respective properties are given in Table 2-1. Based on the site natural period T_n, depth of bedrock H and the average shear wave velocity V_s, soil profiles are defined in the EZ-FRISK program. Once the soil profiles are defined, the appropriate damping and modulus reduction curves are chosen based on the soil classes considered. The program analyse these soil data and derive the site response spectra and the corresponding acceleration time histories. The spectral accelerations of the

ground motions on the surface of four site classes with 5% damping for return periods of 475 and 2475 years are shown in Figure 2-5. As shown in the figure, the ground motion amplifies at almost all periods with the maximum amplification occurring at the site natural period. The acceleration time histories at the generic soil sites in Thimphu, Bhutan for the 475 and 2475 year return periods are respectively shown in Figures 2-6 and 2-7.

Table 2-1 Generic soil sites in Thimphu

Site	*Vs* (m/s)	Depth (m)	*Tn* (s)
Rock	1067	6	0.2
Soft rock	366	37	0.4
Shallow stiff soil	219	27	0.5
Soft soil	112	28	1.0

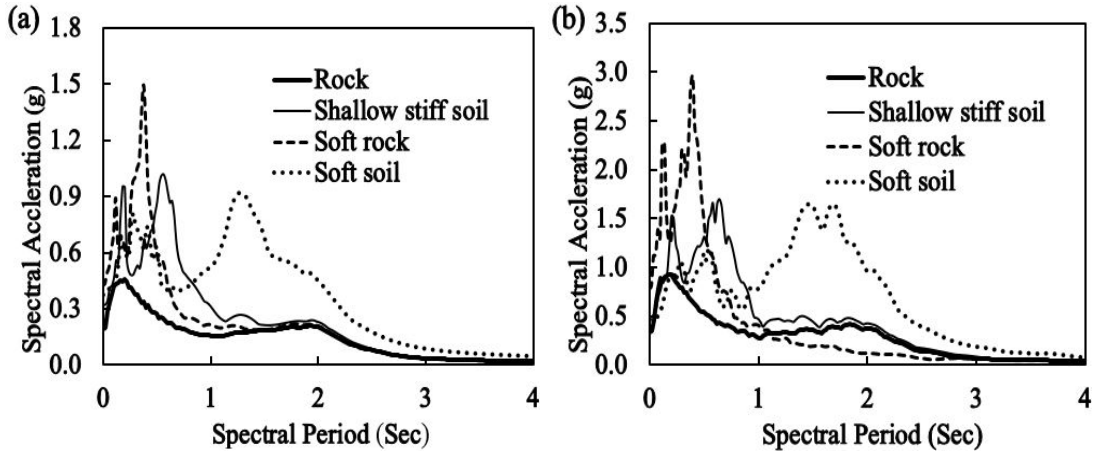

Figure 2-5 Spectral acceleration for four site classes with 5% damping, (a) 475 and (b) 2475 year return periods

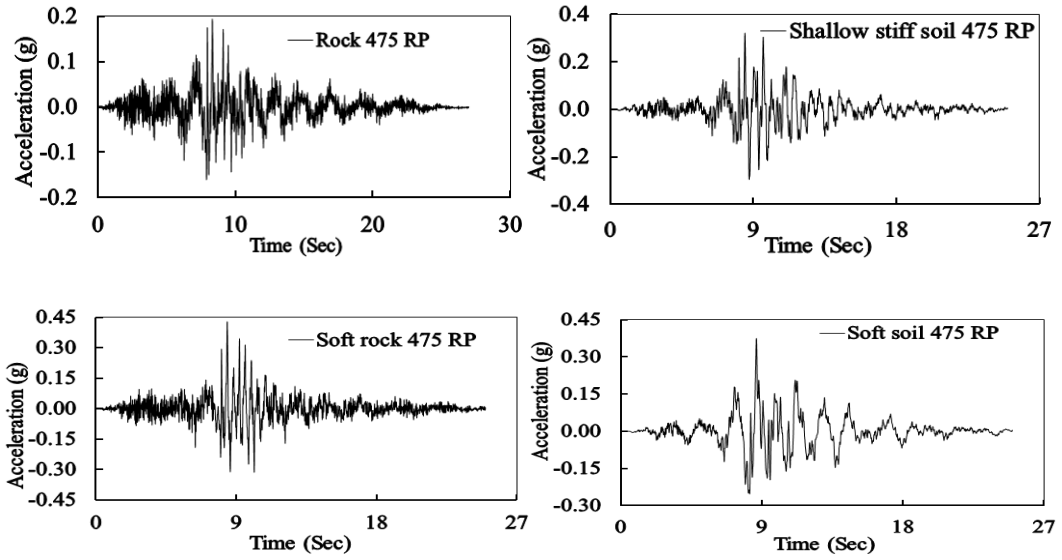

Figure 2-6 Ground motion time histories at generic soil sites for the 475 year return period (RP).

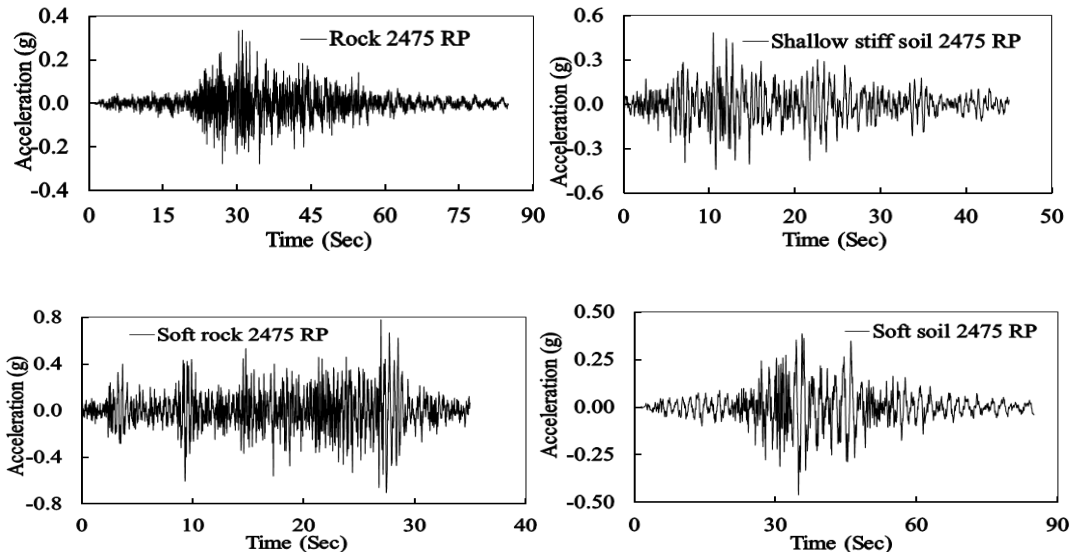

Figure 2-7 Ground motion time histories at generic soil sites for the 2475 year return period (RP).

It is to be noted that the PGA predicted in Thimphu at the rock site for the 475 and 2475 year return periods are respectively 0.21 g and 0.35 g which compares well with the PGA of 0.18 g and 0.36 g for the design basis and maximum considered earthquakes of the Indian Seismic Code for zone V respectively. However, as shown in Figures 2-5 and 2-8, the shapes of the response spectra are quite different which could result in different structural responses. The response spectra of ground motion predicted in Thimphu from PSHA in this study has two peaks corresponding to near field and far field earthquakes.

2.4 Ground Motion from Indian Seismic Code

Indian Seismic Code has four seismic zones designated as zone II, zone III, zone IV and zone V and the corresponding factor assigned to these zones are 0.1, 0.16, 0.24 and 0.36 respectively. These zone factors are the PGA values at respective zones corresponding to the Maximum Considered Earthquake (MCE) or the most severe earthquake considered by the code. Similar to many other international codes, MCE in Indian Seismic Code does not correspond to any probability of occurrences or return periods. The zone factors were assigned purely based on engineering judgement and no probabilistic seismic hazard analyses were carried out to obtain those factors (Jain, 2003; Jain and Murthy, 2005). The code also specifies Design Basis Earthquake (DBE) for which the structures are generally designed. The PGA values for DBE are taken as half the values of MCE. The normalised response spectra of Indian Seismic Code with 5% damping for rock and soil sites are shown in Figure 2-8 (a).

Bhutan is currently following Indian Seismic Code for the design of buildings. Seismic zone V is assumed for Bhutan since Indian states of Arunachal Pradesh and Assam that border Bhutan to the East and South are in zone V of the Indian seismic zonation map. Hence, as per the Indian Seismic Code PGA values in Thimphu are 0.36 g and 0.18 g for MCE and DBE respectively. Although Indian code does not specify return periods for both MCE and DBE, these values are comparable to the PGA values of 0.35 g and 0.21 g predicted from PSHA in Thimphu for the return periods of 2475 and 475 years respectively. However, comparing the response spectra predicted in Thimphu to that of normalised response spectra of Indian Seismic Code, it can be seen that the shapes of the response spectra are quite different. As shown in Figure 2-8 (b), the effect of soil amplification is captured prominently especially for the soft soil site. On the other hand, the normalised response spectra of Indian Seismic Code have no such peaks. Compared to the predicted ground motion response spectra in Figures 2-5 and 2-8, it is obvious that the corner period of the response spectra in Indian Code is low. Therefore, the design spectra could not cover the second peak in the predicted response spectrum as shown in Figure 2-8 (b). These differences in the spectral shapes could result in different structural responses, especially at the soft soil sites.

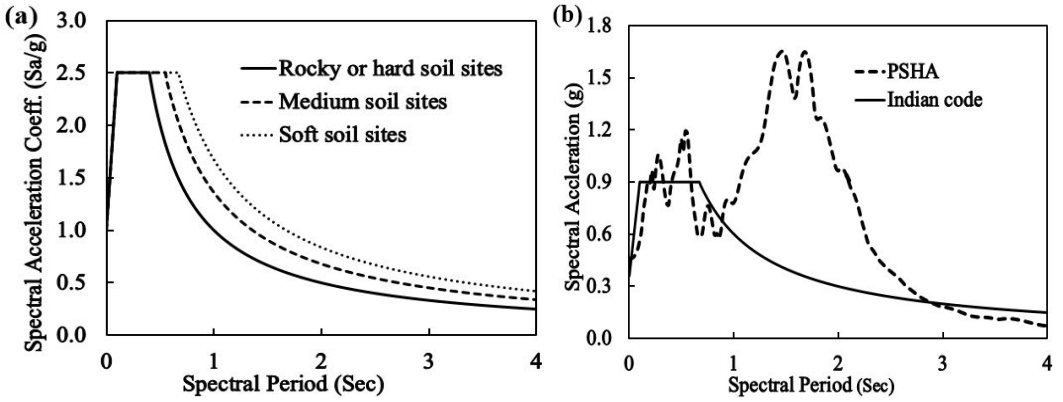

Figure 2-8 (a) Normalised response spectra with 5% damping defined in Indian Seismic Code and (b) comparison of response spectra at soft soil site obtained from PSHA for 2475 year return period and Indian Seismic Code for MCE with 5% damping.

To study the adequacy of using Indian Seismic Code in Bhutan, ground motion time history is derived for soft soil site by matching with the response spectrum of the Indian Seismic Code. Soft soil site is chosen in this study since a notable difference in structural response is expected at the soft soil site owing to the difference in the shapes of the respective response spectra. To make the comparison of structural responses more rational, 1999 Chi-Chi earthquake is again used for matching with the Indian Seismic Code response Spectrum so that the resulted ground motion is in the same phase with the ground motion simulated from the response spectrum predicted from PSHA. Figure 2-9 shows the matching of 1999 Chi-Chi earthquake to Indian code response spectrum at the soft soil site and the resulted ground motion time history for maximum considered earthquake. This ground motion is used together with the ground motion time histories predicted at generic soil sites in Thimphu for the nonlinear dynamic response analysis of three typical buildings in Thimphu in this study.

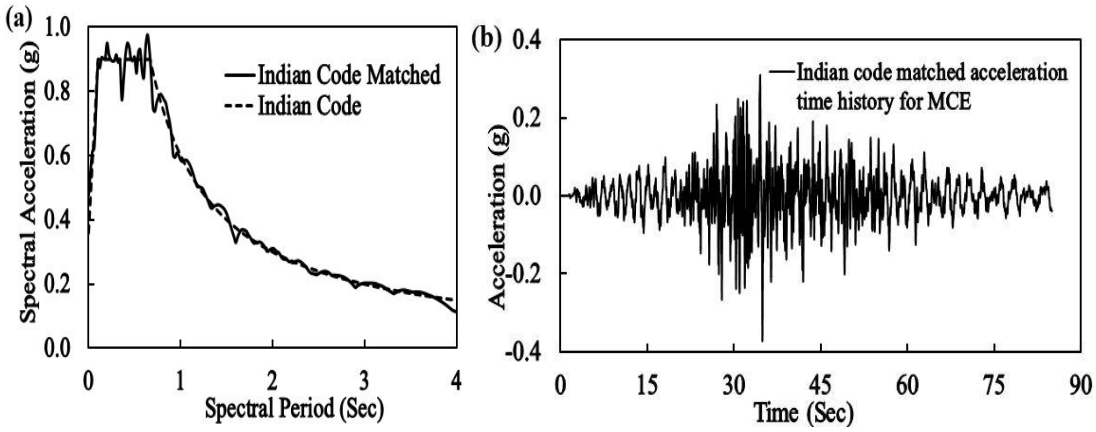

Figure 2-9 (a) Acceleration response spectrum matched to response spectrum of Indian Code at soft soil site for 5% damping and MCE and (b) horizontal ground motion time history derived from the matched spectrum.

2.5 Model Calibration

A four storey reinforced concrete frame building which was pseudo-dynamically tested at the European Laboratory for Structural Assessment (ELSA) is considered for model calibration. The test was conducted for both low level (0.12 g) and high level (0.45 g) ground motions which were generated from the real recorded 1976 Friuli earthquake signal shown in Figure 2-10. The plan and the section elevation of the experimental building are shown in Figure 2-11. The building and test details can be found in Negro et al. (1994), Negro et al. (1996) and Negro and Colombo (1997).

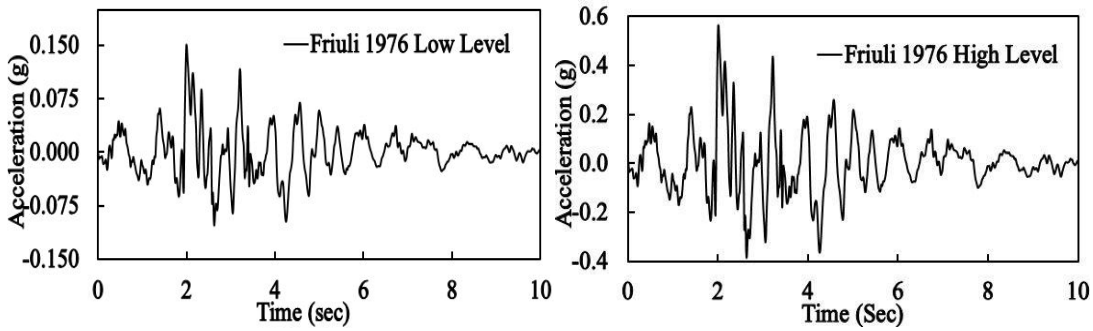

Figure 2-10 Accelerograms from 1976 Friuli Earthquake used in the tests.

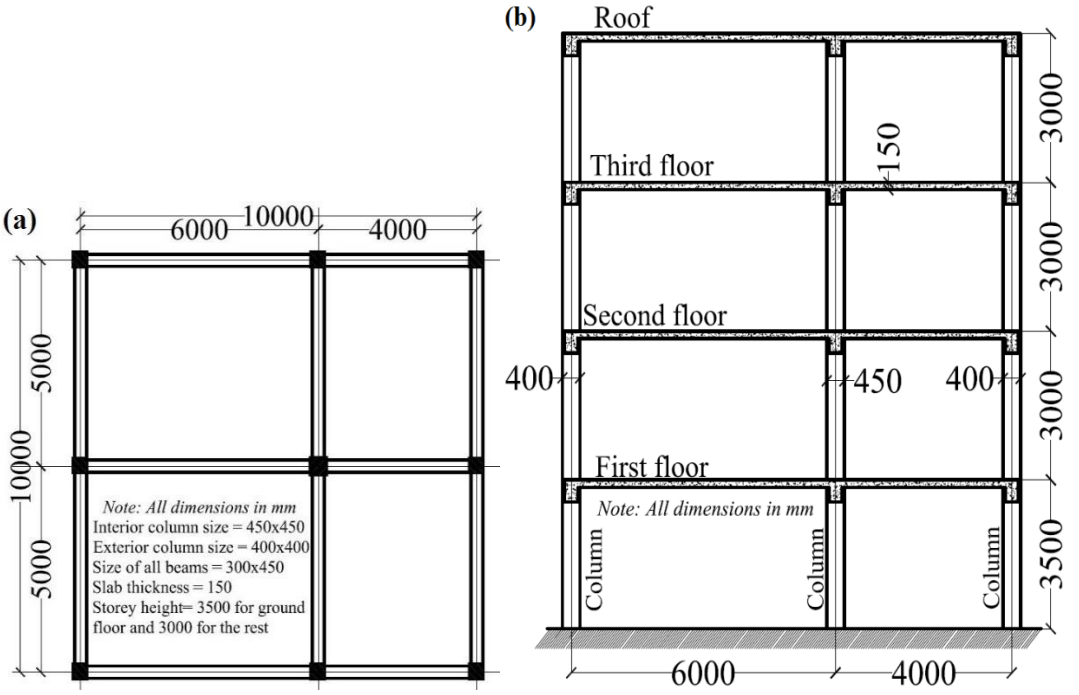

Figure 2-11 Experimental building, (a) beam column layout plan and (b) sectional elevation.

To calibrate the model, nonlinear analysis and performance assessment software, Perform 3D (CSI, 2006) is used for the analyses and simulation of the structural response of the experimental building. The structural response obtained from the numerical simulation is compared with the experimental results to check the accuracy of the calibrated model. Chord rotation model which is based on lumped plasticity model is used in this study since it is computationally inexpensive and is capable of capturing response at high deformation levels required in this study. FEMA 356 (2002) also provides some guidance on this model. Chord rotation model consists of stiff end zones at two ends and two FEMA beams/columns in between that make up the elastic segments.

The main crux of dynamic nonlinear analysis with the use of lumped plasticity model is the definition of Force-Deformation (F-D) relationship. The general F-D diagram of Perform 3D (CSI, 2006) is shown in Figure 2-12 (a). The main idea of Perform 3D F-D relationship is to capture main points designated by Y, U, L, and R and X which respectively represent yield strength, ultimate strength, ductile limit, residual strength and a point which is so large that there is no point in continuing the analysis. In this study, a tri linear F-D relationship defined in Perform 3D (CSI, 2006) and similar to the one defined in Ibarra et al. (2005) and PEER/ATC-72-1 (2010) is used. The F-D relationship is shown in Figure 2-12 (b). As shown in the figure, F-D relationship is defined by stiffness, strength and deformation parameters. Modelling of these parameters is described in the following sub sections.

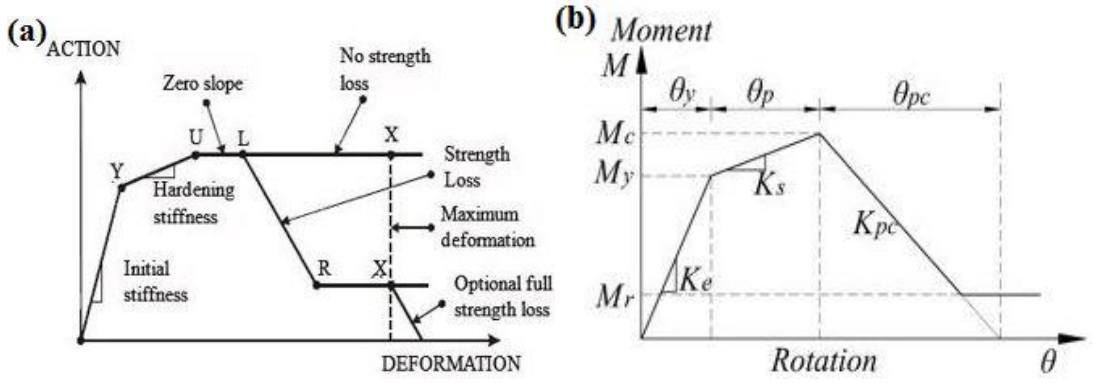

Figure 2-12 (a) General F-D relationship of Perform 3D (CSI, 2006) and (b) F-D relationship used in this study.

2.5.1 Modelling of stiffness parameters

The response of a structure subjected to ground motions is highly dependent on its stiffness parameter. Many researchers have expressed effective stiffness, K_e as the fraction of flexural stiffness of gross section. Based on the data from 255 column tests and considering flexure, shear and bond-slip deformations, Haselton et al. (2008) proposed effective stiffness in the

range of 0.2 EI_g to 0.6 EI_g for higher deformation and 0.35 EI_g to 0.80 EI_g for lower deformation depending on the axial load and aspect ratios, where EI_g is the flexural stiffness of the gross section. Elwood and Eberhard (2006) studied the same test data and proposed an effective stiffness in the range of 0.2 EI_g to 0.7 EI_g for various axial load ratios. Panagiotakos and Fardis (2001) conducted the test on 266 beams and 682 columns to evaluate stiffness, strength and deformation capacities of RC members. Based on the yield rotation estimated from the test data, they estimated the effective stiffness at the yield point of cracked RC members to be approximately 20% of uncracked gross section stiffness. FEMA 356 (2002) specifies the effective stiffness of RC beams to be 50% of the flexural stiffness of gross section while the effective stiffness specified for RC columns ranges from 50% to 70% of flexural stiffness of gross section depending on the axial load. ACI 318-14 (2014) recommends 35% and 70% of gross section stiffness for beams and columns respectively. The high stiffness value recommended by FEMA 356 is reported to be due to the ignorance of bond-slip effect. In this study, effective stiffness proposed by Elwood and Eberhard (2006) has been used. The strain hardening or post-yield stiffness, K_s is estimated from the ultimate moment, yield moment and pre-capping rotation which are defined later. It is found to be 2% to 10% of the effective stiffness to yield for different RC members. Similarly, the effective post capping stiffness, K_{pc} is estimated from the post-capping rotation and the ultimate or capping moment.

It is to be noted that the contribution of the slab to the stiffness of the structure is considered in the numerical calculation as per ACI 318-14 (2014) where monolithic beam and slab is approximated as T-beam and L-beam for interior and exterior beams respectively. Based on the span of beam and depth of slab, the effective width of the beams is either calculated as a quarter of the beam span or as 8 times the depth of slab on either side of the web.

2.5.2 Modelling of strength parameters

Yield moment, M_y of RC members is estimated from the expression provided by Panagiotakos and Fardis (2001). The expression which was based on the number of tests on beams and columns was also validated by Haselton and Deierlein (2007) and found to agree well with the test data. The equation is also found to be in good agreement with the calculation made from basic reinforced concrete theory. From the regression analysis done by Haselton et al. (2008) on a large number of test data, the capping moment, M_c was found to be 1.13 times the yield moment and same has been used in this study. The residual moment, M_r is basically taken as a very small percentage of the capping moment. Perform 3D (CSI, 2006) user guide recommends residual moment as 0.001 times the capping moment and suggests a progressive strength loss instead of sudden loss of strength from U to R point. PEER/ATC 72-1 (2010) also recommends a negligible residual moment or residual strength to be neglected altogether.

FEMA 356 recommends a residual moment as 20% of the capping moment. In this study, a recommendation made by Perform 3D (CSI, 2006) user guide is adopted.

2.5.3 Modelling of deformation parameters

Panagiotakos and Fardis (2001) formulated an empirical equation to calculate yield rotation, θ_y from a large number of test data taking into account flexure, shear and bond slip deformations. The same expression is used for calculating yield rotation in this study. Moreover, the definition of effective stiffness at yield point and yield moment implicitly defines the yield rotation and vice versa. Pre-capping rotation, θ_p which is also called as the plastic rotation is estimated from the expression provided in PEER-ATC-72-1 (2010). Biskinis and Fardis (2010) have also provided an empirical equation for plastic rotation. However, plastic rotation given by Haselton et al. (2008) was found to be more accurate and hence used in this study. There is a limited research on the estimation of post capping rotation, θ_{pc} although it is an important parameter for collapse analysis. The expression proposed by Haselton et al. (2008) for post capping rotation is used in this study.

2.5.4 Modelling of viscous damping

Apart from defining the hysteretic parameters in developing the F-D relationship, it is also important to model non-hysteretic type of damping, i.e., viscous damping. Hysteretic damping is modelled implicitly in the form of cyclic deterioration while viscous damping is usually modelled as a percentage of critical damping in one or more vibration modes. Although distinct vibration modes and periods do not exist in nonlinear response, yet many studies have recommended the use of viscous damping as a percentage of critical damping to be used in the nonlinear analysis. From the study conducted on 85 buildings that were subjected to 8 earthquakes in California, Geol and Chopra (1997) reported 2% to 12% of critical damping for buildings below 35 stories. Satake et al. (2003) conducted vibration test on buildings in Japan and estimated damping in the range of 2-8% for the building height of 10-50m. PEER/ATC 72-1 (2010) recommended 2-4% of the equivalent viscous damping for typical RC building below 30 storeys. Perform 3D (CSI, 2006) recommended 5% modal damping along with a small amount of stiffness proportional Rayleigh damping to damp higher mode displacements. In this study, a combination of 5% modal damping and 0.1% of stiffness proportional Rayleigh damping are used and is found to provide a reliable response predictions.

2.5.5 Shear strength of RC members

In addition to the above parameters, the shear strength of the members is also required to be specified in the program. Among various shear strength models such as those given in Biskinis et al. (2004), Priestley et al. (2009) and Kowalsky and Priestley (2000), revised UCSD model proposed by Kowalsky and Priestly (2000) is found to provide more reliable predictions of the experimental test results. It is hence used in this study to estimate the shear strength of the RC members.

After modelling various parameters and defining the F-D relationship for each RC member, a nonlinear dynamic analysis is carried out for the four storey experimental building for both high-level and low-level input motions. Figures 2-13 and 2-14 show the comparison of the displacement time histories predicted from the numerical analyses and that obtained from the low-level and high-level tests respectively. As shown, a very good agreement has been obtained, indicating the accuracy of the numerical model. It should be noted that a little bit of mismatch is observed in the initial part of the simulation. This is expected because of the use of lumped plasticity model which does not capture initial response well. The same was also observed by other researchers (Haselton et al., 2008; Haselton and Deierlein, 2007). The verified numerical model is used to predict the dynamic responses of RC frame buildings in Thimphu.

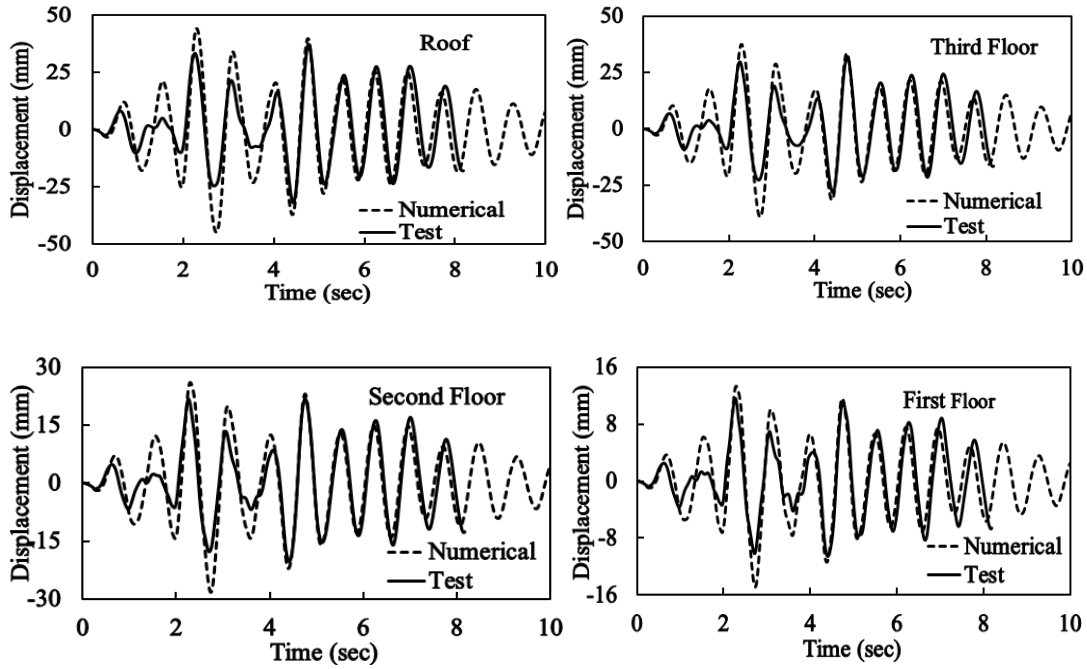

Figure 2-13 Comparison of storey displacements obtained from numerical analyses and test results for low-level test.

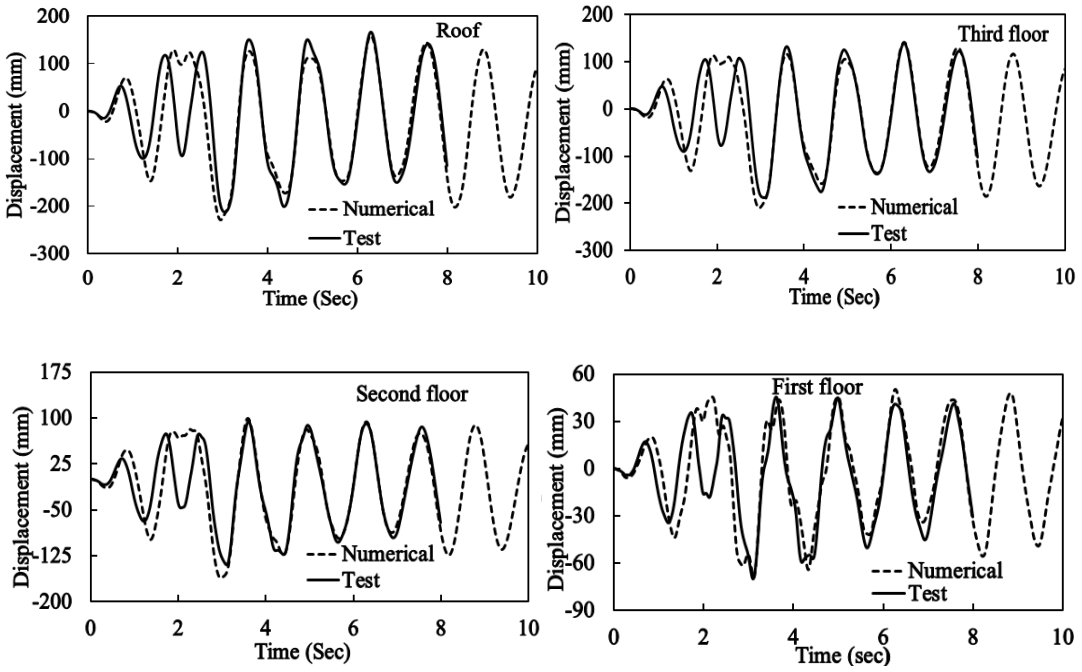

Figure 2-14 Comparison of storey displacements obtained from numerical analysis and test results for high-level test.

2.6 Typical Buildings in Thimphu

The construction of RC buildings had begun in the1970s in Bhutan. Today, RC structures have replaced most of the traditional structures such as adobe and stone masonry buildings in the urban areas. Almost all RC buildings in Thimphu are three to six storeys tall and are mostly rectangular in plan. The ground floor is mainly used for commercial purposes while top floors are used as residential units.

In this study, three typical residential RC buildings are considered. They are selected because they represent the most common RC buildings in Thimphu. They are designated as '6 storey', '3 storey new' and '3 storey old'. '6 storey' is a typical six storey RC building which was designed and built after the adoption of Indian Seismic Code in 1997. Six storey RC buildings are very common in the core area of Thimphu where the population of the city is concentrated. '3 storey new' is a three storey RC building designed and built after the adoption of Indian Seismic Code. '3 storey old' is a three storey RC building built prior to 1997 when no seismic provisions were in place. Both '3 storey old' and '3 storey new' are also common in the core area as well as in the other parts of Thimphu.

It is to be noted that both '6 storey' and '3 storey new' buildings were designed according to the Indian Seismic Code. The details of these buildings such as structural and architectural drawings are obtained from the City Corporation, Thimphu. Since RC buildings built before

1997 were mostly built by local technicians and owners without proper design and drawings, structural details were not documented for these buildings. However, from the non-destructive test conducted by the consultant from Nepal for 15 RC buildings in Thimphu under the Thimphu Valley Earthquake Risk Management Project in 2005, it was found that concrete strength and yield strength of the steel used for these buildings are respectively 15 MPa and 415 MPa. Sizes of RC beams range from 200mmx250mm to 250mmx500mm depending on the span of the beam while column sizes range from 200mmx200mm to 350mmx350mm. The reinforcement ratio of beams ranges from 0.7% to 1.0% while it ranges from 0.8% to 1.5% for columns. This information is used to obtain the structural details of '3 storey old' building. For the purpose of comparison, identical building plan with the same number of beams and columns are considered for '3 storey old' building as that of '3 storey new' building. It is to be noted that only the weight of the infill brick masonry wall is considered and their contribution to stiffness and strength are neglected in the analyses. The details of these buildings are shown in Figures 2-15 and 2-16 and Tables 2-2 to 2-4.

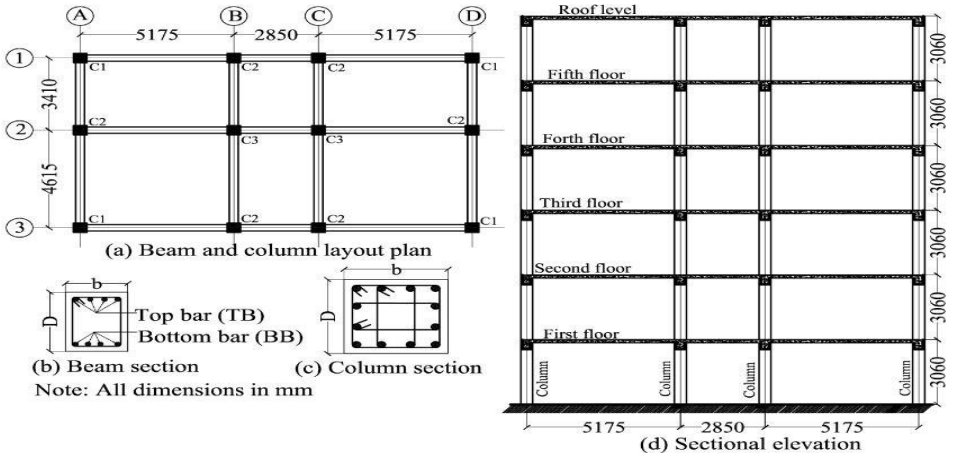

Figure 2-15 Structural details of 6 storey building.

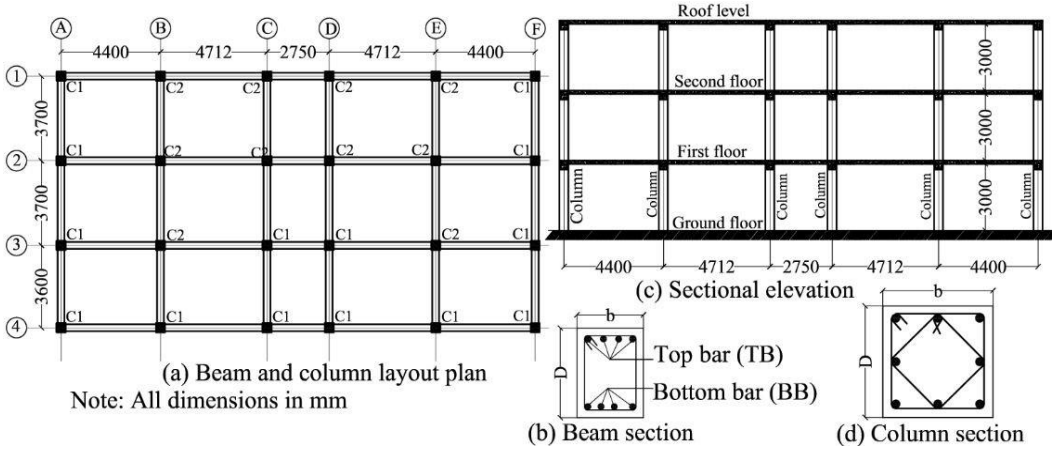

Figure 2-16 Structural details of 3 storey buildings.

Table 2-2 Loading details of typical buildings

Parameters	6 storey	3 storey new	3 storey old
Yield strength of rebars, f_y N/mm^2	415	415	415
Compressive strength of concrete,f_c' N/mm^2	25 for columns, 20 for beams	20	15
Unit weight of reinforced concrete, kN/m^3	25	25	25
Unit weight of bricks, kN/m^3	19.60	19.60	19.60
Superimposed dead load on floors, kN/m^2	1.00	1.00	1.00
Live load on floors, kN/m^2	2.00	2.00	2.00
Lived load on roof, kN/m^2	0.75	0.75	0.75

Table 2-3 Reinforcement details of 6 storey building

RC Members	Dimension (bxD),mm	Reinforcement (Bar dia. in mm)
(a) Floor beams (FB) and Roof beams(RB)		
FB along grid 2& 3	300x450	TB=4-20, BB=2-20+2-16
FB along grid 1	300x450	TB=2-20+2-16, BB=4-16
FB along grid A& D	300x400	TB=2-20+2-16, BB=4-16
FB along grid B& C	300x400	TB=4-20, BB=2-20+2-16
RB along grid 1& 3	300x450	TB=4-16, BB=3-16+1-12
RB along grid 2	300x450	TB=2-20+2-16, BB=4-16
RB along grid A& D	300x400	TB=4-16, BB=3-16+1-12
RB along grid B& C	300x400	TB=4-20, BB=3-20+1-16
Beam stirrups	8@100mmC/C till 2D from either side of column face and 8@150C/C at the center	
(b) Column		
Column C1	450x450	8-20 + 4-16
Column C2	450x450	12-20
Column C3	500x500	4-25+8-20
Column ties	9@90mmC/C throughout	

Table 2-4 Reinforcement details of '3 storey new' and '3 storey old' buildings

RC Members	3 storey new		3 storey old	
	Dimension (bxD),mm	Bar dia. in mm	Dimension (bxD),mm	Bar dia. in mm
(a) Floor beams (FB) and Roof beams(RB)				
FB along grid A,B& C	300x400	TB=4-20, BB=2-20+2-16	250x350	TB=4-12, BB=2-12+2-10
FBs along grid D	300x400	TB=2-20+2-16, BB=4-16	250x350	TB=3-12, BB=3-10
FB along grid 1,3,6&4	300x400	TB=4-20, BB=4-16	250x300	TB=2-12+2-10, BB=3-12
FB along grid 2&5	300x400	TB=4-20, BB=2-20+2-16	250x300	TB=4-12, BB=2-12+2-10
RB along grid A& D	300x400	TB=4-16, BB=2-16+2-12	225x300	TB=3-12, BB=3-10
RB along grid B& C	300x400	TB=2-20+2-16, BB=4-16	225x300	TB=2-12+2-10, BB=3-12
RB along grid 1,3,4&6	300x400	TB=4-16, BB=2-16+2-12	225x300	TB=2-12+1-10, BB=3-10
RB along grid 2&5	300x400	TB=2-20+2-16, BB=4-16	225x300	TB=3-12, BB=3-10
Beam stirrups	8@100mmC/C till 2D from either side of column face and 8@150C/C at the centre		6@150mmC/C throughout	
(b) Column				
Column C1	400x400	8 Nos. 20mm dia.	250x250	4 Nos. 16mm dia.
Column C2	400x400	4-25+4-20	250x250	8 Nos. 12mm dia.
Column ties	8@100mmC/C throughout		6@150mmC/Cthroughout	

2.7 Structural Response of Typical Buildings

Nonlinear response analyses of the three typical buildings in Thimphu are conducted using the ground motions obtained from PSHA at generic soil sites in Thimphu for the 475 and 2475 year return period ground motions. Modelling parameters such as stiffness, strength and deformation capacity of RC members are calculated as described above for model calibration in section 4.

Soil-structure interaction (SSI) has been incorporated for shallow stiff soil, soft rock and soft soil sites to study the effects of SSI in structural response. Columns of typical buildings have rectangular strip footings and founded at 1-2.5 m below the ground level. As such, uncoupled spring model recommended in ASCE/SEI 41-13 for rigid shallow footing is used in this study. The stiffness of embedded footing is calculated as a product of stiffness of footing at the surface and the embedment correction factor given in ASCE/SEI 41-13. The details of modelling SSI for numerical analysis can be found in Thinley and Hao (2016) in chapter 4.

The response of typical buildings is quantified in terms of the period, interstorey drift and displacement. Table 2-5 shows the periods of the typical buildings obtained for different site classes using scant stiffness to yield and uncracked concrete stiffness. Period of the structure is important especially in understanding the response of other quantities such as drift and

displacement. It is to be noted that typical buildings are analysed only for secant stiffness to yield or cracked stiffness in line with the model calibration in section 4. The period of uncracked concrete is calculated solely for the purpose of comparison with the period obtained from the cracked concrete stiffness. As expected, the periods obtained from cracked stiffness are longer than those obtained from uncracked stiffness. However, for the case of uncracked concrete stiffness, the period of '3-storey old' building is longer than that of '6 storey' building. This is due to the use of lower concrete strength and smaller member dimensions in '3 storey old' building, which made the building more flexible than the '6-storey' building. As shown in the table, the period increases as the foundation medium become softer from rock to soft soil. This is due to the reduction of soil stiffness from soft rock to soft soil making the foundation more flexible. The periods of typical buildings obtained in this study are comparable to the period obtained for a four storey RC building in Haselton et al. (2008).

The displacement profiles of the typical buildings estimated at the generic soil sites under 475 and 2475 year return period ground motions are respectively given in Figures 2-17 and 2-18. As shown in the figures, roof displacement is the largest for the 6 storey building which is expected. With exception to the displacement at soft rock site in Figure 2-18 (c) which is due to resonance condition, the roof displacement of '3 storey old' building is more than that of '3 storey new' building at all other soil sites. This is also expected since '3 storey old' building was not designed to any code and used inferior concrete and smaller member dimensions. As shown by the dotted lines, SSI is insignificant under 475 return period but detrimental at soft soil site under 2475 return period ground motions. The interstorey drifts of typical buildings are presented in Figures 2-19 and 2-20 and are described in the next section while assessing the performance of the typical buildings.

Table 2-5 Fundamental periods of typical buildings in seconds for different site classes for the 475 and 2475 year return period (RP)

	Fundamental period using scant stiffness to yield, K_e			Fundamental period with uncracked concrete		
Site class	6 storey	3 storey new	3 storey old	6 storey	3 storey new	3 storey old
Fixed support/Rock	2.126	1.075	1.324	0.867	0.447	0.976
Soft rock 475 RP	2.129	1.076	1.327	0.875	0.450	0.979
Soft rock 2475 RP	2.131	1.077	1.329	0.879	0.452	0.981
Shallow stiff soil 475 RP	2.137	1.080	1.336	0.891	0.457	0.986
Shallow stiff soil 2475 RP	2.146	1.084	1.345	0.907	0.465	0.993
Very soft soil 475 RP	2.222	1.121	1.433	1.030	0.530	1.060
Very soft soil 2475 RP	2.679	1.364	1.870	1.756	0.838	1.429
Indian code soft soil	2.290	1.157	1.514	1.141	0.585	1.122

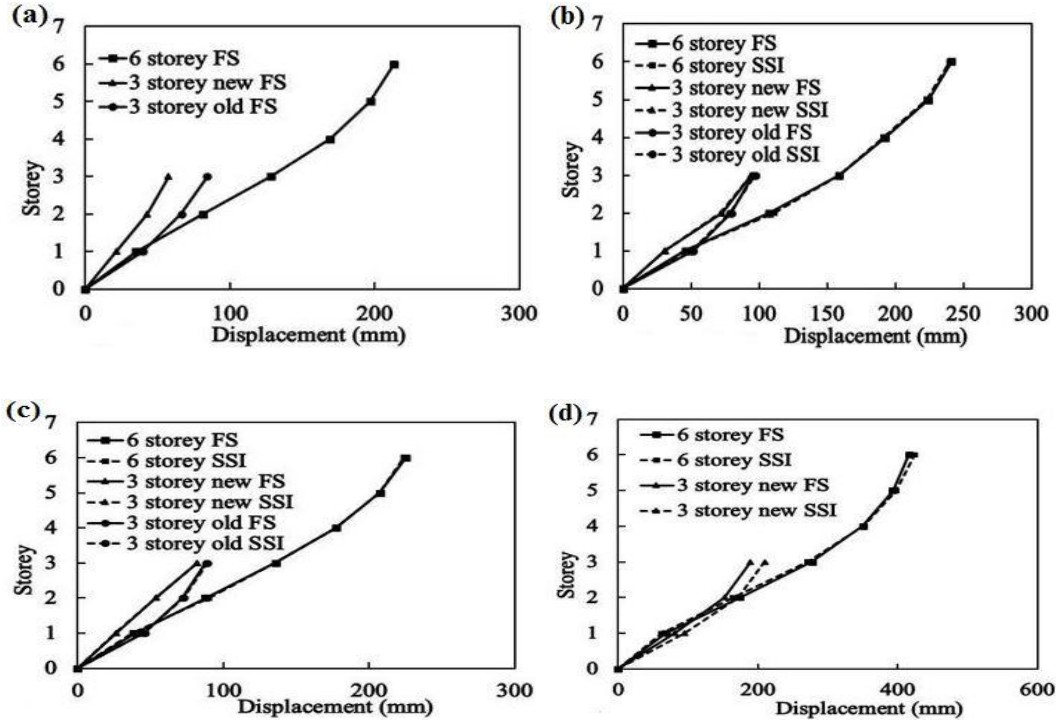

Figure 2-17 Displacement profiles of typical buildings under 475 year return period ground motion, (a) rock; (b) shallow stiff soil; (c) soft rock and (d) soft soil sites.

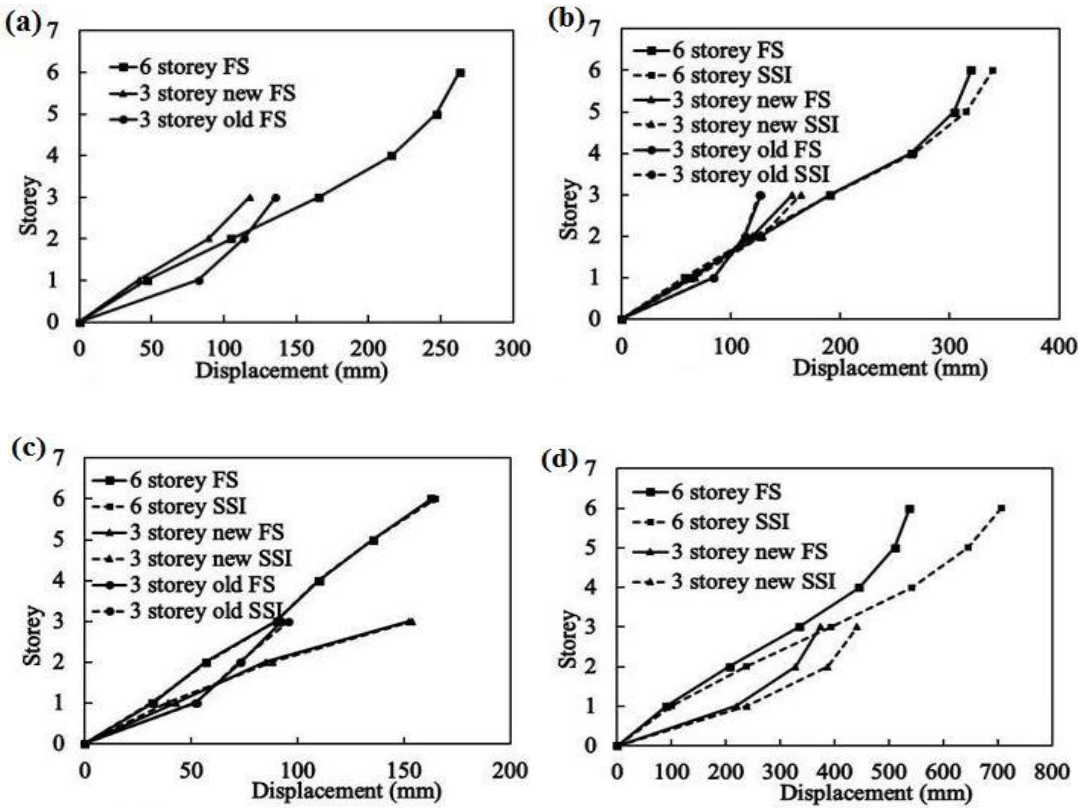

Figure 2-18 Displacement profiles of typical buildings under the 2475 year return period ground motion, (a) rock; (b) shallow stiff soil; (c) soft rock and (d) soft soil sites.

2.8 Performance Evaluation of Typical Buildings and Discussion

The performance of buildings is mostly evaluated based on the inter-storey drift demand. There are many guidelines such as ASCE 41-13 (2014), Vision 2000 (1995) and ATC-40 (1996) that provide correlation between interstorey drift values and the respective performance levels of buildings. Since performances of buildings described by these guidelines are similar in concept, only Vision 2000 is used for the performance evaluation of typical buildings in this study. It is assumed to be applicable for buildings in Thimphu which have been built after the adoption of Indian Seismic Code and Indian ductile detailing code IS 13920 (1993). For the '3 storey old' building which was built prior to 1997 based on some thumb rules with limited or no proper design, application of Vison 2000 for the performance evaluation is a bit tricky since those buildings are not necessarily ductile. Unfortunately, due to the absence of other guidelines to assess such buildings, Vision 2000 is adopted in this study. Table 2-6 shows the performance levels and the corresponding inter-storey drift limits which are also reflected in Figures 2-19 to 2-21 by the vertical lines.

Table 2-6 Performance levels, damage states and interstorey drift limits from Vision 2000

Performance level	Damage state	Interstorey drift (%)
Fully operational	Negligible (No Damage)	<0.20
Operational	Light (Repairable Damage)	<0.50
Life safe	Moderate (Irreparable)	<1.50
Near collapse	Severe	<2.50
Collapse	Complete	>2.50

From Figure 2-19, it is evident that '6 storey' building, although designed according to Indian Seismic Code, is more vulnerable to earthquakes than that of three storey buildings at all soil sites for the return period of 475 years. Even at the rock site, the drift demand exceeds the life safety limit; and at the soft soil site, the drift demand exceeds near collapse limit indicating a total collapse. This could be due to the fact that either the building was not properly designed for lateral load or that the Indian Seismic Code is not adequate enough to be used in Bhutan for the design of medium rise buildings.

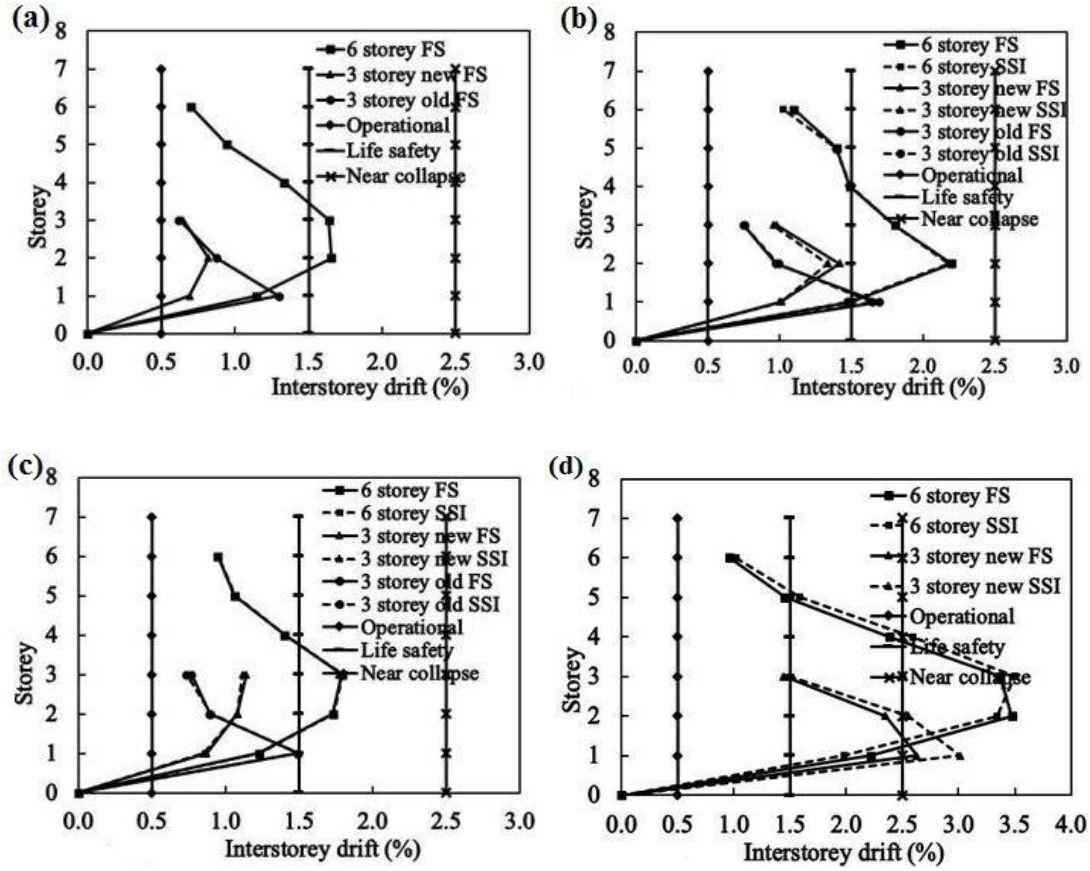

Figure 2-19 Inerstorey drift profiles and performance levels of typical buildings under the 475 return period ground motion, (a) rock; (b) shallow stiff soil; (c) soft rock and (d) soft soil sites.

The inter-storey drift and displacement of '3 storey old' building at soft soil site are not shown in the figures since analysis failed to complete after the initial run and before reaching the peak acceleration of the ground motion owing to the large excessive responses. Looking at the fundamental period of '3 storey old' building in Table 2-5 and the response spectra of soft soil site in Figure 2-5, it can be inferred that the structure could have undergone a resonance condition resulting in a much higher response. This indicates that '3 storey old' building is unstable and more vulnerable than '3 storey new' and '6 storey' buildings at the soft soil site, indicating the improvement of structural safety after performing earthquake-resistant designs.

As expected, '3 storey new' building performs better than '3 storey old' building whose drift demand is lower than the life safety limit at the rock, shallow stiff soil and soft rock sites under the 475 year return period ground motion. However, drift demand crosses near collapse limit at the soft soil site for the same ground motion. On the other hand, the performance of '3 storey old' building is also commendable in spite of being built without proper design and supervision and with the use of lower concrete strength. Its drift demand is within the life safety limit for rock and soft rock sites and between life safety and near collapse limits at

shallow stiff soil site when subjected to the 475 year return period ground motion. This could be partly due to its regular plan configuration and partly to its higher fundamental period which led to lower responses.

Under the 2475 year return period ground motions, drift demand of all three buildings exceeds life safety limit at all sites. '3 storey old' building is more vulnerable than '3 storey new' and '6 storey' building at rock and shallow stiff soil sites with drift demand exceeding well over near collapse limit. At soft rock and soft soil sites, '3 storey new' building is more vulnerable than '6 storey' building. Comparing the fundamental period of '3 storey new' building with that of soft rock and soft soil response spectra in Figure 2-5, it is evident that the building is subjected to higher response acceleration. In fact, the highest drift demand predicted at soft soil site for '3 storey new' building is due to the soil resonance wherein its fundamental period coincides with the site natural period. As shown in Figures 2-19 (c) and 2-20 (c), it is interesting to note that the performance of '6 storey' building at soft rock site under the 2475 year return period ground motion performs better than that when subjected to the 475 year return period ground motion. This can also be referred to the response spectra in Figure 2-5 wherein the 2475 year return period ground motion has lower response acceleration than that of the 475 year return period at the fundamental period of '6 storey' building.

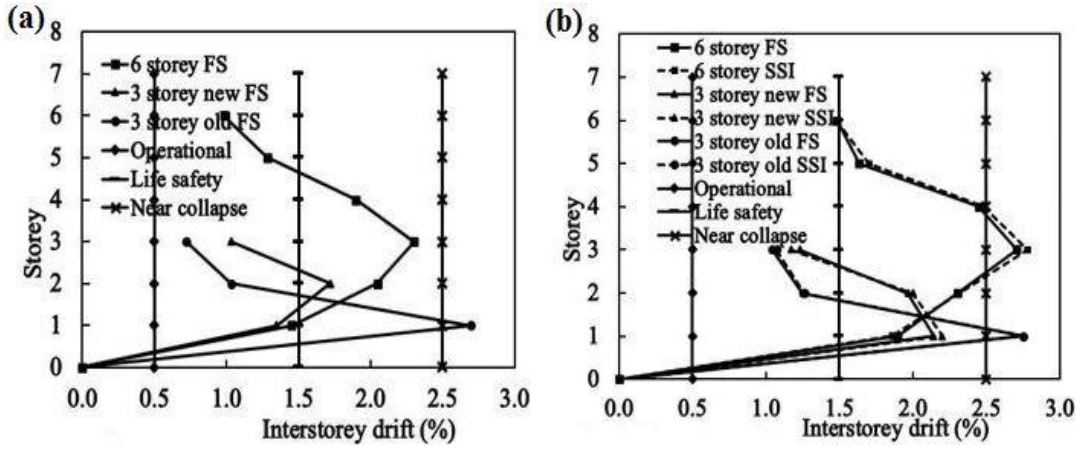

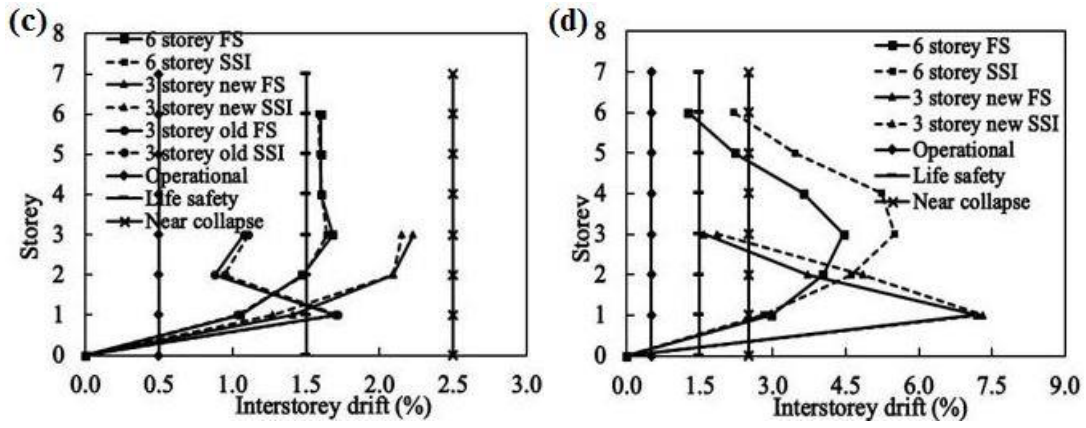

Figure 2-20 Interstorey drift profiles and performance levels of typical buildings under the 2475 return period ground motion, (a) rock; (b) shallow stiff soil; (c) soft rock and (d) soft soil sites.

As shown by dotted lines in the Figures 2-19 and 2-20, SSI has a limited effect at the shallow stiff soil and soft rock sites but has pronounced effect at the soft soil sites especially under the 2475 year return period ground motion. Under the 475 year return period ground motion and at the soft soil site, SSI is found to be slightly detrimental to '6 storey' building whereas it is highly detrimental when subjected to the 2475 year return period ground motion. On the other hand, SSI is beneficial to the '3 storey new' building at the soft soil site under the 475 year return period ground motion and has limited effect under the 2475 year return period ground motion. The effect of SSI on the response of building is in fact found to be dependent on the period of building and the site natural period and stiffness of the soil.

Based on the predicted interstorey drift demand, it can be inferred that typical buildings in Thimphu are generally vulnerable to earthquakes. This could be due to the use of lower concrete strength. Currently, the concrete strength of 20 MPa is being used for buildings in Bhutan whereas, in many parts of the world, concrete with much higher strength is used. The use of lower concrete strength decreases the stiffness and strength and in turn, increases the plastic deformation of the buildings leading to higher drift demand. Moreover, the higher drift demand could also be due to the exclusion of ductile detailing in the model in the case of buildings designed and built after the adoption of Indian Seismic Code in Bhutan. Ductile detailing consists of providing extra reinforcement in the form of development and anchorage lengths especially at the beam-column junctions and at the lapping points of the reinforcements. Although these extra reinforcements are normally included during the construction, yet it is not possible to include these extra bits and pieces of reinforcements in the numerical model. Neglecting the ductile detailing in the model could have resulted in the higher drift demand.

It should be noted that the above observations are obtained from analysis of bare frame structures. In reality, the frame structures have infill masonry wall. The infill masonry walls contribute to stiffness and strength of the concrete frames. These contributions are not considered in the present study. Further study that takes into consideration the masonry walls is needed in the future in assessing the seismic performance of building structures in Bhutan.

2.9 Adequacy of using Indian Seismic Code

The adequacy of using Indian Seismic Code in Bhutan is studied by analysing the typical buildings in Thimphu using the Indian Seismic Code response spectrum matched ground motion at the soft soil site. Since Indian Seismic Code is based on the Maximum Considered Earthquake (MCE), the structural responses obtained from it are compared with that obtained from PSHA at the soft soil site under the 2475 year return period. Although Indian Seismic Code is not based on any return periods, yet many seismic codes such as International Building Code (2006) define MCE as an earthquake having 2% probability of exceedance in 50 years, which is 2475 year return period. Hence, comparison of structural responses from the two is reasonable and logical. Only structural responses of '6 storey' and '3 storey new' buildings are compared since '3 storey old' building was not designed according to the Indian Seismic Code.

Figure 2-21 shows the comparison of interstorey drift estimated at the soft soil site from the Indian Seismic Code matched ground motion and PSHA ground motion under the 2475 year return period. From the figure, it can be seen that interstorey drift and displacement of both the buildings predicted from PSHA in this study are much higher than those predicted from the Indian Seismic Code for both fixed and flexible supports. In the case of fixed support, the maximum interstorey drift predicted from Indian code for '6 storey' building is 2.82% while the corresponding drift obtained from PSHA in this study is 4.45% which is way beyond the near collapse limit of 2.5%. Similarly, the maximum interstorey drifts for '3 storey new' building are 2.72% and 7.18% predicted from ground motions based on Indian code and PSHA respectively for fixed support. A much higher drift demand predicted for '3 storey new' building from PSHA in this study is due to the soil resonance where building period coincides with the site natural period of the soil as shown in Figure 2-22 (a).

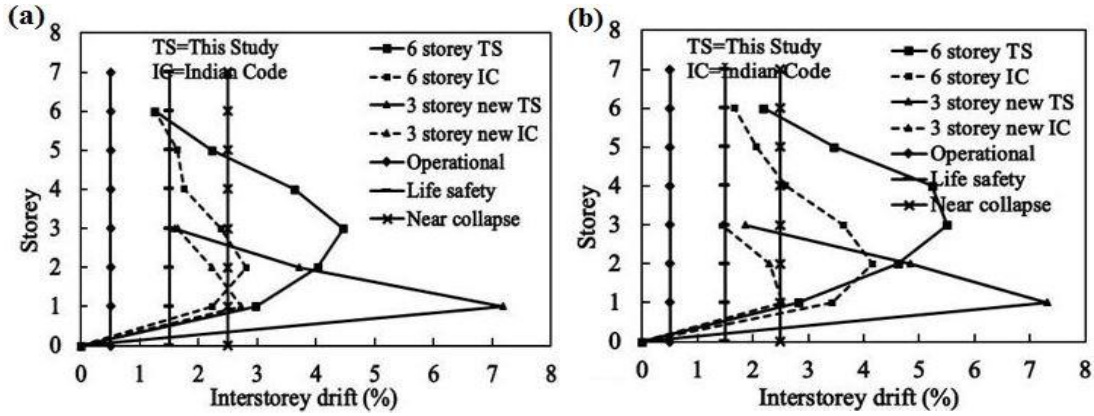

Figure 2-21 Comparison of interstorey drift at the soft soil site estimated from PSHA and Indian Code response spectrum matched ground motion, (a) with fixed support and (b) with SSI.

The main point that can be observed from the comparison is that Indian code underestimates the responses of the buildings. This could be largely due to the shape of response spectra as shown in Figure 2-22 (a) wherein buildings are subjected to higher response spectral acceleration compared to the Indian Code. Although the spectral acceleration at the fundamental vibration period of the '6 storey' building from PSHA does not differ significantly from that defined in Indian Code, a much higher difference in the response is observed. This could be attributed to the fact that ground motion obtained from PSHA has higher Peak Ground Velocity (PGV) as shown in Figure 2-22 (b). The PGV values are respectively 91.61 cm/sec and 47.45cm/sec for the ground motions obtained from PSHA and Indian code at the soft soil site, which also affects the structural responses. In fact, many researchers are in favour of correlating damage to the PGV than PGA. Boatwright et al. (2001) studied correlation among PGA, PGV and intensity of 1994 Northridge earthquake and found that PGV is correlated to intensity much better than PGA. Kaka and Atkinson (2004) also found better correlation between PGV and intensity from the studies made on earthquakes in eastern North America. For the buildings with medium periods, Fajfar et al. (1990) also found PGV the better indicator of damage than PGA.

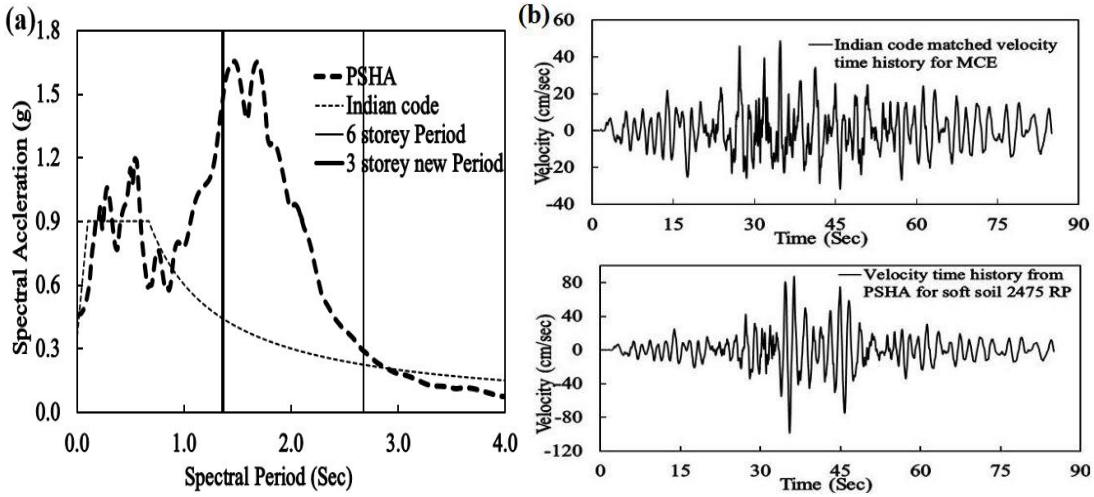

Figure 2-22 (a) The plot of Indian Seismic Code and PSHA response spectra at the soft soil site with 5% damping and (b) comparison of velocity time histories.

The above comparisons show that Indian Seismic Code underestimates the structural response of the typical buildings in Bhutan and its use in Bhutan is questionable. Although only limited structural models are considered in the study, comparing the response spectra obtained from PSHA in Thimphu at generic soil sites and that of the normalised response spectra of Indian Seismic Code in Figures 2-5 and 2-6, it is highly possible that Indian Code could predict different structural responses. Hence, further studies are deemed necessary to better understand the implications of using Indian Code in seismic resistance designs in Bhutan.

2.10 Conclusions

Bhutan locates in one of the most active seismic zones in the world. A lot of significant earthquakes have occurred in the past and inflicted heavy casualties and loss of properties. While the seismic risk is certain, Bhutan is least prepared for it and no comprehensive study of seismic risks of building structures in Bhutan has yet been reported. Bhutan has no seismic design code of its own yet. Prior to 1997, all buildings were either built by technicians based on some thumb rules or designed only for gravity load. Post 1997, Indian Seismic Code has been followed although its applicability to the site conditions in Bhutan is still in question.

The following outcomes are achieved in the study:

1) Design ground motions at the generic soil sites in Thimphu for the return periods of 475 and 2475 years are predicted by carrying out the probabilistic seismic hazard analysis.
2) Typical RC buildings that represent the general building stocks in Bhutan are assessed based on the predicted ground motions by carrying out the nonlinear

dynamic analyses. It was observed that the RC buildings, in general, could suffer moderate to severe damages under the 475 year return period and could even collapse under the 2475 year return period ground motions. In particular, the '6 storey' building could suffer severe damages under the 475 year return period and might collapse under the 2475 year return period ground motions. Except at the soft soil site, three storey building designed according to Indian Seismic Code could remain life safe with moderate damages under the 475 year return period, but could suffer severe damages under the 2475 year return period ground motions. On the other hand, '3 storey old' buildings could suffer moderate to severe damages under the 475 return period and could collapse under the 2475 year return period ground motions.

3) Soil structure interaction is found to have a limited effect at the shallow stiff soil and soft rock sites, while the larger effect is predicted at the soft soil site. SSI is found to be detrimental to '6 storey' building and beneficial to the '3 storey new' building at the soft soil site. The effect of SSI is found to be highly influenced by the period of the building, site natural period of the soil and the stiffness of the soil.
4) Indian Seismic Code underestimates the structural responses of the building structures in Bhutan. Direct application of Indian Seismic Code for the design of buildings in Bhutan needs to be further revisited.

It is to be noted that the PSHA was carried out in 2010 using the Next Generation Attenuation (NGA) models of 2008 available at the time. These NGA models were updated using a more extensive database in 2014. In order to ascertain the implication of the updated NGA models on the structural response of the buildings, the NGA models of 2008 and 2014 are studied and compared in detail. From the comparison, no major discrepancies are observed between the original and the updated NGA models, i.e., a discrepancy of less than 20% is observed for the moment magnitudes greater than or equal to 5.5 and a bit higher discrepancy for the moment magnitudes less than 5.5. Since a large number of sources are used for the PSHA in this study, the contribution of a few earthquake sources with magnitudes less than 5.5 in the generation of the total hazard curve is believed to be insignificant owing to the high seismicity of the region. Hence, the ground motions predicted using the original NGA models would not vary significantly from the ones that can be predicted from the updated NGA models. However, to be on the conservative side, the results of the structural responses and the performance assessment of the typical buildings could at the most vary by a maximum of 20% if the updated NGA models are used for the PSHA.

2.11 References

ACI 318-14 (2014). *Building code requirements for Structural Concrete and Commentary*, American Concrete Institute, Farmington Hills, MI.

Ambraseys, N., & Jackson, D. (2003). A note on early earthquakes in northern India and southern Tibet. *Current Science, 84***,** 570-582.

ASCE/SEI 41-13 (2014). *Seismic Rehabilitation of Existing Buildings*, American Society of Civil Engineers, Reston, Virginia, USA.

ATC-40 (1996). *Seismic Evaluation and Retrofit of concrete Buildings volume 1*. Applied Technology Council, Redwood City, California.

Banerjee, P., & Burgmann, R. (2002). Convergence across the northwest Himalaya from GPS measurements. *Geophysical Research Letters, 29*, 30-1-30-4.

Bilham, R. (2004). Earthquakes in India and the Himalaya: tectonics, geodesy and history. *Annals of Geophysics, 47*, 839-858.

Bilham, R., Gaur, V. K., & Molnar, P. (2001). Himalayan seismic hazard. *Science (Washington), 293***,** 1442-1444.

Bilham, R., Larson, K., Freymueller, J., Jouanne, F., Lefort, P., Leturmy, P., Mugnier, J., Gamond, J., Glot, J., & Martinod, J. (1997). GPS measurements of present-day convergence across the Nepal Himalaya. *Nature, 386*, 61-64.

Biskinis, D. E., Roupakias, G. K., & Fardis, M. N. (2004). Degradation of shear strength of reinforced concrete members with inelastic cyclic displacements. *ACI Structural Journal, 101*(6), 773-783.

Biskinis, D. N., & Fardis, M. N. (2010). Deformations at flexural yielding of members with continuous or lap-spliced bars. *Structural concrete*, 11, 127-138.

Boore, D. M., & and Atkinson, G. M. (2008). Ground motion prediction for the average horizontal component of PGA, PGV and 5% damped PSHA at spectral periods between 0.01s and 10.0s. *Earthquake Spectra, 24***,** 99-138.

Campbell, K., & Bozorgnia, Y. (2006). Next Generation Attenuation (NGA) Empirical Ground Motion Models: Can they be used in Europe? In: *Proceedings of the 1st European Conference on Earthquake Engineering and Seismology*, Geneva, Switzerland, 3-8 September.

Chang, S. W., Bray, J. D., & Seed, R. B. (1996). Engineering implications of ground motions from the Northridge earthquake. *Bulletin of Seismological Society of America, 86***,** 270-288.

Chiou, B. J., & Youngs, R. R. (2008). An NGA model for the average horizontal component of peak ground motion and response spectra. *Earthquake Spectra, 24***,** 173-215.

CSI (2006). *Nonlinear Analysis and Performance Assessment for 3-D Structures.* Computers and Structures, Inc., Berkeley.

Dorji, J. (2009). *Seismic performance of brick infilled RC frame structures in low and medium rise buildings in Bhutan*. Master degree thesis, Centre for Built Environment and Engineering Research, Queensland University of Technology, Brisbane, Australia.

Elwood, K. J., & Eberhard, M. O. (2006*). Effective stiffness of reinforced concrete columns. PEER Research Digest No. 2006-1*, Pacific Earthquake Engineering Research Centre, University of California, Berkeley, California.

EZ-FRISK. *Software for Earthquake Ground Motion Estimation*, Risk Engineering Inc., Boulder, Colorado.

Fajfar, P., Vidic, T., & Fischinger, M. (1990). A measure of earthquake motion capacity to damage medium-period structures. *Soil Dynamics and Earthquake Engineering*, 9, 236-242.

FEMA 356 (2002). *Prestandard and Commentary for the Seismic Rehabilitation of Buildings*. Federal Emergency Management Agency, Washington, DC.

Goel, R. K., & Chopra, A. L. (1997). *Vibration Properties of Buildings Determined from Recorded Earthquake Motions*. UCB/EERC Report 97/14, University of California, Berkeley, California.

GSHAP (1992). Global Seismic Hazard Map of South Asia, Global Seismic Hazard Assessment Program.

Haselton, C. B., & Deierlein, G. G. (2007). *Assessing seismic collapse safety of modern reinforced concrete moment frame buildings*. PEER Report 2007/08, Pacific Earthquake Engineering Research Center, University of California, Berkeley, California.

Haselton, C. B., Goulet, C. A., Mitrani-Reiser, J., Beck, J. L., Deierlein, G. G., Porter, K. A., Stewart, J. P., & Taciroglu, E. (2008). *An assessment to benchmark the seismic performance of a code-conforming reinforced-concrete moment-frame building*. PEER Report 2007/12, Pacific Earthquake Engineering Research Center, University of California, Berkeley, California.

Ibarra, L. F., Medina, R. A., & Krawinkler, H. (2005). Hysteretic models that incorporate strength and stiffness deterioration. *Earthquake engineering & structural dynamics*, *34***,** 1489-1511.

IBC (2006). *International Building Code. International Code Council, Inc. (formerly BOCA, ICBO and SBCCI)* 4051, 60478-5795.

Idriss, I. M. (2008). An NGA empirical model for estimating the horizontal spectral values generated by shallow crustal earthquakes. *Earthquake Spectra*, *24***,** 217-242.

IS 13920 (1993). *Ductile Detailing of Reinforced Concrete Structures Subjected to Seismic Forces – Code of Practice*, Bureau of Indian Standards, New Delhi, India.

IS-1893 (2002). *Criteria for Earthquake Resistant Design of Structures –Part I: General provisions and buildings*, Bureau of Indian Standards, New Delhi, India.

Jain, S. K. (2003). Review of Indian Seismic code IS 1893 (Part 1). *The Indian Concrete Journal*, 1414-1422.

Jain, S. K., & Murthy, C. V. R. (2005). *Proposed Draft Provisions and Commentary on Indian Seismic Code IS 1893 (Part 1)*. Department of Civil Engineering, Indian Institute of Technology Kanpur.

JBoatwright, J., Thywissen, K., & Seekins, L. (2001). Correlation of ground motion and intensity for the 17 January 1994 Northridge, California earthquake. *Bulletin of Seismological Society of America*, *91*, 739-752.

Kaka, S. I., & Atkinson, G. M. (2004). Relationships between instrumental ground motion parameters and Modified Mercalli Intensity in eastern North America. *Bulletin of Seismological Society of America*, *94* (5), 1728–1736.

Kowalsky, M. J., & Priestley, M. J. N. (2000). Improved analytical model for shear strength of circular reinforced concrete columns in seismic regions. *ACI Structural Journal*, *97* (3).

McGuire, R. K. (2004). Seismic Hazard and Rick Analysis. Earthquake Engineering Research Institute, Berkeley, 240.

Motegi. (2001). Bhutan need not worry about a major earthquake disaster. *Geological Survey of Bhutan*.

Negro, P., & Colombo, A. (1997). Irregularities induced by non-structural masonry panels in framed buildings. *Engineering Structures, 19***,** 576-585.

Negro, P., Pinto, A., Verzeletti, G., & Magonette, G. (1996). PsD test on four-story R/C building designed according to Eurocodes. *Journal of Structural Engineering, 122***,** 1409-1417.

Negro, P., Verzeletti, G., Magonette, G., & Pinto, A. (1994). Test on a four storey full scale RC frame designed according to Eurocode 8 and 2. Preliminary report, Joint Research Centre, Italy.

Pagliaroli, A., & Lanzo, G. (2008). Selection of real accelerograms for the seismic response analysis of the istorical town of Nicastro (Southern Italy) during the March 1638 Calabria earthquake. *Engineering Structures, 30,* 2211-2222.

Panagiotakos, T. B., & Fardis, M. N. (2001). Deformations of reinforced concrete members at yielding and ultimate. *ACI Structural Journal, 98* (2), 135-148.

PEER-ATC-72-1 (2010*). Modelling and Acceptance Criteria for seismic Design and Analysis of Tall Buildings*. Applied Technology Council/Pacific Earthquake Engineering Research Centre.

Priestley, M. J. N., Verma, R., & Xiao, Y. (2009). Seismic shear strength of reinforced concrete columns. *Journal of Structural Engineering, 120* (8), 2310-2329.

Report. (2009). *Joint report on September 21 2009 Bhutan Earthquake,* Royal Government of Bhutan and UNDP, Thimphu.

Rodriguez-Marek, A., Bray, J. D., & Abrahamson, N. (1999). *Characterization of site response, general site categories.* PEER Report 1999/03, University of California, Berkeley, CA.

Satake, N., Suda, K., Arakawa, T., Sasaki, A., & Tamura, Y. (2003). Damping evaluation using full scale data of buildings in Japan. *Journal of Structural Engineering, 129* (4), 470-477.

Thinley, K., & Hao, H. (2016). Seismic response analysis and performance assessment of masonry infilled RC buildings in Bhutan with and without soft storey. *Advances in Structural Engineering*, DOI: 10.1177/1369433216661336.

UNDP Report. (2006). *Report on Thimphu Valley Earthquake Risk Management Program*, Standards and Quality Control Authority, Ministry of Works and Human Settlement, Thimphu, Bhutan.

Vision-2000 (1995). *Performance Based Seismic Engineering of Buildings: conceptual framework, vol I and II.* Structural Engineers Association of California, Sacramento.

Walling, M. Y., & W. K. Mohanty, W. K. (2009). An overview on the seismic zonation and micro zonation studies in India. *Earth-Science Reviews, 96,* 67-91.

CHAPTER 3 SEISMIC PERFORMANCE OF REINFORCED CONCRETE FRAME BUILDINGS IN BHUTAN BASED ON FUZZY PROBABILITY ANALYSIS

3.1 Abstract

Seismic performance of reinforced concrete (RC) frame buildings is mostly assessed based on the distinct interstorey drift limits defined by many existing guidelines. In reality, damage of a structure is a continuous process under the action of the load and also depends on a number of factors. Therefore damage can be more logically defined with a fuzzy performance level than a distinct interstorey drift limit. In this paper, probability and fuzzy set theory are used to estimate the realistic failure probabilities of the RC buildings in Bhutan by considering randomness in material and geometrical parameters and fuzziness in the damage criteria. Three typical RC frame buildings in Thimphu, Bhutan and the ground motions predicted at the generic soil sites in Thimphu are used for the structural response prediction. Rosenbluth Point Estimate Method is used for modelling the statistical variation of the input parameters and the computer program Perform 3D (CSI, 2006) is used for carrying out the dynamic nonlinear analysis of the buildings. Monte Carlo Simulation is employed to validate the accuracy of the Rosenbluth Point Estimate Method and determine the statistical distribution of the response quantities. Soil structure interaction (SSI) is considered at the soft soil site using the uncoupled spring model. Based on the mean and standard deviation of the intersotrey drifts obtained from the analyses, the fuzzy failure probabilities of the buildings are estimated. It is found that under the 475 year return period ground motions, typical buildings experience a high probability of irreparable and severe damages, while the high probability of severe damage and complete collapse are predicted under the 2475 year return period ground motions. SSI is found to be detrimental to the 3 storey building, while no significant effect is observed to the 6 storey building.

3.2 Introduction

Interstorey drift is the most important response quantity that is commonly used to indicate the performance of buildings under seismic action. Many existing guidelines such as ASCE/SEI 41-13 (2014), ATC-40 (1996) and Vision 2000 (1995) specify interstorey drift limits corresponding to the performance level of buildings and accordingly, many researchers have assessed the performance of buildings based on these guidelines. Moreover, several seismic design codes have also imposed drift limit during the design stage to ensure the intended performance of buildings. For example, Indian Seismic Code, IS 1893 (2002) restricts the inter

storey drift to 0.4% at the design load level. Similarly, Australian Seismic Code, AS1170.4 (2007) limits the inter storey drift at any floor to 1.5% for structure collapse prevention.

There are a number of studies that used interstorey drift to assess the seismic performance of existing RC buildings in various parts of the world. Lynch et al. (2011), Duan and Hueste (2012) and Rezaei and Massumi (2014) studied the seismic performance of existing RC buildings designed according to the respective seismic codes in Southern California, China and Iran, respectively. The interstorey drift demands were estimated from the nonlinear dynamic analyses and compared with the performance limits of ASCE/SEI 41-13 (2014) to ascertain the performance of the RC buildings. Similarly, the performance of existing RC buildings in Canada, central United States and Nepal were respectively studied by Sadjadi at el. (2007), Kueht and Hueste (2009) and Chaulagain et al. (2015). Nonlinear dynamic analyses were carried out to estimate the interstorey drift demands which were then compared with the performance limits such as Vision 2000 and FEMA 356 (2000) for assessing the performance. Panagiotakos and Fardis (2000), Kim and Kim (2009) and Raju et al. (2012) also investigated the seismic performance of RC buildings designed according to the Eurocode 8 (1998), International Building Code, IBC (2003) and Indian Seismic Code, respectively. The performance of the buildings was similarly assessed based on the interstorey drift limits and pushover curves.

In all the above studies, the seismic performance of the RC buildings was assessed based on the distinct interstorey drift limits without considering uncertainties in the input parameters. In reality, structural parameters such as material strength, stiffness and dimensions inevitably vary from their design values owing to many factors such as the variations of quality control during construction and inevitable deterioration during service. Therefore, under the action of earthquake ground motion, structural responses are influenced by these uncertain parameter variations. Owing to these uncertainties, the estimated interstorey drift of buildings based on these design parameters could vary to a certain extent. On the other hand, the damage criteria are commonly regarded and more logically modelled as fuzzy. This is because the damage is indeed itself a fuzzy definition and a continuous process. For example, as per the Australian Seismic Code, it is acceptable to say that a building structure would collapse if the interstorey drift is equal to or larger than 1.5%. However, it is not logical to conclude that the same structure absolutely would not collapse if the interstorey drift is 1.499%. Therefore, damage criteria are more reasonably modelled as fuzzy. However, only very limited number of studies such as Kirke and Hao (2004), Gu and Lu (2005) and Pakdamar and Güler (2008) had considered fuzziness in modelling the damages of the buildings. These studies, however, had

either ignored the uncertainties in the structural parameters or were just applied only to simple two-dimensional building frames.

This study is geared towards assessing the seismic performance of reinforced concrete frame buildings in Bhutan in a more holistic and realistic manner by taking into account both the random structural parameter variations and the fuzziness in damage criterion definition. Assessing the realistic performance of RC buildings for the expected earthquakes has long been overdue in Bhutan. The country is located on one of the most active seismic zones in the Himalaya and the destructive earthquakes such as the one that occurred in Nepal on 25th April 2015 cannot be ruled out in Bhutan at any time. The structures in Bhutan are equally vulnerable, if not more, as those in Nepal. A number of RC buildings in Bhutan were built without any kind of engineering design and technical specifications. Although RC buildings built in Bhutan after the adoption of Indian Seismic Code in 1997 have been designed according to Indian Seismic Code, their performance under the seismic action is still not known. Fewer studies were done on the seismic performance of RC buildings in Bhutan (UNDP Report, 2006; Dorji, 2009; Thinley et al., 2017). However, they are either fully deterministic analysis based or are based on the linear elastic analysis. Since there are a number of uncertainties inherent with the structures and they invariably exhibit nonlinear behaviour under seismic excitation, performance predicted by these studies is not necessarily realistic. Hence to safeguard the loss of lives and properties during seismic events, the realistic performance assessment of RC buildings in Bhutan has become a very high priority.

In this study, three typical RC frame buildings that represent the general RC building stocks in Bhutan are considered for the seismic performance assessment. Ground motions predicted for the site conditions in Bhutan for 475 and 2475 year return periods are used for the analyses. The effect of soil structure interaction is considered by introducing spring support at the soft soil site. Rosenbluth Point Estimate Method (Rosenbluth, 1981) is used to calculate the statistical variations of random structural parameters and the dynamic nonlinear analysis and performance assessment software, Perform 3D (CSI, 2006) is used for the response prediction of the buildings. The structural responses predicted by considering the statistical variations of random variables by Rosenbluth Point Estimate Method are verified using Monte Carlo Simulation technique. The fuzzy probability analysis is then used to estimate the damage probabilities of buildings by introducing triangular membership function for modelling the fuzzy damage criteria. The drift limits specified by Structural Engineers Association of California (SEAOC) in Vision 2000 document is used for the definition of damage boundaries and construction of membership function. In general, the RC building designed according to the Indian Seismic Code have the high probability of undergoing irreparable damage and

severe to complete collapse under the 475 and 2475 year return period ground motions, respectively. The high probability of severe damage and complete collapse are predicted under the 475 and 2475 year return period ground motions, respectively in case of the RC building not designed to any standard.

3.3 Ground Motion Time Histories

Located right on the junction of tectonic plates where the Indo-Australian plate is continuously being subducted under the Eurasian plate, Bhutan has experienced a number of earthquakes of various sizes in the past. However, owing to its isolation for the larger part of its history combined with the lack of in-house technical capabilities, none of the earthquakes occurred in Bhutan were quantitatively recorded or studied in detail. In the absence of the ground motion record, the earthquake ground motions predicted in chapter 2 by Thinley et al. (2017) from probabilistic seismic hazard analysis (PSHA) are used in this study. They considered 18 seismic source zones within a distance of 400 km from Thimphu, Bhutan for PSHA. The ground motion time histories at generic soil sites predicted in Thimphu, Bhutan for the 475 and 2475 year return periods are shown in Figures 3-1 and 3-2. The corresponding response spectra are shown in Figure 3-3. These predicted ground motions will be used as inputs in this study. More detailed information regarding PSHA and seismic ground motion prediction can be found in chapter 2 of this thesis.

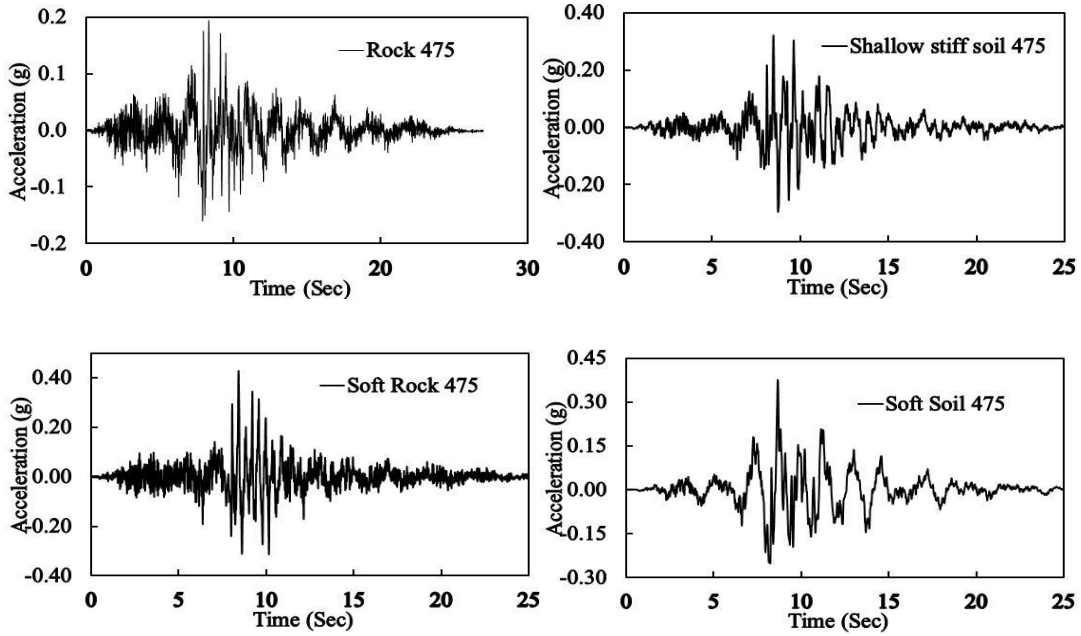

Figure 3-1 Ground motion time histories at generic soil sites in Thimphu for 475 year return periods.

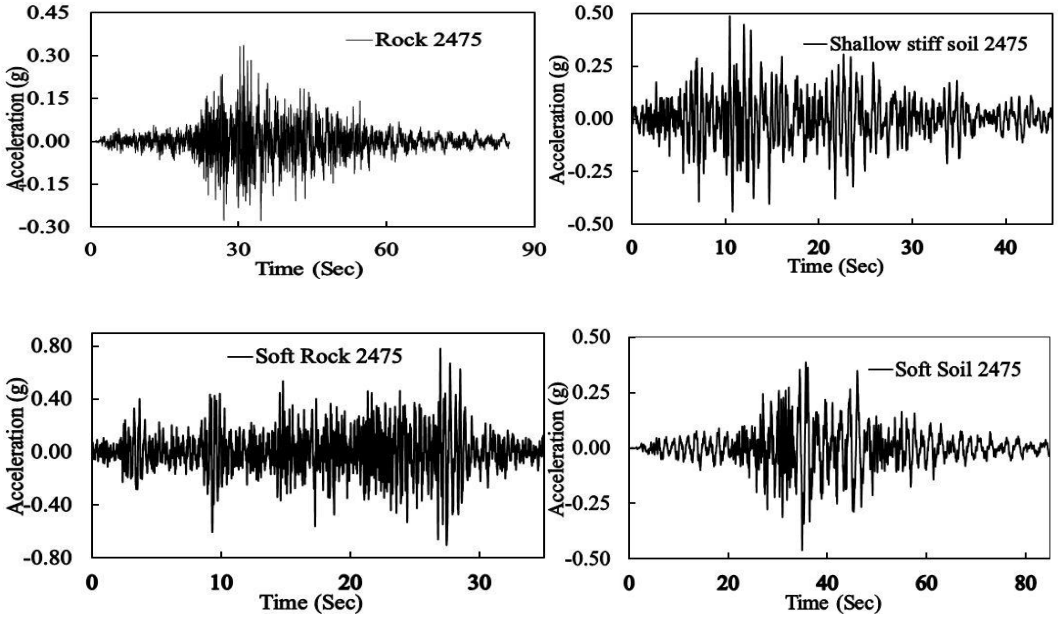

Figure 3-2 Ground motion time histories at generic soil sites in Thimphu for 2475 year return periods.

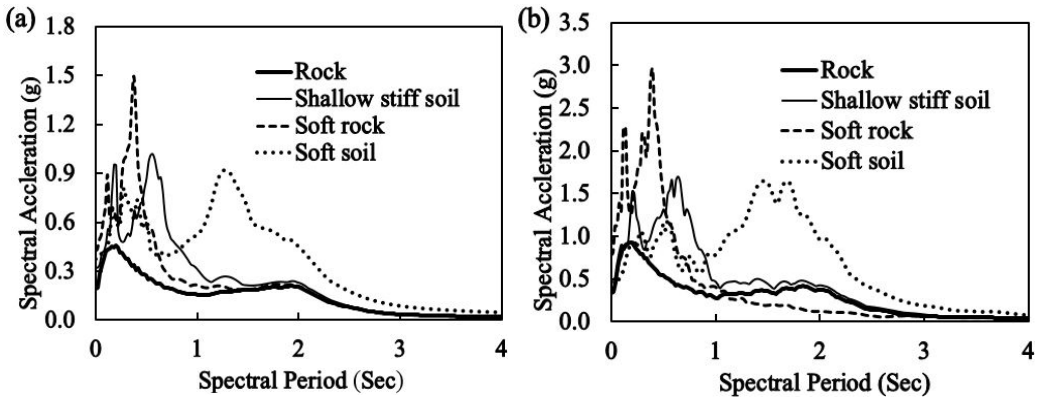

Figure 3-3 Ground motion response spectra at different sites for (a) 475 and (b) 2475 year return periods.

3.4 Structural model for performance assessment

3.4.1 Case study buildings

RC frame buildings are very common in the urban areas of Bhutan and their construction has been started as early as the 1970s. However, only in 1997, the country has adopted Indian Seismic Code for the seismic design of RC buildings. Until 1997, RC buildings in Bhutan were only designed for gravity load or were just built based on some primitive thumb rules. As such, in addition to the RC buildings that were designed and built according to Indian Seismic Code, there are a number of RC buildings which were built without any kind of seismic provision. In this study, three typical buildings denoted as '6 storey', '3 storey new'

and ‘3 storey old’ buildings are considered for assessing the performance. The ‘6 storey’ and ‘3 storey new’ buildings were designed according to the Indian Seismic Code while ‘3 storey old’ building was not designed to any standard but was built by local technicians based on some thumb rules prior to 1997. Since RC buildings built prior to 1997 were directly constructed at the site without proper design and drawings, there are no records of structural details available for these buildings. Hence, the geometry of ‘3 storey old’ building is assumed identical to that of ‘3 storey new’ building in this study. This is done so as to compare the performance of buildings built prior to and after the adoption of Indian Seismic Code in 1997.

Beam and column layout plans and sectional elevations of the ‘6 storey’ and ‘3 storey’ buildings are shown in Figures 3-4 and 3-5, respectively. As shown in the figures, ‘6 storey’ building has three bays along the x-direction and two bays along the y-direction, while ‘3 storey’ buildings have five and three bays along the x and y-directions, respectively. The notations, C1, C2 and C3 represent the column markings which are detailed in Tables 3-1 and 3-2 for dimensions and reinforcements. The centre to centre spacing between the columns and floor to floor height of the buildings are given in the figures in millimetres.

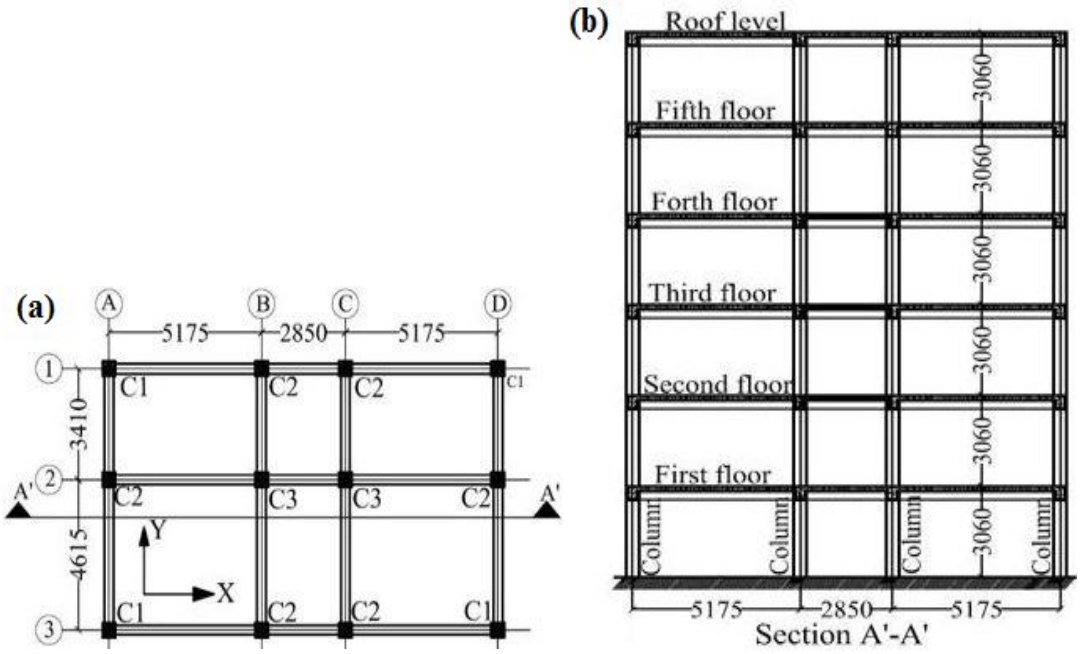

Figure 3-4 (a) Beam and column layout plan and (b) sectional elevation of 6 storey building.

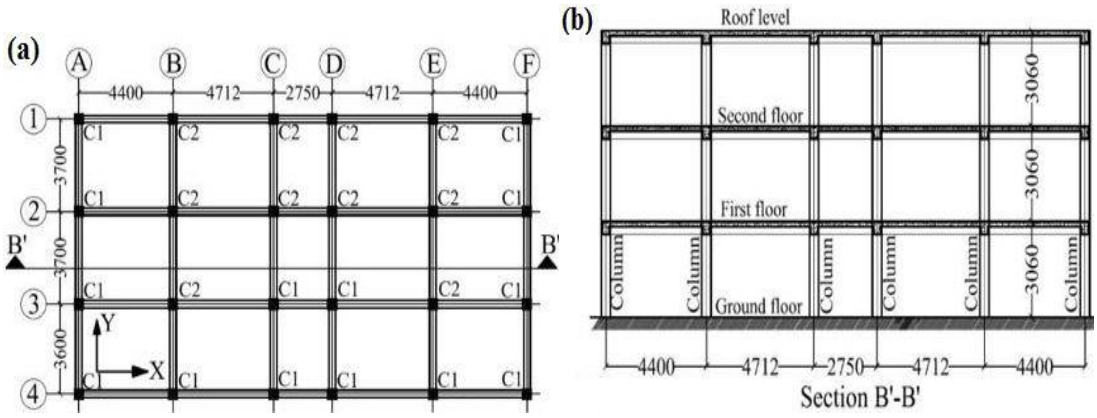

Figure 3-5 (a) Beam and column layout plan and (b) sectional elevation of 3 storey buildings.

The '6 storey' and '3 storey new' buildings are the existing buildings in Thimphu and their structural details are obtained from Thimphu City Corporation in the form of architectural and structural drawings. The design live load of 2 kN/m^2 on floors and 0.75 kN/m^2 on roofs were used for these buildings. The superimposed dead load of 1 kN/m^2 was also applied on floors. The concrete compressive strength of 25 MPa was used for columns and 20 MPa for beams and slabs for '6 storey' building, while 20 MPa is used for all structural members of '3 storey new' building. The steel yield strength of 415 MPa was specified for the reinforcement used for these buildings. The clear cover depth of 40 mm and 25 mm were respectively used for beams and columns of these buildings. A slab thickness of 150 mm was used for all floors of these buildings.

In the absence of the structural drawings, the structural details of the '3 storey old' building such as member dimension, reinforcement ratio and compressive strength of concrete are adopted from the result of non-destructive tests conducted on 15 such old buildings in Thimphu under the Thimphu Valley Earthquake Risk Management Project in 2005 (UNDP Report, 2006). The structural details of these buildings were found to be very much similar since they were built based on similar kind of thumb rules. As observed from the non-destructive tests, 15 MPa concrete and 415 MPa steel are respectively adopted for the '3 storey old' building. The concrete cover depth of 20 mm for beams and columns and the slab thickness of 100 mm are also adopted for the building.

The cross section of beams and columns showing the arrangement of reinforcement are shown in Figure 3-6. The member dimensions and reinforcement details of typical buildings are given in Tables 3-1 and 3-2. The reinforcements provided for beams and columns are denoted by the number of bars followed by the diameter of the bar. For instance, referring Figure 3-6 (a) and Table 3-1, the reinforcements provided for the top and bottom of the floor beams (FB)

along x-direction are respectively denoted by ‘4-20’ and ‘2-20+2-16’. The notation, ‘4-20’ denotes 4 numbers of 20 mm diameter bar, while ‘2-20+2-16’ denotes 2 numbers of 20 mm diameter bar and 2 numbers of 16 mm diameter bar. The reinforcement provided for the other beams and columns can be similarly read from the tables. Depending on the number of bars specified for columns, the main reinforcement and ties were arranged as shown in Figure 3-6 (b). To account for the contribution of a slab to the stiffness of the structure, interior and exterior monolithic beams and slab are approximated as T and L beams, respectively. The effective width of T and L beams are calculated as per ACI 318-14 (2104) depending on the span of beam and depth of the slab. The columns of typical buildings have square strip footings and are founded at a shallow depth of 1.5 to 2 m from the ground level.

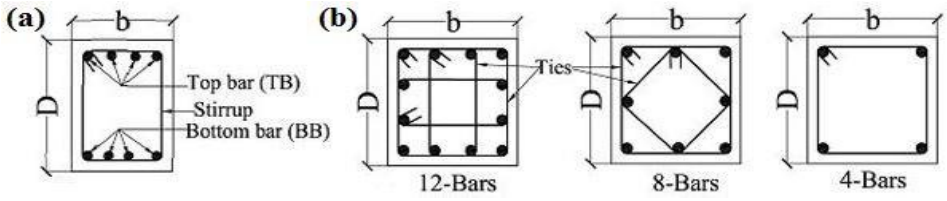

Figure 3-6 (a) Typical beam cross section showing top and bottom reinforcement of beam and (b) column cross sections with a different number of reinforcement bars.

Table 3-1 Dimension and reinforcement details for RC members for '6 storey' building

RC Members	Dimension (bxD),mm	Reinforcement (Bar dia. in mm)	
(a) Floor Beams (FB) and Roof Beams (RB)			
		Top bars	Bottom Bars
FB along X	300x450	4-20	2-20+2-16
FB along Y	300x400	4-20	2-20+2-16
RB along X	300x450	2-20+2-16	4-16
RB along Y	300x400	2-20+2-16	4-16
Beam stirrups		8@100 mm at column face and 8@150 mm C/C at the center	
(b) Column			
Column C1	450x450	8-20 + 4-16	
Column C2	450x450	12-20	
Column C3	500x500	4-25+8-20	
Column ties		10@90 mm C/C throughout	

Table 3-2 Dimension and reinforcement details of RC members for '3 storey new' and '3 storey old' buildings

	3 storey new			3 storey old		
RC Members	Dimension (bxD),mm	Reinforcement (Bar dia. in mm)		Dimension (bxD),mm	Reinforcement (Bar dia. in mm)	
(a) Floor Beams (FB) and Roof Beams (RB)						
		Top Bars	Bottom Bars		Top Bars	Bottom Bars
FB along X	300x400	4-20	2-20+2-16	250x350	4-12	2-12+2-10
FB along Y	300x400	2-20+2-16	4-16	250x300	3-12	3-12
RB along X	300x400	2-20+2-16	4-16	225x300	3-12	3-12
RB along Y	300x400	4-16	2-16+2-12	225x300	2-12+1-10	3-10
Beam stirrups		8@100 mm C/C at column face and 8@150 mm C/C at the center			6@150 mm C/C throughout	
(b) Column						
Column C1	400x400	8-20		250x250	4-16	
Column C2	400x400	4-25+4-20		250x250	8-12	
Column ties		8@100 mm C/C throughout			6@150 mm C/C throughout	

3.4.2 Numerical model

The chord rotation model, which is based on the lumped plasticity model, is used for modelling the RC members. The application of chord rotation model in modelling an RC member is shown in Figure 3-7 (a). It consists of a stiff end zone and a plastic hinge at each end of the member with elastic segments in the middle. The trilinear force-deformation (F-D) relationship of Perform 3D (CSI, 2006) which is similar to Ibarra et al. (2005) is used for the numerical simulation. The chord rotation model has end moment as force and end rotation as deformation. The F-D relationship is defined by stiffness (K), strength (M) and deformation (θ) parameters and is shown in Figure 3-7 (b). It is also called backbone curve and defines the hysteretic response of the component. Defining these parameters forms the main crux of modelling RC members for nonlinear dynamic analysis.

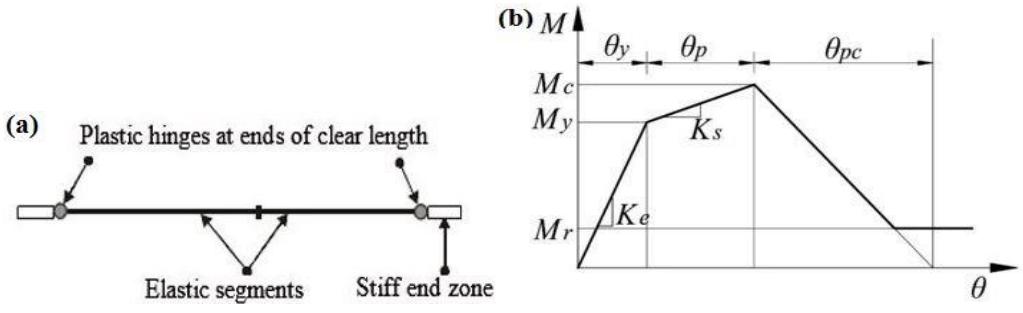

Figure 3-7 (a) Implementation of chord rotation model of Perform 3D (CSI, 2006) and (b) F-D relationship used for numerical model.

In order to predict the structural response correctly, the numerical model was previously calibrated with the experimental results. The experimental results of a four storey RC frame building which was pseudo-dynamically tested at the European Laboratory for Structural Assessment (ELSA) were used for the model calibration. The details of the experimental building and test procedure can be found in Negro et al. (1994), Negro et al. (1996), Negro and Colombo (1997). Using the structural details of experimental building and the ground motion used for the test, the response of the experimental building is correctly predicted by the numerical model. The details of model calibration can be found in Thinley et al. (2014). In calibrating the numerical model, stiffness, strength and deformation parameters are estimated as those given in the following paragraph. The F-D relationship and hence the stiffness, strength and deformation parameters of RC beams and columns of the typical buildings are similarly defined.

The yield moment M_y is estimated from the expression given by Panagiotakos and Fardis (2001) which was developed based on the number of tests on beams and columns. The expression was also validated by Haselton and Deierlein (2007) and found to agree well with the test data. The capping moment M_c is taken as $1.13M_y$ that was proposed by Haselton et al. (2008) from the regression analyses of the number of test data. As recommended in Perform 3D (CSI, 2006), the residual moment M_r is taken as 0.001 times the capping moment. The effective stiffness or secant stiffness K_e is estimated from the expression given by Elwood and Eberhard (2006) and ranges from 0.2 EI_g to 0.7 EI_g depending on the axial load ratio, where EI_g is the flexural stiffness of the gross section. The pre-capping rotation θ_c and post-capping rotation θ_{pc} are estimated from the expression proposed by Haselton et al. (2008) based on the number of test results. Depending on the structural details of the RC members, the values of pre-capping and post-capping rotations were found to range from 0.03 to 0.07 radian and 0.07 to 0.1 radian, respectively. These details were used for calibrating the model with the experimental results in Thinley et al. (2014) and same details are used for estimating the nonlinear response of the typical buildings in this study. In addition, a 5% modal damping is used in combination with a small amount of stiffness proportional Rayleigh damping (0.1%) which is used to damp out high-frequency vibrations. The geometrical nonlinearity in the form of P-delta effect is also included in the analyses. The details of modelling RC members can be found in chapter 2.

The effect of soil-structure interaction (SSI) is considered only at the soft soil site since it was found to be insignificant at the other soil sites in the previous study (Thinley et al., 2014). Hence, fixed support is assumed at the rock, shallow stiff soil and soft rock sites, while the equivalent spring supports are used to model the flexible support at the soft soil site. More

specifically, the three translational and three rotational springs along the three mutually perpendicular directions are provided at the support of each column to simulate the effect of soil flexibility as shown in Figure 3-8 (a). Owing to the complexity of incorporating the frequency dependent dynamic foundation impedance function in the analysis, only the static equivalent springs are used to model the soil. The stiffness of these springs is estimated from the expressions given in ASCE/SEI 41 (2014). These expressions are simplified for the square footings used in this study and are given in Table 3-3. As given in Table 3-3 and shown in Figure 3-8 (a), K_x, K_y and K_z are the translational spring stiffness along the x, y and z-directions, respectively. Similarly, K_{rx} and K_{ry} are the rocking stiffness along the x and y-directions, respectively and K_{tz} is the torsional stiffness along the z-direction. As represented in Figure 3-8 (b), the size of the square footing, B = 2.2 m and 3.5 m for '3 storey new' and '6 storey' buildings and were respectively founded at the depth, D_f = 1.5 m and 2 m from the soil surface. The depth of the footing pad, d = 0.35 m and 0.75 m and the effective depth of foundation, h = 1.03 m and 1.63 m were respectively used for the column footings of '3 storey new' and '6 storey' buildings. The shear modulus of soil, G is dependent on the shear wave velocity of soil and response spectral acceleration of ground motion at the short period. It is calculated to be 4.05 MPa and 0.46 MPa, respectively for the 475 and 2475 year return period ground motions at the soft soil site. The Poisson's ratio used for the soft soil is v = 0.45. SSI is not considered for '3 storey old' building since analyses failed to run at soft soil site owing to very large response.

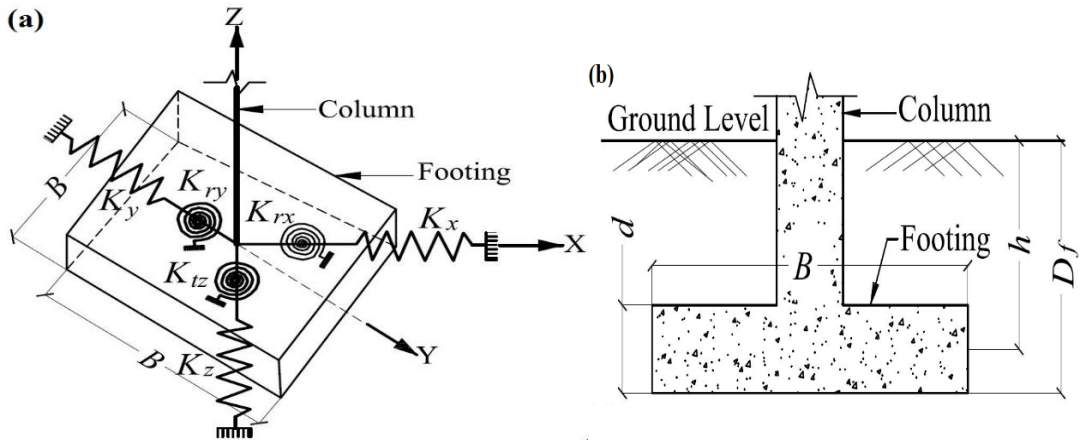

Figure 3-8 (a) Provision of translational and rotational springs in the three mutually perpendicular directions and (b) section of typical square column footing.

Table 3-3 The stiffness of springs for various degrees of freedom.

Degree of Freedom	Stiffness of soil springs at the bottom of square footing founded at the shallow depth, D_f
Translation along x axis	$K_x = \frac{4.6GB}{2-v}\left[\left\{1+0.21\sqrt{\frac{D_f}{B}}\right\}\left\{1+1.6\left(\frac{2hd}{B^2}\right)^{0.4}\right\}\right]$
Translation along y-axis	$K_y = \frac{4.6GB}{2-v}\left[\left\{1+0.21\sqrt{\frac{D_f}{B}}\right\}\left\{1+1.6\left(\frac{2hd}{B^2}\right)^{0.4}\right\}\right]$
Translation along z-axis	$K_z = \frac{2.35GB}{1-v}\left[\left\{1+0.22\frac{D_f}{B}\right\}\left\{1+0.32\left(\frac{2d}{B}\right)^{0.67}\right\}\right]$
Rocking along x-axis	$K_{rx} = \frac{0.5GB^3}{1-v}\left[1.0+2.5\frac{d}{B}+5\frac{d^2}{B^2}\left(\frac{d}{D_f}\right)^{-0.2}\right]$
Rocking along y-axis	$K_{ry} = \frac{0.5GB^3}{1-v}\left[1.0+1.4\left(\frac{d}{B}\right)^{0.6}\left\{1.5+3.7\left(\frac{d}{B}\right)^{1.9}\left(\frac{d}{D_f}\right)^{-0.6}\right\}\right]$
Torsion along z-axis	$K_{tz} = 1.04GB^3\left[1.0+5.2\left(\frac{d}{B}\right)^{0.9}\right]$

3.5 Modelling of uncertainties

In the probabilistic seismic assessment of buildings, there are a number of uncertainties that need to be considered. These are static loading, ground motion, structural configuration and boundary condition, modelling, material and geometrical uncertainties. In this study, only material and geometrical uncertainties are considered for the structural response estimation. Loading and modelling uncertainties are expected to have limited effect since the numerical model used in this study was previously calibrated with the experimental results. Ground motions used in this study are considered as deterministic as they were specifically predicted for the site conditions in Bhutan from PSHA for both the 475 and 2475 year return periods. The material and geometrical parameters that significantly influence the response of the structures are considered in this study. The designed values of these parameters are taken as the mean, while the coefficient of variation (CoV) and distribution pattern are considered as described below.

3.5.1 Compressive strength of concrete, f_c

In the absence of sufficient test, Indian Standard for Plain and Reinforced Concrete, IS 456 (2000) recommended standard deviation for various grades of concrete. For the concrete

design strength of 20 MPa and 25 MPa, the standard deviation of 4 MPa is recommended while the standard deviation of 3.5 MPa is recommended for the design strength of 15 MPa. This results in the CoV of 0.23, 0.20 and 0.16 for the design strengths of 15 MPa, 20 MPa and 25 MPa, respectively. Mirza et al. (1979) suggested CoV of concrete to be 0.18 and 0.14, respectively for average and excellent quality control during construction. Barlett and MacGregor (1996) also estimated similar CoV (0.186) while investigating the relationship between the cast in place concrete. In a separate study undertaken by Ellingwood (1977), the CoV of concrete strength was estimated to be 0.21. All these researchers assumed concrete properties to be normally distributed. Since Indian codes are followed in Bhutan, the CoV recommended by Indian code is used in this study. The compressive strength of concrete is assumed to be normally distributed in line with the above researchers. The mean, CoV and probability distribution of these parameters are given in Table 3-4.

3.5.2 Modulus of elasticity of concrete, E_c

Modulus of elasticity of concrete is closely related to the compressive strength of concrete (f_c). Indian code for Plain and Reinforced Concrete, IS 456 (2000) provide the following relationship between the two with the variation of 20%.

$$E_c = 5000\sqrt{f_c} \tag{3.1}$$

where E_c and f_c are in MPa. Similar relationships are also provided by other codes (AS3600, 2002; BS 8110, 1985) depending on the weight, compressive strength and density. CoV suggested by Mirza et al. (1979) is in between 0.08-0.10. Similar to the compressive strength of concrete, the coefficient of variations of 0.23, 0.20 and 0.16 are assumed with normal distribution for the modulus of elasticity of concrete resulted from the concrete design strength of 15 MPa, 20 MPa and 25 MPa, respectively.

3.5.3 Yield strength of steel, f_y

Variability of the strength of steel reinforcement significantly influences the outcome of the analysis. Basu et al. (2004) conducted the test on 500 sample rebars designated as Fe 415 as per Indian standard. The mean yield strength and corresponding coefficient of variation were found to be 509 MPa and 0.089, respectively. Mirza and MacGregor (1979) tested 4000 samples of grade 40 and 60 bars. For average quality control during construction, the estimated mean yield strength and coefficient of variation were 337 MPa and 0.107 respectively for grade 40 bars and 503 MPa and 0.093 for grade 60 bars. In studying the seismic fragility of highway bridges, Nielson and DesRoches (2007) had also taken the coefficient of variation of rebar as 0.08. In line with these studies, the coefficient of variation of 0.090 is assumed with

the normal distribution. Modulus of elasticity of steel is reported to have very small CoV and is considered as deterministic in this study.

3.5.4 Member Dimensions, *M*

Many studies assumed CoV in between 0.03 and 0.05 with normal distribution for statistical variation of geometrical dimensions. Low and Hao (2001) assumed CoV of 0.05 for all dimensions while investigating the reliability of reinforced concrete slab under explosive loading. Similarly, Kirke and Hao (2004) used CoV of 0.03 with normal distribution in estimating the failure probabilities of reinforced concrete structures in Singapore. Another researcher also recommended the use of normal distribution for the variation of dimension (Mirza and MacGregor, 1979). In this study, CoV of 0.05 and the normal distribution is assumed. It is to be noted that only the variation of width and depth of structural members is considered while the span of beams and height of columns are considered to be constant.

Table 3-4 Mean, CoV and distribution type of the material and geometrical parameters

Variables	6 storey building columns		3 storey new and beams of 6 storey buildings		3 storey old building		Probability Distribution
	Mean (MPa)	CoV	Mean (MPa)	CoV	Mean (MPa)	CoV	
E_c	25000.00	0.16	22361.00	0.20	19365.00	0.23	Normal
f_c	25.00	0.16	20.00	0.20	15.00	0.23	Normal
f_y	415.00	0.09	415.00	0.09	415.00	0.09	Normal
Dimension	As in Table 3-1	0.05	As in Table 3-1&2	0.05	As in Table 3-2	0.05	Normal

3.6 Probabilistic Structural Response Estimation

With the involvement of the number of parameters and their uncertainties, estimation of probabilistic nonlinear responses of structures is not straightforward. In this study, Rosenbluth Point Estimate Method (RPEM) (Rosenbluth, 1981) is employed to estimate the probabilistic structural response quantities. This method was found to accurately estimate the moments of a function whose variables are normally distributed (Low and Hao, 2001). Monte Carlo Simulation method (MCSM) is used to verify the accuracy of RPEM and also to determine the statistical distribution of response quantities. These methods are briefly described in the following sections. Since interstorey drift is the most important response quantity related to the damages of structures, the term response quantity in this study invariably refers to the interstorey drift of buildings.

3.6.1 Rosenbluth Point Estimate Method

This method was first developed by Rosenbluth (1981) and is computationally very efficient and straightforward for uncertainty analysis. It is capable of estimating statistical moments of a model output involving a number of random variables. The basic procedure of this method involves the consideration of two point estimates at one standard deviation on either side of the mean value for each variable. The performance function is then estimated for every possible combination of these point estimates. Depending on the number of variables involved, the number of point estimates and the number of possible combination of these point estimates are respectively given by $2n$ and 2^n, where n is the number of variables. The mean and standard deviation of the performance function are calculated from the output of 2^n simulations.

In this study, four parameters are considered, namely modulus of elasticity of concrete (E_c), compressive strength of concrete (f_c), yield strength of steel reinforcement (f_y) and member dimension (M) for the estimation of structural responses of typical buildings. As a result, there are 8 point estimates and 16 possible combinations of these four parameters. Table 3-5 shows the application of RPEM for the '3 storey new' building. In the table, E_c^+, f_c^+, f_y^+ and M^+ represent the mean plus one standard deviation and E_c^-, f_c^-, f_y^- and M^- represent mean minus one standard deviation that together make 8 point estimates and 16 possible combinations.

For every combination of these parameters, Perform 3D (CSI, 2006) is employed to carry out dynamic nonlinear analyses using the ground motions at generic soil sites in Thimphu. The structural response quantities such as interstorey drifts and displacements are estimated from the nonlinear analyses. The mean, standard deviation and skewness are then calculated from the 16 response quantities estimated from the 16 combinations. The RPEM is similarly applied to the estimations of the responses of '6 storey' and '3 storey old' buildings.

Table 3-5 Possible combination of four parameters using RPEM for '3 storey new' building.

Combination No.	Combination	E_c (MPa)	f_c (Mpa)	f_y (MPa)	D (mm)
1	$E_c^+ f_c^+ f_y^+ M^+$	26833.20	24.00	452.35	420
2	$E_c^+ f_c^+ f_y^- M^+$	26833.20	24.00	377.65	420
3	$E_c^+ f_c^- f_y^- M^+$	26833.20	16.00	377.65	420
4	$E_c^- f_c^- f_y^- M^+$	17888.80	16.00	377.65	420
5	$E_c^+ f_c^- f_y^+ M^+$	26833.20	16.00	452.35	420
6	$E_c^- f_c^- f_y^+ M^+$	17888.80	16.00	452.35	420
7	$E_c^- f_c^+ f_y^+ M^+$	17888.80	24.00	452.35	420
8	$E_c^- f_c^+ f_y^- M^+$	17888.80	24.00	377.65	420
9	$E_c^- f_c^- f_y^- M^-$	17888.80	16.00	377.65	380
10	$E_c^- f_c^- f_y^+ M^-$	17888.80	16.00	452.35	380
11	$E_c^- f_c^+ f_y^+ M^-$	17888.80	24.00	452.35	380
12	$E_c^+ f_c^+ f_y^+ M^-$	26833.20	24.00	452.35	380
13	$E_c^+ f_c^- f_y^+ M^-$	26833.20	16.00	452.35	380
14	$E_c^+ f_c^+ f_y^- M^-$	26833.20	24.00	377.65	380
15	$E_c^+ f_c^- f_y^- M^-$	26833.20	16.00	377.65	380
16	$E_c^- f_c^+ f_y^- M^-$	17888.80	24.00	377.65	380

3.6.2 Monte Carlo Simulation Method

MCSM is basically a very simple procedure that solves a deterministic problem a number of times to build up a statistical distribution of output quantity (Liang and Hao, 2007). It is capable of estimating very precise output and normally used as reference point for verifying other probabilistic results. However, it is computationally very expensive and requires a large number of simulations to arrive at the converged solution. It is not practical to use this method for an everyday problem. Hence, this method is only applied to '3 storey new' building just to validate the reliability of RPEM.

Using this method, a number of random variables are generated for the four considered parameters based on their mean, standard deviation and distribution pattern given in Table 3-4. The dynamic nonlinear analyses are carried out using these randomly generated parameters to estimate the interstorey drift and displacement of the building. Unlike in the RPEM where only 16 analyses are required for the four considered parameters, analysis has to be continued until the mean and standard deviation of response quantities remain virtually unchanged in MCSM. Normally, a large number of simulations in the range of a few hundred to even thousands are required to arrive at the converged solution of response quantities. In this study, a variance reduction technique called stratified sampling is employed to reduce the number of simulations. Initially, 600 random variables are generated for each parameter and with the use

of stratified sampling technique, 250 random variables are randomly selected for each parameter and similarly tabulated as in Table 3-5. Nonlinear dynamic analyses are then run starting from the first combination of these random variables and estimated the interstorey drifts and displacements for each combination. The mean and standard deviation of these response quantities are calculated after every analysis/simulation. It is observed that mean interstorey drift at the rock, shallow stiff soil and soft rock sites remained almost constant after 100 simulations while it required 150 simulations to arrive at the constant mean for the soft soil site condition. Figure 3-9 shows the convergence of mean interstorey drift with the number of simulations at the four soil sites. As shown in Figure 3-10, standard deviations of interstorey drifts at the four soil sites remain constant after 200 simulations indicating the convergence of standard deviation. Hence, after 200 simulations, both mean and standard deviation of interstorey drifts of '3 storey new' building converged. This is possible because of the use of stratified sampling technique otherwise the number of simulations to reach convergence could have been much more.

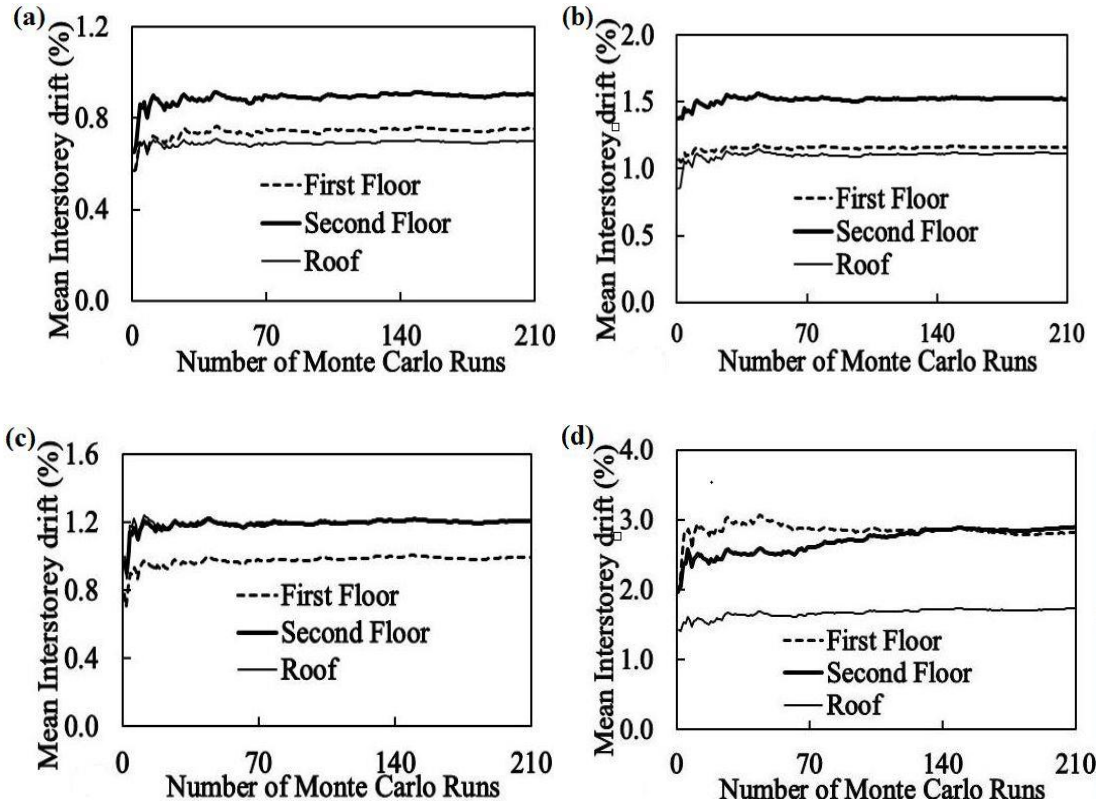

Figure 3-9 The convergence of mean interstorey drift obtained from Monte Carlo Simulation method at (a) rock; (b) shallow stiff soil; (c) soft rock and (d) soft soil sites.

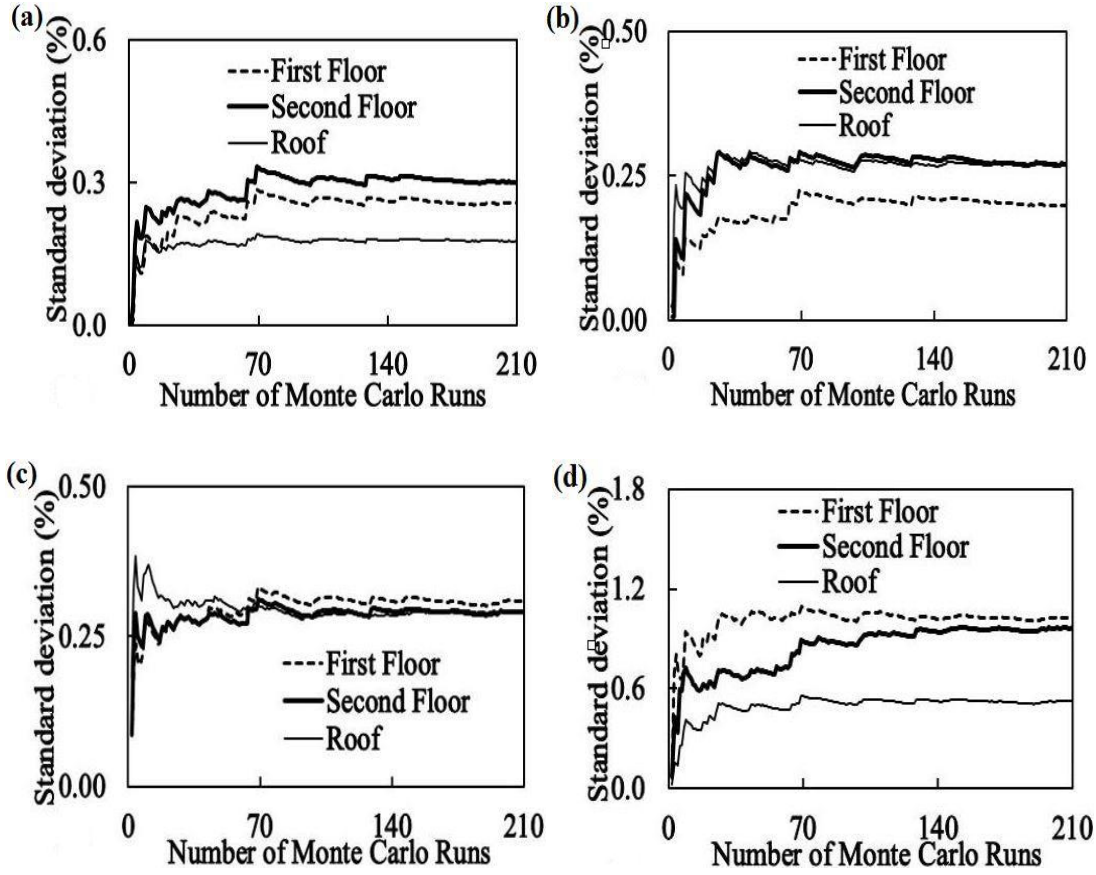

Figure 3-10 Convergence of standard deviation of interstorey drift obtained from Monte Carlo Simulation Method at (a) rock; (b) shallow stiff soil; (c) soft rock and (d) soft soil sites.

3.6.3 Validation of Rosenbluth Point Estimate Method

To validate the structural responses predicted by RPEM, the converged mean and standard deviation of interstorey drifts of '3 storey new' building are compared with the corresponding values obtained from MCSM. Table 3-6 shows the comparison of these values. The profiles of mean interstorey drift and standard deviation obtained from these methods are shown in Figures 3-11 and 3-12. From the table and figures, it can be observed that mean interstorey drift and standard deviation predicted by both the methods are very close to each other. Considering the complexity of estimating structural responses, that is comparing 16 simulations required for RPEM to 200 simulations for MCSM, it can be stated that RPEM is very efficient, practical and sufficiently accurate for the probabilistic response prediction. Hence, only RPEM is used for the structural response estimation of the '6 storey' and '3 storey old' buildings in this study.

Table 3-6 Comparison of interstorey drift and standard deviation obtained from RPEM and MCSM

	First Floor		Second Floor		Roof	
	Mean	Std. Dev	Mean	Std. Dev	Mean	Std. Dev
a) Rock site						
Rosenbluth	0.740	0.261	0.862	0.289	0.674	0.187
MonteCarlo	0.750	0.263	0.901	0.307	0.695	0.179
b) Shallow stiff soil site						
Rosenbluth	1.136	0.198	1.525	0.344	1.121	0.317
MonteCarlo	1.158	0.198	1.524	0.318	1.111	0.314
c) Soft rock site						
Rosenbluth	0.959	0.291	1.162	0.285	1.134	0.287
MonteCarlo	0.992	0.308	1.205	0.29	1.207	0.288
e) soft soil site						
Rosenbluth	2.887	1.221	2.399	0.818	1.523	0.551
MonteCarlo	2.818	1.074	2.557	0.967	1.728	0.565

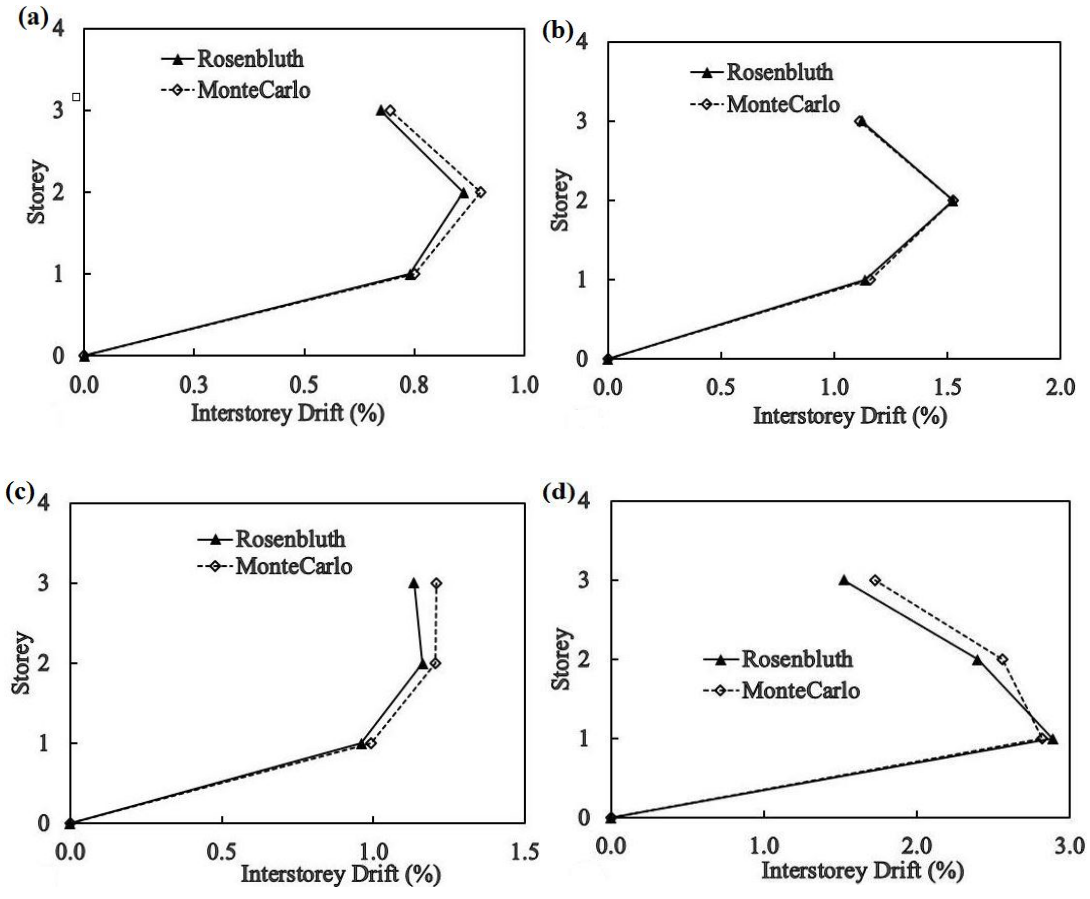

Figure 3-11 Comparison of mean interstorey drift obtained from RPEM and MCSM at (a) rock; (b) shallow stiff soil; (c) soft rock and (d) soft soil sites.

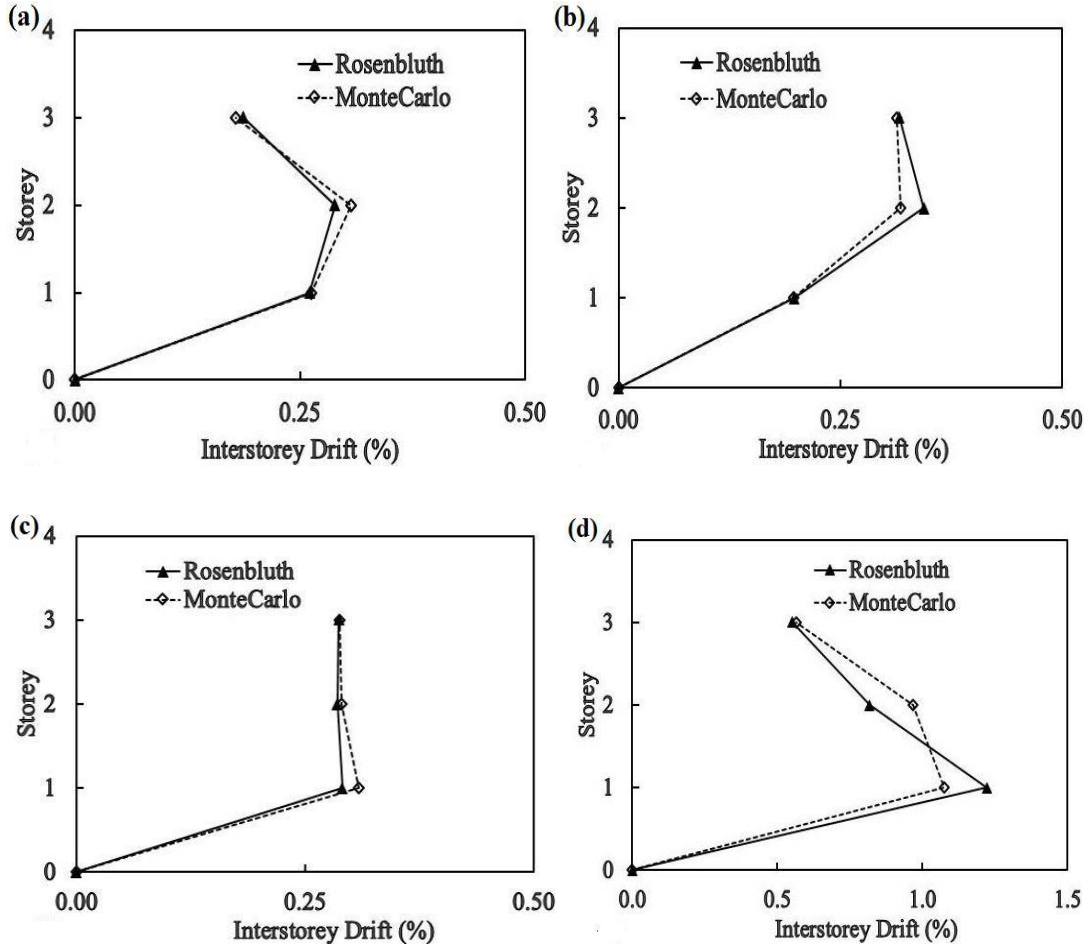

Figure 3-12 Comparison of interstorey drift standard deviation obtained from RPEM and MCSM at (a) rock; (b) shallow stiff soil; (c) soft rock and (d) soft soil sites.

3.6.4 Determination of statistical distribution of structural responses

MCSM is also used to determine the statistical distribution of the response quantity which, in this case, is the interstorey drift. It is found that interstorey drift of '3 storey new' building is lognormally distributed. The popularly used Kolmogorov-Smirnov test is carried out which confirmed the lognormal distribution of interstorey drifts with the significance level of 0.05 for rock and soft soil sites and significance level of 0.01 for shallow stiff soil and soft rock sites. The Kolmogorov-Smirnov test statistic values for interstorey drift at second floor along with the critical values for 0.05 and 0.01 significance levels are given in Table 3-7. As shown in the table, test statistic values at rock and soft soil sites are less than the critical value for 0.05 significance level, while the test values at shallow stiff soil and soft rock sites are less than the critical value for 0.01 significance level. Figure3-13 shows the plot of actual cumulative distribution function to that of fitted cumulative distribution function at the second floor level for different soil sites. As shown in the figure, the two cumulative distribution

functions are very close to each other thereby confirming the lognormal distribution function. The K-S test is conducted for interstorey drift at the second floor level since the response is the largest at this level.

Table 3-7 K-S test statistic values of interstorey drift at the second floor.

Soil Sites	Test values at 2nd floor	Critical value for α=0.05	Critical value for α=0.01
Rock Site	0.09000	0.093849	0.112481
Shallow Stiff Soil	0.11364	0.093849	0.112481
Soft Rock	0.11214	0.093849	0.112481
Soft Soil	0.05942	0.093849	0.112481

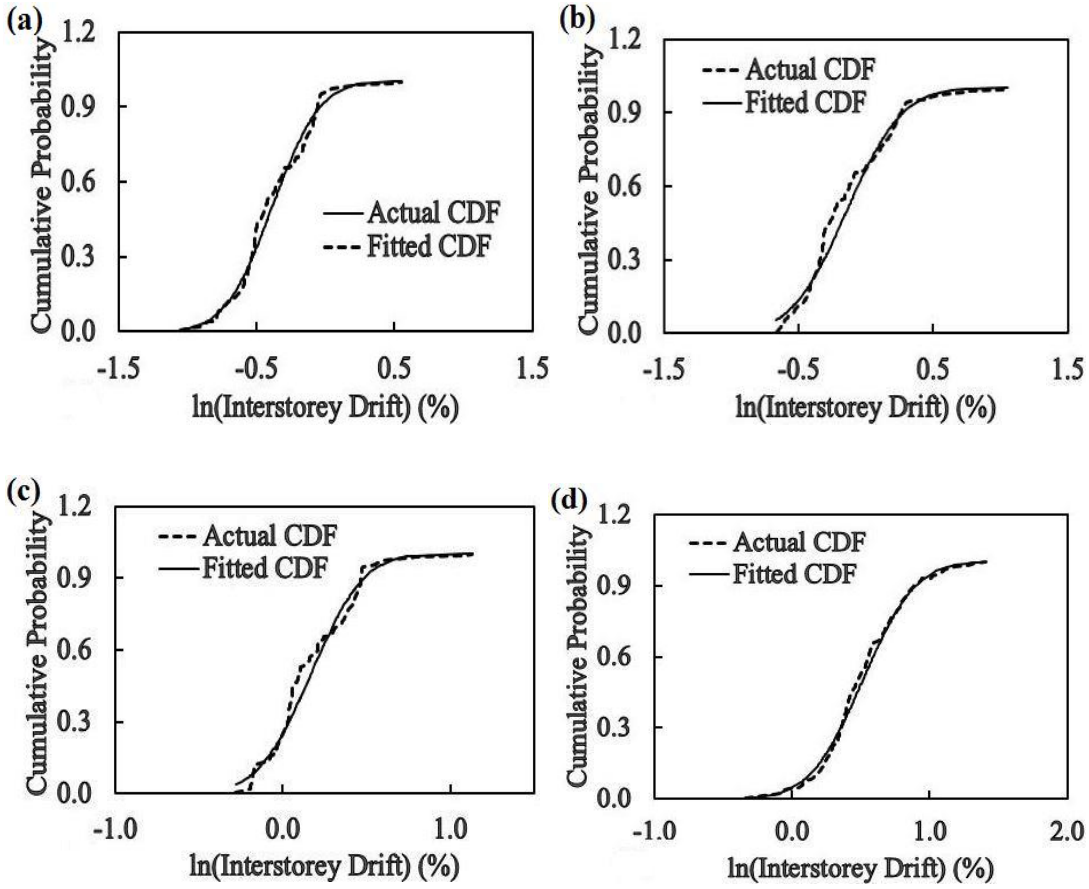

Figure 3-13 Comparison of actual and fitted CDF at (a) rock; (b) shallow stiff soil; (c) soft rock and (d) soft soil sites.

3.7 Fuzzy failure probability analysis

The performance of buildings is mostly evaluated based on the interstorey drift demand. Many guidelines such as ASCE/SEI-41 13 (2014), ATC 40 (1996) and Vision 2000 (1995) define

performance levels of buildings with corresponding damage states and interstorey drifts. In the absence of the interstorey drift limits specified for the RC buildings in Bhutan, interstorey drift limits defined in Vision 2000 is used for defining the damage boundary in this paper. Given the probabilistic distribution of the maximum interstorey drift obtained above, damage probabilities of typical buildings can be estimated from

$$P_f = P(D_m \geq D_c) = \int_{D_c}^{\infty} f_D(D) dD \tag{3.2}$$

where D_m = maximum interstorey drift, D_c = interstorey drift limits defined in Table 3-8 and $f_D(D)$ is the probability density function.

Table 3-8 Performance levels, damage states and interstorey drift limits from Vision 2000

Performance level	Damage state	Interstorey drift (%)
Fully operational	Negligible (No Damage)	<0.20
Operational	Light (Repairable	<0.50
Life safe	Moderate (Irreparable)	<1.50
Near collapse	Severe	<2.50
Collapse	Complete	>2.50

Equation (3.2) estimates damage probabilities based on the distinct damage boundaries wherein structure is considered to be damaged if $D_m \geq D_c$ and not damaged if $D_m < D_c$. In reality, a structure cannot have a fixed damage boundary since damage is dependent on many factors. For instance, it is not logical to describe a structure as moderately damaged when the maximum interstorey drift is 1.499% and severely damaged when the maximum interstorey drift is 1.500%. Hence, it is logical to define a fuzzy region in between the damage boundaries given in Table 3-8 to estimate the damage probabilities of the structures. Zadeh (1965) first introduced fuzzy sets to tackle with the real world situations that are virtually imprecise in nature. According to fuzzy set theory, a fuzzy region is defined by a lower and upper fuzzy limit in combination with a membership function (Wu et al., 1999). Introducing a fuzzy region to the distinct damage boundary limits in Table 3-8, the fuzzy failure probabilities of typical buildings can be estimated from Zhao et al. (1996)

$$P_{ff} = P(D_m \geq D_c) = \int_{D_L}^{D_U} \mu(D) f_D(D) dD \tag{3.3}$$

where D_U and D_L are respectively upper and lower fuzzy limit and $\mu(D)$ is the membership function.

In the fuzzy region, structure may fail even when $D_m < D_c$ or may not fail when $D_m \geq D_c$. It is to be noted that the definition of a membership function is quite complex and subjective. It is often based on some experts' knowledge (Low and Hao, 2001; Wu et al., 1999). In this study, a triangular membership function is adopted due to its simplicity and a high level of accuracy. As shown in Figure 3-14, the triangular membership function is constructed by linearly extending each damage state to the midpoint of the next damage state (Kirke and Hao, 2004). The midpoint of damage limit is assigned the membership function of 1 indicating the most likelihood of damage occurring of the respective damage state. For example, irreparable damage has the drift limit of 0.5% to 1.5% which gives the midpoint value of 1.0%. Hence, the membership function of irreparable damage varies linearly from 0 at 0.35% drift (midpoint of repairable damage) to 1 at 1% drift. It then decreases linearly from 1 to 0 again at 2% drift which is the midpoint of severe damage. In the same manner, the membership functions of other damage states are defined.

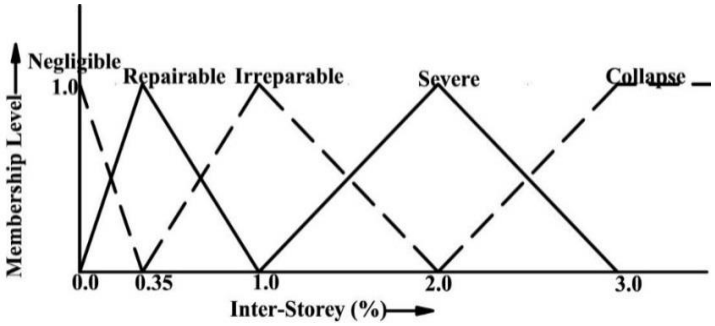

Figure 3-14 Triangular membership function adopted in this study.

3.8 Numerical results and discussion

Having verified the accuracy of RPEM in the previous section, it is now extended to calculate the structural responses of '6 storey' and '3 storey old' buildings at the different soil sites for both the 475 and 2475 year return period ground motions. As mentioned in the previous section, SSI is considered only at the soft soil site. As such, fixed support is considered when the typical buildings are analysed for the ground motions predicted at the rock, shallow stiff soil and the soft rock sites, while an equivalent spring support is considered when the buildings are analysed for the ground motions predicted at the soft soil site. The buildings are also analysed with fixed support for the ground motion predicted at the soft soil to study the structural responses estimated with and without considering SSI. The mean fundamental periods of the typical buildings for the first three modes are given in Table 3-9.

Table 3-9 Fundamental period of typical buildings for uncracked and cracked concrete

Building	Fundamental period with uncracked concrete			Fundamental period using secant stiffness to yield, K_e		
	Mode 1	Mode 2	Mode 3	Mode 1	Mode 2	Mode 3
6 storey	0.867	0.274	0.15	2.126	0.662	0.357
3 storey new	0.447	0.14	0.08	1.075	0.329	0.182
3 storey old	0.976	0.337	0.213	1.324	0.376	0.172

The fundamental period is the main parameter that governs the response of the buildings. As shown in Table 3-9, the period of building increases as it enters from elastic to the inelastic range. For '6 storey' and '3 storey new' buildings, the first mode period is increased by a factor of 2.45 and 2.40, respectively while the first mode period is increased by a factor of 1.36 for '3 storey old' buildings. The increase in period is highly dependent on the value of the secant stiffness used for modelling the RC members of the buildings. Many researchers such as Calvi et al. (2006), Dunand et al. (2006) and Katsanos et al. (2012) reported a similar factor by which the period of RC buildings is increased when subjected to ground motions. Eurocode 8 (1998) proposed a period increment factor of 2. The increase in period is mainly due to the reduction in structural stiffness of buildings when undergoing nonlinear behaviour under the ground motion. It can be seen in Table 2-9 that, the first modal period of '3 storey old' building for the case of uncracked concrete is more than that of '6 storey' building. This is due to the use of a very low concrete grade, smaller dimensions of RC members and less reinforcement area which contributed in making '3 storey old' building more flexible than that of '6 storey' building.

The mean and standard deviation of interstorey drift obtained at different soil site for the 475 and 2475 year return period ground motions are given in Tables 3-10 to 3-12. The tables also feature the storey level where the maximum interstorey drift occurs. The mean interstorey drift profiles for the same are shown in Figures 3-15 and 3-16. The interstorey drift profiles estimated with fixed and spring support are respectively shown in the figures by solid and dotted lines. It is to be noted that analyses failed to run at the soft soil site for 14 out of 16 possible combinations of random variables for the '3 storey old' building. It is due to the excessive responses that resulted from the smaller mean member dimension, insufficient reinforcement and very low concrete grade for the '3 storey old' building. Hence the mean interstorey drift and its standard deviation of the '3 storey old' building are not estimated at soft soil site.

Table 3-10 Mean maximum interstorey drift and corresponding standard deviation of '6 storey' building

		475 year return period			2475 year return period			
Site class	Support Type	Mean (%)	Std. Dev. (%)	Floor Level	Mean (%)	Std. Dev. (%)	Floor Level	Probability distribution
Rock	Fixed	1.518	0.210	2	2.268	0.171	2	Log normal
Shallow stiff	Fixed	1.854	0.344	2	2.537	0.335	3	Log normal
Soft rock	Fixed	1.607	0.237	2	1.552	0.156	3	Log normal
Soft soil	Fixed	2.985	0.485	2	4.642	0.424	3	Log normal
Soft soil	Spring	2.976	0.475	3	4.727	0.685	3	Log normal

Table 3-11 Mean maximum interstorey drift and corresponding standard deviation of '3 storey new' building

		475 year return period			2475 year return period			
Site class	Support Type	Mean (%)	Std. Dev. (%)	Floor Level	Mean (%)	Std. Dev. (%)	Floor Level	Probability distribution
Rock	Fixed	0.862	0.289	2	1.704	0.516	2	Log normal
Shallow stiff	Fixed	1.525	0.344	2	2.399	0.588	1	Log normal
Soft rock	Fixed	1.162	0.285	2	1.925	0.520	3	Log normal
Soft soil	Fixed	2.887	1.221	1	6.320	1.447	1	Log normal
Soft soil	Spring	3.277	1.081	1	7.190	0.874	1	Log normal

Table 3-12 Mean maximum interstorey drift and corresponding standard deviation of '3 storey old' building

		475 year return period			2475 year return period			
Site class	Support Type	Mean (%)	Std. Dev. (%)	Floor Level	Mean (%)	Std. Dev. (%)	Floor Level	Probability distribution
Rock	Fixed	1.854	0.401	1	2.489	0.206	1	Log normal
Shallow stiff	Fixed	2.462	0.136	1	2.586	0.358	1	Log normal
Soft rock	Fixed	1.930	0.453	1	2.268	0.297	2	Log normal

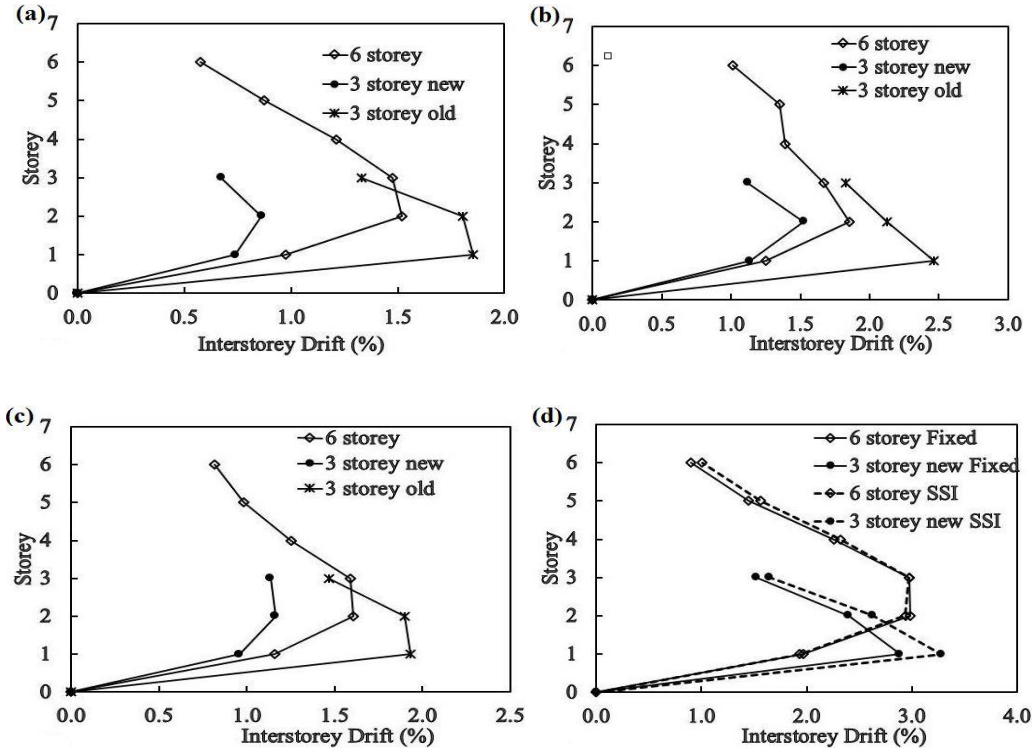

Figure 3-15 Mean interstorey drift profiles for typical buildings subjected to 475 year return period ground motions at (a) rock; (b) shallow stiff soil; (c) soft rock and (d) soft soil sites.

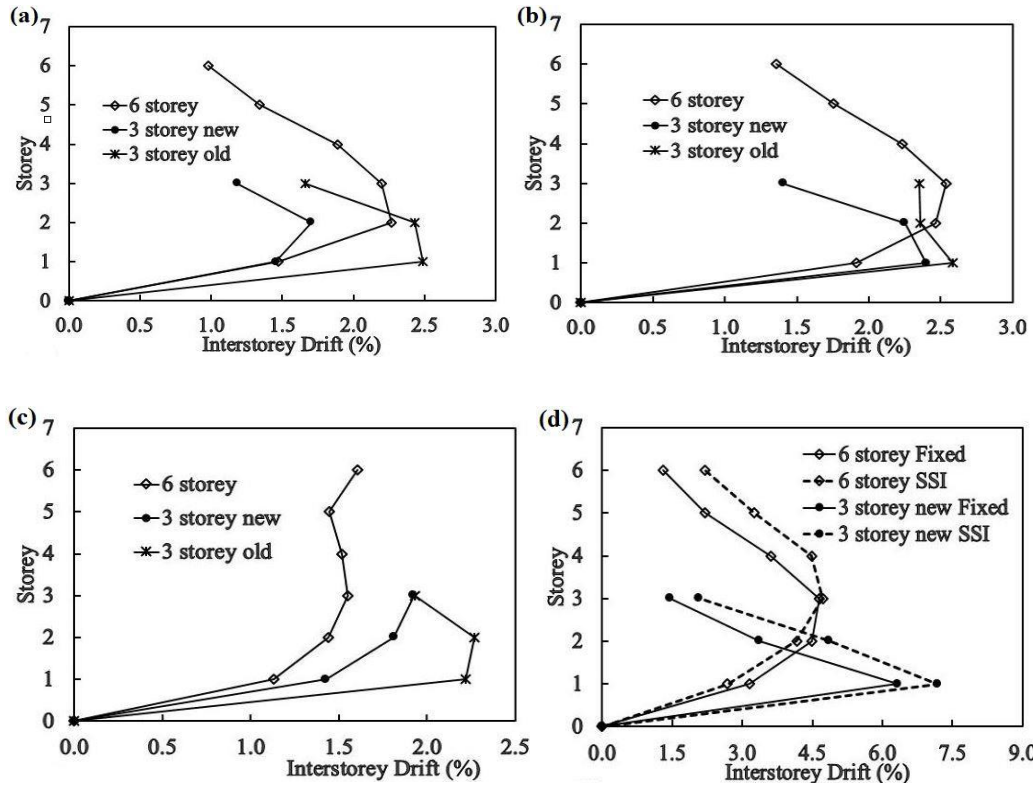

Figure 3-16 Mean interstorey drift profiles for typical buildings subjected to 2475 year return period ground motions at (a) rock; (b) shallow stiff soil; (c) soft rock and (d) soft soil sites.

Observing the mean maximum interstorey drift of typical buildings in Tables 3-10 to 3-12 and comparing with the drift limits of Vision 2000 in Table 3-8, it can be seen that the performance of the '3 storey new' building is superior to that of '6 storey' and '3 storey old' buildings under the ground motions predicted in Thimphu. On the other hand, '3 storey old' building is found to be the most vulnerable structure with higher interstorey drift values. From Table 3-10, it can be observed that '6 storey' building undergoes severe damage at the rock, shallow stiff soil and soft rock sites, while it collapses at soft soil site under the 475 year return period ground motions. Under the 2475 year return period ground motions, the '6 storey' building undergoes severe damage at rock and soft rock sites and collapses at shallow stiff soil and soft soil sites. It is interesting to note that interstorey drift value at soft rock site for the 475 year return period ground motion is higher than that of the 2475 year return period ground motion. This is found to be due to the higher spectral acceleration value of the 475 year return period ground motion corresponding to the fundamental period of the '6 storey' building.

Similarly, '3 storey new' building experiences irreparable damage at rock site, severe damage at shallow stiff soil and soft rock sites and collapses at soft soil site for the 475 year return period ground motions. As for the 2475 year return period ground motion, the '3 storey new' building experiences severe damage at the rock, shallow stiff soil and soft rock sites while it collapses at the soft soil sites. An extremely large interstorey drift predicted at soft soil site corresponding to the 2475 year return period ground motion is found to be due to the resonance wherein the fundamental period of the '3 storey new' building coincides with the site natural period of the soft soil.

With the mean interstorey drift in between 1.5% and 2.5%, the '3 storey old' building experiences severe damage at the rock, shallow stiff soil and soft rock sites under the 475 year return period ground motion. The building also suffers severe damage at rock and soft rock sites, but collapses at shallow stiff soil site under the 2475 year return period ground motion. As noted earlier, the analysis failed to run for 14 out of 16 combinations of random variables at soft soil site due to the large excessive response. This implies that the '3 storey old' building collapses at soft soil site for both the 475 and 2475 year return period ground motions.

As shown in Figures 3-15(d) and 3-16(d), SSI is slightly detrimental for the typical buildings with higher interstorey drift values as compared to the fixed support case. It can also be observed from Figure 3-16(c) that the interstorey drift profile of '3 storey new' building at soft rock site is quite unique and similar to the displacement profile of the buildings. This could be due to the significant contribution from the second mode, whose period correspond to much higher spectral acceleration than that of the first mode period as observed from Figure-3(b) and Table 3-9.

The maximum interstorey drift values in Tables 3-10 to 3-12 and interstorey drift profiles in Figures 3-15 and 3-16 also highlight the occurrence of the maximum interstorey drift at different levels of the buildings for different return periods of ground motion. The interstorey drift pattern of the building is highly influenced by the ratio of beam to column stiffness, intensity of ground motion and contribution from higher modes (Akkar et al., 2004; Alavi and Krawinkler, 2004; Adiyanto et al., 2011; Moniri, 2014). As the ratio of beam to column stiffness increases, the maximum interstorey drift shifts to the lower storeys and vice versa. Similarly, increase in the intensity of ground motion causes the maximum interstorey drift to shift towards the lower storeys, while the effect of higher modes shifts the maximum interstorey drift to the upper storeys. The maximum interstorey drift of '6 storey' building occurs at the second floor for 475 year return period ground motion and shifts to the third floor for 2475 year return period ground motion. Matching the fundamental periods in Table 3-9 to that of response spectral acceleration values in Figure 3-3, the shift of the maximum interstorey drift to the third floor could be due to the sizeable contribution of the second and third modes. While evaluating the seismic performance of 6 storey, 10 storey and 15 storey buildings under the near-fault ground motions, Moniri (2014) also reported the influence of higher modes to the 6 storey building. Moreover, the higher stiffness of columns in comparison to beams of the '6 storey' building also contributed role in shifting it to the upper floor. The occurrence of the maximum interstorey drift of '3 storey new' building under the 475 year return period ground motion is at the second floor level at the rock, shallow stiff soil and soft rock sites while it is at the first floor level at the soft soil site. Under the 2475 year return period ground motion, the maximum interstorey drift shifts to the first storey level at the shallow stiff soil and soft soil sites. This could be due to the increase in the intensity of ground motion which causes the maximum interstorey drift to shift towards the lower floors. The occurrence of the maximum interstorey drift at the third floor level under the 2475 year return period ground motion at the soft rock site is due to the influence of the second mode as evident from matching the fundamental periods to the response spectra in Figure 3-3(b). With exception to the maximum interstorey drift at the soft rock site under 2475 year return period ground motion, the maximum interstorey drift of '3 storey old' building occurs at the first floor level under both the 475 and 2475 year return period ground motions . As can be estimated from Table 3-2, beams are stronger than columns for '3 storey old' building and hence the higher value of beam to column stiffness ratio, which in combination with the influence of the first mode result in the maximum interstorey drift to occur at the first floor level for the '3 storey old' building.

The damages predicted above are solely based on the distinct drift limits and a single mean interstorey drift value. Referring to Table 3-10 for '6 storey' building, it can be observed that

severe damage is predicted at the rock site when subjected to both the 475 and 2475 year return period ground motions although there is a significant difference in their interstorey drift values. The predicted interstorey drift values are 1.518% and 2.268% when subjected to the 475 and 2475 year return period ground motions, respectively. In practice, a building would undergo different damages since the 2475 year return period ground motion is more severe than that of the 475 year return period ground motion. Similarly, severe damage is predicted for both the '6 storey' and '3 storey old' buildings, although '6 storey' building has lower interstorey drift value of the two. This is the main limitation of assessing the performance of structures based on the distinct damage boundary and using the deterministic or single interstorey drift value. Probabilistic and fuzzy probabilistic analysis are hence used to provide the more reasonable quantitative assessment of the damage probability.

Based on the probabilistic information in Tables 3-10 to 3-12 and damage limits in Table 3-8, damage probabilities of typical buildings are estimated from Equations (3.2). However, as discussed in the previous section, the damage probabilities determined from Equation (3.2) is based on the distinct damage boundaries which are not realistic and practical. Although it provides a reasonable indication of the damage of structures, yet it still has the ambiguity in defining the damage boundaries as discussed above. Hence, fuzzy probability theory is employed to solve the ambiguity of damage boundaries by introducing the membership function in Equation (3.3). Using the triangular membership function as shown in Figure 3-14, the damage probabilities of the typical buildings are calculated. The damage probabilities of typical buildings with fixed support for 475 and 2475 year return period ground motions are given in Tables 3-13 to 3-15. Table 3-16 shows the damage probabilities of the '6 storey' and '3 storey new' buildings incorporating SSI for the same ground motions.

Table 3-13 Failure probabilities of '6 storey' building with fixed support.

	Damage Category				
Site Class	Negligible (%)	Repairable (%)	Irreparable (%)	Severe (%)	Collapse (%)
a) Conventional analysis from 475 year return period ground motion					
Rock	0.000	0.000	49.379	50.594	0.026
Shallow stiff	0.000	0.000	15.169	79.994	4.837
Soft rock	0.000	0.000	35.909	63.857	0.234
Soft soil	0.000	0.000	0.005	17.132	82.864
b) Fuzzy analysis from 475 year return period ground motion					
Rock	0.000	0.018	48.305	51.374	0.303
Shallow stiff	0.000	0.006	22.826	68.719	8.448
Soft rock	0.000	0.013	40.159	58.668	1.160
Soft soil	0.000	0.000	0.143	20.850	79.007
c) Conventional analysis from 2475 year return period ground motion					
Rock	0.000	0.000	0.000	90.692	9.308
Shallow stiff	0.000	0.000	0.006	48.129	51.864
Soft rock	0.000	0.000	38.563	61.437	0.000
Soft soil	0.000	0.000	0.000	0.000	100.000
d) Fuzzy analysis from 2475 year return period ground motion					
Rock	0.000	0.000	0.324	72.531	27.145
Shallow stiff	0.000	0.000	0.470	47.109	52.420
Soft rock	0.000	0.000	44.766	55.199	0.035
Soft soil	0.000	0.000	0.000	0.000	100.000

Table 3-14 Failure probabilities of '3 storey new' building with fixed support.

	Damage Category				
Site Class	Negligible (%)	Repairable (%)	Irreparable (%)	Severe (%)	Collapse (%)
a) Conventional analysis from 475 year return period ground motion					
Rock	0.001	6.262	90.688	3.022	0.027
Shallow stiff	0.000	0.000	50.867	48.557	0.577
Soft rock	0.000	0.029	88.256	11.674	0.041
Soft soil	0.000	0.072	14.310	32.615	53.003
b) Fuzzy analysis from 475 year return period ground motion					
Rock	0.038	30.652	63.057	6.192	0.060
Shallow stiff	0.000	0.273	48.590	49.628	1.510
Soft rock	0.000	6.199	73.542	20.121	0.138
Soft soil	0.001	0.848	14.385	31.341	53.425
c) Conventional analysis from 2475 year return period ground motion					
Rock	0.000	0.004	38.819	53.376	7.801
Shallow stiff	0.000	0.000	2.907	58.472	38.621
Soft rock	0.000	0.004	26.797	55.488	17.711
Soft soil	0.000	0.000	0.000	0.075	99.925
d) Fuzzy analysis from 2475 year return period ground motion					
Rock	0.000	0.886	38.169	51.246	9.699
Shallow stiff	0.000	0.001	6.335	52.904	40.760
Soft rock	0.000	0.579	27.834	51.915	19.672
Soft soil	0.000	0.000	0.000	0.143	99.857

Table 3-15 Failure probabilities of '3 storey old' building with fixed support.

	Damage Category				
Site Class	Negligible (%)	Repairable (%)	Irreparable (%)	Severe (%)	Collapse (%)
a) Conventional analysis from 475 year return period ground motion					
Rock	0.000	0.000	18.289	75.025	6.686
Shallow stiff	0.000	0.000	0.000	62.017	37.983
Soft rock	0.000	0.000	15.751	73.381	10.868
b) Fuzzy analysis from 475 year return period ground motion					
Rock	0.000	0.023	24.272	65.674	10.032
Shallow stiff	0.000	0.000	0.000	53.725	46.275
Soft rock	0.000	0.027	21.197	64.476	14.300
c) Conventional analysis from 2475 year return period ground motion					
Rock	0.000	0.000	0.000	53.561	46.439
Shallow stiff	0.000	0.000	0.004	42.540	57.456
Soft rock	0.000	0.000	0.343	75.883	23.774
d) Fuzzy analysis from 2475 year return period ground motion					
Rock	0.000	0.000	0.036	51.058	48.906
Shallow stiff	0.000	0.000	0.346	43.126	56.528
Soft rock	0.000	0.000	3.474	66.301	30.225

Table 3-16 Probabilities of '6 storey' and '3 storey new' buildings at soft soil site incorporating SSI.

	Damage Category				
Structure	Negligible (%)	Repairable (%)	Irreparable (%)	Severe (%)	Collapse (%)
a) Conventional analysis from 475 year return period ground motion					
6 storey	0.000	0.000	0.002	15.854	84.144
3 storey new	0.000	0.000	1.475	24.216	74.309
b) Fuzzy analysis from 475 year return period ground motion					
6 storey	0.000	0.000	0.090	20.205	79.705
3 storey new	0.000	0.004	2.567	23.727	73.701
c) Conventional analysis from 2475 year return period ground motion					
6 storey	0.000	0.000	0.000	0.001	99.999
3 storey new	0.000	0.000	0.000	0.000	100.000
d) Fuzzy analysis from 2475 year return period ground motion					
6 storey	0.000	0.000	0.000	0.019	99.981
3 storey new	0.000	0.000	0.000	0.000	100.000

Comparing the damage probabilities predicted from conventional and fuzzy analyses in Tables 3-13 to 3-15, it can be observed that the difference in damage probabilities predicted from the two analyses ranges from 1% to 28%. However, this comparison excludes the damage

probability at soft soil site where there is 100% damage with excessive interstorey drifts. In general, the damage probabilities predicted by the two methods are comparable without significant variation. However, the damage probabilities predicted by fuzzy analyses are more practical since ambiguity of damage boundary is considered in the analysis. If the damages are to be converted into a monetary figure, even a very small difference could be very significant. Hence, an analysis that considers the fuzziness in damage criteria is more practical and gives more rational seismic loss estimations.

Based on the fuzzy probability analyses, it can be observed from Tables 3-13 to 3-15 that the typical buildings in Bhutan experience a high probability of irreparable and severe damages at the rock, shallow stiff soil and soft rock sites and high probability of collapse at the soft soil site under the ground motions considered. The '3 storey new' and '3 storey old' buildings respectively exhibit the best and the worst performances among the three typical building types. For example, the probabilities of collapse from fuzzy probability analysis at shallow stiff soil site under the 475 year return period ground motion are 1.51%, 8.45% and 46.28% for '3 storey new', '6 storey' and '3 storey old' buildings, respectively. Similarly, the probabilities of collapse at the shallow stiff soil site under 2475 year return period ground motion are 40.76%, 52.42% and 56.53% respectively for '3 storey new', '6 storey' and '3 storey old' buildings. Comparing the failure probability values at soft soil site in Tables 3-13 to 3-14 and Table 3-16 for fixed and spring support, it is evident that SSI has no significant effect on '6 storey' building while it has a detrimental effect on '3 storey new' building. For instance, the probability of collapse with and without consideration of SSI at the soft soil site for the '6 storey' building are 79.71% and 79.01%, respectively under the 475 year return period ground motion. Under the same ground motion, the probability of collapse of '3 storey new' buildings with and without consideration of SSI are 73.70% and 53.42%, respectively.

The high damage probability of the '3 storey old' building is expected since it was not properly designed and its structural details were assumed in line with the structural details of the buildings built prior to the adoption of Indian Seismic Code in 1997. As shown in Table 3-3, the structural members and reinforcement used for '3 storey old' building are very nominal in addition to the use of 15 MPa concrete. However, it is not expected for the '6 storey' and '3 storey new' buildings to experience the high probability of irreparable and severe damages. They were designed according to the Indian Seismic Code and were expected to perform better than that predicted in this study. The high probability of damage could be due to the use of low concrete strength in the current construction practice in Bhutan, which results in large interstorey drift. The large interstorey drift and hence the high probability of damage could also be due to the inability of incorporating ductile detailing in the modelling. The high

probability of damages also questions the adequacy of directly using Indian Seismic Code in Bhutan.

3.9 Conclusion

A comprehensive study on the performance of RC buildings in Bhutan is carried out. Three typical RC buildings in Bhutan are considered for the probabilistic seismic assessment. Unlike in many studies where the performance of buildings is assessed based on the distinct interstorey drift limits, a more rational approach based on the fuzzy probability analysis is employed in this study.

The main outcome that transpired from this study is the prediction of logical and realistic damage probabilities of the RC buildings in Bhutan. The results reveal that RC buildings in Bhutan are very susceptible to seismic damages. Under the ground motions considered in this study, none of the buildings can be immediately occupied and there is also a very small probability of remaining them in the operational state. As expected, '3 storey new' and '6 storey' buildings, which were designed following the Indian Seismic Code perform better than that of '3 storey old' building. However, these buildings also suffer higher probability of irreparable and severe damages under the 475 year return period ground motion at rock, shallow stiff and soft rock sites while the high probability of severe damage and higher probability of collapse are predicted under the 2475 year return period ground motion. As for the '3 storey old' building that was built before the adoption of Indian Seismic Code, high probability of severe damage is predicted under the 475 year return period ground motion and almost an equal probability of severe damage and complete collapse are predicted under the 2475 year ground motion at rock, shallow stiff soil and soft rock sites. At the soft soil sites, high probability of collapse is predicted for '3 storey new' and '6 storey' buildings under the ground motions of both the return periods. On the other hand '3 storey old' building suffers complete collapse at the soft soil site.

It is observed that high probability of damages experienced by RC buildings in Bhutan could be mainly due to the use of low concrete grade in the construction. The highest grade of concrete currently used for the construction of buildings in Bhutan is 25 MPa, while in many existing buildings concrete grade of as low as 15 MPa was used. The low concrete grade reduces the stiffness of the building which in turn results in the high deformation and hence the high damages of RC buildings during the seismic excitations. It is also possible that the direct use of Indian Seismic Code for the design of RC buildings in Bhutan is not adequate as concluded in chapter 2. Hence, the use of higher concrete strength and investigating the direct

use of Indian Seismic Code in Bhutan could be the way forward for improving the performance of these buildings.

In addition to the realistic information on the performance of RC buildings in Bhutan, this study could also shed light on the performance of RC buildings in the Himalayan region such as Nepal and North Eastern India where the construction types and seismicity are very much similar.

3.10 References

ACI 318-14 (2014). *Building code requirements for Structural Concrete*. American Concrete Institute, Detroit, MI.

Adiyanto, M. I., Faisal, A., & Majid, T. A. (2011). Nonlinear Behaviour of Reinforced Concrete Building under Repeated Earthquake Excitation. In: *Proceedings of the International Conference on Computer and Software Modelling*, Singapore.

Akkar, S., Gülkan, P., & Yazgan, U. (2004). A simple procedure to compute the interstory drift for frame type structures. In: *Proceedings of the 13th World Conference on Earthquake Engineering,* Vancouver, B. C., Canada, 1-6 August.

Alavi, B., & Krawinkler, H. (2004). Behavior of moment-resisting frame structures subjected to near-fault ground motions. *Earthquake Engineering Structural Dynamics, 33* (6), 687-706.

AS 3600 (2002). *Concrete Structures*. Standards Australia International.

AS1170.4 (2007). *Australian Standard for structural design actions. Part 4: Earthquake actions in Australia*. Standards Australia.

ASCE/SEI 41-13 (2014). *Seismic Rehabilitation of Existing Buildings*. American Society of Civil Engineers, Reston, Virginia.

ATC-40 (1996). *Seismic Evaluation and Retrofit of Concrete Buildings volume 1*. Applied Technology Council, Redwood City, California.

Barlett, F. M., & MacGregor, J. G. (1996). Statistical analysis of the compressive strength of concrete in structures. *ACI Material, 93* (2), 158-68.

Basu, P. C., Shylamoni, P., & Roshan, A. D. (2004). Characterisation of steel reinforced for RC structures: An overview and related issues. *The Indian Concrete Journal*, 19-30.

BS 8110 (1985). *Structural use of concrete –Part I Code of practice for design and construction*. British Standard.

Calvi, G. M., Pinho, R., & Crowley, H. (2006). State-of-the-knowledge on the period elongation of RC buildings during strong ground shaking. In: *Proceedings of the 1st European Conference on Earthquake Engineering and seismology*, Geneva, Switzerland.

Chaulagain, H., Rodrigues, H., Spacone, E., & Varum, H. (2015). Seismic response of current RC buildings in Kathmandu Valley. *Structural Engineering and Mechanics, 53* (4), 791-818.

CSI (2006). *Nonlinear Analysis and Performance Assessment for 3-D Structures.* Computers and Structures, Inc., Berkeley.

Dorji, J. (2009). *Seismic performance of brick infilled RC frame structures in low and medium rise buildings in Bhutan*. Master degree thesis. Brisbane, Australia, Centre for Built Environment and Engineering Research, Queensland University of Technology, OLD, Australia.

Duan, H., & Hueste, M. B. D. (2012). Seismic performance of a reinforced concrete frame building in China. *Engineering Structures*, 41, 77-89

Dunand, F., Guéguen, P., Bard, P. Y., Rodgers, J., & Celebi, M. (2006). Comparison of the dynamic parameters extracted from weak, moderate and strong building motion. In: *Proceedings of the 1st European Conference of Earthquake Engineering and Seismology*, Geneva, Switzerland, 1021.

Ellingwood, B. (1977). Statistical analysis of RC beam-column interaction. *Journal of Structural Division, ASCE, 103* (ASCE 13061 Proceeding).

Elwood, K. J., & Eberhard, M. O. (2006). *Effective stiffness of reinforced concrete columns*. Research Digest No. 2006-1, Pacific Earthquake Engineering Research Centre, PEER, University of California, Berkeley, California.

Eurocode 8 (2002). *Design of Structures for earthquake resistance–Part 1: General rules, seismic actions and rules for buildings*. European Standard, NF EN, 1.

FEMA 356 (2000). *Prestandard and Commentary for the Seismic Rehabilitation of Buildings*. Federal Emergency Management Agency, American Society of Civil Engineers, Reston, Virginia.

Gu, X., & Lu, Y. (2005). A fuzzy–random analysis model for seismic performance of framed structures incorporating structural and non-structural damage. *Earthquake Engineering and Structural Dynamics, 34* (10), 1305-1321.

Haselton, C. B., & Deierlein, G. G. (2007). *Assessing seismic collapse safety of modern reinforced concrete moment frame building*s. Report No. 2007/08, Pacific Earthquake Engineering Research Center, PEER, University of California, Berkeley, California.

Haselton, C. B., Goulet, C. A., Mitrani-Reiser, J., Beck, J. L., Deierlein, G. G., Porter, K. A., Stewart, J. P., & Taciroglu, E. (2008). *An assessment to benchmark the seismic performance of a code-conforming reinforced-concrete moment-frame building*. Report No. 2007/12, Pacific Earthquake Engineering Research Center, PEER, University of California, Berkeley, California.

Ibarra, L. F., Medina, R. A., & Krawinkler, H. (2005). Hysteretic models that incorporate strength and stiffness deterioration. *Earthquake Engineering and Structural Dynamics, 34*, 1489-1511.

IBC (2003). *International Building Code*. International Code Council, Falls Church, VA.

IS 1893 (2002). *Criteria for Earthquake Resistant Design of Structures –Part I: General provisions and buildings*. Bureau of Indian Standards, New Delhi; 2002.

IS 456 (2000). *Indian Standards for Plain and Reinforced Concrete*. Bureau of Indian Standards, New Delhi, India.

Katsanos, E. I., Sextos, A. G., & Elnashai, A. S. (2012). Period elongation of nonlinear systems modeled with degrading hysteretic rules. In: *Proceedings of the 15th World Conference on Earthquake Engineering*, Lisbon.

Kim, T., & Kim, J. (2009). Seismic demand of an RC special moment frame building. *The Structural Design of Tall Buildings, 18* (2), 137-147.

Kirke, A., & Hao, H. (2004). Estimation of failure probabilities of RC frame structures in Singapore to the simulated largest credible ground motion. *Engineering Structures, 26*, 139-150.

Kueht, E., & Hueste, M. B. (2009). Impact of code requirements in the central United States: Seismic performance assessment of a reinforced concrete building. *Journal of Structural Engineering, 135* (4), 404-413.

Liang, J., & Hao, H. (2007). Effect of uncertain earthquake source parameters on ground motion simulation using the empirical Green's function method. In: *Proceedings of Australian Earthquake Engineering Society 2007 Conference*, Wollongong, New South Wales, Australia.

Low, H. S., & Hao, H. (2001). Reliability analysis of reinforced concrete slabs under explosive loading. *International Journal of Structural Safety, 23* (2), 157-78.

Lynch, K. P., Rowe, K. L., & Liel, A. B. (2011). Seismic performance of reinforced concrete frame buildings in Southern California. *Earthquake Spectra, 27* (2), 399-418.

Mirza, S. A., & MacGregor, J. G. (1979). Variability of mechanical properties of reinforcing bars. *Journal of Structural Division, ASCE, 105*, 751-66.

Mirza, S. A., & MacGregor, J. G. (1979). Variations in dimensions of reinforced concrete members. *Journal of Structural Division, ASCE, 105*, 921-37.

Mirza, S. A., Hatzinikolas, M., & MacGregor, J. G. (1979). Statistical descriptions of strength of concrete. *Journal of Structural Division, ASCE, 80*, 167-76.

Moniri, H. (2014). *Evaluation of Seismic Performance of Reinforced Concrete Buildings Using Incremental Dynamic Analysis (IDA) for Near Field Earthquakes*. Ph.D. thesis. Eastern Mediterranean University, Cyprus.

Negro, P., & Colombo, A. (1997). Irregularities induced by non-structural masonry panels in framed buildings. *Engineering Structures, 19*, 576-585.

Negro, P., Pinto, A., Verzeletti, G., & Magonette, G. (1996). PsD test on four-story R/C building designed according to Eurocodes. *Journal of Structural Engineering, 122*, 1409-1417.

Negro, P., Verzeletti, G., Magonette, G., & Pinto, A. (1994). *Test on a four storey full scale RC frame designed according to Eurocode 8 and 2*. Preliminary report, Joint Research Centre, Italy.

Nielson, B. G., & DesRoches, R. (2007). Seismic fragility methodology for highway bridges using a component level approach. *Earthquake Engineering and Structural Dynamics, 36* (6), 823-839.

Pakdamar, F., & Güler, K. (2008). Fuzzy logic approach in the performance evaluation of reinforced concrete structures (flexible performance). In: *Proceedings of the 14th World Conference on Earthquake Engineering*, Beijing, China, October 12-17.

Panagiotakos, T. B., & Fardis, M. N. (2001). Deformations of reinforced concrete members at yielding and ultimate. *Structural Journal, 98* (2), 135-148.

Panagiotakos, T. B., & Fardis, M. N. (2004). Seismic performance of RC frames designed to Eurocode 8 or to the Greek codes 2000. *Bulletin of Earthquake Engineering, 2* (2), 221-259.

Raju, K. R., Cinitha, A., & Iyer, N. R. (2012). Seismic performance evaluation of existing RC buildings designed as per past codes of practice. *Sadhana, 37* (2), 281-297.

Rezaei, E., & Massumi, A. (2014). Seismic performance of reinforced concrete frame buildings designed by Iranian seismic code. *Journal of Seismology and Earthquake Engineering, 16* (3), 209-217.

Rosenbluth, E. (1981). Two-point estimates in probabilities. *Applied Mathematical Modelling, 5* (5), 329-335.

Sadjadi, R., Kianoush, M. R., & Talebi, S. (2007). Seismic performance of reinforced concrete moment resisting frames. *Engineering Structures, 29* (9), 2365-2380.

Thinley, K., Hao, H., & Tashi, C. (2014). Seismic performance of reinforced concrete buildings in Bhutan. In: *Proceedings of Australian Earthquake Engineering Society 2014 Conference*, Lorne, Victoria, Australia, 21-23 November.

Thinley, K., Hao, H., & Tashi, C. (2017). Seismic Performance of Reinforced Concrete Buildings in Thimphu, Bhutan. *International Journal of Structural Stability and Dynamics***,** *17* (7), 1750074.

UNDP Report (2006). *Report on Thimphu Valley Earthquake Risk Management Program*. Standards and Quality Control Authority, Ministry of Works and Human Settlement, Thimphu, Bhutan.

Vision 2000 (1995). *Performance Based Seismic Engineering of Buildings; conceptual framework*. Structural Engineers Association of California, Sacramento, CA.

Wu, C., Hao, H., & Zhou, Y. (1999). Fuzzy-random probabilistic analysis of rock mass responses to explosive loads. *Computers and Geotechnics, 25*, 205-225.

Zadeh, L. A. (1965). Fuzzy sets. *Information and control, 8* (3), 338-353.

Zhao, G., Li, Y., & Wang, H. (1996). *Application of fuzzy-random probability theory to structural reliability*. Application of statistics and probability, Rotterdam, Balkema, ISBN 9054105631.

CHAPTER 4 SEISMIC RESPONSE ANALYSIS AND PERFORMANCE ASSESSMENT OF MASONRY INFILLED RC BUILDINGS IN BHUTAN WITHOUT AND WITH SOFT STOREY

4.1 Abstract

Bhutan locates in a high seismicity region but has no seismic design code of its own. Recent devastating earthquake in Nepal, which is located in the same region as Bhutan and with similar construction types, raises the concern on the seismic safety of building structures in Bhutan. This study is aimed at assessing the performance of masonry infilled and soft storey RC frame buildings in Bhutan under the 475 and 2475 year return period ground motions predicted from the Probabilistic Seismic Hazard Analysis. A nonlinear strut model is used to model the infill wall and the influence of openings and soil-structure interaction are considered in the analyses. The result suggests that the masonry infilled RC frame buildings in Bhutan could suffer repairable and irreparable damages under the 475 year return period ground motions and severe damages and even collapse under the 2475 year return period ground motion. The buildings with the soft storey are found to be more vulnerable than the normal masonry infilled RC buildings. The design recommendation of Indian Seismic Code improves the performance of soft storey buildings but cannot fully negate the soft storey effect. This study is the first such effort in assessing the performance of general building stocks in the high seismicity Bhutan. The results can guide the seismic strengthening options and can be used for further loss predictions for seismic preparedness of the country.

4.2 Introduction

Reinforced concrete frame with masonry infill wall is the most common building structures in Bhutan and also in the other parts of the world. Simplicity in construction method combined with the cheap and readily available construction materials led to the construction of masonry infilled RC buildings in all parts of the world. However, owing to the complexity in comprehending the interaction of infill wall with the surrounding RC frame, engineers normally design these buildings as a bare frame (Asteris et al., 2011; Crisafulli et al., 2000). In reality, the addition of infill wall drastically changes the load transfer mechanism from frame action to more of a truss action resulting in an increase in axial forces and a decrease in bending moments in the columns (Murty and Jain, 2000). The seismic demand of infilled frame buildings also changes due to the sizeable reduction of the natural period as compared

to that of bare frame buildings (Asteris et al., 2011). Hence, designing the infilled frame as a bare frame would grossly approximate the intended performance of the buildings. This was demonstrated during the past earthquakes such as 2001 Gujarat earthquake and the very recent 2015 Nepal earthquake where a number of masonry infilled RC buildings were either collapsed or badly damaged.

In Bhutan, masonry infilled RC buildings were not even designed as bare frames until 1997 although the construction of these buildings has been started in the early 1970s. Bhutan still has no seismic design code of its own. Only in 1997, the country has adopted Indian Seismic Code for the design of buildings by simply assuming the seismicity of Bhutan in par with the neighbouring states of India. While the buildings built prior to 1997 were not designed to any specifications, the masonry infilled RC buildings built after the adoption of Indian Seismic Code were mostly designed as bare frames. Moreover, the applicability of Indian Seismic Code to the site conditions in Bhutan has never been studied. Hence, in the event of an earthquake such as the one in Nepal, there exists a real risk to the thousands of masonry infilled RC buildings that are currently standing today. The risk is further enhanced by the presence of a number of masonry infilled RC buildings with the open first storey which were either not designed to any standard or just designed as the normal bare frames. As proven to the world time and again, masonry infilled RC buildings with the open first storey were the major victims of the earthquakes in the past.

On the other hand, Bhutan is located on one of the most active seismic regions in the Himalaya where the Indo-Australian Plate is continuously being subducted under the Eurasian Plate. During the last seven and half decades, 32 earthquakes of engineering significance have occurred in Bhutan causing huge loss to lives and properties (Dorji, 2009). A number of big earthquakes had also occurred just outside Bhutan such as the 1897 M_w=8.7 Shillong Plateau, 1934 M_w=8.3 Bihar-Nepal border, 1947 M_w=7.7 upper Assam and 1950 M_w=8.6 Arunachal Pradesh earthquakes (Walling and Mohanty, 2009). Similar earthquakes cannot be ruled out in Bhutan anytime soon. Banerjee and Bürgmann (2002) and Bilham et al. (2001) had already reported the high probability of one or two big earthquakes occurring in the Himalayan region based on the seismic gap hypothesis.

In spite of high seismic risk and presence of a large number of masonry infilled RC buildings, there is no real study carried out on the performance of these buildings in Bhutan. Dorji (2009) studied the performance of masonry infilled frame buildings in Bhutan, but only used the two-dimensional building model and ground motions from other regions that do not necessarily represent those expected in Bhutan. Thinley et al. (2017) had undertaken the similar studies, using seismic ground motions predicted based on Probabilistic Seismic Hazard Analysis

(PSHA) for Bhutan, but only considered bare frame buildings. Hence, there is a real need to assess the performance of existing infilled RC buildings in Bhutan to ascertain their vulnerability on the one hand and to come up with the possible retrofitting and design strategies on the other hand.

This study is carried out to more realistically assess the performance of masonry infilled RC buildings in Bhutan using the ground motions predicted for Thimphu, Bhutan from PSHA at different soil sites for both the 475 and 2475 year return periods. Three typical masonry infilled RC buildings that represent the general building stocks in the country are considered for the study. The buildings are also studied for the soft storey effects by removing infill wall from the ground floor. The numerical models are first calibrated with the experimental results and then used for predicting the structural responses of the respective buildings. The effects of openings and soil-structure interaction are considered in the analyses. In the absence of the reference performance limits for the masonry infilled buildings in Bhutan, the performance limits specified by Ghobarah (2004) is used for assessing the infilled frame buildings. The adequacy of design provisions recommended by Indian Seismic Code for the soft storey building is also investigated. From this study, it is observed that the masonry infilled RC buildings in Bhutan would suffer repairable to irreparable damages under the 475 year return period ground motions while severe damage to complete collapse is predicted when subjected to the 2475 year return period ground motion. The soft storey buildings are found to be more vulnerable than the fully infilled RC buildings. The incorporation of design provision as per the Indian Seismic Code improves the performance of the building with the soft storey, but an alternative of strengthening only the columns of the soft storey has almost the same effect with more advantages.

4.3 Ground motions

Being located on one of the most active seismic zones in the region, a large number of earthquakes of various sizes have occurred in Bhutan. However, these earthquakes were neither recorded nor studied in detail. In the absence of the ground motions specific to the site conditions in Bhutan, Thinley et al. (2017) conducted a Probabilistic Seismic Hazard Analysis (PSHA) considering 18 seismic source zones within a distance of 400 km from Thimphu, Bhutan. Based on PSHA, they predicted ground motions at different soil sites for the return periods of 475 and 2475 years. These ground motions are used for assessing the performance of the buildings in this study since they were specifically predicted for the site conditions in Bhutan. Figure 4-1 shows the acceleration response spectra of ground motions at different soil sites for 475 and 2475 year return periods at 5% damping.

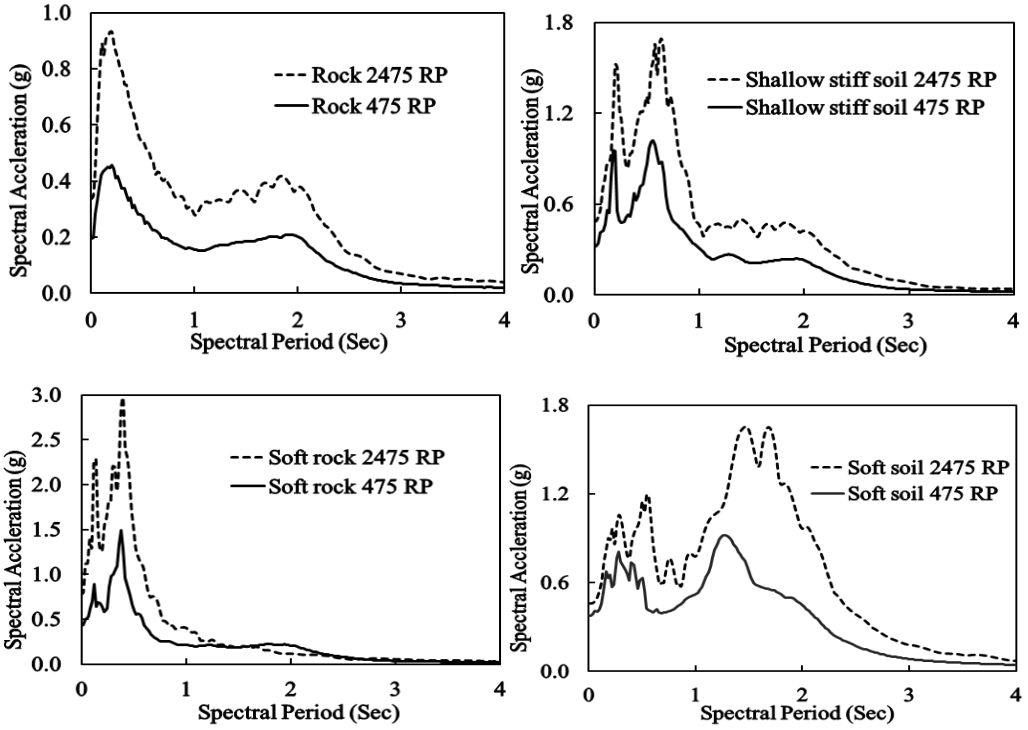

Figure 4-1 Acceleration response spectra at generic soil sites for 475 and 2475 year return period (RP) ground motions at 5% damping.

4.4 Typical buildings considered for study

Three masonry infilled RC buildings that represent the general building stocks in Bhutan are considered in this study. They are denoted as '6 storey', '3 storey new' and '3 storey old' buildings. '6 storey' and '3 storey new' buildings represent those designed and built as per the Indian Seismic Code, while '3 storey old' building represents that built prior to 1997 before the adoption of Indian Seismic Code. Brick masonry of 250mm and 125mm thick are used for all buildings as exterior and interior partition walls respectively. The masonry wall and column layout plan of these typical buildings are shown in Figure 4-2. The reinforcement and member dimension details are given in Table 4-1.

‘6 storey' and '3 storey new' buildings are the real buildings that are currently standing in Thimphu. The structural and architectural details of these buildings are obtained from the Thimphu municipal corporation. The yield strength of reinforcement used for these buildings is 415 MPa. The concrete strength of 25 MPa for columns and 20 MPa for rest of the RC members are specified for ‘6 storey building’, while 20 MPa for all RC members is specified for ‘3 storey new’ building. The live loads on floors and on the roof used for the design of these buildings are 2 kN/m^2 and 0.75 kN/m^2, respectively. Since the compressive strength of masonry wall has never been determined in Bhutan, it is adopted from the studies of Kaushik et al. (2007). From a number of experimental studies carried out on the Indian brick masonry

walls, the mean compressive strength of the brick masonry with intermediate (1:4) and weak (1:6) mortars were respectively found to be 6.6 MPa and 4.1 MPa. They also found the modulus of elasticity of masonry walls in the range of $250f_m$ to $1100f_m$, where f_m is the compressive strength of masonry wall. In this study, f_m=6.6 MPa and modulus of elasticity of $550f_m$ are adopted for '6 storey' and '3 storey new' buildings. They are assumed to be applicable to brick masonry in Bhutan since the study was conducted on Indian bricks which are also used in Bhutan. In addition, the cracking strength of 0.35 MPa is used as per Dolšek and Fajfar (2002).

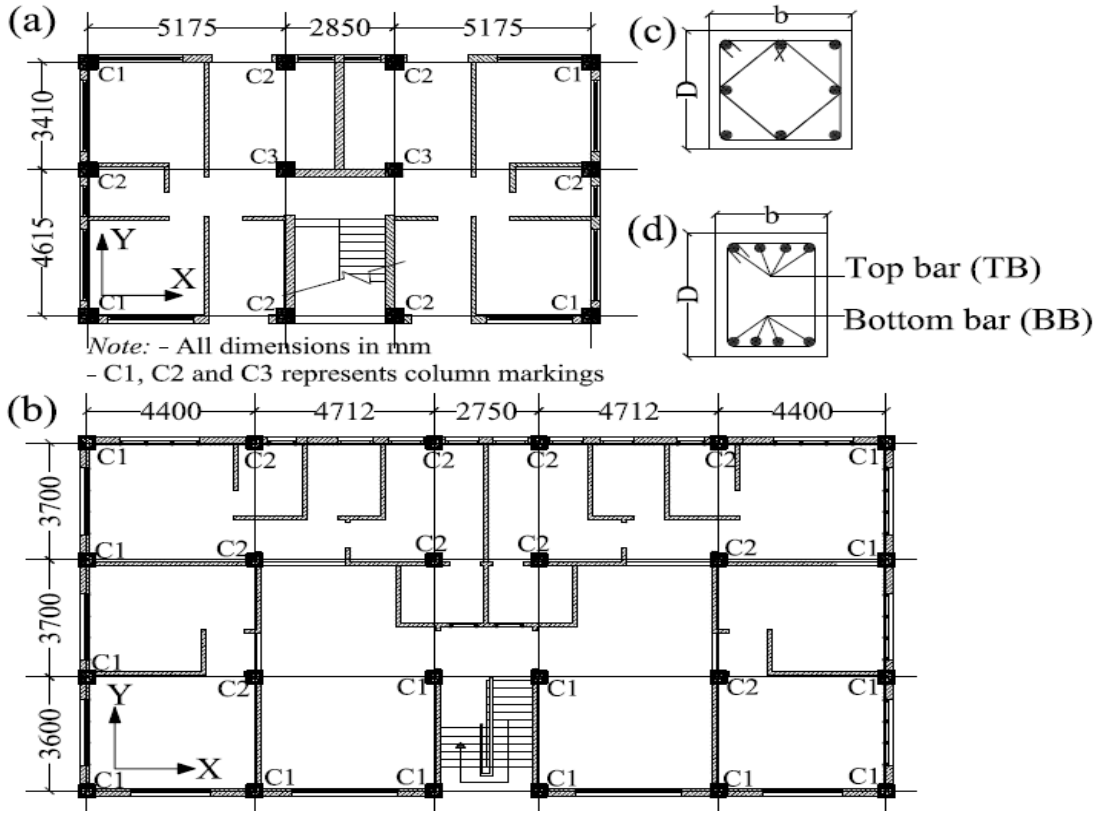

Figure 4-2 Masonry wall and column layout plan for (a) 6 storey; (b) 3 storey; (c) typical column cross section and (d) typical beam cross section.

Since there are no reliable drawings and design details available for the buildings built before 1997, the plan and elevation of the '3 storey old' building are assumed identical to that of '3 storey new' building. However, structural details such as member dimension, reinforcement, concrete grade and masonry details are adopted from the result of a non-destructive test conducted on 15 masonry infilled RC buildings under the Thimphu Valley Earthquake Risk Management Project (UNDP, 2006). The majority of the buildings examined under the project were built prior to 1997 and very similar structural details were observed in all these buildings in spite of some differences in the general layout plan. The yield strength of reinforcement

and the concrete strength used are 415 MPa and 15 MPa respectively. The compressive strength of 4.1 MPa and cracking strength of 0.25 MPa are used corresponding to weak mortar (6:1).

Table 4-1 Reinforcement and member dimensions of typical buildings

	6 storey	3 storey new	3 storey old
(a) Floor Beams (FB) and Roof Beams(RB) reinforcement			
FB along X	TB=4-20, BB=2-20+2-16	TB=4-20, BB=2-20+2-16	TB=4-12, BB=2-12+2-10
FB along Y	TB=4-20, BB=2-20+2-16	TB=2-20+2-16, BB=4-16	TB=3-12, BB=3-10
RB along X	TB=2-20+2-16, BB=4-16	TB=2-20+2-16, BB=4-16	TB=3-12, BB=3-10
RB along Y	TB=2-20+2-16, BB=4-16	TB=4-16, BB=2-16+2-12	TB=2-12+1-10, BB=3-10
Beam stirrups	8@100mmC/C till 2D from either side of column face and 8@150C/C at the centre		6@150mmC/C throughout
(b) Column reinforcement			
Column C1	8-20 + 4-16	8-20	4-16
Column C2	12-20	4-25+4-20	8-12
Column C3	4-25+8-20		
Column ties	10@90mmC/C throughout	8@100mmC/C throughout	6@150mmC/C throughout
(c) Dimensions			
Beams along X	300mm x 450mm	300mm x 400mm	250mm x 350mm
Beams along Y	300mm x 400mm	300mm x 400mm	250mm x 300mm
Columns C1 & C2	450mm x 450mm	400mm x 400mm	250mm x 250mm
Columns C3	500mm x 500mm		
Slab depth	150mmm	150mmm	100mmm

4.5 Numerical modelling and model calibration

Basically, numerical modelling of masonry infilled RC building consists of modelling the RC members and infill wall which when combined together are expected to simulate the composite response of the infilled RC building. The modelling of RC members and infill wall followed by model calibration are described in the following sections.

4.5.1 Modelling of RC members

The chord rotation model which is based on the lumped plasticity model is used for modelling the beams and columns. It is computationally inexpensive and is capable of capturing the structural response at higher deformation level. It consists of a stiff end zone and a plastic hinge at the each end of elastic beam/column as shown in Figure 4-3(a). A tri-linear force-deformation (F-D) relationship implemented in Perform 3D (CSI, 2006) software and very similar to the one developed by Ibarra et al. (2005) is employed in this study. As shown in

Figure 4-3(b), the F-D relationship is characterised by stiffness, strength and deformation parameters of the component.

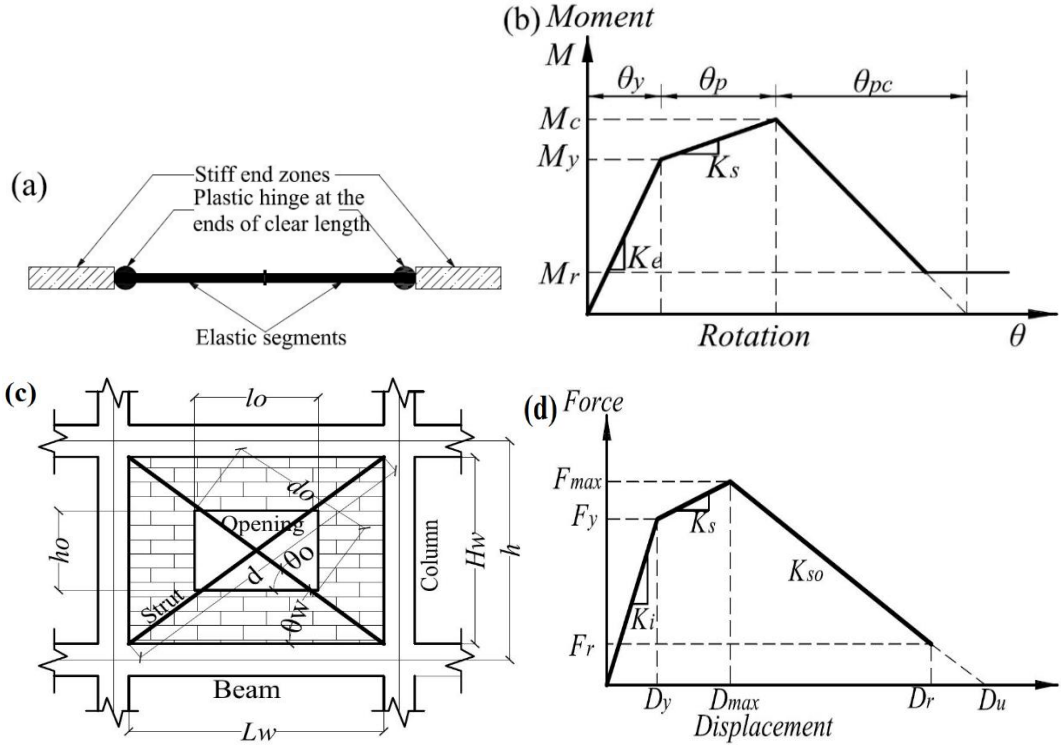

Figure 4-3 (a) Chord rotation model; (b) F-D relationship of RC members; (c) masonry infilled wall representation by equivalent strut and (d) F-D relationship of equivalent strut model.

Effective stiffness, *Ke* is normally expressed as a fraction of the flexure stiffness of a gross section in the number of studies (ACI 318-14, 2014; FEMA-356, 2000; Panagiotakos and Fardis, 2001). In this study, the effective stiffness is estimated from the expressions given by Elwood and Eberhard (2009) which were developed from the test data of 255 columns. It varies from $0.20EIg$ to $0.7EI_g$ depending on the magnitude of the axial load, where E is the modulus of elasticity of RC member and I_g is the moment of inertia of the gross section. The yield moment M_y and yield rotation θ_y are obtained from the equations given by Panagiotakos and Fardis (2001). These equations were experimentally verified by Haselton and Deierlein (2006) and found to agree well with the test data. As proposed by Haselton et al. (2008) from a number of experimental tests, the capping moment M_c is taken as $1.13M_y$. The residual moment M_r is taken as 0.001 times the capping moment as recommended in the Perform 3D (CSI, 2006) user guide. The pre-capping rotation θ_c and post-capping rotation θ_{pc} are estimated from the expressions proposed by Haselton (2008) which are also given in PEER-ATC-71-1 (2010). In addition to 3% modal damping, a small amount of stiffness proportional Rayleigh damping (0.1%) is used in the analyses to damp out the higher mode displacements. The material nonlinearity in the form of P-delta effect is also included in the analyses. The

contribution of the slab to the stiffness of the beam is taken into account by approximating the exterior and interior beams as L and T-beam respectively. Based on the span and the overall depth of beams, the effective width of the beams is estimated from the expressions given in ACI 318-14 (2014).

4.5.2 Modelling of masonry infill wall

A macro model in the form of a diagonal strut is used to model infill wall in this study. While the diagonal length, thickness and material of equivalent strut are taken same as that of the infill wall, a number of equations were proposed to determine the width of the strut. One group of researchers simply estimate the width of the strut as a fraction of the diagonal length of the wall while the other group estimate it based on the relative stiffness of the wall and frame (Holmes, 1961; Smith and Carter, 1969; Mainstone, 1974; Penelis and Kappos, 1997). The equation proposed by Mainstone (1974) for estimating the width of the diagonal strut was adopted by FEMA-274 (1997) and the same is used in this study. As shown in Figure 4-3(c), a strut in each diagonal direction is used to model the infill wall. Each diagonal strut is characterised by a force-deformation relationship as shown in Figure 4-3(d). There are a number of studies that define the F-D relationship of a single strut model. However, many are centred on the F-D relationship developed by Panagiotakos and Fardis (1996) which is briefly described here. Referring Figure 4-3(d), the initial stiffness, K_i and secant stiffness, K_s are given by

$$K_i = \frac{G_w L_w t_w}{H_w} \tag{4.1}$$

$$K_s = \frac{E_w w t_w}{d} \tag{4.2}$$

where G_w, L_w, t_w, H_w, E_w, w and d are respectively the shear modulus, length, thickness, height, modulus of elasticity, width and the diagonal length of the infill wall. The negative stiffness of the softening branch K_{so} is recommended to be less than 10% of the initial stiffness. The force corresponding to yield point is estimated from the expression

$$F_y = f_{tp} t_w L_w \tag{4.3}$$

where f_{tp}= cracking strength of the infill wall. The maximum strength of infill is assumed as $1.3F_y$ while the residual strength F_r is assumed to be less than $0.1F_y$. The displacements corresponding to the yield point D_y, maximum strength D_{max} and at residual strength D_r are given by

$$D_y = \frac{F_y}{K_i} \tag{4.4}$$

$$D_{max} = D_y + \frac{F_{max} - F_y}{K_s} \tag{4.5}$$

$$D_r = \frac{F_{max} - F_r}{K_{so}} \tag{4.6}$$

In this study, the initial stiffness of infill wall and force at yield point are estimated from Equations (4.1) and (4.3) respectively. The maximum strength is taken as $1.67F_y$ as per Dolšek and Fajfar (2008). The residual strength is taken as $0.1Fy$. The displacements at the maximum strength, D_{max} is assumed to occur at the storey drift of 0.20% for short infill wall and 0.15% for the long infill wall with window, while the displacement at collapse, D_u is taken as $5D_{max}$ as given in Dolšek and Fajfar (2008).

4.5.3 Calibration of the model

The four storey RC building which was pseudo-dynamically tested at the European Laboratory of Structural Assessment (ELSA) is considered for model calibration. The tested building was 10mx10m in plan and was designed according to Eurocodes 2 and 8 for high ductility class. An accelerogram artificially derived from the real recorded 1976 Friuli earthquake with factored nominal peak ground acceleration of 0.45g was used for the tests. The details of the experimental building and pseudo-dynamic tests can be found in Negro and Verzeletti (1996) and Negro et al. (1994).

The uniformly infilled RC frame and infilled frame with open first storey building are numerically modelled using the F-D relationships of RC frame and infill wall described in the above sections. The stiffness, strength and deformation parameters of RC frames and infill walls are estimated as defined in the modelling of RC members and modelling of infilled wall sections using the geometrical and material properties of the experimental building. The Perform 3D (CSI, 2006) program is then employed to estimate the structural responses of the experimental buildings using the ground motions used for the test. The storey displacements predicted from the numerical model is compared with the corresponding displacements obtained from the pseudo-dynamic tests. Figure 4-4(a) and 4-4(b) respectively depict the comparison of storey displacements obtained from the numerical analyses and experimental tests for the infilled frame and the soft storey buildings. From the figure, it can be seen that a very good match is achieved, indicating the accuracy of the numerical model. However, some difference in the displacement amplitudes can be observed especially at the first and second floor levels. This could be mainly due to the flexibility of the foundation slab resulted during the pseudo-dynamic test. Since it is quite complicated to assess the flexibility of the foundation

slab, it is not incorporated in the numerical model. Hence the displacement amplitudes lower than that of the test results are estimated by the numerical model. The higher displacement amplitude could also be due to its inability to incorporate the actual viscous damping during the test. Since pseudo-dynamic tests are conducted at a slower speed than the real time, a much lower damping could have actually used during the test. Similar observations were also made by Negro and Colombo (1997) and Smyrou et al. (2011) while calibrating the numerical model using the same experimental test results.

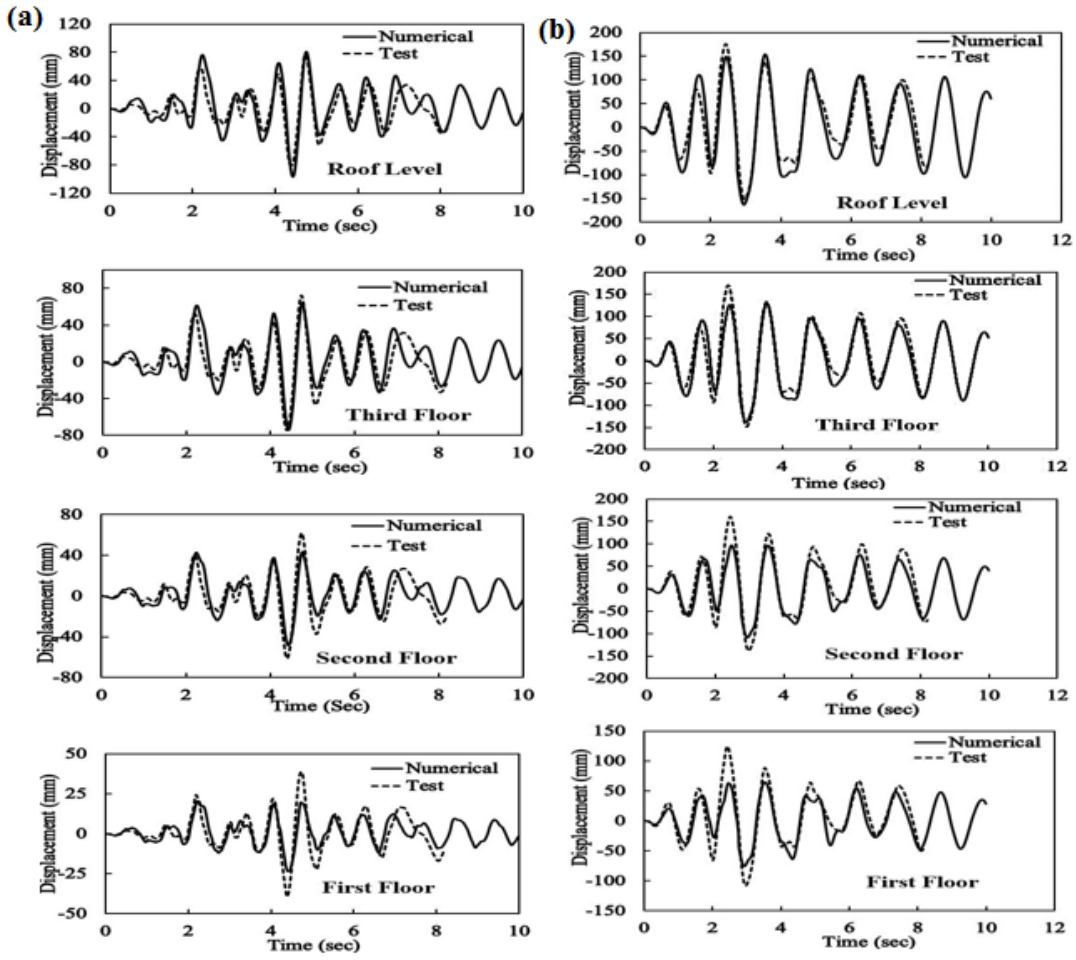

Figure 4-4 Comparisons of displacement time histories obtained from numerical analyses and experimental tests for (a) infilled frame building and (b) soft storey building.

4.6 Incorporation of opening and soil-structure interaction

4.6.1 Incorporation of opening

Due to the uncertainties in regard to the size and position of openings, prediction of structural response of infilled frame buildings with an opening is very complex. The most general understanding currently known is that the presence of opening reduces the stiffness and strength of the infill wall. As a result, many researchers such as Al-Chaar (2002), Asteris et

al. (2012), Dawe and Seah (1988), Decanini et al. (2012), Durrani and Luo (1994), Mondal and Jian (2008) and Smyrou (2006) have proposed reduction factor for the infill wall with openings. The reduction factor is multiplied by the effective width of the masonry infill wall with the opening which in turn modifies its strength and stiffness. The reduction factors proposed by each researcher vary to a great extent. In this study, reduction factor, R_f proposed by Durrani and Luo (1994) and given in Equation (4.7) is used since it approximately represents the mean reduction factors proposed by different researchers.

$$R_f = 1 - \left[1 - \frac{(dsin(2\theta) - d_o \sin(\theta + \theta_o))^2}{2L_w H_w \sin(2\theta)}\right]^2 \tag{4.7}$$

The parameters involved in Equation (4.7) can be referred from Figure 4-3(c).

4.6.2 Incorporation of soil-structure interaction (SSI)

The effect of SSI is approximately incorporated in the analyses by introducing uncoupled spring support according to the soil conditions at different sites. Owing to the complexity of incorporating the frequency dependent dynamic foundation impedance function in the analysis, only static springs are used to model the soil. The mass of foundation and radiation damping are neglected in the analyses. For the square footings founded at the shallow depth, the stiffness coefficients of the springs are estimated from ASCE/SEI 41-13 (2014) as given below:

$$K_{xy} = \frac{4.6GB}{2-\nu}\left\{\left[1 + 0.21\sqrt{\frac{D_f}{B}}\right]\left[1 + 1.6\left(\frac{2hd}{B^2}\right)^{0.4}\right]\right\} \tag{4.8}$$

$$K_z = \frac{2.35GB}{1-\nu}\left\{\left[1 + 0.22\frac{D_f}{B}\right]\left[1 + 0.32\left(\frac{2d}{B}\right)^{0.67}\right]\right\} \tag{4.9}$$

$$K_{xx} = \frac{0.5GB^3}{1-\nu}\left[1 + 2.5\frac{d}{B} + 5\frac{d^2}{B^2}\left(\frac{d}{D_f}\right)^{-0.2}\right] \tag{4.10}$$

$$K_{yy} = \frac{0.5GB^3}{1-\nu}\left\{1 + 1.4\left(\frac{d}{B}\right)^{0.6}\left[1.5 + 3.7\left(\frac{d}{B}\right)^{1.9}\left(\frac{d}{D_f}\right)^{-0.6}\right]\right\} \tag{4.11}$$

$$K_{zz} = 1.04GB^3\left[1 + 5.2\left(\frac{d}{B}\right)^{0.9}\right] \tag{4.12}$$

where K_{xy}, K_z, K_{xx}, K_{yy}, K_{zz} are horizontal stiffness along the x and y-axes, vertical stiffness along the z-axis, rocking stiffness along the x-axis, rocking stiffness along the y-axis and torsional stiffness along the z-axis respectively. A typical column footing showing various notations and axes is shown in Figure 4-5. The size of the square footing for '6 storey', '3

storey new' and '3 storey old' buildings are respectively *B*=3.5m, 2.2m and 1.5m and founded at a depth ranging from D_f=1.2 to 2.5m below the ground level. The depth of the footing pad used for '6 storey', '3 storey new' and '3 storey old' are respectively, *d*=0.75m, 0.50m and 0.35m. The effective depth of foundation ranges from *h*=1.0m to 2.0m. The effective shear modulus of soil, *G* is estimated from the shear wave velocity of soil and the respective response spectral acceleration at the short period. The Poisson's ratio, *v* used for the calculation of soil stiffness at shallow stiff soil, soft rock and soft soil sites are respectively 0.35, 0.25 and 0.45.

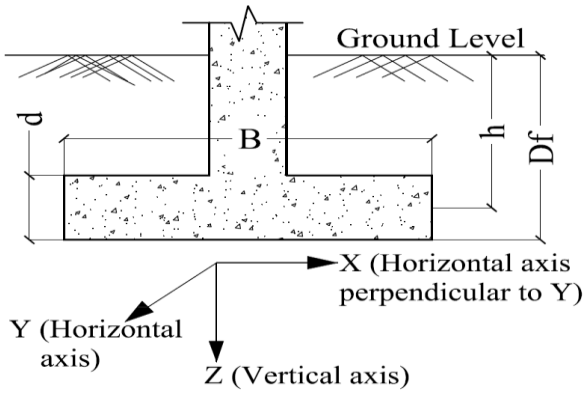

Figure 4-5 Column footing details showing various notations and axes.

4.7 Structural response of masonry infilled RC buildings

After calibrating the numerical models, nonlinear analyses of typical buildings are carried out at different soil sites under the 475 and 2475 year return period ground motions. The nonlinear analyses are first carried out for the as built masonry infilled RC buildings described in section 3. To study the response of soft storey buildings, infill walls are removed from the ground floor of these buildings and carried out the another set of nonlinear analyses. The structural responses in the form of fundamental period, interstorey drift and energy dissipation are then estimated for the infilled and soft storey buildings. The structural responses of the bare frame buildings estimated in Thinley et al. (2014) are compared with that of infilled and soft storey buildings. The pushover analyses are also carried out to better understand the response of these buildings. It is to be noted that the terms 'infilled' 'soft storey' and 'bare' mentioned in this paper refer to normal masonry infilled RC building, masonry infilled RC building with open first storey and RC frame building without masonry infill wall respectively.

The fundamental periods estimated for '6 storey' building are 2.12 sec, 0.26 sec and 1.10 sec respectively for bare, infilled and soft storey frames. The periods of 1.08 sec, 0.12 sec and 0.89 Sec are respectively estimated for bare, infilled and soft storey frames of '3 storey new' building and the periods of corresponding frames of the '3 storey old' building are 1.32 sec,

0.14 sec and 2.38 sec respectively. It is evident that the introduction of masonry infill wall drastically reduces the fundamental period of the building. The first modal period is approximately reduced by 8-10 times with the addition of infill wall. This could be due to the predominant use infill walls within the frames resulting in the significant increase in the stiffness of the buildings. The sizeable reduction of the fundamental period is also observed in the case of '6 storey' and '3 storey new' soft storey buildings. However, it is just opposite in the case of '3 storey old' soft storey building wherein its first modal period is 1.79 times higher than the corresponding bare frame building. The removal of infill wall from the ground floor in combination with the weaker ground floor columns could have made it more flexible.

Figures 4-6 to 4-8 respectively display the comparison of interstorey drift profiles of '6 storey', '3 storey new' and '3 storey old' buildings estimated at the various soil sites under the 475 and 2475 year return period ground motions. It can be observed from the figures that the structural responses exhibited by the infilled, bare and soft storey buildings are quite distinct and vary to a large extent. The maximum interstorey drift of the soft storey building invariably occurs at the first floor level while it varies from one floor to another for infilled and bare frame buildings depending on the stiffness of beams and columns, intensity of ground motion and the possible contribution from higher modes. As expected, the minimum and the maximum interstorey drift values are exhibited by the buildings at the rock and the soft soil sites respectively. With exception to the Figure 4-6(d) which is due to the resonance condition, the maximum interstorey drift values of bare and soft storey buildings are comparable to each other with some deviation. However, the maximum interstorey drift values of the masonry infilled buildings are significantly lower than the bare and soft storey buildings. This is attributed to the much higher lateral stiffness of the infilled frame buildings as compared to the bare frame buildings. It can be also observed from the figures that the soft storey effect becomes more prominent with the increase in the intensity of ground motion and the decrease in the stiffness of the soil media.

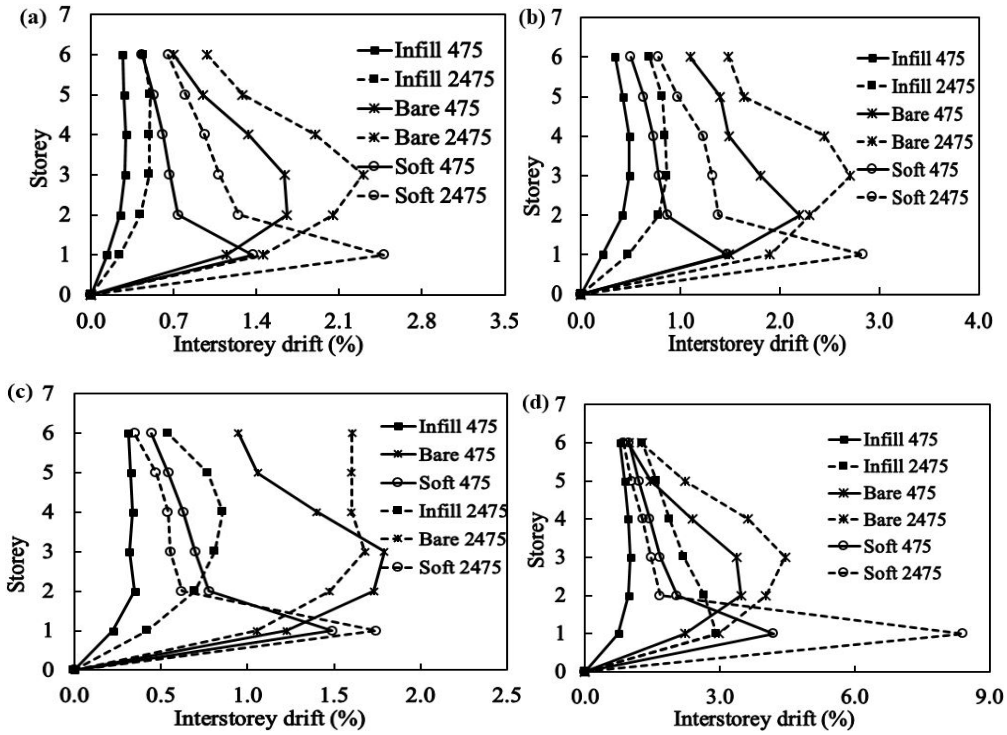

Figure 4-6 Interstorey drift profiles of '6 storey' infilled, bare and soft storey frame buildings subjected to the 475 and 2475 year return period ground motions at (a) rock; (b) shallow stiff soil; (c) soft rock and (d) soft soil sites.

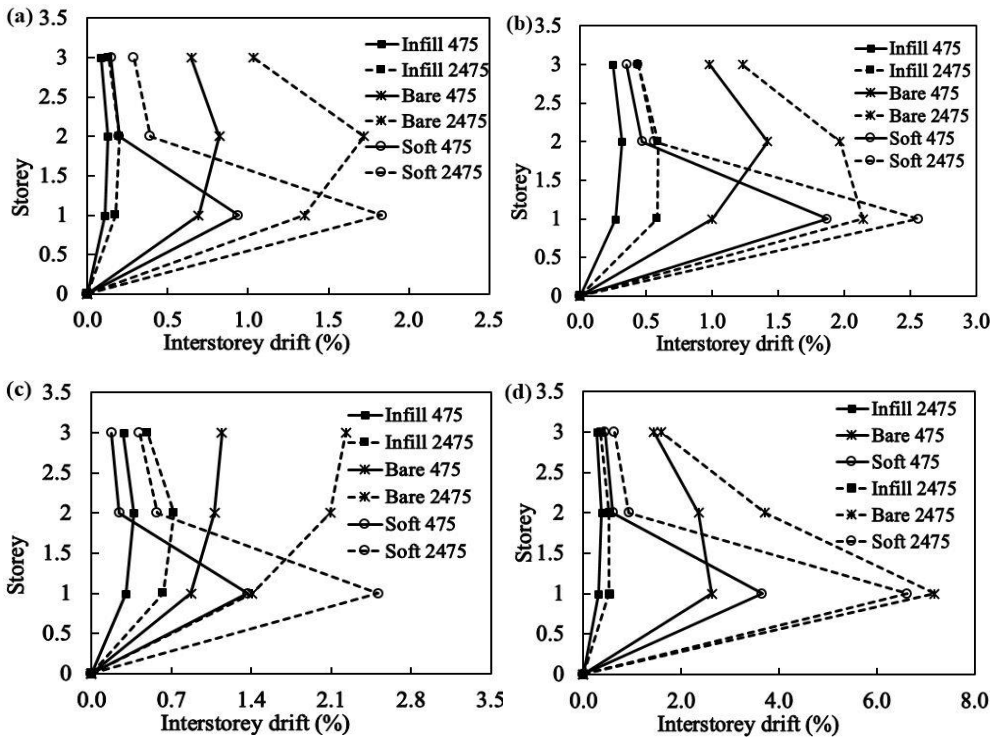

Figure 4-7 Interstorey drift profiles of '3 storey new' infilled, bare and soft storey frame buildings subjected to the 475 and 2475 year return period ground motions at (a) rock; (b) shallow stiff soil; (c) soft rock and (d) soft soil sites.

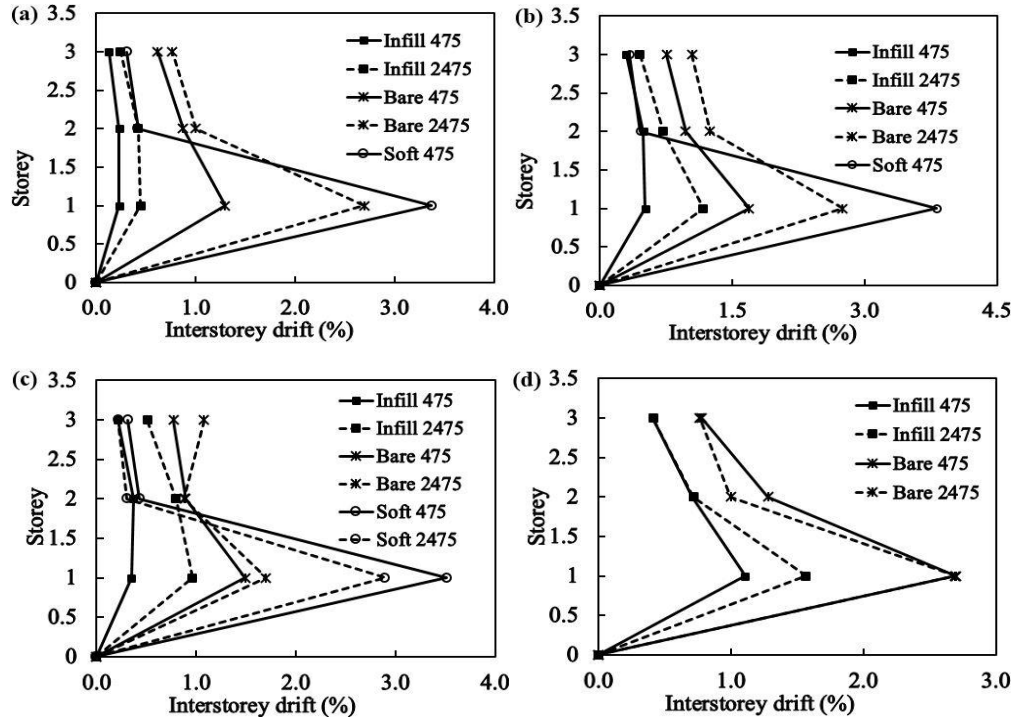

Figure 4-8 Interstorey drift profiles of '3 storey old' infilled, bare and soft storey frame buildings subjected to the 475 and 2475 year return period ground motions at (a) rock; (b) shallow stiff soil; (c) soft rock and (d) soft soil sites.

Figure 4-9 highlights the results of pushover analyses carried out on the three typical buildings. As illustrated in the figure, the maximum strength of infilled frame building is approximately 1.5 times higher than that of the corresponding bare frame building. The response of soft storey building is in between the bare and infilled frame buildings for '6 storey' and '3 storey new' buildings but is lower than both the buildings for the '3 storey old' building. This is due to the weak ground floor columns of '3 storey old' building which becomes more flexible when infill wall is removed. The figure also reveals the higher stiffness and lower ductility of infilled frame buildings as compared to the bare frame buildings. Similar observations were also made by Sattar and Liel (2010) for the pre-1975 California masonry infilled RC buildings.

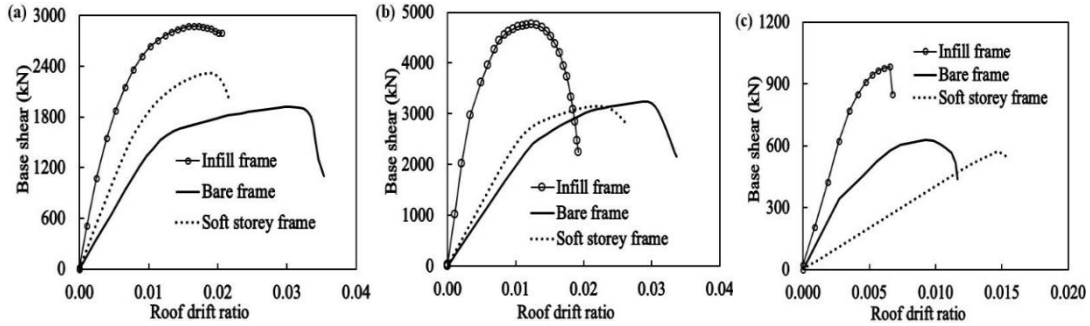

Figure 4-9 Pushover curves for bare, infilled and soft storey frames for (a) 6 storey; (b) 3 storey new and (c) 3 storey old buildings.

The energy dissipated by different components of typical buildings at the soft soil sites for both the 475 and 2475 year return period ground motions is given in Table 4-2. As for the bare '6 storey' and '3 storey new' buildings, majority of energy is dissipated by beams with some contribution from columns. This is expected since both the buildings were designed according to Indian Seismic Code conforming to the strong column and weak beam design concept. On the other hand, entire energy dissipation occurs in columns of '3 storey old' bare frame building. This is also expected since beams are stronger than columns wherein the inelastic action is concentrated in columns. In the case of the infilled frame buildings, most energy is dissipated by infill wall with a sizeable contribution from columns. As given in the table, the dissipation of energy by frames increases with increase in the intensity of ground motion, while the contribution from infill wall decreases. In the case of the soft storey buildings, most energy is dissipated by columns with some contribution from infill wall. The contribution of columns in dissipating seismic energy further increases with the increase in the intensity of ground motions. The dissipation of maximum energy by infill wall at low intensity ground motion clearly confirms infill wall as the first building component to undergo damages during earthquakes.

Table 4-2 Proportion of energy dissipated by different components of buildings at soft soil site under the 475 and 2475 year return period ground motions

	475 Year Return Period			2475 Year Return Period		
Building components	6 storey	3 storey new	3 storey old	6 storey	3 storey new	3 storey old
a) Bare Frames						
Beams	87.9%	67.7%	0.1%	84.2%	61.9%	0.0%
Columns	12.1%	32.3%	99.9%	15.8%	38.1%	100.0%
b) Infilled frames						
Infilled walls	68.6%	100.0%	62.9%	53.2%	96.7%	75.7%
Beams	8.9%	0.0%	0.0%	18.1%	0.0%	0.0%
Columns	22.5%	0.0%	37.1%	28.8%	3.3%	24.3%
c) Soft storey frames						
Infilled walls	17.0%	13.3%	0.0%	16.7%	3.5%	0.0%
Beams	24.6%	0.0%	0.0%	12.6%	0.1%	0.0%
Columns	58.4%	86.7%	100.0%	70.7%	96.4%	100.0%

4.8 Response of soft storey buildings designed according to Indian Seismic Code

The soft storey defined in Indian Seismic Code is the building storey whose lateral stiffness is less than 70% of the storey above or less than 80% of the average lateral stiffness of the three storeys above. The typical masonry infilled RC buildings with the open first storey in Bhutan

do qualify as the soft storey buildings. According to the Indian Seismic Code, beams and columns of the soft storey floors should be designed for 2.5 times the storey shears and moments estimated for the bare frame. Factor 2.5 is applied to all buildings with soft stories notwithstanding the extent of irregularities. Similarly, Eurocode 8 (1996) recommends the member forces of the soft storey beams and columns be increased by a factor α, which is given by

$$\alpha = \left(1 + \frac{\Delta V_{Rw}}{\sum V_{Sd}}\right) \leq q \tag{4.13}$$

where ΔV_{Rw} is the total reduction of infill wall resistance as compared to the adjacent infilled storey and $\sum V_{Sd}$ is the sum of seismic shear forces in the vertical members of the soft storey. The factor q varies from 1.5 to 4.68 depending on the ductility class and regularity of building. From the extensive studies conducted by Fardis and Panagiotakos (1997), it was found that increasing the resistance of beams only increases the ductility demand of the columns. Hence, they recommended only the lateral resistance of columns to be increased and same have been adopted by the later version of Eurocode 8 (2002).

Only very limited studies have been conducted to examine the adequacy of empirical factor recommended by Indian Seismic Code for the soft storey buildings. Kaushik et al. (2009) studied various strengthening options of soft storey buildings including the provision of Indian Seismic Code. However, the study was based on the pushover analysis which might not provide real response under the dynamic action. To assess the effectiveness of Indian Seismic Code and the recommendations of Fardis and Panagiotakos (1997), the typical soft storey buildings considered in the previous section are analysed with two strengthening measures. The first case is by following the provision of Indian Seismic Code and denoted as 'Soft-Indian Code'. In the second case, only the moments and shears of the ground floor (GF) columns estimated for the bare frame are multiplied by a factor of 2.5 and denoted as 'Soft-GF columnsx2.5' based on the recommendation of Fardis and Panagiotakos (1997). Since structural responses obtained at different sites exhibit a very similar trend, only the responses obtained at shallow stiff soil site under the 475 year return period ground motion are shown in this paper. Figure 4-10 depicts the interstorey drift profiles of soft storey typical buildings and their comparison with the corresponding unstrengthened soft storey and normal infilled frame buildings.

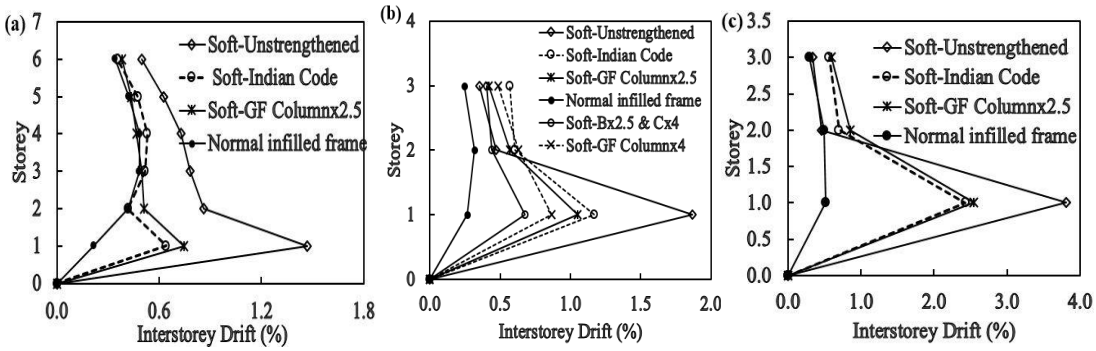

Figure 4-10 Interstorey drift profiles of soft storey frames strengthened with different options (a) 6 storey; (b) 3 storey new and (c) 3 storey old buildings at shallow stiff soil site subjected to the 475 return period ground motion.

It can be observed from the figure that there is a significant reduction in interstorey drift when the resistance of beams and columns of soft storey floor are increased by 2.5 times. The interstorey drifts of unstrengthened '6 storey', '3 storey new' and '3 storey old' soft storey buildings are 2.29, 1.59 and 1.56 higher than the corresponding Indian code designed soft storey buildings respectively. However, the interstorey drift of Indian code designed soft storey buildings and the soft storey buildings with only the ground floor columns being strengthened by the factor of 2.5 are very close to each other. Their drift values vary only by 5-15%. This shows that there is no measurable advantage in increasing the resistance of soft storey beams but certainly adds to the cost of strengthening the beams. As studied by Fardis and Panagiotakos (1997), increasing the resistance of soft storey beams could transfer a more inelastic action to columns, rendering them more vulnerable.

To further study the response of soft storey buildings, two more strengthening cases are considered. In the third case, moments and shears of the first storey beams estimated for bare frames are increased by a factor of 2.5 while the ground floor columns are increased by a factor of 4.0, thereby preserving the weak beam strong column design concept. In the fourth case, only the moments and shears of the ground floor columns are multiplied by factor 4.0. The analyses are carried out only for the '3 storey new' soft storey building for these two cases at the shallow stiff soil sites for the 475 year return period ground motion. The resulting interstorey drifts are shown in Figure 4-10(b). As shown in the figure, there is a slight improvement in the last two cases, but increasing the strength of columns by 4 times significantly increases the cost on the one hand and applicability issues on the other hand. As can be noted, all these strengthening options which are expected to make up for the absence of infill wall on the ground floor are not able to reproduce the response of the normal infilled frame building.

4.9 Performance of masonry infilled and soft storey buildings

The performance of buildings is mostly assessed based on the interstorey drift demand. There are many guidelines such as Vision 2000 (1995), ATC-40 (1996), FEMA 356 (2000) and ASCE/SEI 41-13 (2014) that define interstorey drift limits corresponding to the performance levels of the buildings. However, there are very limited studies undertaken on the correlation of interstorey drifts with the performance levels of the masonry infilled RC buildings. Ghobarah (2004) and ŠIPOŠ and SIGMUND (2014) are two of the very few studies that proposed the correlation of interstorey drift limits and the corresponding performance levels specifically for the masonry infilled RC buildings. They were both derived from a large number of analytical and numerical data obtained from the masonry infilled RC buildings. In the absence of the performance criteria developed for the buildings in Bhutan, the performance criteria specified by Ghobarah (2004) is used in this study since they are more completely defined than that of ŠIPOŠ and SIGMUND (2014).

Unlike the masonry infilled RC frames and the general RC buildings, there is no performance criterion specifically developed for the soft storey buildings. In this study, the performance criteria of Vision 2000 (1995) which are mostly used for assessing the bare frame buildings are used to assess the performance of the soft storey buildings. Since the overall response of the soft storey buildings is governed by the ground floor columns which are devoid of infill walls, it is reasonable to use performance criteria of bare frame buildings. Moreover, the interstorey drift values of Vision 2000 compare well with the experimental results of the soft storey columns tested by Wilson et al. (2008). The performance criteria and the corresponding interstorey drift limits proposed by Ghobarah (2004) and Vision 2000 (1995) are given in Table 4-3.

Table 4-3 Interstorey drift limits and corresponding performance levels and damage states of masonry infilled and general RC frame buildings.

Performance levels	Damage state	Interstorey drift (IDR) limit (%)	
		Ghobarah (2004)	Vision 2000
Fully Operational (FO)	Slight	<0.1	<0.2
Operational (O)	Repairable	0.1≤IDR<0.4	<0.5
Life Safety (LS)	Irreparable	0.4≤IDR<0.7	<1.5
Near Collapse (NC)	Severe	0.7≤IDR≤0.8	<2.5
Collapse (C)	Complete	IDR>0.8	>2.5

Figures 4-11 and 4-12 respectively show the interstorey drift profiles and the performance levels of the typical masonry infilled RC buildings at the generic soil sites for the 475 and 2475 year return period ground motions. The interstorey drift profiles obtained by analysing

the buildings with fixed support (FS) and with SSI are shown in solid and dotted lines respectively. From the figures, it can be observed that the maximum interstorey drift of '3 storey new' building is in between 0.1% to 0.4% at all soil sites under the 475 year return period ground motion. This indicates that the building would remain within the operational limit with some repairable damages. When the intensity of ground motion is increased to the 2475 year return period, '3 storey new' building undergoes repairable damage at the rock site but experiences irreparable damages at shallow stiff soil and soft soil sites. At the soft rock site, the building undergoes severe damage and enters the near collapse limit. In regard to the '6 storey' building, the repairable damage is predicted at rock and soft rock sites, while irreparable damage and complete collapse are respectively predicted at the shallow stiff soil and soft soil sites under the 475 year return period ground motion. Under the 2475 year return period ground motion, '6 storey building undergoes irreparable damages at the rock site but collapses at all other sites with the maximum interstorey drifts well beyond 0.8%. The performance of '3 storey old' building is similar to that of '6 storey' building although its maximum interstorey drifts at shallow stiff soil and soft rock sites are significantly higher than that of '6 storey' building. This is due to the definition of performance levels within the distinct interstorey drift limits.

As shown by the doted lines, SSI has no significant effect on buildings at the soft rock site and slightly detrimental effect at the shallow stiff soil site under the return periods of both the 475 and 2475 years. However, SSI has a significant effect at the soft soil site with a large deviation of interstorey drifts from the fixed base case. The performance of '3 storey new' buildings is observed to be as expected since it remains operational under the 475 year return period ground motion and life safe under the 2475 year return period ground motion corresponding to the intended design objective. However, the performance of '6 storey' building is not very satisfactory although it was also designed to Indian Seismic Code. This could be due to the inadequate design on the one hand and inadequacy of Indian Seismic Code for the site conditions in Bhutan on the other hand. It could also be due to the use of very low concrete grade in spite of having 6 full floors. Although the performance of '3 storey old' building is inferior of the three buildings, it performs satisfactorily under the 475 year return period ground motion. The presence of infill wall could have strengthened the weak RC frames thereby increasing the overall stiffness of the buildings.

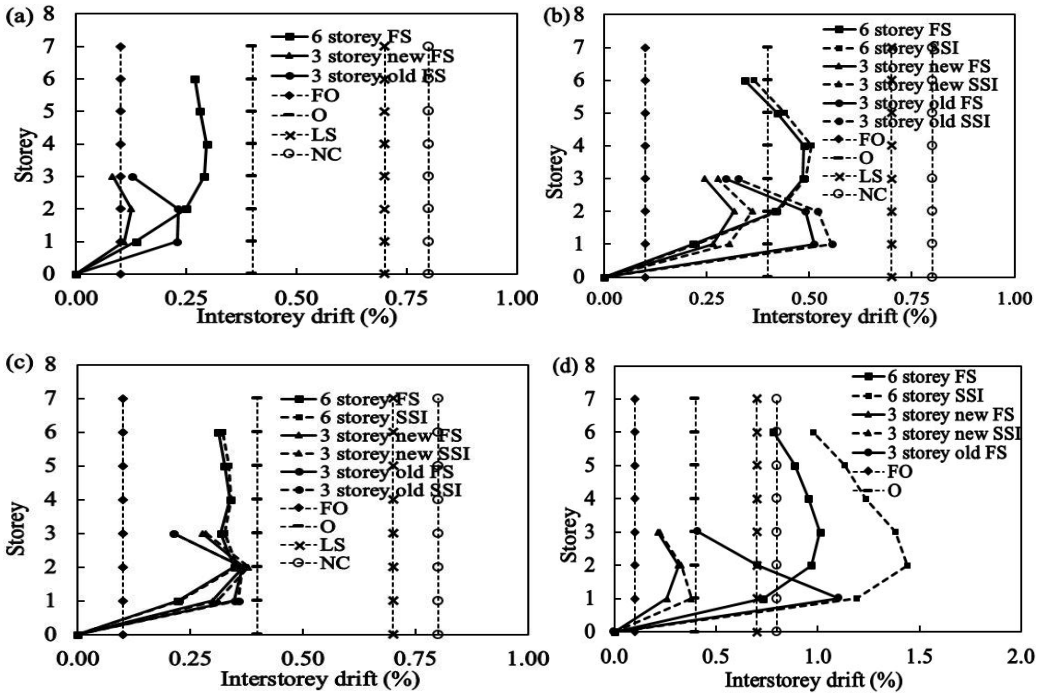

Figure 4-11 Performance levels and interstorey drift profiles of masonry infilled RC buildings subjected to the 475 year return period ground motions at (a) rock; (b) shallow stiff soil; (c) soft rock and (d) soft soil sites with fixed support (FS) and with SSI.

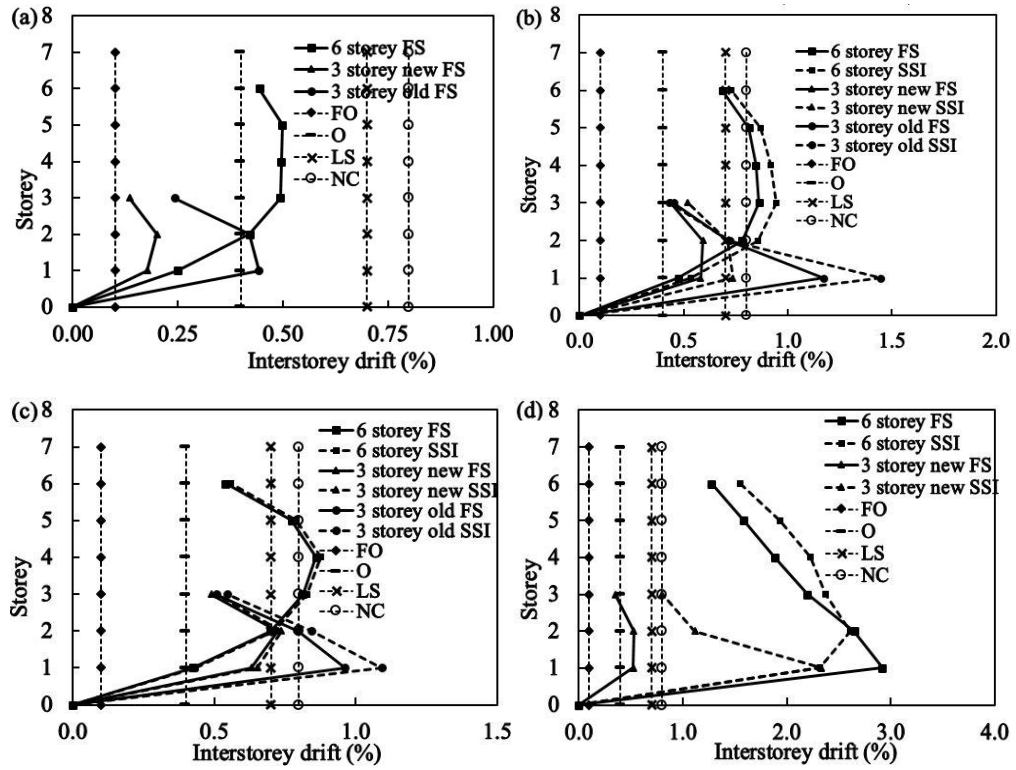

Figure 4-12 Performance levels and interstorey drift profiles of masonry infilled RC buildings subjected to the 2475 year return period ground motions at (a) rock; (b) shallow stiff soil; (c) soft rock and (d) soft soil sites with fixed support (FS) and with SSI.

The performance of the soft storey buildings under the 475 and 2475 year return period ground motions at the various soil sites can be inferred from Figures 4-13 and 4-14. As shown in the figures, the performance of the soft storey buildings is fully governed by the interstorey drift at the first floor level. The effect of SSI was found to be similar to that of masonry infilled RC buildings and hence are not considered here. As shown in Figure 4-13, the '3 storey old' soft storey building collapses under the 475 year return period ground motion irrespective of the soil sites. Both '6 storey' and '3 storey new' soft storey building remain within the life safety limit at the rock and soft rock sites and collapse at the soft soil site. At the shallow stiff soil sites, only '6 storey' building remain life safe while '3 storey new' building exceeds the life safety limit. However, under the 2475 return period ground motion, '3 storey' old building collapses at all soil sites while the '3 storey new' building remain within the near collapse limit at the rock site and collapses at the other sites. The '6 storey' building collapses at shallow stiff and soft soil sites and remains within the near collapse limit at the rock and soft rock sites. Comparing Figure 4-11 to Figure 4-13 and Figure 4-12 to Figure 4-14, it can be observed that soft storey buildings are more vulnerable to earthquakes than the masonry infilled RC buildings. Unlike the masonry infilled RC buildings where the '3 storey new' building exhibits the best performance, '6 storey' building performs better in the case of the soft storey buildings. This could be due to the higher strength and stiffness of the ground floor columns of '6 storey' buildings compared to that of '3 storey new' building.

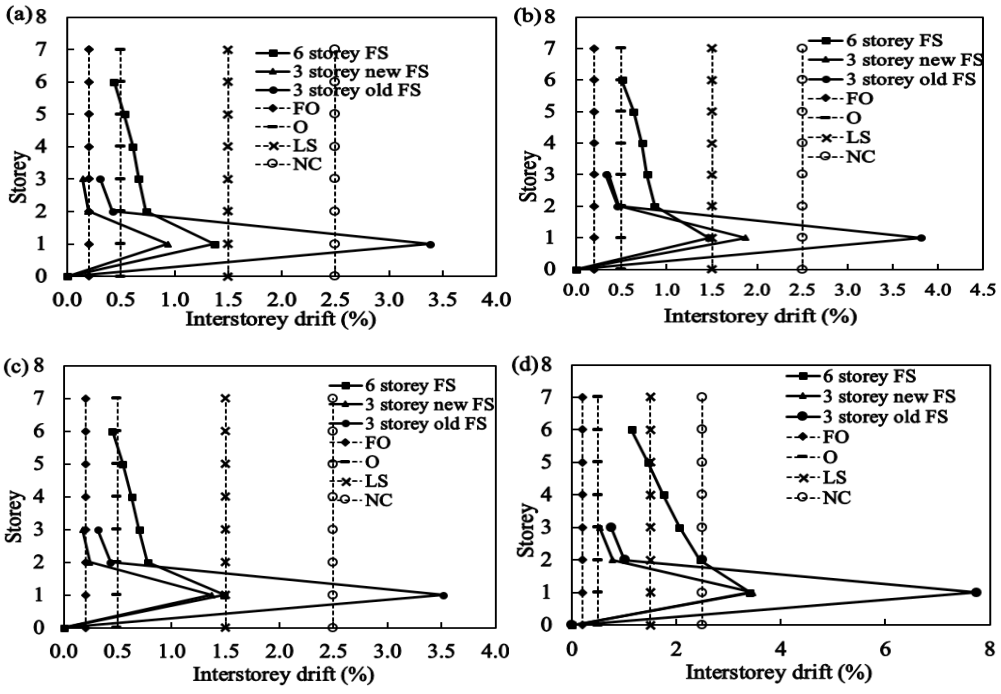

Figure 4-13 Performance levels and interstorey drift profiles of soft storey buildings subjected to the 475 year return period ground motions at (a) rock; (b) shallow stiff soil; (c) soft rock and (d) soft soil sites.

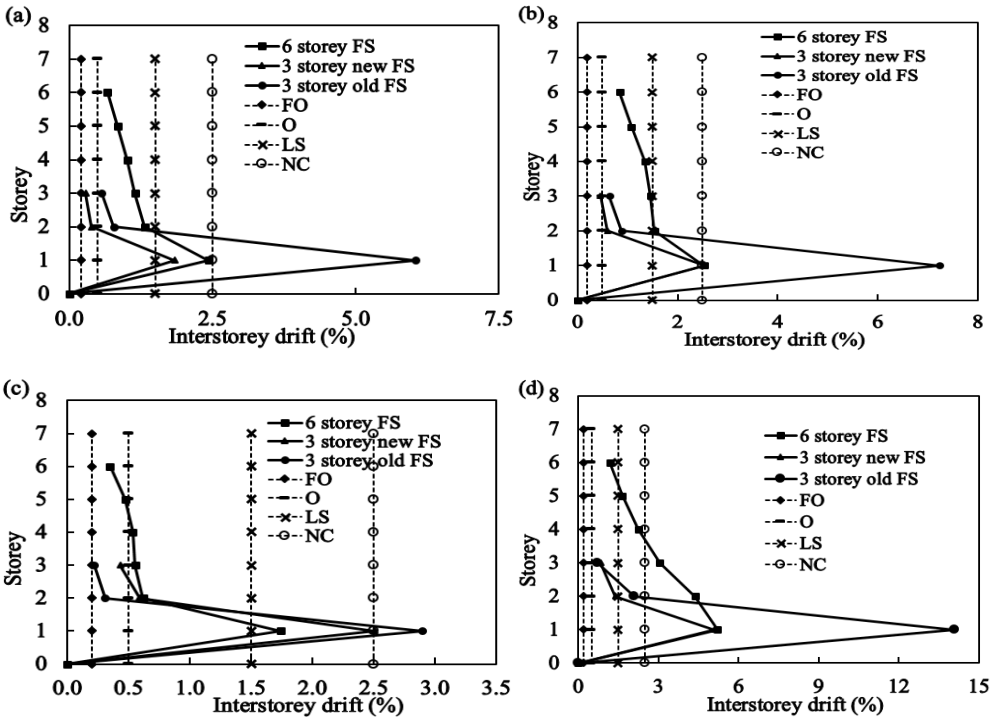

Figure 4-14 Performance levels and interstorey drift profiles of soft storey buildings subjected to the 2475 year return period ground motions at (a) rock; (b) shallow stiff soil; (c) soft rock and (d) soft soil sites.

4.10 Summary and conclusion

The seismic performance of masonry infilled RC buildings in Bhutan is assessed using the ground motions predicted in Bhutan at various soil sites for the 475 and 2475 year return periods. The numerical model is first calibrated with the experimental results and then applied to estimate the structural responses and performances of the masonry infilled and soft storey RC buildings. The effects of openings and the flexibility of foundation are considered in the analyses. The design provision for soft storey buildings as per the Indian Seismic Code is studied and compared with the design recommendations proposed by other researchers. It is found that:

1. Under the 475 year return period ground motion, the masonry infilled RC buildings in Bhutan, in general, could remain life safe but would experience repairable to irreparable damages depending on the soil conditions. Under the 2475 year return period ground motion, the properly designed buildings could survive with irreparable and severe damages, but poorly designed buildings and the buildings built before the adoption of Indian Seismic Code could collapse.

2. The effect of SSI is highly significant at the soft soil sites as found in chapter 2 and needs to be incorporated in the design.
3. Soft storey building strengthened according to Indian Seismic Code improves the performance of the building. However, strengthening only the columns of the soft storey leads to almost the same performance if beams of the floor are also strengthened. Strengthening the soft storey beams and columns by large factors do improve performance but cannot replicate the performance of infilled frame buildings.
4. Regular configuration of infill wall in the RC frames certainly improves the performance of the buildings through the increase of stiffness and strength and greatly reducing the interstorey drift. Irregular arrangement of infill wall such as that of the soft storey is highly detrimental to the performance of the building.
5. The performance of the soft storey buildings is found to be highly influenced by the strength and stiffness of the soft storey columns.

4.11 References

ACI 318-14 (2014). *Building code requirements for structural concrete*. Detroit, Mich, American concrete institute.

Al-Chaar, G. (2002). *Evaluating strength and stiffness of unreinforced masonry infill structures*. No. ERDC/CERL-TR-02-1. Engineer Research and Development Centre Champaign, US Army Corps of Engineers.

ASCE/SEI 41-13 (2014). *Seismic rehabilitation of existing buildings*. American Society of Civil Engineers.

Asteris, P. G., Giannopoulos, I. P., & Chrysostomou, C. Z. (2012). Modeling of infilled frames with openings. *Open Construction and Building Technology Journal, 6* (1), 81-91.

Asteris, P. G, Antoniou, S., Sophianopoulos, D., & Chrysostomou, C. Z. (2011). Mathematical macromodeling of infilled frames: State of the art. *Journal of Structural Engineering, 137* (12), 1508-1517.

ATC-40 (1996). *Seismic evaluation and retrofit of concrete building volume 1*. Applied Technology Council, Redwood city, California.

Banerjee, P., & Bürgmann, R. (2002). Convergence across the northwest Himalaya from gap measurements. *Geophysical Research Letters, 29* (13), 30-1-30-4.

Bilham, R., Gaur, V. K., & Molnar, P. (2001). Himalayan seismic hazard. *Science (Washington), 293* (5534), 1442-1444.

Crisafulli, F. J. (1997). *Seismic behaviour of reinforced concrete structures with masonry infills.* PhD Thesis, University of Canterbury, New Zealand.

Crisafulli, F. J., & Carr, A. J. (2007). Proposed macro-model for the analysis of infilled frame structures. *Bulletin of the New Zealand Society for Earthquake Engineering, 40* (2), 69-77.

Crisafulli FJ, Carr AJ and Park R (2000) Analytical modelling of infilled frame structures-a general review. *Bulletin-New Zealand Society for Earthquake Engineering*. 33(1): 30-47.

CSI (2006). *Nonlinear Analysis and Performance Assessment for 3-D Structures.* Computers and Structures, Inc., Berkeley.

Dawe, J., & Seah, C. (1988). Lateral load resistance of masonry panels in flexible steel frames. *Brick and Block Masonry (8th IBMAC) London, Elsevier Applied Science* 2, 606-616.

Decanini, L., Liberatore, L., & Mollaioli, F. (2012). The influence of openings on the seismic behaviour of infilled framed structures. In: *15th World Conference on Earthquake Engineering*, Lisbon, Portugal.

Deierlein, G. G., Reinhorn, A. M., & Willford, M. R. (2010). *Nonlinear structural analysis for seismic design*. NEHRP Seismic Design Technical Brief, No. 4.

Dolšek, M., & Fajfar, P. (2002). Mathematical modelling of an infilled RC frame structure based on the results of pseudo-dynamic tests. *Earthquake engineering & structural dynamics, 31* (6), 1215-1230.

Dolšek, M., & Fajfar, P. (2008). The effect of masonry infills on the seismic response of a four-storey reinforced concrete frame—a deterministic assessment. *Engineering Structures, 30* (7), 1991-2001.

Dorji, J. (2009). *Seismic performance of brick infilled RC frame structures in low and medium rise buildings in Bhutan.* Master's degree Thesis, Queensland University of Technology, Australia.

Durrani, A. J., & Luo, Y. (1994). *Seismic retrofit of flat-slab buildings with masonry infills.* Technical report, National Centre for Earthquake Engineering Research, pp. 1-8.

Elwood, K. J., & Eberhard, M. O. (2009). Effective stiffness of reinforced concrete columns. *ACI Structural Journal, 106* (4), 476.

Eurocode 8 (2002). *Design of Structures for earthquake resistance–Part 1: General rules, seismic actions and rules for buildings*. European Standard, NF EN, 1.

Fardis, M., & Panagiotakos, T. (1997). Seismic design and response of bare and masonry-infilled reinforced concrete buildings part ii: Infilled structures. *Journal of Earthquake Engineering, 1* (3): 475-503.

FEMA-274 (1997). *NEHRP commentary on the guidelines for the seismic rehabilitation of buildings*. Washington DC.

FEMA-356 (2000). *Prestandard and commentary for the seismic rehabilitation of buildings*. Washington DC, Federal Emergency Management Agency.

Ghobarah, A. (2004). On drift limits associated with different damage levels. In: *International workshop on performance-based seismic design*, Dept. of Civil Engineering, McMaster University, No. 28.

Hao, H., & Tashi, C. (2012). Earthquake ground motion prediction and its influence on building structures in Bhutan. In: *12th International Symposium on structural engineering*, China.

Haselton, C. B. (2008). *Beam-column element model calibrated for predicting flexural response leading to global collapse of RC frame buildings*. Report, Pacific Earthquake Engineering Research Center.

Haselton, C., & Deierlein, G. (2006). Toward the codification of modelling provisions for simulating structural collapse. In: *8th National Conference on Earthquake Engineering* (100th Anniversary Earthquake Conference), pp. 18-22.

Haselton, C. B., Goulet, C. A., Mitrani-Reiser, J., Beck, J. L., Deierlein, G. G., Porter, K. A., Stewart, J. P., & Taciroglu, E. (2008). *An assessment to benchmark the seismic performance of a code-conforming reinforced-concrete moment-frame building*. Report (2007/1), Pacific Earthquake Engineering Research Centre.

Hendry, A. (1998). *Structural masonry*. 2nd ed. London, UK: Palgrave Macmillan, London.

Holmes, M. (1961). Steel frames with brickwork and concrete infilling. *Proceedings of the Institution of Civil Engineers* 19(4): 473-478.

Ibarra, L. F., Medina, R. A., & Krawinkler, H. (2005). Hysteretic models that incorporate strength and stiffness deterioration. *Earthquake engineering & structural dynamics*, *34* (12), 1489-1511.

IS-1893 (2002). *Criteria for earthquake resistant design of structures*. Bureau of Indian Standards, New Delhi, India.

Kaushik, H. B., Rai, D. C., & Jain, S. K. (2007). Stress-strain characteristics of clay brick masonry under uniaxial compression. *Journal of materials in Civil Engineering*, *19* (9), 728-739.

Kaushik, H. B., Rai, D. C., & Jain, S. K. (2009). Effectiveness of some strengthening options for masonry-infilled RC frames with open first story. *Journal of structural engineering, 135* (8), 925-937.

Mainstone, R. (1974). *Supplementary note on the stiffness and strength of infilled frames*. 2ed edition, Institution of Civil Engineers, London, UK, pp. 57-90.

Mondal, G., & Jain, S. K. (2008). Lateral stiffness of masonry infilled reinforced concrete (RC) frames with central opening. *Earthquake Spectra*, *24* (3), 701-723.

Murty, C., & Jain, S. K. (2000). Beneficial influence of masonry infill walls on seismic performance of RC frame buildings. In: *12th World Conference on Earthquake Engineering*, Auckland, New Zealand.

Negro, P., & Colombo, A. (1997). Irregularities induced by non-structural masonry panels in framed buildings. *Engineering Structures*, *19* (7), 576-585.

Negro, P., & Verzeletti, G. (1996). Effect of infills on the global behaviour of RC frames: Energy considerations from pseudo dynamic tests. *Earthquake engineering & structural dynamics*, *25* (8), 753-773.

Negro, P., Verzeletti, G., Magonette, G., & Pinto, A. (1994). *Test on a four storey full scale RC frame designed according to Eurocode 8 and 2*. Preliminary report, Joint Research Center, Italy.

Panagiotakos, T., & Fardis, M. (1996). Seismic response of infilled RC frames structures. In: *11th World Conference on Earthquake Engineering*, Acapulco.

Panagiotakos, T. B., & Fardis, M. N. (2001). Deformations of reinforced concrete members at yielding and ultimate. *ACI Structural Journal, 98* (2), 135-148.

Paulay, T., & Priestley, M. (1992). *Seismic design of reinforced concrete and masonry buildings*. New York: John Wily and Sons Inc.

PEER-ATC-71-1 (2010). *Modelling and acceptance criteria for seismic design and analysis of tall buildings.* Pacific Earthquake Engineering Research Center.

Penelis, G., & Kappos, A. (1997). *Earthquake resistant concrete structures*. London: EP & FN SPON, London.

Sattar, S., & Liel, A. B. (2010). Seismic performance of reinforced concrete frame structures with and without masonry infill walls. In: *9th US National and 10th Canadian conference on earthquake engineering*, Toronto, Canada.

Šipoš, T. K., & Sigmund, V. (2014). Damage assessment of masonry infilled frames. In: *2nd European Conference on Earthquake Engineering and Seismology*, Istanbul, Turkey.

Smith, BS and Carter C (1969) A method of analysis for infilled frames. In: *Institute of Civil Engineers*, Thomas Telford, No. 44, pp. 31-48.

Smyrou, E. (2006). *Implementation and verification of a masonry panel model for nonlinear dynamic analysis of infilled RC frames*. Master Degree Thesis, ROSE School.

Smyrou, E., Blandon, C., Antoniou, S., Pinho, R., & Crisafulli, F. (2011). Implementation and verification of a masonry panel model for nonlinear dynamic analysis of infilled RC frames. *Bulletin of Earthquake Engineering, 9* (5), 1519-1534.

Thinley, K., Hao, H., & Tashi, C. (2017). Seismic Performance of Reinforced Concrete Buildings in Thimphu, Bhutan. *International Journal of Structural Stability and Dynamics***,** *17* (7), 1750074.

Thinley, K., Hao, H., & Tashi, C. (2014). Seismic performance of reinforced concrete buildings in Bhutan. In: *Australian Earthquake Engineering Society 2014 Conference*, Lorne, Victoria, Australia.

UNDP (2006). *Report on Thimphu valley earthquake risk management program.* Standards and Quality Control Authority, Ministry of Works and Human Settlement, Thimphu, Bhutan.

Vision 2000 (1995). *Performance Based Seismic Engineering of Buildings; conceptual framework*. Structural Engineers Association of California, Sacramento, CA.

Walling, M. Y., & Mohanty, W. K. (2009). An overview on the seismic zonation and micro zonation studies in India. *Earth-Science Reviews, 96* (1), 67-91.

Wilson, J., Lam, N., & Rodsin, K. (2008). Collapse modelling of soft storey buildings. In: *Australian Structural Engineering Conference (ASCE)*, Melbourne, Australia, 26-27 June 2008.

CHAPTER 5 SEISMIC DAMAGE PREDICTION OF MASONRY INFILLED RC BUILDINGS WITHOUT AND WITH SOFT STOREY IN BHUTAN BASED ON FUZZY PROBABILITY ANALYSIS

5.1 Abstract

The need to predict the realistic performances of the masonry infilled RC buildings without and with soft storey in Bhutan has been dearly felt for quite some time. The country is located right on the inter-plate boundary in the Himalaya where the Indo-Australian plate is continuously being subducted under the Eurasian plate. Masonry infilled RC buildings without and with soft storey are very common building structures in the urban centres and more than 50% of them were built without any kind of engineering design. In spite of the high seismic risk, the seismic damage assessment of these buildings has not been realistically carried out until now. This study is aimed at predicting the realistic damage probabilities of the masonry infilled RC buildings without and with soft storey in Bhutan considering the randomness in the material and geometrical parameters and the fuzziness in the damage criteria. The ground motions predicted in Bhutan from the Probabilistic Seismic Hazard Analysis for the 475 and 2475 year return periods are used for the analyses. Rosenbluth Point Estimate Method is used for modelling the statistical variation of the input parameters and the Perform 3D (CSI, 2006) program is used for estimating the response quantities. Monte Carlo Simulation is employed to validate the accuracy of the Point Estimate Method. It is found that the masonry infilled RC buildings without soft storey have the high probability of undergoing repairable and severe damages under the 475 and 2475 year return period ground motions respectively; while the high probability of irreparable damage and severe to complete collapse are predicted for the soft storey buildings for the corresponding earthquake ground motions. These results highlight the expected damages of the current building stocks in Bhutan and provide quantitative information for effective strengthening options to minimize the earthquake impacts in the high-seismicity country.

5.2 Introduction

Predicting the seismic damages of the existing masonry infilled reinforced concrete (RC) buildings without and with soft storey in Bhutan has become the nation's main priority today. All urban centres of the country are predominated by the masonry infilled RC buildings both with and with soft storey. Prior to the adoption of Indian Seismic Code, IS 1893 (2002) in 1997, a majority of these buildings were constructed without any kind of design. The country still does not have seismic design code of its own and the buildings are still being designed

following the Indian Seismic Code. Moreover, even after the adoption of the Indian code, the masonry infilled RC buildings are commonly designed as bare frames ignoring the contribution of infill wall to the strength and stiffness of the buildings. As evident from a number of studies, the presence of infill walls drastically changes the structural responses of the infilled frame buildings when subjected to seismic excitation (Asteris and Cotsovos, 2012; Dolsek and Fajfar, 2008; Murthy and Jain, 2000). Hence, there exist a mix of masonry infilled RC buildings which were either not at all designed or not properly designed to lateral loads. It is paramount to predict the damages of these buildings to ascertain the realistic seismic risk of the country so as to be prepared for the future seismic events.

The need to predict the seismic performance of building structures is further enhanced by the location of the country in the highly active seismic region in the Himalaya. The country sits right on the inter-plate boundary where the Indo-Australian plate is continuously being sub-ducted under the Eurasian plate. A number of earthquakes had occurred in the past both within and just outside the country's territory. In fact, during the last seven and half decades, Bhutan experienced 32 earthquakes of engineering significance taking away lives and damaging properties (Dorji, 2009). The more recent M6.1 earthquake that occurred in September 2009 in the eastern Bhutan had taken 13 lives and damaged hundreds of rural homes, schools and monasteries. The 2011 M6.9 Sikkim earthquake was also disastrous to the rural homes in the western Bhutan although it occurred some distance away from Bhutan. It is worth mentioning here that some of the big Himalayan earthquakes such as 1897 Shillong Plateau earthquake, 1934 Bihar-Nepal earthquake and 1950 Assam earthquake had all occurred very close to Bhutan. It is possible that such large earthquakes could also occur in Bhutan owing to the same geographical location and with the presence of highly active faults such as Main Boundary Thrust and Main Central Thrust faults (Walling and Mohanty, 2009). In fact, based on the concept of seismic gap combined with the geomorphological and geophysical evidence along the Himalaya, Bilham et al. (1997) and Banerjee and Bürgmann (2002) had already reported the overdue of one or more big earthquakes in the Himalayan region. Being located in the proximity of the Assam seismic gap, the likelihood of big earthquakes cannot be ruled out in Bhutan.

In spite of this worrying situation, realistic prediction of the performance of masonry infilled RC buildings without and with soft storey in Bhutan has not been carried out. There are very few studies undertaken on the seismic assessment of buildings in Bhutan, but they are either based on bare frames or are deterministic in nature. Employing the ground motions from El-Centro, Kobe and Northridge earthquakes, Dorji (2009) studied the seismic performance of masonry infilled RC buildings in Bhutan. This study may not leads to realistic predictions

owing to the use of ground motions from other sites. The recent studies carried out by Hao and Tashi (2012) and Thinley et al. (2014) used earthquake ground motions predicted for Bhutan from the Probabilistic Seismic Hazard Analysis, but ignored the contribution of masonry infill wall in the numerical model. In a recent study undertaken by Thinley and Hao (2015), the contribution of the masonry walls in the numerical model was considered, but the study adopted the design values in the deterministic analyses. This study extends the analysis reported by Thinley and Hao (2015) by considering possible statistical fluctuations of structural parameters and the fuzziness of damage criteria for a more realistic fuzzy probabilistic analysis of masonry infilled RC buildings in Bhutan subjected to earthquake ground motions. Moreover, RC frame buildings with soft storey, which has been proven the most vulnerable to seismic loads but are not considered in the previous study, is also the focus of the present study.

The three typical masonry infilled RC buildings, without and with soft storey, i.e. ground floor open, and built prior to and after the adoption of Indian Seismic Code are considered for the analyses. The ground motions predicted in chapter 2 of this thesis from the Probabilistic Seismic Hazard Analysis by Thinley et al. (2017) for the 475 and 2475 year return periods are used in the analysis. For more realistic prediction of structural responses, the effects of opening in the masonry wall and soil-structure interaction are considered in the numerical model. A nonlinear strut model is used to model the infill wall while the RC beams and columns are modelled using the FEMA beam and FEMA column components respectively. The numerical model was previously calibrated with the experimental results in Thinley and Hao (2015). The Rosenbluth Point Estimate Method is employed for modelling the statistical variation of the material and geometrical parameters and the computer program Perform 3D (CSI, 2006) is used for estimating the nonlinear structural response of the buildings. The Monte Carlo Simulation Method is used to validate the accuracy of the Rosenbluth Point Estimate Method. Based on the estimated probabilistic distributions of the interstorey drift and adopting the triangular membership function, fuzzy damage probabilities of the masonry infilled RC buildings without and with soft storey are estimated in accordance with the interstorey drift limits defined in Ghobarah (2004) and Vision 2000 (1995) respectively. From this study, it is observed that the masonry infilled RC buildings without soft storey are very likely to experience repairable and severe damages under the 475 and 2475 year return period ground motions respectively, while those with soft storey have the high probability of experiencing irreparable damage and severe to complete collapse under the 475 and 2475 year return period ground motions, respectively.

Although located in a high seismicity region, rigorous study of the building responses to seismic loadings is very limited. The results presented in this paper are from the first comprehensive fuzzy probabilistic study on the performances of masonry infilled RC buildings subjected to earthquake ground motions in Bhutan. They can be used as guide for strengthening existing structures in the country to mitigate seismic hazards, which has become a more compelling issue after the recent Nepal earthquake in the same region with similar construction types.

5.3 Description of Buildings considered for the Study

Three typical masonry infilled RC buildings without soft storey representing the general building stocks in the country are initially considered. They are denoted as '6 storey', '3 storey new' and '3 storey old' and abbreviated as 6S, 3SN and 3SO respectively. The '6 storey' and '3 storey new' buildings represent the 6 storey and 3 storey buildings designed and built according to the Indian Seismic Code, while the '3 storey old' building represents the 3 storey buildings which were built prior to 1997 without following any standard design. The 3 storey buildings are very common in all the urban centres in the country while the buildings with 4 to 6 storeys are mostly concentrated in the capital city, Thimphu. The plan and sectional elevation of these buildings are shown in Figure 5-1.

The '6 storey' and '3 storey new' are the real existing buildings built in 2009 in Thimphu. The details of these buildings are obtained from the Thimphu City Corporation in the form of structural and architectural drawings. The cross-sectional dimension of beams and columns and their longitudinal and transverse reinforcements are shown in Table 5-1. The compressive strength of the concrete used for the beams and slabs of these buildings is 20 MPa, while the compressive strength of 25 MPa and 20 MPa are respectively used for the columns of '6 storey' and '3 storey new' buildings. The compressive strength of the brick masonry used is 6.07 MPa corresponding to the medium mortar mix consisting of cement to sand ratio of 1:4. The unit weight of reinforced concrete and brick masonry are respectively taken as 25 kN/m^3 and 19.6 kN/m^3 as specified in the structural drawings. The yield strength of reinforcement used is 415 MPa for all the buildings. The live load of 2 kN/m^2 and 0.75 kN/m^2 are respectively applied on the floors and roofs of the buildings. The superimposed dead load of 1kN/m^2 is also applied on all the floors. The clear cover of 40 mm and 25 mm are respectively specified for columns and beams of these buildings.

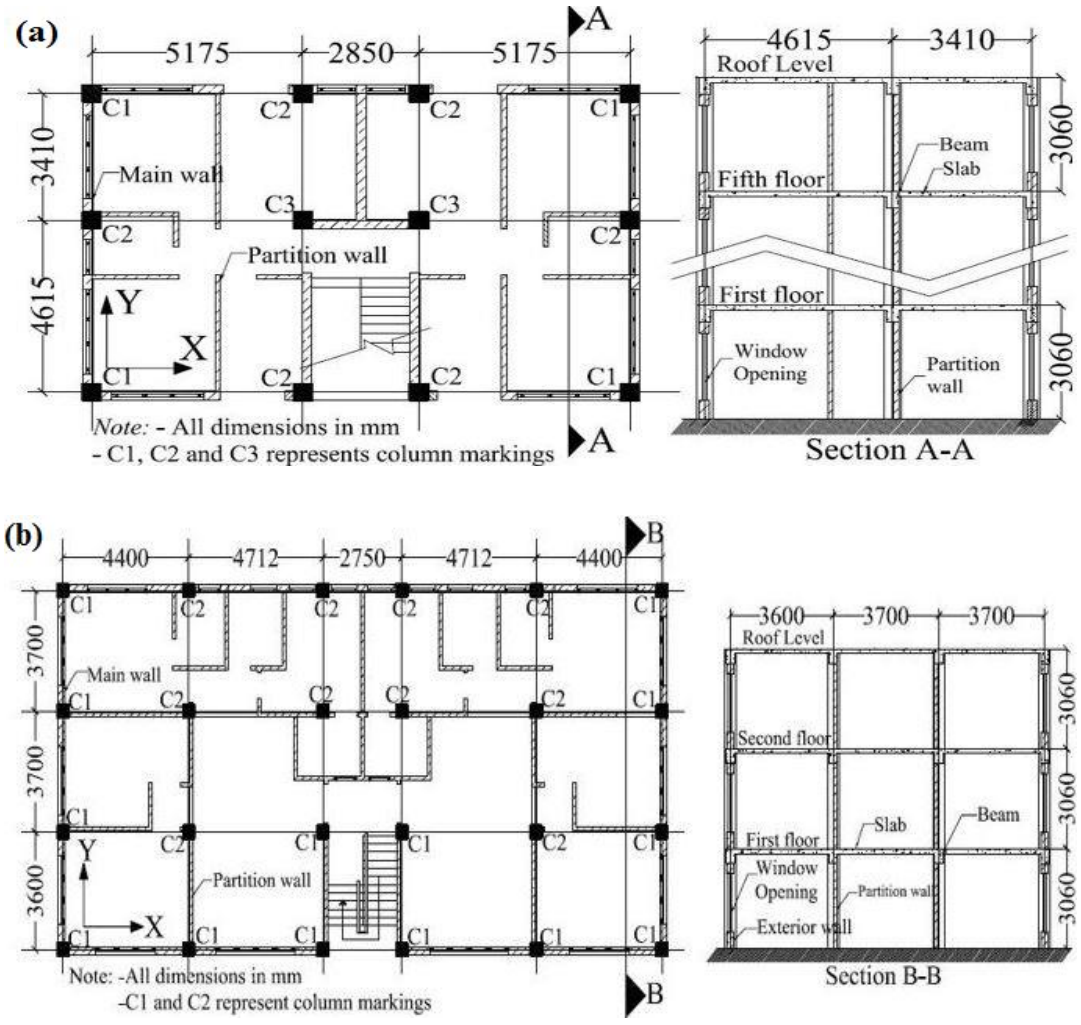

Figure 5-1 Plan and sectional elevation of typical buildings, (a) 6 storey and (b) 3 storey buildings.

It is to be noted that design information of '3 storey old' building is not available since they were directly built at the site by the local technicians without any kind of design. Therefore, there are no records of structural and architectural details for those buildings. Hence, the plan and elevation of the '3 storey old' building are assumed identical to that of the '3 storey new' building. However, its structural details such as the beam and column sizes, concrete strength and reinforcement details are derived from the result of the non-destructive test conducted on 15 old masonry infilled RC buildings under the Thimphu Valley Earthquake Risk Management Project in 2005 (UNDP Report, 2006). It was found that the concrete strength of 15 MPa and steel yield strength of 415 MPa were mostly used for those buildings and the same have been adopted in this study for the '3 storey old' building. The compressive strength of brick masonry is assumed as 3.77 MPa corresponding to weak mortar consisting of cement to sand ratio of 1:6. The member dimensions and the reinforcement details are also assumed

similar to the ones found in the majority of the 15 tested buildings which are given in Table 5-1.

For simplicity, the masonry infilled RC buildings with soft storey considered in this study are obtained by removing infill walls from the ground floor of the above three building models. They are respectively denoted as soft storey '6 storey', '3 storey new' and '3 storey old' buildings. With exception to the infill walls in the ground floors, all other architectural and structural details of the masonry infilled RC buildings with soft storey are considered identical to the corresponding masonry infilled RC buildings without soft storey. This is justifiable since masonry infilled RC buildings with or without soft storeys are commonly designed as bare frames even today in Bhutan. Hence, removing the infill walls from the ground floor of the masonry infilled RC buildings without soft storey well represent the soft storey RC buildings in Bhutan.

Table 5-1 Reinforcement and member dimension details of the typical buildings

	6 storey (6S)		3 storey new (3SN)		3 storey old (3SO)	
a) Beam reinforcement						
	Top Bar	Bottom Bar	Top Bar	Bottom Bar	Top Bar	Bottom Bar
Floor beams along X	4-20	2-20+2-16	4-20	2-20+2-16	4-12	2-12+2-10
Floor beams along Y	4-20	2-20+2-16	2-20+2-16	4-16	3-12	3-10
Roof beams along X	2-20+2-16	4-16	2-20+2-16	4-16	3-12	3-10
Roof beams along Y	2-20+2-16	4-16	4-16	2-16+2-12	2-12+1-10	3-10
Beam stirrups	8@100C/C		8@100C/C		6@150C/C	
b) Column reinforcement						
Column C1	8-20 + 4-16		8-20		4-16	
Column C2	12-20		4-25+4-20		8-12	
Column C3	4-25+8-20					
Column ties	10@90C/C		8@100C/C		6@150C/C	
c) RC member dimension						
Beams along X	300mm x 450mm		300mm x 400mm		250mm x 350mm	
Beams along Y	300mm x 450mm		300mm x 400mm		250mm x 300mm	
Columns C1 & C2	450mm x 450mm		400mm x 400mm		250mm x 250mm	
Columns C3	500mm x 500mm					
Slab thickness	150mm		150mm		100mm	

5.4 Ground Motions

Despite the occurrence of many earthquakes in the past, there is no ground motion record available in Bhutan. Even today, the country has no seismic station to record the ground

motions in the area. In the absence of the recorded ground motion data, those predicted at the generic soil sites in Thimphu in chapter 2 of this thesis by Thinley et al. (2017) for the 475 and 2475 year return periods are used in this study. They were predicted from the Probabilistic Seismic Hazard Analysis (PSHA) using 18 seismic source zones located within the distance of 400 km from Thimphu. Since these ground motions were specifically developed for the site conditions in Bhutan, they are believed to provide more representative seismic motions in Bhutan. The acceleration time histories of ground motions at the generic soil sites for the 475 and 2475 year return periods are shown in Figure 5-2.

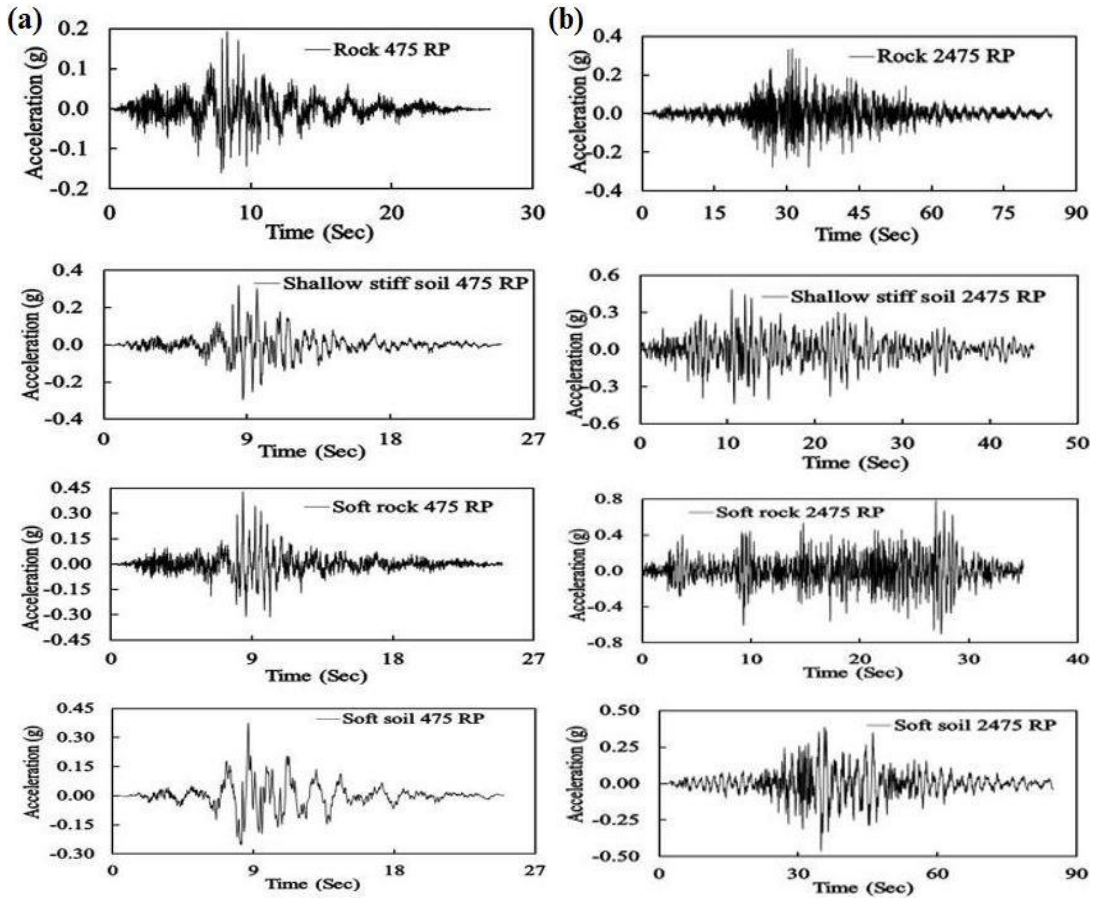

Figure 5-2 Acceleration time histories of ground motions at rock, shallow stiff soil, soft rock and soft soil sites for (a) 475 and (b) 2475 year Return Periods(RP).

5.5 Numerical Modelling

The numerical model previously calibrated against the experimental results for the masonry infilled and soft storey RC buildings in chapter 4 of this thesis by Thinley and Hao (2016) is adopted in this study. It consists of modelling the RC members and infill wall which are briefly described below. In addition, the effects of the opening and soil structure interaction are

incorporated in the numerical model for the realistic estimation of structural response and damage to earthquake ground excitations.

5.5.1 Modelling of RC members

The reinforced concrete beams and columns are modelled using the chord rotation model which is based on the lumped plasticity approach. It consists of the stiff zone at the ends and FEMA beam or FEMA column component in the middle. The FEMA component constitutes a plastic hinge and an elastic segment as shown in Figure 5-3(a). The tri-linear force-deformation (F-D) relationship implemented in Perform 3D (CSI, 2006) software is used to define the stiffness, strength and deformation parameters of the RC members as shown in Figure 5-3(b).

The effective stiffness or secant stiffness to yield, K_e is estimated from the expression given by Elwood and Eberhard (2009) which was derived from the test data of 255 columns. Depending on the axial load, the effective stiffness is adopted in the range of $0.2EI_g$ to $0.7EI_g$, where E is the modulus of elasticity of RC member and I_g is the moment of inertia of the gross section. The yield moment, M_y and yield rotation, θ_y are estimated from the equations given by Panagiotakos and Fardis (2001) which were validated by Haselton and Deierlein (2007) using a large number of experimental test data. The capping moment, M_c is taken as $1.13M_y$ as proposed by Haselton et al. (2008) based on test data. The residual moment, M_r is taken as $0.001M_c$ as recommended in the Perform 3D (CSI, 2006) user guide. The deformation parameters such as pre-capping rotation, θ_p and post capping rotation, θ_{pc} are obtained from the expressions of Haselton et al. (2008). The estimation of the stiffness, strength and deformation parameters from the respective expressions completely define the F-D relationship of the RC members. To incorporate the contribution of the slab to the stiffness of the beams, the exterior and interior beams are respectively approximated as L and T-beams. The effective width of these beams is calculated from the expression given in ACI 318-14 (2014) based on their span and overall depth.

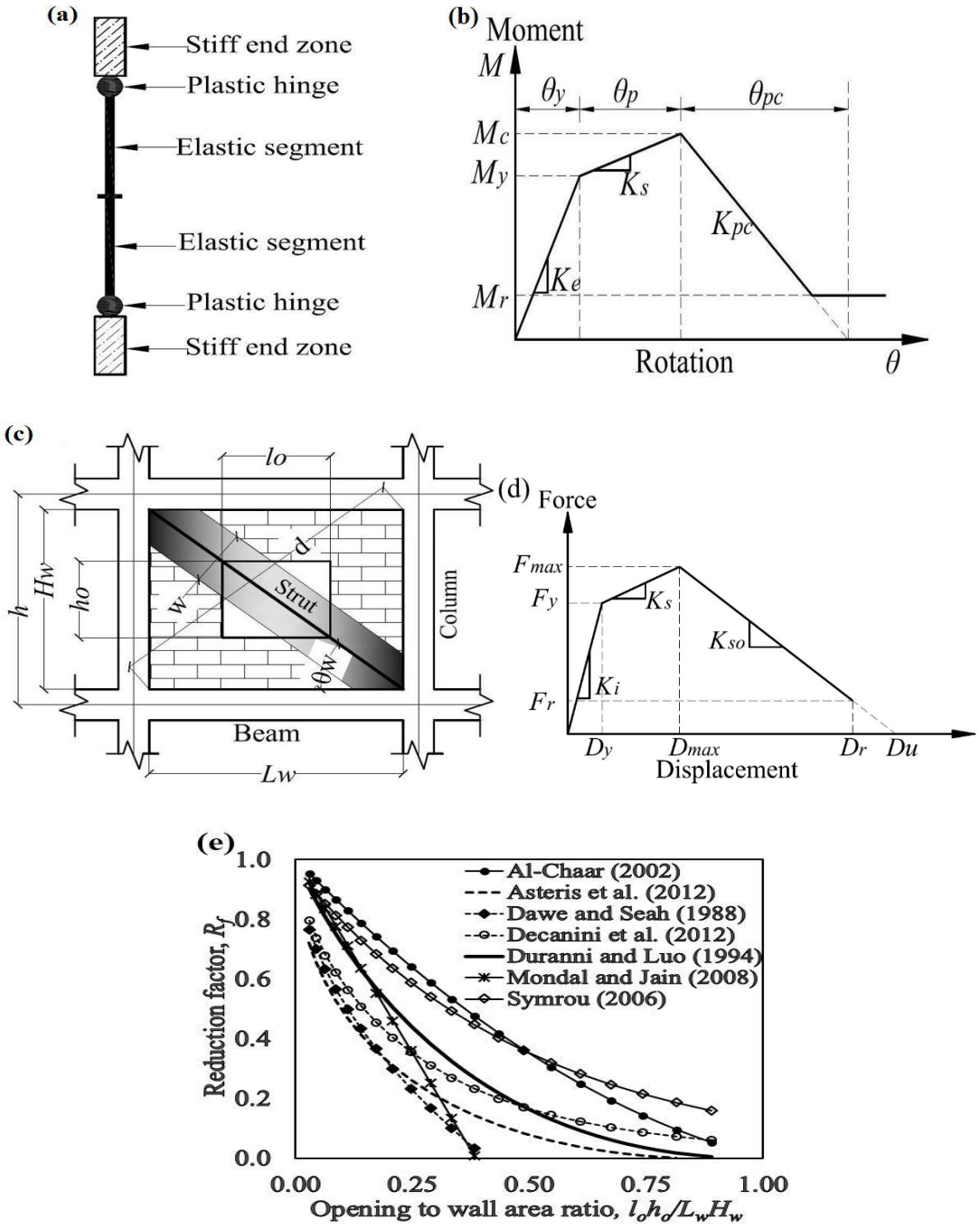

Figure 5-3 Numerical modelling of masonry infilled RC frame, (a) chord rotation model; (b) F-D relationship of RC members; (c) masonry infill wall representation by equivalent strut; (d) F-D relationship of the equivalent strut model and (e) comparison of reduction factors.

5.5.2 Modelling of masonry infill wall

A single equivalent strut model available in the Perform 3D (CSI, 2006) software is used to model the infill walls as shown in Figure 5-3(c). The force-deformation envelope developed by Panagiotakos and Fardis (1996) is employed as shown in Figure 5-3(d). The initial stiffness, K_i and secant stiffness, K_s are obtained from

$$K_i = \frac{G_w L_w t_w}{H_w} \tag{5.1}$$

$$K_s = \frac{E_w w t_w}{d} \tag{5.2}$$

where G_w is the shear modulus of the infill wall and is calculated to be 40% of the modulus of elasticity of the infill wall, E_w. L_w, H_w, t_w and d are respectively the length, height, thickness and diagonal length of the infill wall as shown in Figure 5-3(c). The equivalent strut width, w is estimated from the equation proposed by Mainstone (1974) and adopted in FEMA 274 (1997). It is given by

$$w = 0.175d\left[\sqrt[4]{\left\{\frac{(E_w t_w sin2\theta_w)}{4EIH_w}\right\}}\right]^{-0.4} \tag{5.3}$$

where E and I are the modulus of elasticity and moment of inertia of the column respectively. The angle between the diagonal strut and the horizontal direction is represented by θ_w as shown in Figure 5-3(c). The negative stiffness, K_{so} of the softening branch is taken as $0.1K_i$. The force corresponding to the yield point is estimated from

$$F_y = f_{tp} t_w L_w \tag{5.4}$$

where f_{tp} is the cracking strength of the masonry wall. The maximum strength, F_{max} and the residual strength, F_r of the infill wall are respectively taken as $1.3F_y$ and $0.1F_y$ as in Panagiotakos and Fardis (1996). The displacements corresponding to the yield point, maximum strength and the residual strength are estimated from

$$D_y = \frac{F_y}{K_i} \tag{5.5}$$

$$D_{max} = D_y + \frac{F_{max} - F_y}{K_s} \tag{5.6}$$

$$D_r = \frac{F_{max} - F_r}{K_{so}} \tag{5.7}$$

The above modelling was calibrated in a previous study against testing data (Thinley and Hao, 2016). The same modelling procedures are followed in this study.

5.5.3 Incorporation of opening and soil structure interaction (SSI) in the model

The presence of opening reduces the strength and stiffness of the infill wall and is normally incorporated in the numerical model by introducing the reduction factor. For the infill walls with opening, the equivalent width of the diagonal strut is multiplied by the reduction factor

to obtain the revised strength and stiffness of the infill wall. The reduction factor proposed by different researchers such as AL-Chaar (2002), Asteris et al. (2011), Dawe and Seah (1989), Decanini et al. (2012), Durrani and Luo (1994), Mondal and Jain (2008) and Smyrou (2006) are compared for the ratios of the area of opening at the centre of the wall, $l_o h_o$ to the overall area of the wall, $L_w H_w$ as shown in Figure 5-3(e). The notations l_o and h_o are respectively the length and height of the opening as illustrated in Figure 5-3(c). As observed from Figure 5-3(e), the reduction factor proposed by Durrani and Luo (1994) represent the mean of all these factors and therefore it is used in this study. It is given by the expression

$$R_f = 1 - \left[1 - \frac{(dsin(2\theta_w) - d_o \sin(\theta_w + \theta_o))^2}{2L_w H_w \sin(2\theta_w)}\right]^2 \quad (5.8)$$

where d_o and θ_o are respectively the diagonal length of the opening and the angle made by the diagonal length of the opening with the horizontal direction. The other notations are the same as those in the above equations.

In this study, SSI is considered only at the soft soil site for masonry infilled RC buildings without soft storey. It was observed from the previous studies that the effect of SSI is not very significant at the rock, shallow stiff soil and soft rock sites (Thinley et al., 2014; Thinley and Hao, 2015). The uncoupled spring model is used to represent the rigid column footings which are founded at the shallow depth of 1.2 m to 2.5 m. Since it is quite difficult to include the frequency dependent dynamic foundation impedance function in nonlinear analysis, only the static springs are used. The equivalent stiffness coefficients of the springs are estimated from ASCE/SEI 41-13 (2014). The effective shear modulus, of the soil is estimated from the shear wave velocity of the soil and response spectral acceleration at the short period. The size of the square footing, B = 3.5 m, 2.2 m and 1.5 m and the corresponding depth of footing pad, d = 0.75 m, 0.50 m and 0.35 m are respectively specified for '6 storey', '3 storey new' and '3 storey old' buildings. The effective depth of foundation, ranges from 1.0 m to 2.0 m depending on the overall foundation depth and the depth of footing pad. The Poisson's ratio is taken as 0.45 for the soft soil site.

5.6 Estimation of Probabilistic Structural Responses

5.6.1 Consideration of uncertainties

The most influential material and geometrical uncertainties are considered for the probabilistic structural response estimations in this study. The other uncertainties such as modelling are not expected to have a significant effect since the numerical model used in this study was previously calibrated with the experimental results. The ground motions used in this study are

considered as deterministic as they were specifically predicted from PSHA for the site conditions in Bhutan. However, it is acknowledged that strong earthquake ground motion in an engineering site is expected to vary significantly from location to location, and event to event. It is very difficult to quantitatively model these variations. The present study concentrates on modelling the variations of structural parameters on responses. Modelling the influences of statistical variations of ground motions on structural responses is deemed necessary, which could be a future research topic.

The material uncertainties considered in this study are the compressive strength of masonry wall, f_m, the compressive strength of concrete, f_c and the yield strength of steel, f_y since they are found to significantly influence the structural responses amongst the other parameters. The modulus of elasticity of the reinforced concrete and masonry wall are also empirically related to their respective compressive strength. The geometrical uncertainties considered are the depth, *D* and width, *b* of the RC beams and columns and the thickness of main masonry wall, t_m and partition wall, t_p. The design values of these parameters are taken as the respective mean values, while the coefficient of variation (CoV) and probability distribution have been taken from a number of past studies and guidelines as discussed in the following sub-sections. Due to the absence of information regarding their cross-correlation, these parameters are assumed to be statistically independent of each other. The material and geometrical uncertainties considered in this study along with the CoV and distribution types are given in Table 5-2.

Table 5-2 Mean and coefficient of variation of material and geometrical parameters

	6 storey building		**3 storey new building**		**3 storey old building**		
Variables	**Mean**	**CoV**	**Mean**	**CoV**	**Mean**	**CoV**	**Probability Distribution**
fm	6.07 MPa	0.20	6.07 MPa	0.20	3.77 MPa	0.24	Normal
fc (columns)	25 MPa	0.16	20 MPa	0.20	15 MPa	0.23	Normal
fc (others)	20 Mpa	0.20	20 MPa	0.20	15 MPa	0.23	Normal
fy	415 Mpa	0.09	415.00	0.09	415 MPa	0.09	Normal
t_m	250 mm	0.05	250 mm	0.05	250 mm	0.05	Normal
t_p	125 mm	0.05	125 mm	0.05	125 mm	0.05	Normal
D and b	As in Table 5-1	0.05	As in Table 5-1	0.05	As in Table 5-1	0.05	Normal

5.6.1.1 Compressive strength of masonry wall (f_m)

The compressive strength of the brick masonry walls used in this study is adopted from the results of a number of prism tests conducted by Kaushik et al. (2007) on Indian bricks. They found the mean compressive strengths of the brick masonry with medium and weak cement mortars to be 6.07 MPa and 3.77 MPa respectively with the respective CoV of 0.20 and 0.24.

These values are assumed to be applicable in Bhutan since Indian bricks with similar cement-sand mortar compositions are used in Bhutan. Other studies such as Gumaste et al. (2007) and Sarangapani et al. (2005) also provided similar values of compressive strength on the Indian brick masonry. The compressive strength of masonry wall is assumed to be normally distributed.

5.6.1.2 Compressive strength of concrete (f_c)

The CoV of concrete has been suggested by many researchers and vary from 0.14 to 0.21. For the concrete casted with average and with the excellent quality control during construction, Mirza et al. (1979) suggested a CoV of 0.18 and 0.14 respectively. The other researchers such as Barlet and MacGregor (1996) and Ellingwood (1977) suggested the CoV of 0.186 and 0.21 respectively. In this study, the CoV of 0.23, 0.20 and 0.16 for the concrete compressive strength of 15 MPa, 20 MPa and 25 MPa are respectively adopted as recommended by Indian Standard for Plain and Reinforced Concrete, IS 456 (2000). The normal distribution is assumed similar to the above studies.

5.6.1.3 Yield strength of steel (f_y)

The coefficient of variation of 0.09 with the normal distribution is assumed for the statistical variation of the yield strength of steel. This is mainly based on the number of tests conducted by Basu et al. (2004) on the Indian reinforcing bars. They tested 500 samples of Fe415 grade steel and reported the mean and CoV of 509MPa and 0.0893 respectively. Similarly, Mirza and MacGregor (1979) tested 4000 samples of grade 40 and 60 bars and obtained the respective mean and CoV of 337 MPa and 0.107 for grade 40 bars and 503 MPa and 0.093 for grade 60 bars respectively. The modulus of elasticity of steel is reported to have very small CoV and is therefore considered as deterministic in this study.

5.6.1.4 Member dimension (M_d)

In line with the other researchers, the CoV of 0.05 and normal distribution are assumed for the statistical variation of geometrical dimensions. While investigating the reliability of reinforced concrete slab under explosive loading, Low and Hao (2001) assumed CoV of 0.05 for all dimensions. The CoV of 0.03 and normal distribution were assumed by Kirke and Hao (2004) in estimating the failure probabilities of the RC buildings in Singapore. In this study, the statistical variation of dimension is only applied to the beam and column cross sections and to the thickness of masonry infill walls.

5.6.2 Estimation of structural responses

The estimation of structural responses involving a number of statistical parameters is quite complicated. Since the material and geometrical parameters considered in this study are normally distributed, Rosenbluth Point Estimate Method (RPEM) is employed to model the statistical variation of parameters. For the normally distributed variables, this method was found to estimate the accurate moments of a function (Kirke and Hao, 2004). The accuracy of the RPEM is verified by using the Monte Carlo Simulation Method (MCSM). These methods are briefly described in the following sections.

5.6.2.1 Rosenbluth Point Estimate Method (RPEM)

Rosenblueth (1975) first developed this method for estimating the statistical response quantities involving several parameters which may be correlated or uncorrelated. It is a quite straightforward, computationally efficient and only requires a little knowledge of probability concept. The procedure involves the consideration of two point estimates at one standard deviation on either side of the mean value for each variable. The performance function is estimated for every possible combination of these point estimates. Depending on the number of variables considered, the number of point estimates and the number of possible combinations of the point estimates are respectively given by $2n$ and 2^n, where n is the number of random parameters considered. Since four statistical parameters are considered in this study, namely f_m, f_c, f_y and M_d, they result into 8 point estimates as given below.

f_m^+, f_m^-, f_c^+, f_c^-, f_y^+, f_y^-, M_d^+ and M_d^-

where f_m^+, f_c^+, f_y^+ *and* M_d^+ represent the respective parameters with mean plus one standard deviation while f_m^-, f_c^-, f_y^- and M_d^- represent the mean minus one standard deviation. These 8 point estimates give rise to 16 possible combinations.

Perform 3D (CSI, 2006) program is employed to carry out the nonlinear analyses for each of these combinations using the ground motions described in section 3. The structural response quantities such as interstorey drifts and displacements are estimated from the nonlinear analyses corresponding to each of these 16 combinations. The mean and standard deviation are then estimated from the 16 response quantities estimated from the 16 combinations. This method is initially applied to the masonry infilled '3 storey new' RC buildings without soft storey to estimate the probabilistic response quantities which are later validated by the MCSM.

5.6.2.2 Monte Carlo Simulation Method (MCSM)

This method is very close to the real answer and normally used as a reference to validate the other probabilistic results. It involves solving the deterministic problem many times to build up a statistical distribution of the output quantity. However, it requires a large number of simulations to arrive at the converged solution and is not practical for an everyday problem. In this study, it is only used to validate the RPEM and determining the statistical distribution of the output quantity. This method is applied only to the masonry infilled '3 storey new' building without soft storey for the said purposes.

Based on the mean, standard deviation and distribution pattern of the statistical parameters given in Table 5-2 for the masonry infilled '3 storey new' building, 1000 random variables are initially generated for each parameter. Using the stratified sampling technique, 250 random variables are finally selected for each parameter from 1000 random variables. The nonlinear analyses are then carried out starting from the first combination of these random variables until the mean and standard deviation of the response quantities remain virtually unchanged. The response quantities in this study mainly refer to the interstorey drift which is more closely related to the damage of the buildings. It is observed that the mean and standard deviation of the interstorey drift and displacement remained almost constant after 150 simulations, indicating the convergence of the solution. This is possible owing to the use of the stratified sampling technique without which the number of simulations to arrive at the converged solution could have been substantially larger. Figures 5-4 and 5-5 respectively depict the convergence of mean interstorey drift and its standard deviation at the generic soil sites under the 475 year return period ground motions.

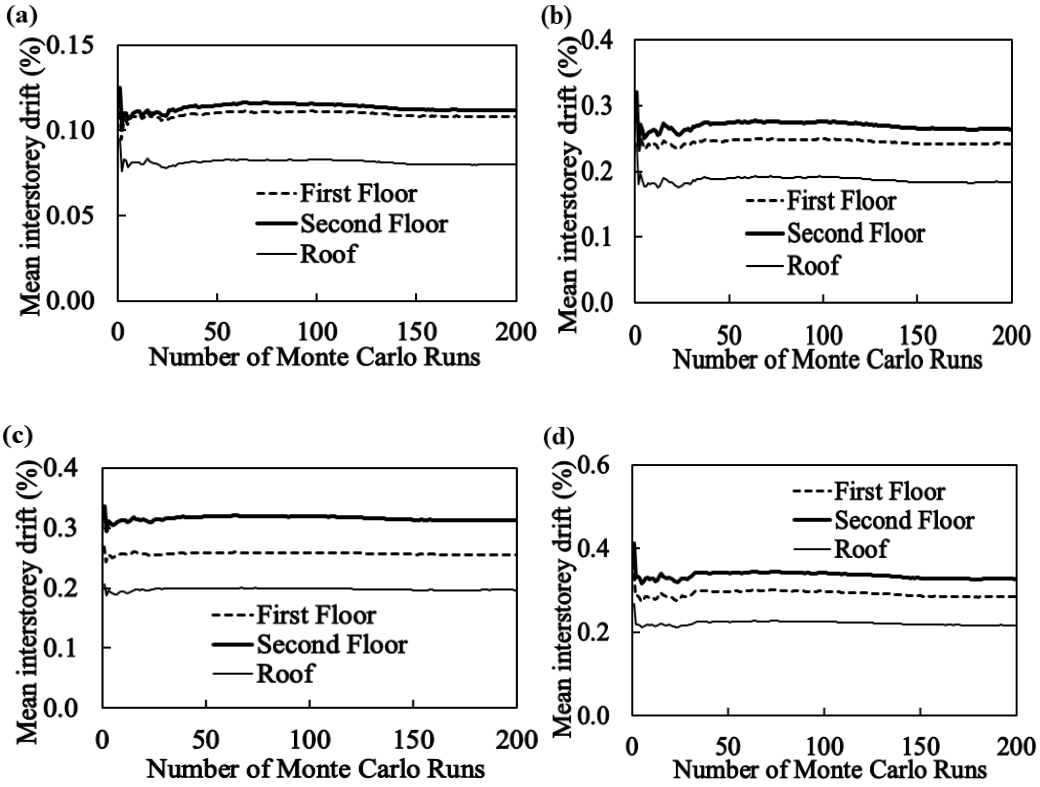

Figure 5-4 The convergence of mean interstorey drift obtained from Monte Carlo Simulation Method, (a) rock; (b) shallow stiff soil; (c) soft rock and (d) soft soil sites.

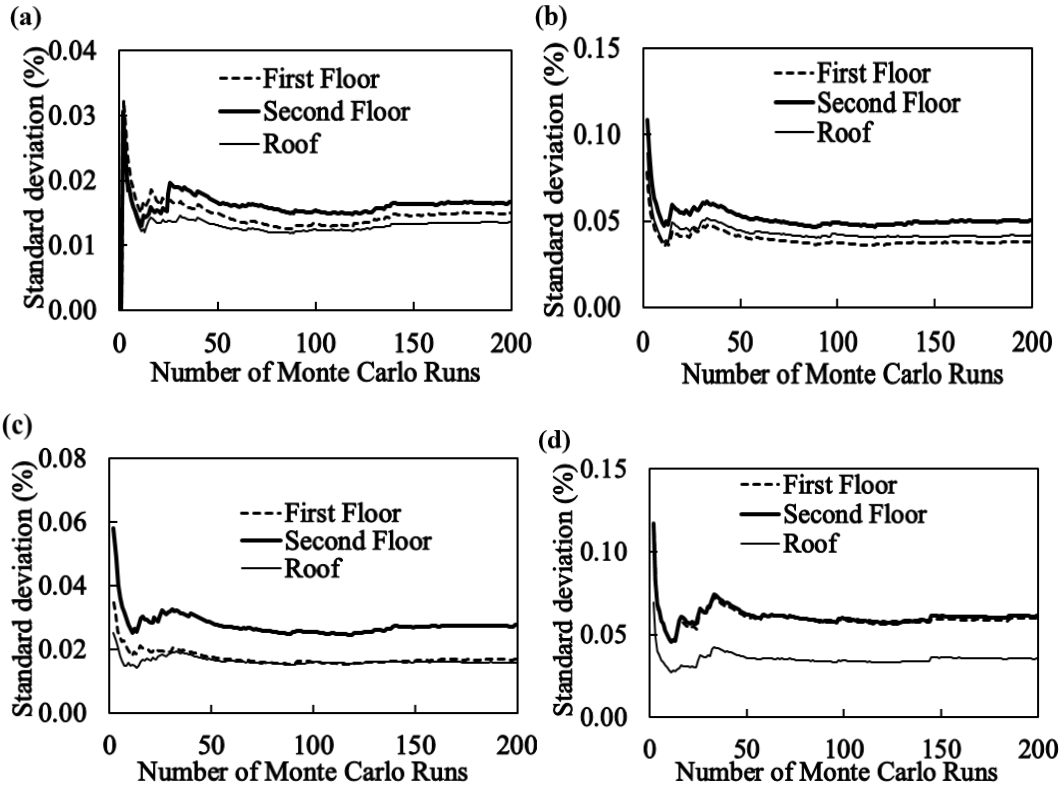

Figure 5-5 The convergence of standard deviation obtained from Monte Carlo Simulation Method, (a) rock; (b) shallow stiff soil; (c) soft rock and (d) soft soil sites.

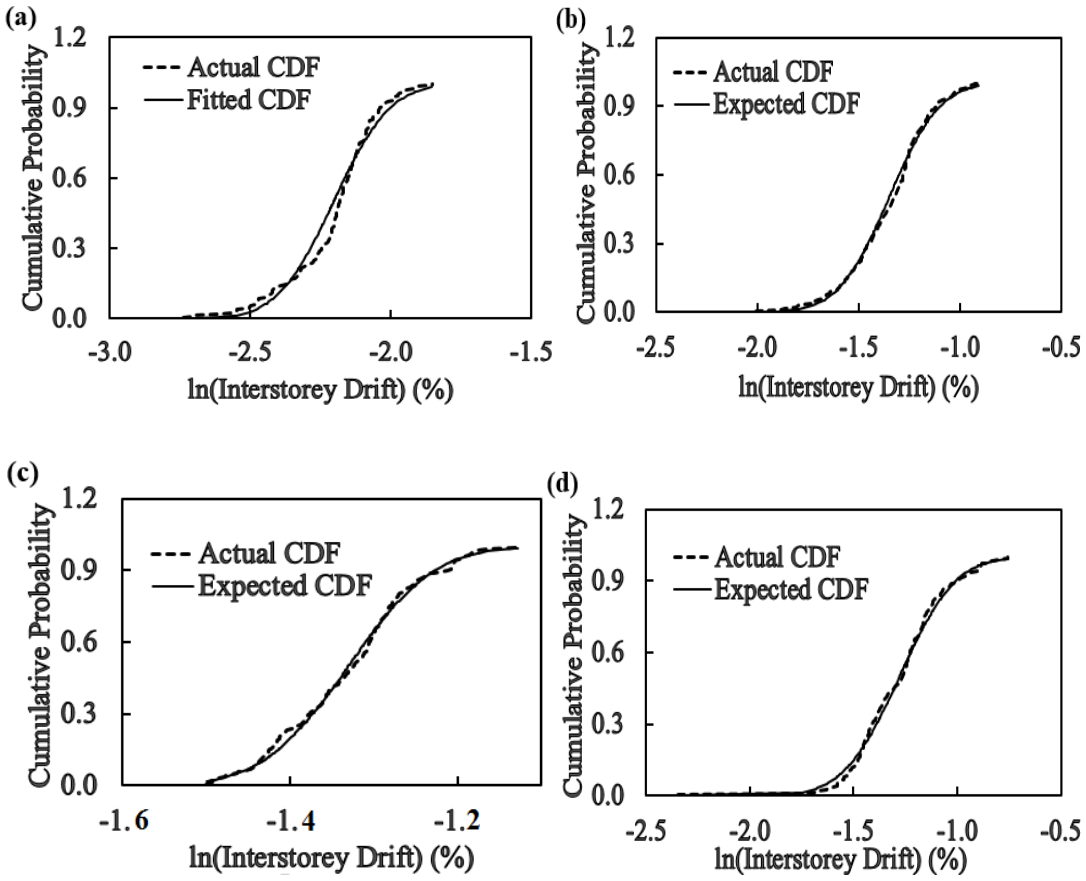

Figure 5-6 Comparison of actual and fitted CDF, (a) rock; (b) shallow stiff soil; (c) soft rock and (d) soft soil sites.

To validate the RPEM, the converged mean interstorey drift and standard deviation obtained from Monte Carlo Simulation Method are compared with the corresponding mean interstorey drift and standard deviation obtained from the RPEM. Table 5-3 shows the comparison of the results obtained from the two methods. From the table, it can be seen that the mean interstorey drift and standard deviation obtained from the two methods are very close to each other. This shows the capability of RPEM in estimating the probabilistic structural response quantities with sufficient accuracy.

In addition, the data obtained from the MCSM are also be used to determine the statistical distribution of the response quantity. It is observed that the interstorey drifts obtained from the MSCM are lognormally distributed. The commonly used Kolmogorov-Smirnov goodness of fit test is carried out to verify the observed distribution. Table 5-4 shows the K-S test statistic values of the interstorey drift at three floors and the critical values for 0.10 and 0.05 significance levels. From the table, it can be observed that most of the test statistic values are lower than the critical value of 0.10 significance level, while very few are lower than the critical value of 0.05 significance level. This confirms that most of them pass K-S test with

10% significance level and a few pass with 5% significance level, indicating a very good fit. The plot of actual cumulative distribution function (CDF) and fitted cumulative distribution function of the interstorey drift at the second floor level is shown in Figure5-6. As shown in the figure, a very close match is obtained confirming the lognormal distribution. Similar observations are also made for the interstorey drift at first floor and roof level, which are not shown here for brevity.

Table 5-3 Mean interstorey drift and standard deviation obtained from RPEM and MCSM under the 475 year return period ground motions

	First Floor		Second Floor		Roof	
	Mean (%)	Std Dev (%)	Mean (%)	Std Dev (%)	Mean (%)	Std Dev (%)
a) Rock site						
Rosenbluth	0.117	0.019	0.128	0.021	0.091	0.019
MonteCarlo	0.110	0.016	0.122	0.018	0.083	0.015
b) Shallow stiff soil site						
Rosenbluth	0.275	0.054	0.304	0.070	0.213	0.054
MonteCarlo	0.262	0.048	0.284	0.060	0.195	0.048
c) Soft rock site						
Rosenbluth	0.284	0.024	0.354	0.032	0.222	0.033
MonteCarlo	0.265	0.020	0.323	0.028	0.210	0.020
e) soft soil site						
Rosenbluth	0.322	0.078	0.366	0.078	0.241	0.042
MonteCarlo	0.301	0.065	0.338	0.065	0.227	0.037

Table 5-4 K-S statistic values of interstorey drift and critical values

	K-S Test Statistic values at different soil sites				Critical value for α=0.1	Critical value for α=0.05
Storey	Rock Site	Shallow Stiff	Soft Rock	Soft Soil		
1	0.9451	0.0388	0.0653	0.0448	0.0865	0.0960
2	0.0930	0.0587	0.0888	0.0510	0.0865	0.0960
3	0.0801	0.0324	0.0544	0.0546	0.0865	0.0960

5.6.3 Probabilistic results and discussion

Having validated the accuracy of the RPEM and determined the statistical distribution of the response quantities in the previous section, RPEM is further employed to estimate the probabilistic response quantities of the other building models considered in this study. The mean maximum interstorey drifts of masonry infilled RC buildings without and with soft storey are given in Tables 5-5 and 5-6 and the mean interstorey drift profiles are shown in

Figures 5-7 and 5-8 respectively. It is to be noted that the analysis failed to run completely at the soft soil site for masonry infilled '3 storey old' building without soft storey under the 2475 year return period ground motion because of the excessive responses, indicating complete failure of the building. Similarly, the analysis failed to run completely for the masonry infilled '3 storey old' building with soft storey under both the 475 and 2475 year return period ground motions at the soft soil site. Hence their mean interstorey drifts and deviations are not shown in the respective tables and figures. The fundamental period of the masonry infilled RC buildings without and with soft storey estimated from the mean structural parameters are given in Table 5-7.

Table 5-5 Mean maximum interstorey drift and corresponding standard deviation for typical masonry infilled RC buildings in Bhutan

		475 year return period			2475 year return period			
Site class	Support Type	Mean (%)	Std. Dev. (%)	Floor Level	Mean (%)	Std. Dev. (%)	Floor Level	Probability distribution
a) 6 storey building								
Rock	Fixed	0.287	0.050	3	0.509	0.095	4	Log normal
Shallow stiff	Fixed	0.470	0.027	3	0.856	0.115	4	Log normal
Soft rock	Fixed	0.338	0.043	3	0.831	0.077	4	Log normal
Soft soil	Fixed	1.012	0.194	3	2.781	0.258	1	Log normal
Soft soil	Spring	1.413	0.243	2	2.903	0.597	2	Log normal
b) 3 storey new building								
Rock	Fixed	0.128	0.021	2	0.195	0.066	2	Log normal
Shallow stiff	Fixed	0.304	0.070	2	0.576	0.103	2	Log normal
Soft rock	Fixed	0.354	0.032	2	0.737	0.057	2	Log normal
Soft soil	Fixed	0.366	0.078	2	0.598	0.144	2	Log normal
Soft soil	Spring	0.439	0.094	1	1.933	0.483	1	Log normal
c) 3 storey old building								
Rock	Fixed	0.265	0.079	1	0.447	0.135	1	Log normal
Shallow stiff	Fixed	0.511	0.045	1	1.182	0.150	1	Log normal
Soft rock	Fixed	0.372	0.024	1	0.999	0.128	1	Log normal
Soft soil	Fixed	1.260	0.250	1	2.045	0.734	1	Log normal
Soft soil	Spring	1.981	0.330	1				Log normal

Table 5-6 Mean maximum interstorey drift and corresponding standard deviation for typical soft storey buildings in Bhutan

		475 year return period			2475 year return period			
Site class	Support Type	Mean (%)	Std. Dev. (%)	Floor Level	Mean (%)	Std. Dev. (%)	Floor Level	Probability distribution
a) 6 storey building								
Rock	Fixed	1.384	0.294	1.000	2.569	0.604	1.000	Log normal
Shallow stiff	Fixed	1.596	0.288	1.000	2.972	0.634	1.000	Log normal
Soft rock	Fixed	1.491	0.308	1.000	1.621	0.226	1.000	Log normal
Soft soil	Fixed	3.977	0.279	1.000	8.034	0.415	1.000	Log normal
b) 3 storey new building								
Rock	Fixed	0.960	0.333	1.000	1.781	0.533	1.000	Log normal
Shallow stiff	Fixed	1.812	0.235	1.000	2.968	0.570	1.000	Log normal
Soft rock	Fixed	1.327	0.317	1.000	2.218	0.343	1.000	Log normal
Soft soil	Fixed	3.368	1.142	1.000	5.702	1.827	1.000	Log normal
c) 3 storey old building								
Rock	Fixed	3.312	0.816	1.000	4.319	0.401	1.000	Log normal
Shallow stiff	Fixed	3.538	0.643	1.000	4.515	0.569	1.000	Log normal
Soft rock	Fixed	3.358	0.721	1.000	3.186	0.163	1.000	Log normal

Table 5-7 Fundamental period of typical buildings using scant stiffness to yield

	Period (Sec)			Participation factor		
Building	1st mode	2nd mode	3rd mode	1st mode	2nd mode	3rd mode
(a) Infilled frame buildings						
6 storey	0.288	0.092	0.052	0.709	0.122	0.021
3 storey new	0.124	0.034	0.023	0.639	0.050	0.009
3 storey old	0.159	0.040	0.027	0.559	0.056	0.008
(b) Soft storey buildings						
6 storey	1.102	0.180	0.042	0.908	0.001	0.000
3 storey new	0.892	0.072	0.024	0.895	0.000	0.000
3 storey old	2.380	0.105	0.027	0.992	0.000	0.000

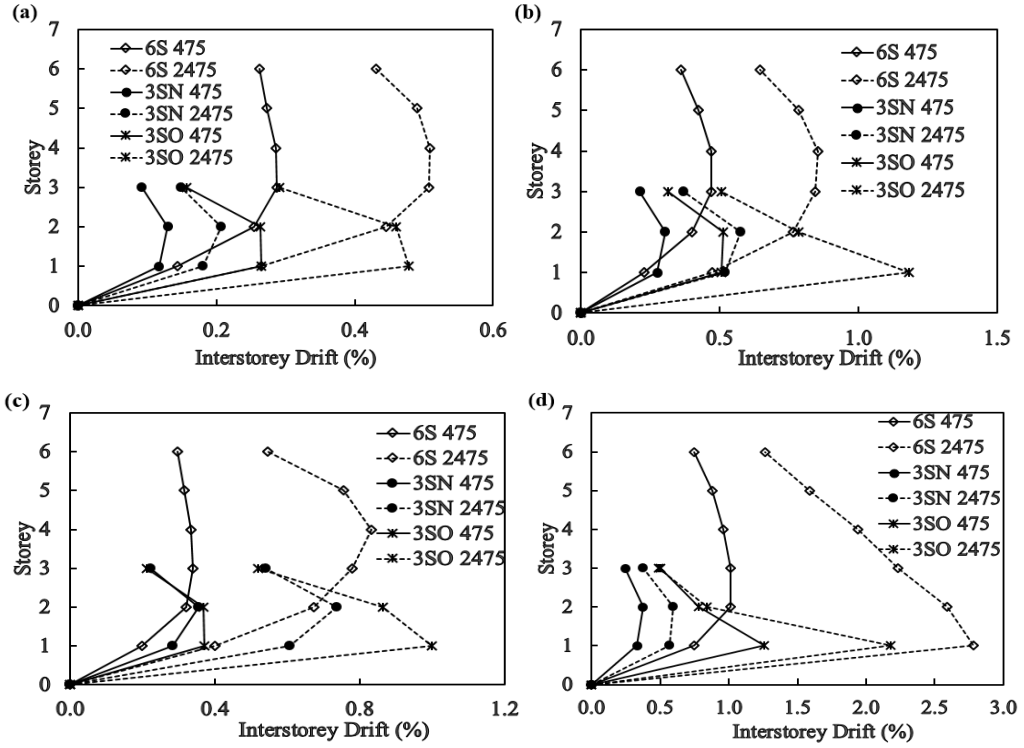

Figure 5-7 Mean interstorey drift profiles of masonry infilled RC buildings without soft storey under the 475 and 2475 return period ground motions with fixed support, (a) rock; (b) shallow stiff soil; (c) soft rock and (d) soft soil sites.

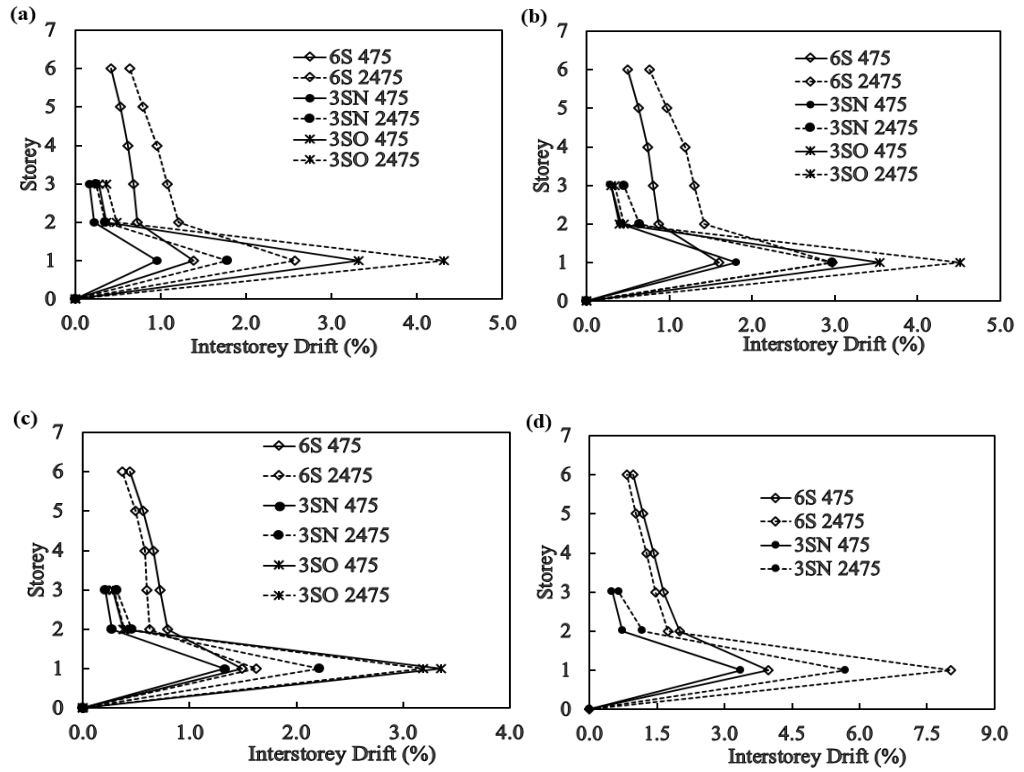

Figure 5-8 Mean interstorey drift profiles for masonry infilled RC buildings with soft storey subjected to the 475 and 2475 return period ground motions, (a) rock; (b) shallow stiff soil; (c) soft rock and (d) soft soil sites.

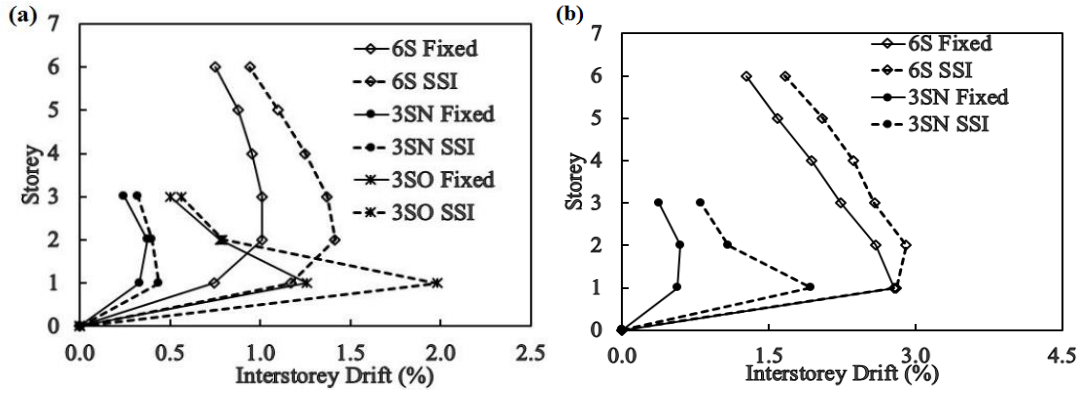

Figure 5-9 Comparison of mean interstorey drift profiles of masonry infilled RC buildings without soft storey at the soft soil site with and without considering SSI, (a) 475 and (b) 2475 year return period ground motion.

From Table 5-5 and Figure 5-7, it can be observed that the maximum interstorey drift of the masonry infilled buildings without soft storey could occur at any floor level, depending on the relative stiffness of the beams and columns at various floors of the building, intensity of ground motion and the contribution from the higher modes (Akkar et al., 2004; Alavi and Krawinkler, 2004; Adiyanto et al., 2011). The maximum interstorey drift normally occurs at the floor where the ratio of column to beam stiffness is the least. As shown, except at the soft soil site, the maximum interstorey drift of the masonry infilled '6 storey' building without soft storey occurs at the third and fourth floors under the 475 and 2475 year return period ground motions respectively. The shift from third to the fourth floor is because of the higher mode contributions to the response. As observed from Table 5-7, the contribution from the second and third modes is significant with sizeable participation factors. The occurrence of the maximum interstorey drift at the first floor under the 2475 year return period ground motion at the soft soil site could be due to the increase in the intensity of the ground motion. In the case of masonry infilled '3 storey new' building without soft storey, the maximum interstorey drift occurs at the second floor at all soil sites with fixed support. The increase in the intensity of ground motion has no effect in shifting the maximum interstorey drift to the lower floor which could be due to the higher stiffness of the columns. At the soft soil site with spring support, the maximum interstorey drift occurs at the first floor level confirming the influence of the foundation flexibility and increase in the intensity of ground motion. The occurrence of maximum interstorey drift at the first floor level for the masonry infilled '3 storey old' building without soft storey is quite obvious owing to the smaller column to beam stiffness ratio and the influence of the first mode. As observed from Table 5-6 and Figure 5-8, the maximum interstorey drift of masonry infilled RC buildings with soft storey always occurs at

the first floor level. This is obvious since stiffness of the ground floor is considerably reduced owing to the removal of the infill wall from the ground floor.

From Figures 5-7 and 5-8, it can be observed that the interstorey drift increases by 1.5 to 3 times when the intensity of ground motion is increased from 475 to 2475 year return period at the various soil sites. The soft storey effect can be observed by comparing the interstorey drift values in Tables 5-5 and 5-6 and Figures 5-7 and 5-8. From the tables, the interstorey drifts of the masonry infilled RC buildings with soft storey are 3 to 13 times higher than that of the masonry infilled RC buildings without soft storey. Moreover, the fundamental periods of the masonry infilled RC buildings with soft storey are much higher than the periods of the corresponding masonry infilled RC buildings without soft storey as given in Table 5-7. These indicate the significant change in the structural response when the masonry wall is removed from the ground floor. It is interesting to note that the first mode period of the '3 storey old' building with soft storey is around twice as that of the '6 storey' building with soft storey. This could be largely due to a very weak ground floor columns of the '3 storey old' building rendering the building very flexible.

The effect of soil structure interaction can be observed from Figure 5-9, wherein the mean interstorey drift profiles estimated with and without considering SSI are compared. As shown, including SSI in calculation always results in higher interstorey drifts for all the building models considered. Under 475 year return period ground motion, SSI effect is found significant on '3 storey old' and '6 storey' buildings, but insignificant on the '3 storey new' buildings. However, SSI effect becomes significant on '3 storey new' building when subjected to the 2475 year return period ground motion. This is because the effect of SSI depends on the site natural period of soil, fundamental period of the building, ground motion intensity and the level of nonlinear responses. The above observations demonstrate that neglecting SSI effect in structural response calculation may lead to inaccurate predictions.

5.7 Fuzzy Failure Probability analyses and Prediction of Damages

Interstorey drift is the most important response quantity which is used to define the damages of the building structures. Many guidelines provide a correlation between the interstorey drift values and the corresponding damage states of the buildings (FEMA 356, 2002; ATC 40, 1996; Vision 2000, 1995; ASCE/SEI 41-13, 2014). These correlations were however developed mainly for the general building structures and not specific to the masonry infilled RC buildings. In this study, the performance criteria developed by Ghobarah (2004) specifically for the masonry infilled RC buildings is used to correlate the damages of the masonry infilled RC buildings without soft storey in Bhutan. They were derived from a

number of analytical and experimental studies on the masonry infilled RC buildings and are assumed to be applicable to Bhutan. Similarly, there is paucity of performance criteria for the masonry infilled RC buildings with soft storey. In this study, the performance criteria of Vision 2000 (1995) which are mostly used for assessing the damages of the bare frame RC buildings are employed to evaluate the damages of the soft storey buildings. This is justifiable since the performance of the soft storey buildings is governed by the response of the ground floor columns which are devoid of infill walls. The interstorey drift values and the corresponding damage states specified by Ghobarah (2004) and Vision 2000 are given in Table 5-8.

Table 5-8 Damage states and corresponding interstorey drift limits

Performance levels	Damage state	Interstorey drift (IDR) limit (%)	
		Ghobarah (2004)	Vision 2000
Fully Operational (FO)	Slight	<0.1	<0.2
Operational (O)	Repairable	0.1≤IDR<0.4	<0.5
Life Safety (LS)	Irreparable	0.4≤IDR<0.7	<1.5
Near Collapse (NC)	Severe	0.7≤IDR≤0.8	<2.5
Collapse (C)	Complete	IDR>0.8	>2.5

Based on the probabilistic information of the maximum interstorey drift given in Tables 5-5 and 5-6 and the performance criteria in Table 5-8, the damage probabilities of the masonry infilled RC buildings without and with soft storey can be conventionally estimated from the equation below.

$$P_f = (D \geq D_c) = \int_{D_c}^{\infty} f_D(D) dD \tag{5.9}$$

where D is the maximum interstorey drift demand given in Tables 5-5 and 5-6 for buildings with and without soft storey respectively, $f_D\ (D)$ is its probability density function and D_c is the critical interstorey drift value correlated to the damage given in Table 5-8. The damage probabilities predicted by Equation (5.9) are based on the fixed damage boundary wherein the structure is said to be damaged if $D \geq D_c$ and not damaged if $D < D_c$. However, the damage is a continuous process under the action of the load and is more appropriate to be defined with a fuzzy set. In other words, damage of a structure is not only dependent on the randomness of the input parameters but also on the fuzziness of the damage criteria (Zhao et al., 1995). For instance, referring to the interstorey drift limits of Vision 2000, it is not logical to categorize a building as severely damaged when the interstorey drift is 2.499% and completely collapsed when the interstorey drift value is 2.501%. Hence, it is more logical to define a fuzzy region between the damage boundaries given in Table 5-8 to estimate the fuzzy damage probabilities.

According to the fuzzy set theory, the fuzzy region is defined by introducing membership function in between the lower and upper fuzzy region. In the fuzzy region, the structure may fail even if $D < D_c$ and may not fail if $D \geq D_c$. Based on the random-fuzzy probability theory, the fuzzy failure probability of the structure can be obtained from

$$P_{ff} = P(D \geq D_c) = \int_{D_L}^{D_u} \mu(D) f_D(D) dD \tag{5.10}$$

where D_U and D_L are respectively the upper and the lower fuzzy limits and $\mu(D)$ is the membership function (Wu et al., 1999). The membership function is normally determined from the fuzzy statistic test, but in the absence of data, it is often determined based on the judgement of some experts (Zhao et al., 1995). A commonly used triangular membership function shown in Figure 5-10 is adopted in this study. It is constructed by extending the damage state to the midpoint of the next damage stage. The midpoint of damage limit is assigned the membership function of 1.0 since it is most likely that the damage would occur at the midpoint of the respective damage limits. The membership function, $\mu(D)$ =1 and $\mu(D)$ =0 respectively indicate 100% and 0% failure probabilities.

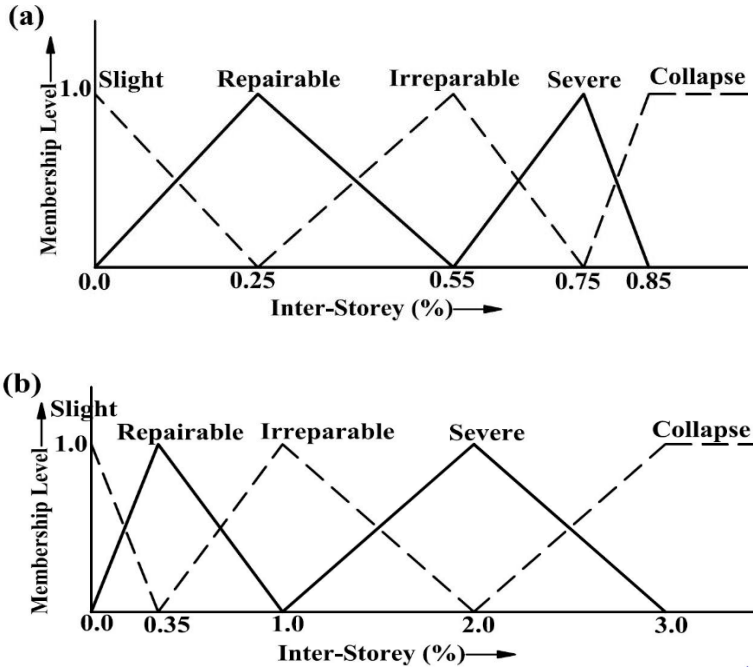

Figure 5-10 Triangular membership function used for the estimation of the fuzzy failure probabilities of the masonry infilled RC buildings, (a) without and (b) with soft storey.

The damage probabilities obtained from the conventional probability analysis using Equation (5.9) and fuzzy probability analysis using Equation (5.10) are given in Table 5-9 for the masonry infilled RC buildings without and with soft storey at the shallow stiff soil site under the 475 year return period ground motion. As observed from the table, the damage

probabilities predicted from the two analyses are comparable to one another with some variation. As discussed above, the damages predicted by the conventional analyses are based on the fixed damage boundaries, which provide good damage indication of the buildings although with some ambiguity in the damage boundaries. With the consideration of fuzzy region in between the damage boundaries, the fuzzy probability analyses take into consideration the ambiguity in the damage boundary definition. Hereafter, only fuzzy probability analysis is used to estimate the damage probabilities of the masonry infilled RC buildings without and with soft storey at all soil sites and under both the 475 and 2475 year return period ground motions.

The fuzzy failure probabilities estimated at the generic soil sites under the 475 and 2475 return period ground motions for the masonry infilled RC buildings without and with soft storey are given in Tables 5-10 to 5-12. As mentioned earlier, the soil-structure interaction is considered only for the masonry infilled RC buildings without soft storey at the soft soil site and the damage probabilities estimated considering SSI are termed as 'Soft soil (SSI)' in Tables 5-10 to 5-12.

Table 5-9 Comparison of failure probabilities obtained from fuzzy and conventional probability analyses at shallow stiff soil site under the 475 year return period ground motion

	Damage Category				
Building	Slight (%)	Repairable (%)	Irreparable (%)	Severe (%)	Collapse (%)
a) Conventional analysis - Masonry infilled					
6 storey	0.000	0.286	99.714	0.000	0.000
3 storey new	0.004	87.182	12.740	0.061	0.012
3 storey old	0.000	0.310	99.674	0.017	0.000
b) Fuzzy analysis - Masonry infilled					
6 storey	0.000	26.733	73.253	0.014	0.000
3 storey new	4.144	74.464	21.099	0.279	0.014
3 storey old	0.000	14.619	82.650	2.731	0.000
c) Conventional analysis - Soft storey					
6 storey	0.000	0.000	39.405	60.173	0.422
3 storey new	0.000	0.000	10.617	88.286	1.096
3 storey old	0.000	0.000	0.000	4.031	95.968
d)Fuzzy analysis - Soft storey					
6 storey	0.000	0.041	41.709	56.755	1.495
3 storey new	0.000	0.000	22.633	73.267	4.100
3 storey old	0.000	0.000	0.018	6.388	93.594

Table 5-10 Fuzzy failure probabilities of '6 storey' masonry infilled RC buildings with and without soft storey

	Damage Category				
Site Class	Slight (%)	Repairable (%)	Irreparable (%)	Severe (%)	Collapse (%)
a) Infilled frame building-475 return period ground motions					
Rock	2.208	83.427	14.364	0.001	0.000
Shallow stiff soil	0.000	26.733	73.253	0.014	0.000
Soft rock	0.027	70.440	29.533	0.000	0.000
Soft soil	0.000	0.000	0.665	7.259	92.075
Soft soil (SSI)	0.000	0.000	0.003	0.090	99.907
b) Infilled frame building-2475 return period ground motions					
Rock	0.000	20.779	68.623	9.961	0.637
Shallow stiff soil	0.000	0.003	4.436	28.762	66.799
Soft rock	0.000	0.000	2.675	34.130	63.194
Soft soil	0.000	0.000	0.000	0.000	100.000
Soft soil (SSI)	0.000	0.000	0.000	0.000	100.000
c) Soft storey building-475 return period ground motions					
Rock	0.000	1.115	60.142	38.075	0.668
Shallow stiff soil	0.000	0.041	41.709	56.755	1.495
Soft rock	0.000	0.434	51.328	46.871	1.367
Soft soil	0.000	0.000	0.000	0.000	100.000
d) Soft storey building-2475 return period ground motions					
Rock	0.000	0.000	4.014	44.964	51.022
Shallow stiff soil	0.000	0.000	0.667	25.489	73.844
Soft rock	0.000	0.002	38.581	60.667	0.750
Soft soil	0.000	0.000	0.000	0.000	100.000

Table 5-11 Fuzzy failure probabilities of '3 storey new' masonry infilled RC building with and without soft storey

	Damage Category				
Site Class	Slight (%)	Repairable (%)	Irreparable (%)	Severe (%)	Collapse (%)
a) Infilled frame building-475 return period ground motions					
Rock	47.927	52.060	0.013	0.000	0.000
Shallow stiff soil	4.144	74.464	21.099	0.279	0.014
Soft rock	0.970	64.685	33.730	0.593	0.022
Soft soil	0.261	57.911	41.150	0.664	0.015
Soft soil (SSI)	0.069	39.799	55.359	4.398	0.375
b) Infilled frame building-2475 return period ground motions					
Rock	18.421	80.404	1.175	0.000	0.000
Shallow stiff soil	0.000	9.813	64.224	22.575	3.388
Soft rock	0.000	0.000	15.067	68.180	16.753
Soft soil	0.001	11.017	55.084	24.534	9.364
Soft soil (SSI)	0.000	0.034	0.641	1.571	97.755
c) Soft storey building-475 return period ground motions					
Rock	0.031	23.810	64.596	11.252	0.310
Shallow stiff soil	0.000	0.000	22.633	73.267	4.100
Soft rock	0.000	2.540	63.572	33.135	0.753
Soft soil	0.000	0.003	2.044	21.540	76.414
d) Soft storey building-2475 return period ground motions					
Rock	0.000	0.676	33.964	52.796	12.564
Shallow stiff soil	0.000	0.000	0.440	24.348	75.212
Soft rock	0.000	0.000	6.370	65.822	27.808
Soft soil	0.000	0.000	0.026	1.344	98.630

Table 5-12 Fuzzy failure probabilities of '3 storey old' masonry infilled RC building with and without soft storey

	Damage Category				
Site Class	Slight (%)	Repairable (%)	Irreparable (%)	Severe (%)	Collapse (%)
a) Infilled frame building-475 return period ground motions					
Rock	8.152	80.118	11.686	0.043	0.001
Shallow stiff soil	0.000	14.619	82.650	2.731	0.000
Soft rock	0.000	59.334	40.666	0.000	0.000
Soft soil	0.000	0.000	0.185	1.692	98.123
Soft soil (SSI)	0.000	0.000	0.000	0.000	100.000
b) Infilled frame building-2475 return period ground motions					
Rock	0.000	25.845	71.329	2.815	0.011
Shallow stiff soil	0.000	0.000	0.001	0.132	99.867
Soft rock	0.000	0.000	0.303	5.575	94.122
Soft soil	0.000	0.000	0.000	0.003	99.997
c) Soft storey building-475 return period ground motions					
Rock	0.000	0.000	0.565	17.331	82.104
Shallow stiff soil	0.000	0.000	0.018	6.388	93.594
Soft rock	0.000	0.000	0.197	13.353	86.450
Soft soil	0.000	0.000	0.000	0.000	100.000
d) Soft storey building-2475 return period ground motions					
Rock	0.000	0.000	0.000	0.000	100.000
Shallow stiff soil	0.000	0.000	0.000	0.008	99.992
Soft rock	0.000	0.000	0.000	0.914	99.086
Soft soil	0.000	0.000	0.000	0.015	99.985

From Table 5-10, it can be observed that the masonry infilled ‘6 storey’ building without soft storey has the high probability of undergoing repairable damages at the rock and soft rock sites, irreparable damage at the shallow stiff soil site and complete collapse at the soft soil site under the 475 year return period ground motion. Under the 2475 year return period ground motion, the building could suffer irreparable damage at the rock site and complete collapse at the soft soil site. At the shallow stiff soil and soft rock site, the building has around 30% and 64% probabilities of undergoing severe damage and complete collapse, respectively. In regard to the masonry infilled ‘6 storey’ building with soft storey, high probability of irreparable damage is predicted at the rock site and almost an equal probability of irreparable and severe damages are predicted at the soft rock site under the 475 year return period ground motion. At the shallow stiff soil site, the building has 40% and 60% probability of undergoing irreparable and severe damages respectively. When the 2475 year return period ground motion is considered, the building could experience almost an equal probability of severe damage and complete collapse at the rock site, while it has the high probability of experiencing complete

collapse and severe damage at the shallow stiff soil and soft rock sites respectively. The building has the 100% probability of complete collapse at the soft soil site under both the 475 and 2475 year return period ground motions.

Referring to the Table 5-11, except at the soft soil site with SSI, where the high probability of irreparable damage is predicted, the masonry infilled '3 storey new' building without soft storey has the high probability of experiencing repairable damages at all soil sites under the 475 year return period ground motion. When the 2475 year return period ground motion is considered the building has the high probability of undergoing repairable, irreparable, severe and irreparable damages at the rock, shallow stiff soil, soft rock and soft soil sites respectively. At the soft soil site with flexible support, high probability of complete collapse is predicted. On the other hand, the masonry infilled '3 storey new' building with soft storey is likely to experience irreparable damage at the rock and soft rock sites and severe damage at the shallow stiff soil site under the 475 year return period ground motion. At the soft soil site, a high probability of complete collapse is predicted under the same ground motion. Under the 2475 year return period ground motion, the building has a high probability of experiencing severe damage at rock and soft rock sites and a very high probability of complete collapse at the shallow stiff soil and soft soil sites.

From Table 5-12, it can be observed that the masonry infilled '3 storey old' building without soft storey could experience high probability of repairable damage at the rock and soft rock sites and almost 100% probability of irreparable damage and complete collapse at the shallow stiff soil and soft soil sites under the 475 year return period ground motion. Except at the rock site where a high probability of irreparable damage is predicted, the probability of undergoing complete collapse is more than 90% at all other sites under the 2475 year return period ground motion. In the case of the masonry infilled '3 storey old' RC building with soft storey, more than 80% and 100% probabilities of complete collapse are predicted at all soil sites under the 475 and 2475 year return period ground motions respectively, indicating this type of structures is the most vulnerable when subjected to earthquake ground excitations.

The above results indicate that masonry infilled '3 storey new' RC building without soft storey is expected to suffer the least damage followed by the masonry infilled '6 storey' RC building without soft storey. The masonry infilled '3 storey old' RC building without soft storey is expected to experience the most severe damage because it was not properly designed while the other two buildings were designed and built according to the Indian Seismic Code. The results for the masonry infilled '3 storey new' building without soft storey also confirm that the intended design objectives, i.e., buildings remaining operational under the 475 year return period ground motion and are life safe when subjected to the 2475 year return period ground

motion, are achieved. However, the results for the masonry infilled '6 storey' building without soft storey indicate that it could not meet the design objectives mentioned above although it was designed according to the Indian Seismic Code. This indicates that the building was either not properly designed or that the Indian Seismic Code may not be directly applicable to the design of building structures in Bhutan because of the different ground motion characteristics.

It is interesting to note that the damage probabilities predicted for the masonry infilled '3 storey old' RC building without soft storey are comparable to that of the masonry infilled '6 storey' RC building without soft storey under the 475 year return period ground motion, although it was not designed to any standard. This could be due to the beneficial effect of the infill wall wherein the weaker RC frames of '3 storey old' building are strengthened by the addition of the infill walls and resulting in the overall increase in the stiffness of the building. However, under the 2475 year return period ground motion, the performance of the masonry infilled '6 storey' RC building without soft storey is better than that of the corresponding '3 storey old' building. This could be due to the transfer of lateral load from infill wall to RC frames as the intensity of the ground motion is increased. The RC frame of the '3 storey old' building being much weaker than that of the '6 storey' building undergoes more damages under the increased intensity of ground motion. The results also reveal that the damage probabilities predicted by considering SSI are higher than that without considering it. This indicates the detrimental effect of SSI.

As expected, the masonry infilled RC buildings with soft storey are more vulnerable to seismic ground excitations as compared to the masonry infilled RC buildings without soft storey. The damage of the soft storey building is highly influenced by the strength and stiffness of the ground floor columns. As the intensity of the ground motion increases, the inelastic action of the soft storey building is increasingly being borne by the ground floor columns. Hence, the ground floor columns with higher strength and stiffness suffer lower damage. The high probability of complete collapse predicted for the masonry infilled '3 storey old' building with soft storey is mainly due to its weak column.

5.8 Summary and Conclusion

Bhutan is located in one of the most active seismic regions in the Himalaya. The majority of the buildings in the urban centres consist of the masonry infilled RC buildings without and with soft storey whose performance under the earthquake ground motions is literally unknown. More than half of these buildings were not designed to any standard while the rest were designed according to the Indian Seismic Code whose applicability to the building structures in Bhutan is not studied. This study is aimed at predicting the damage probabilities

of the masonry infilled RC buildings without and with soft storey in Bhutan so as to derive the most effective mitigation measures of the impending seismic risk in the country. Fuzzy failure probabilities of the building models subjected to the predicted ground motions in Bhutan corresponding to the 475 and 2475 year return period ground motions are used in the analyses. The following conclusions can be drawn from this study:

1. The masonry infilled RC buildings without soft storey designed and built according to the Indian Seismic Code are likely to experience repairable damage under the 475 year return period ground motion and irreparable to severe damage under the 2475 year return period ground motion.
2. The old masonry infilled RC buildings without soft storey are likely to suffer repairable to irreparable damage under the 475 year return period ground motion and irreparable to complete collapse under the 2475 year return period ground motion.
3. The masonry infilled RC buildings with soft storey designed according to the Indian Seismic Code are likely to experience irreparable to severe damage under the 475 year return period ground motion and severe to complete collapse under the 2475 year return period ground motion.
4. The old masonry infilled RC buildings with soft storey built without engineering design could undergo irreparable to severe damage under the 475 year return period ground motion and complete collapse under the 2475 year return period ground motion.

The findings and the results presented in this study provide very useful information on the damage probabilities of buildings in Bhutan. The results could be especially useful for seismic loss estimation and seismic mitigation studies in the country.

5.9 References

ACI-318-14 (2014). *Building code requirements for structural concrete.* American concrete institute, Detroit, MI.

Adiyanto, M. I., Faisal, A., & Majid, T. A. (2011). Nonlinear Behaviour of Reinforced Concrete Building under Repeated Earthquake Excitation. In: *Proceedings of the International Conference on Computer and Software Modelling*, Singapore.

Akkar, S., Gülkan, P., & Yazgan, U. (2004). A simple procedure to compute the interstory drift for frame type structures. In: *Proceedings of the 13th World Conference of Earthquake Engineering*, Vancouver, British Columbia, Canada.

Alavi, B., & Krawinkler, H. (2004). Behavior of moment-resisting frame structures subjected to near-fault ground motions. *Earthquake Engineering and Structural Dynamics, 33* (6), 687-706.

Al-Chaar, G. (2002). *Evaluating strength and stiffness of unreinforced masonry infill structures*. Report No. ERDC/CERL-TR-02-1, Engineer Research and Development Centre Champaign, US Army Corps of Engineers, Illinois, USA.

ASCE/SEI 41-13 (2014). *Seismic Rehabilitation of Existing Buildings*. American Society of Civil Engineers, Reston, Virginia, USA.

Asteris, P. G., & Cotsovos, D. (2012). Numerical investigation of the effect of infill walls on the structural response of RC frames. *Open Construction and Building Technology Journal, 6* (1), 164-181.

Asteris, P. G., Chrysostomou, C. Z., Giannopoulos, I. P., & Smyrou, E. (2011). Masonry infilled reinforced concrete frames with openings. In: *Proceedings of the 3rd International Conference on Computational Methods in Structural Dynamics and Earthquake Engineering*, Greece.

ATC-40 (1996). *Seismic Evaluation and Retrofit of concrete Buildings volume 1*. Applied Technology Council, Redwood City, California, USA.

Banerjee, P., & Burgmann, R. (2002). Convergence across the northwest Himalaya from GPS measurements. *Geophysical Research Letters, 29*, 30-1-30-4.

Barlett, F. M., & MacGregor, J. G. (1996). Statistical analysis of the compressive strength of concrete in structures. *ACI Material, 93* (2), 158-68.

Basu, P. C., Shylamoni, P., & Roshan, A. D. (2004). Characterisation of steel reinforced for RC structures: An overview and related issues. *The Indian Concrete Journal.*

Bilham, R., Larson, K., Freymueller, J., Jouanne, F., Lefort, P., Leturmy, P., Mugnier, J., Gamond, J., Glot, J., & Martinod, J. (1997). GPS measurements of present-day convergence across the Nepal Himalaya. *Nature, 386*, 61-64.

CSI (2006). *Nonlinear Analysis and Performance Assessment for 3-D Structures.* Computers and Structures, Inc., Berkeley.

Dawe, J., & Seah, C. (1989). Lateral load resistance of masonry panels in flexible steelframes. In: *8th Internation Brick and Block Masonry Conference*, Dublin, Ireland, 19-21 September, pp. 606-616.

Decanini, L., Liberatore, L., & Mollaioli, F. (2012). The influence of openings on the seismic behaviour of infilled framed structures. In: *Proceedings of the 15 World Conference on Earthquake Engineering*, Lisbon, Portugal, 24-28 September.

Dolšek, M., & Fajfar, P. (2008). The effect of masonry infills on the seismic response of a four-storey reinforced concrete frame—a deterministic assessment. *Engineering Structures, 30* (7), 1991-2001.

Dorji, J. (2009). *Seismic performance of brick infilled RC frame structures in low and medium rise buildings in Bhutan*. Master degree thesis, Centre for Built Environment and Engineering Research, Queensland University of Technology, Brisbane, Australia..

Durrani, A. J., & Luo, Y. (1994). *Seismic retrofit of flat-slab buildings with masonry infills.* Technical Report, National Center for Earthquake Engineering Research, San Francisco, CA, pp. 1-8.

Ellingwood, B. (1977). Statistical analysis of RC beam-column interaction. *Journal of the Structural Division, ASCE, 103.*

Elwood, K. J., & Eberhard, M. O. (2009). Effective stiffness of reinforced concrete columns. *ACI Structural Journal, 106*,(4), 476.

FEMA 356 (2002). *Prestandard and Commentary for the Seismic Rehabilitation of Buildings.* Federal Emergency Management Agency, Washington DC, USA.

FEMA-274 (1997). *Guidelines for the Seismic Rehabilitation of Buildings*. Federal Emergency Management Agency, Washington DC, USA.

Ghobarah, A. (2004). On drift limits associated with different damage levels. In: *Proceedings of the International workshop on performance-based seismic design*, Department of Civil Engineering, McMaster University, Hamilton, ON, Canada, 28 June -1 July.

Gumaste, K., Rao, K. N., Reddy, B. V., & Jagadish, K. (2007). Strength and elasticity of brick masonry prisms and wallettes under compression. *Materials and structures, 40* (2), 241-253.

Hao, H., & Tashi, C. (2012). Earthquake ground motion prediction and its influence on building structures in Bhutan. In: *Proceedings of the 12th International Symposium on Structural Engineering*, Wuhan, China, 17-19 November.

Haselton, C. B., & Deierlein, G. G. (2007). *Assessing seismic collapse safety of modern reinforced concrete moment frame buildings*. PEER Report 2007/08, Pacific Earthquake Engineering Research Center, University of California, Berkeley, California.

Haselton, C. B., Goulet, C. A., Mitrani-Reiser, J., Beck, J. L., Deierlein, G. G., Porter, K. A., Stewart, J. P., & Taciroglu, E. (2008). *An assessment to benchmark the seismic performance of a code-conforming reinforced-concrete moment-frame building*. PEER Report 2007/12, Pacific Earthquake Engineering Research Center, University of California, Berkeley, California.

IS 1893 (2002). *Criteria for Earthquake Resistant Deisgn of Structures*. Bureau of Indian Standards, New Delhi, 2002.

IS 456 (2000). *Indian Standards for Plain and Reinforced Concrete*. Bureau of Indian Standards, New Delhi, India.

Kaushik, H. B., Rai D. C., & Jain, S. K. (2007). Stress-strain characteristics of clay brick masonry under uniaxial compression. *Journal of materials in Civil Engineering, 19* (9), 728-739.

Kirke, A., & Hao, H. (2004). Estimation of failure probabilities of RC frame structures in Singapore to the simulated largest credible ground motion. *Engineering Structures, 26* (1), 139-150.

Low, H. S., & Hao, H. (2001). Reliability analysis of reinforced concrete slabs under explosive loading. *International Journal of Structural Safety, 23* (2), 157-78.

Mainstone, R. (1974). *Supplementary note on teh stiffness and strength of infilled frames*. In *Institution of Civil Engineers*, London, UK.

Mirza, S. A., & MacGregor, J. G. (1979). Variability of mechanical properties of reinforcing bars. *Journal of the Structural Division, ASCE, 105*, 751-766.

Mirza, S. A., Hatzinikolas, M., & MacGregor, J. G. (1979). Statistical descriptions of strength of concrete. *Journal of the Structural Division, ASCE, 80*, 167-76.

Mondal, G., & Jain, S. K. (2008). Lateral stiffness of masonry infilled reinforced concrete (RC) frames with central opening. *Earthquake Spectra, 24* (3), 701-723.

Murty, C. V. R., & Jain, S. K. (2000). Beneficial influence of masonry infill walls on seismic performance of RC frame buildings. In: *Proceedings of the 12th World Conference on Earthquake Engineering*, Auckland, New Zealand, 30 January-4 February.

Panagiotakos, T. B., & Fardis, M. N. (2001). Deformations of reinforced concrete members at yielding and ultimate. *ACI Structural Journal, 98* (2), 135-148.

Panagiotakos, T., & Fardis, M. (1996). Seismic response of infilled RC frames structures. In: *Proceedings of the 11th World Conference on Earthquake Engineering*, Acapulco, Mexico, 23-28 June.

Rosenblueth, E. (1975). Point estimates for probability moments. In: *Proceedings of the National Academy of Sciences, 72* (10), 3812-3814.

Sarangapani, G., Venkatarama, R. B., & Jagadish, K. (2005). Brick-mortar bond and masonry compressive strength. *Journal of materials in Civil Engineering, 17* (2), 229-237.

Smyrou, E. (2006). *Implementation and verification of a masonry panel model for nonlinear dynamic analysis of infilled RC frames*. Master's degree thesis, ROSE School, Pavia.

Thinley, K., & Hao, H. (2015). Seismic assessment of masonry infilled reinforced concrete frame buildings in Bhutan. In *Proceedings of the Pacific Earthquake Engineering Conference*, Sydney, NSW, Australia, 6-8 November.

Thinley, K., & Hao, H. (2016). Seismic response analyses and performance assessment of masonry-infilled reinforced concrete frame buildings in Bhutan without and with soft storey. *Advances in Structural Engineering***,** 1369433216661336.

Thinley, K., Hao, H., & Tashi, C. (2017). Seismic Performance of Reinforced Concrete Buildings in Thimphu, Bhutan. *International Journal of Structural Stability and Dynamics***,** *17* (7), 1750074.

Thinley, K., Hao, H., & Tashi, C. (2014). Seismic performance of reinforced concrete buildings in Bhutan. In: *Proceedings of the Australian Earthquake Engineering Society Conference*, Lorne, VIC, Australia. 21-23 November.

UNDP Report (2006). *Report on Thimphu Valley Earthquake Risk Management Program*. Standards and Quality Control Authority, Ministry of Works and Human Settlement, Thimphu, Bhutan.

Vision 2000 (1995). *Performance Based Seismic Engineering of Buildings; conceptual framework*. Structural Engineers Association of California, Sacramento, CA.

Walling, M. Y., & Mohanty, W. K. (2009). An overview on the seismic zonation and micro zonation studies in India. *Earth-Science Reviews, 96*, 67-91.

Wu, C., Hao, H., & Zhou, Y. (1999). Fuzzy-random probabilistic analysis of rock mass responses to explosive loads. *Computers and Geotechnics, 25* (4), 205-225.

Zhao, G., Li, Y., & Wang, H. (1995). Application of fuzzy-random probability theory to structural reliability. *Application of Statistics and Probabilitty ICASP, 7,* 753-755.

CHAPTER 6 SEISMIC FRAGILITY ANALYSIS OF MASONRY INFILLED REINFORCED CONCRETE FRAME BUILDINGS IN BHUTAN

6.1 Abstract

This study is focused on developing fragility curves for the masonry infilled RC buildings in Bhutan using both spectral accelerations at first mode period with 5% damping, S_a (T_1, 5%) and peak ground acceleration, PGA as intensity measures. Fragility curve serves as an important tool for the estimation of seismic damages and losses, providing retrofitting decisions and preparing disaster response plan. Bhutan, being located on one of the high seismic areas in the Himalaya and being home to a number of masonry infilled RC buildings, it is paramount to assess the performance of these buildings so as to prepare the effective disaster response plan in the country. Three typical masonry infilled RC buildings representing the general building stocks in the country are selected for the development of fragility curves. The effect of material uncertainty is studied by statistically varying the material parameters using Rosenbluth point estimate method. Incremental dynamic analyses are performed using 22 selected ground motion records to determine S_a (T_1, 5%) and PGA values corresponding to the specified interstorey drift criteria representing slight damage, repairable, irreparable, severe and collapse damage states for each ground motion record. Fragility curves are generated from the lognormal mean and standard deviation of S_a (T_1, 5%) and PGA values of various damage states estimated from 22 ground motion records. To give justice to the existence of a number of masonry infilled buildings with the open ground floor in Bhutan, fragility curves are similarly developed for this type of buildings for various damage states.

6.2 Introduction

The masonry infilled RC buildings are the most dominant and popular building structures in the urban areas of Bhutan where the population of the country is concentrated. The construction of these buildings was started in the 1970s and has then gradually replaced the traditional stone masonry buildings. In the capital city, Thimphu, almost all the traditional buildings are now replaced by the masonry infilled RC buildings as shown in Figure 6-1. Moreover, the construction of masonry infilled RC buildings has also begun in some rural areas in Bhutan. However, there is a huge concern for the safety of these buildings during the earthquakes. Bhutan does not have seismic design code of its own even to this day. The country has adopted Indian Seismic Code, IS 1893 (2002) for the design of buildings only in 1997. This implies that all buildings built prior to 1997 were not designed to any standard but were built entirely based on the limited experience of the local technicians. There is also a

concern for the safety of the buildings built after the adoption of Indian Seismic Code. This is owing to the fact that engineers would not necessarily have followed the Indian Seismic Code properly in the design of buildings since the number of engineers in the late 1990s and early 2000s was insufficient and not properly trained for performing the structural design of buildings. Moreover, the applicability of Indian Seismic Code for the design of buildings in Bhutan has not been examined and the suitability of its direct application is very much questionable owing to the difference in many conditions such as site conditions, construction materials, and workmanship, etc. Hence, the safety of masonry infilled RC buildings built both prior to and after the adoption of Indian Seismic Code needs to be studied to understand the performances of these buildings should an earthquake strikes Bhutan.

Figure 6-1 Typical masonry infilled RC buildings in Thimphu, Bhutan.

On the other hand, Bhutan is located on the eastern Himalaya which is the least studied section of the Himalaya. From the limited investigations carried out on the seismicity of Bhutan Himalaya, there are contrasting views put forward by different researchers. Some researchers such as Gahalaut et al. (2011) and Drukpa et al. (2006) consider Bhutan Himalaya as the low seismic zone since there are no records of earthquakes with magnitude, M_w greater than 7 occurred in Bhutan in the last 200 years. Gahalaut et al. (2011) suggested that the low seismicity of Bhutan Himalaya could be due to the changes in stress caused by the 1897 Shilling Plateau earthquake and also due to the slow convergence rate as compared to western Himalaya. On the other hand, from the paleo seismic investigation, Kumar et al. (2010) deduced that there is a strong probability of a large medieval earthquake occurring in Bhutan. However, the real fact is that Bhutan is surrounded by a number of big Himalayan earthquakes

that occurred in the past as shown in Figure 6-2. The 1934 Bihar-Nepal (M_w=8.1), 2011 Sikkim (M_w=6.9) and the most recent 2015 Gorkha (M_w=7.8) earthquakes occurred in the west, the 1950 Assam (M_w=8.6) in the east and the 1897 Shilling Plateau (M_w=8.1) to the south of Bhutan. It was also reported that big earthquake of $M_w > 7$ had occurred in Bhutan in the spring of 1713 and had destroyed buildings in all districts of Bhutan (Ambraseys and Jackson, 2003). Recently, Hetényi et al. (2016) confirmed that this very earthquake was actually occurred on 4th May 1714 and had a magnitude of 8 ± 0.5 based on the damage and paleo seismological observations. In addition, as reported and listed by Drukpa et al. (2006), 30 earthquakes in the magnitude range of 4.2-6.75 had occurred in Bhutan since 1937. The list excludes the recent M_w=5.5 and M_w=6.1 earthquakes that occurred in 2009 in the eastern Bhutan. It is evident from these earthquakes that Bhutan is indeed located in one of the most active seismic zones in the Himalaya and the big earthquakes such as the recent Gorkha earthquake cannot be ruled out in Bhutan.

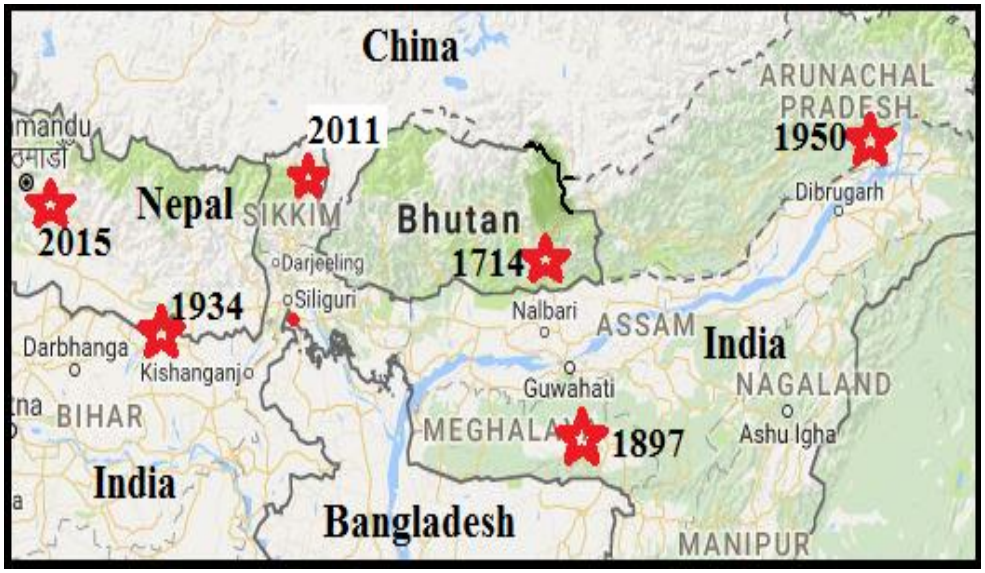

Figure 6-2 Approximate location of the big Himalayan earthquakes in and around Bhutan as indicated by the red star.

The presence of masonry infilled RC buildings constructed with and without proper design combined with the location of the country in the high seismic area makes it necessary to investigate the seismic safety of these buildings. However, there are very limited studies carried out on the seismic performance of the masonry infilled RC buildings in Bhutan. Through the initiative of the Government of Bhutan, 15 masonry infilled RC buildings in Thimphu, Bhutan were assessed employing the consultants from Nepal and local engineers. From the field observations and non-destructive test data, it was reported that only one building was found to satisfy the design requirement of the Indian Seismic Code (UNDP Report, 2006). This study was the first such study in Bhutan, but was very preliminary and

mainly based on the linear elastic analyses and also on the visual judgement of the consultants. Dorji (2009) studied the performance of masonry infilled RC buildings in Bhutan using 2 dimensional (2D) RC frame and subjecting it to three ground motion records from other regions. The predictions of the latter study are not necessarily realistic because of the simplified structural models and the somehow arbitrarily selected three ground motion records. Thinley and Hao (2016), Thinley and Hao (2017), and Thinley et al. (2017) recently studied the seismic performance of RC frame buildings with or without masonry infilled RC buildings in Bhutan employing the ground motions obtained at generic soil sites from the Probabilistic Seismic Hazard Analysis (PSHA).

This study is an extension of the previous studies. It aims at assessing the damages of the masonry infilled RC buildings in Bhutan through the development of fragility curves for various damage states by taking into consideration of possible random variations in ground motions and structural material parameters. The three typical masonry infilled RC buildings that epitomize the general building stocks in the country and are analysed in the previous studies are considered again for the fragility analysis. To model the possible random variations in ground motion characteristics, 22 ground motion records with their geometric mean acceleration response spectrum compatible to the predicted acceleration response spectrum for the shallow stiff soil site from PSHA (Thinley et al., 2017) are selected from PEER ground motion database. The damage states specified by Ghobarah (2004) are used for defining the damages of masonry infilled RC buildings. The numerical model of the masonry infilled RC frame which was previously calibrated with the experimental test results in Thinley and Hao (2016) is used in this study. The nonlinear analysis and performance assessment software, Perform 3D (CSI, 2006) is used for carrying out Incremental Dynamic Analysis (IDA) to estimate intensity measures corresponding to each damage level for each ground motion record. The random variations of material parameters is considered by employing Rosenbluth Point Estimate Method (Rosenblueth, 1975). The fragility curves are developed for each damage state using both Peak Ground Acceleration, PGA and spectral acceleration at first mode period with 5% damping, S_a (T_1, 5%) as intensity measures. The effect of soil-structure interaction (SSI) is not considered in this study since it was observed to be less significant from the previous studies (Thinley and Hao, 2016; Thinley et al., 2017).

Similarly, the fragility curves are also developed for the masonry infilled RC buildings with the open ground floor which are commonly referred to as soft storey buildings since they are also very common in Bhutan. For simplicity, the building models used for developing fragility curves for soft storey buildings are actually derived from the masonry infilled RC buildings originally considered in this study by removing infill walls from the ground floor of the

respective buildings. It is to be noted that masonry infilled RC buildings in this study refer to the general masonry infilled RC buildings, while the soft storey buildings refer to the masonry infilled RC buildings with the open ground floor throughout this manuscript.

The fragility curves developed in this study for the masonry infilled and soft storey buildings in Bhutan give more comprehensive predictions of the performances of the respective buildings. They can be used in the development of seismic risk response plan and appropriate retrofitting options.

6.3 Development of fragility curves

Fragility function defines the probability of reaching or exceeding a level of damage state, *DS* under the given ground motion intensity measure, *IM*. As reported by Rossetto and Elnashai (2003), there are four approaches of deriving fragility functions, namely empirical, judgemental, analytical and hybrid methods. In an empirical method, fragility curves are derived by statistically analysing the observed field data, while the opinion of experts is used in the judgemental method. Analytical and hybrid fragility curves are respectively derived from the dynamic structural analysis and from the combination of the other three methods (Calvi et al., 2006; Pejovic and Jankovic, 2016). In this study, the analytical method is used for generating the fragility curves of the masonry infilled RC buildings since there are no observed damage data or the data available from the expert's opinion in Bhutan. The analytical method has the advantage of providing the analyst with the control of data in terms of choosing *IM* levels and deciding the number of analyses at each level. In line with many other researchers, the two-parameter lognormal distribution function is used to define fragility function. Mathematically, it is defined as

$$P[DM \geq DM^{DS}/IM] = \Phi\left[\frac{\ln(IM)-\mu_{ln}}{\sigma_{ln}}\right] \tag{6.1}$$

where *P*[.] denotes the probability of damage measure, *DM* being at or exceeding a particular damage measure, DM^{DS} corresponding to the specified damage state, *DS* for a given seismic intensity level defined by the earthquake intensity measure, *IM*. Φ is the standard cumulative probability function, while μ_{ln} and σ_{ln} denote the mean and standard deviation of *ln* (*IM*) respectively. For lognormally distributed *IM*, the median of *IM* is the same as the mean of ln (*IM*).

Damage measure, *DM* is an observable quantity related to the damage of the structure. It is obtained from the nonlinear dynamic analysis for the various intensity level of ground motion. The most common *DM* used for the fragility analysis of buildings is the interstorey drift since

it correlates well with the observed damage of the buildings. The other observable quantities such as the maximum base shear, node rotation, peak roof drift and some damage indices defined based on these damage response quantities are also used as *DM* (Vamvatsikos and Cornell, 2002). In this study, interstorey drift is used as *DM* as in many previous studies. On the other hand, the intensity measure, *IM* characterises the intensity of a ground motion. PGA and spectral acceleration at the first mode period with 5% damping, S_a (T_1, 5%) are commonly used as *IM*, although both possess their respective strengths and weaknesses. It is quite straightforward to use PGA as *IM* and is also easy for common people to understand since it is used in many standards to define seismic hazard. However, PGA does not reveal important characteristics of an earthquake such as frequency content and time duration during the stronger part of an earthquake (Dumova-Jovanoska, 2000). Similarly, S_a (T_1, 5%) is found to be effective for structures with responses dominated by the first mode (Shome et al., 1998). However, S_a (T_1, 5%) does not incorporate the inevitable changes in the period of vibration when structure enters from the linear to the nonlinear range with the decrease in effective stiffness, and cannot effectively represent the responses contributed from higher modes. In this study, both the S_a (T_1, 5%) and PGA are used as *IM* in the analysis. The discussion in the use of other *IM* such as peak ground velocity, peak acceleration demand, peak velocity demand and peak displacement demand can be found in Shahi et al. (2014).

As given in Equation (6.1), the development of fragility curves basically requires the estimation of *DM* for various intensity levels of earthquake ground motion *IM*. Incremental Dynamic Analysis (IDA) and multiple stripe analysis are the two analytical approaches commonly employed to estimate *DM* and *IM* for fragility analysis (Baker, 2015). IDA is a powerful computational method that estimates a range of structural responses from elastic to inelastic and finally to collapse or global dynamic instability (Vamvatsikos and Cornell, 2002). Multiple stripe analysis involves performing analysis at a specified set of *IM* levels which are obtained from a different set of ground motions. In this study, IDA is used to estimate *DM* and *IM* to derive the fragility curves of the masonry infilled RC buildings in Bhutan. All in all, the development of fragility curves requires the selection of ground motion records, selection of prototype masonry infilled RC buildings, numerical modelling of the building models, consideration of uncertainties, the definition of damage states and finally the performance of incremental dynamic analysis (IDA). They are subsequently described below.

6.3.1 Selection of Ground Motion

The selection of ground motions is one of the most important steps for the seismic fragility analysis of structures since they are the major sources of uncertainties. Ideally, it is desirable to employ ground motions that occurred within the area of interest. However, there are no

ground motion acceleration records available in Bhutan, although it is located in one of the most active seismic zones in the Himalaya. In this study, 22 ground motions are selected from the PEER Ground Motion Database (PGMD) in line with the seismicity and soil sites in Bhutan. It was shown in the previous studies that 10 to 20 records are normally adequate for the estimation of seismic demands with sufficient accuracy when S_a (T_1, 5%) is used as intensity measures (Shome, 1999). In this study the selected ground motions have moment magnitude, M_w between 6.5 and 8, epicentral distance between 5 and 70 km and are recorded on sites with the shear wave velocity, V_{s30} of 450 to 750 m/s, corresponding to the shallow stiff soil site which is commonly found in Bhutan.

More importantly, the ground motions are selected in such a way that the geometric mean spectrum of the selected ground motions is compatible with the target spectrum as shown in Figure 6-3. In the absence of the design spectrum for Bhutan and strong motion record in the country, the acceleration response spectrum at shallow stiff soil site predicted by Thinley et al. (2017) from the Probabilistic Seismic Hazard Analysis (PSHA) for 475 year return period in Thimphu, Bhutan is therefore used as the target spectrum. Unlike in the case of amplitude scaling and spectrum matching processes which respectively result in high energy content at higher modes and same energy content over all records, the mean spectrum matching minimizes the amplification at higher modes and maintains the original record characteristics (Mazzoni et al., 2012). The mean spectral matching initially involves scaling the spectral acceleration of the individual ground motions at all periods so that the maximum spectral acceleration of the suite is equal to or less than the maximum spectral acceleration of the target spectrum. The additional scale factor is then applied to the entire ground motions in such a way that the mean square error between the spectral acceleration of the resulted mean spectrum and the target spectrum is minimized. The mean square error method is commonly used in many studies such as Pejovic and Jankovic (2016) in scaling the ground motions since it is effective and capable of selecting ground motions whose response spectra is very close to the target spectrum. The details of the ground motions selected are given in Table 6-1.

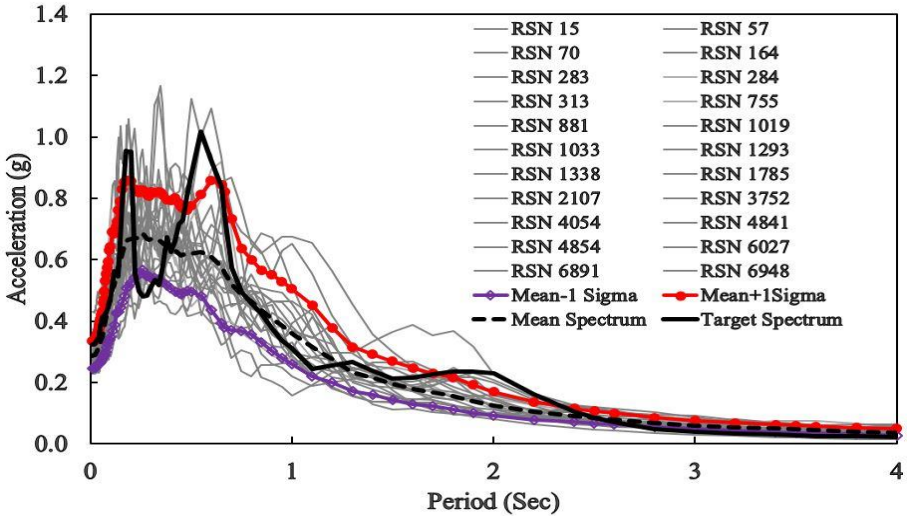

Figure 6-3 Selected ground motion spectra with their geometric mean and target spectrum

Record No.	Earthquake	Year	Station	Mw	Dist. (km)	Vs30 (m/sec)	PGA (g)
15	Kern County	1952	Taft Lincoln School	7.4	38.9	385.4	0.16
57	San Fernando	1971	Castaic - Old Ridge Route	6.6	22.6	450.3	0.32
70	San Fernando	1971	Lake Hughes	6.6	27.4	425.3	0.15
164	Imperial Valley	1979	Cerro Prieto	6.5	15.2	471.5	0.17
283	Irpinia	1980	Arienzo	6.9	52.9	612.8	0.03
284	Irpinia	1980	Auletta	6.9	9.6	476.6	0.06
313	Corinth	1981	Corinth	6.6	10.3	361.4	0.24
755	Loma Prieta	1989	Coyote Lake Dam	6.9	20.3	561.4	0.15
881	Landers	1992	Morongo Fire Station	7.3	17.4	396.4	0.22
1019	Northridge	1994	Lake Hughes	6.7	35.8	425.3	0.09
1033	Northridge	1994	Littlerock Brainard Can	6.7	46.6	485.7	0.07
1293	Chi-Chi	1999	HWA046	7.6	51.8	617.5	0.09
1338	Chi-Chi	1999	ILA050	7.6	66.9	621.1	0.06
1785	Hector Mine	1999	Fun Valley	7.1	54.7	388.6	0.08
2107	Denali_ Alaska	2002	Carlo (temp)	7.9	50.9	399.4	0.10
3752	Landers	1992	Forest Falls Post Office	7.3	45.3	436.1	0.09
4054	Bam	2003	Mohammad Abad	6.6	46.2	574.9	0.07
4841	Chuetsu-oki	2007	Joetsu Yasuzukaku	6.8	25.5	655.5	0.15
4854	Chuetsu-oki	2007	Nadachiku Joetsu City	6.8	35.9	570.6	0.12
6027	El Mayor	2010	Ocotillo Wells	7.2	67.7	361.2	0.09
6891	Darfield	2010	CSHS	7.0	43.6	638.4	0.09
6948	Darfield	2010	OXZ	7.0	30.6	481.6	0.13

6.3.2 Selection of Masonry infilled RC buildings

With the start of its construction in the early 1970s, the urban centres today are fully dominated by the masonry infilled RC buildings in Bhutan. The traditional stone masonry buildings which once dominated the urban centres are fast being replaced by the masonry infilled RC buildings. Moreover, the construction of masonry infilled RC buildings has also penetrated in some rural areas in Bhutan today. The buildings built prior to the adoption of the Indian Seismic Code in 1997 were not designed to lateral loads and most of them are of three storeys in height. With the adoption of the Indian Seismic Code from 1997, the height of the building gradually increased from three to four and currently the buildings up to six storeys are permitted in the capital city, Thimphu. Hence there exists a variety of masonry infilled RC buildings that were constructed with and without any kind of standard design and with the height ranging from 2 to 6 storeys. To represent these buildings, three typical masonry infilled RC buildings namely '6 storey', '3 storey new' and "3 storey old' are considered in this study. The '6 storey' and '3 storey new' are respectively the real typical masonry infilled RC buildings in Thimphu that were designed according to the Indian Seismic code. Since buildings built prior to the adoption of the Indian Seismic Code were mostly built by the local technician without any kind of design, there are no credible structural and architectural details available for those buildings. Hence, the '3 storey old' building model is the dummy masonry infilled RC buildings intended to represent those built prior to the adoption of the Indian Seismic Code. While the architectural details are assumed the same as that of the '3 storey new' existing buildings, its structural details are aligned with the typical structural details of the buildings built prior to 1997. The structural details such as the RC member sizes, amount of reinforcement and the strength of concrete and steel are adopted from the test result of the non-destructive test conducted on the 15 old masonry infilled RC buildings under the Thimphu Valley Earthquake Risk Management Project (TVERMP) in 2005 (UNDP Report, 2006). While '6 storey' masonry infilled RC buildings are more or less confined to the capital city, Thimphu, both '3 storey new' and '3 storey old' masonry infill buildings are very common in all urban centres in Bhutan including Thimphu. The column and masonry wall layout plan of the buildings and the reinforcement detailing in beams and columns are shown in Figure 6-4. The member dimension and reinforcement details of the buildings are given in Table 6-2.

The concrete compressive strengths, f_c of 25 MPa for columns and 20 MPa for other RC members were specified for '6 storey' building. As for '3 storey new' and '3 storey old' buildings, f_c of 20 MPa and 15 MPa were respectively specified for all RC members. The modulus of elasticity of concrete is taken as $E_c=5000(f_c)^{1/2}$ as per the Indian Standard for Plain and Reinforced Concrete, IS 456 (2000). The yield strength of steel, f_y used for all buildings is 415 MPa. The compressive strength of masonry, f_m used for '6 storey' and '3 storey new'

is 6.07 MPa while 3.77 MPa has been assumed for '3 storey old' building. The modulus of elasticity of masonry is taken as E_m=550f_m as recommended by Kaushik et al. (2007) and proposed in FEMA 306. The thickness of main and partition masonry walls are 250 mm and 125 mm respectively.

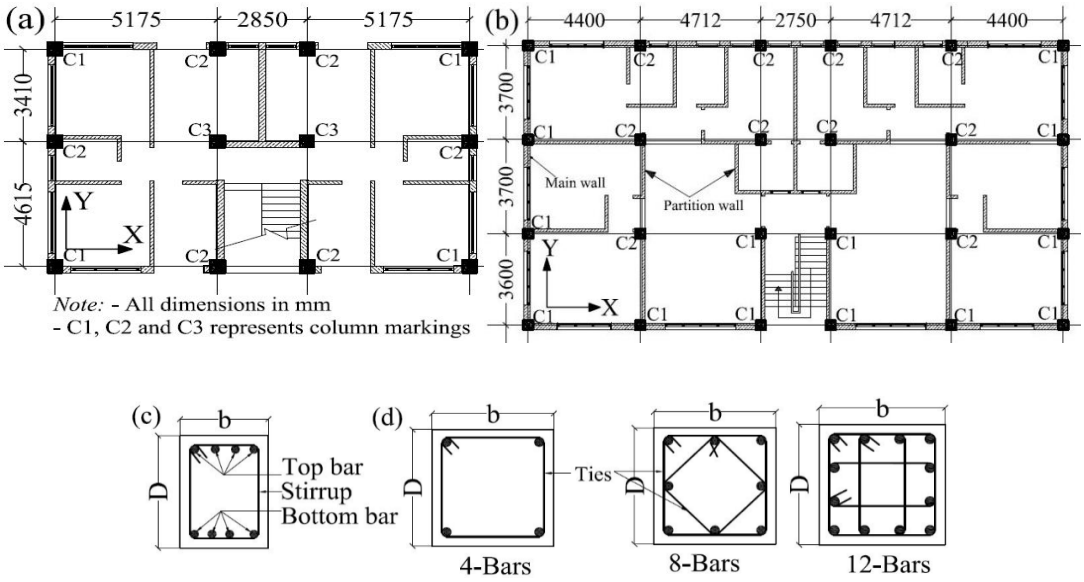

Figure 6-4 Column and masonry wall layout plan of (a) 6 storey and (b) 3 storey buildings. Reinforcement arrangement details of (c) beams and (d) columns.

Table 6-1 Reinforcement and member dimension details of the typical buildings

	6 storey		3 storey new		3 storey old	
(a) Floor Beams (FB) and Roof Beams(RB) reinforcement						
	Top Bar	Bottom Bar	Top Bar	Bottom Bar	Top Bar	Bottom Bar
FB along X	4-20	2-20+2-16	4-20	2-20+2-16	4-12	2-12+2-10
FB along Y	4-20	2-20+2-16	2-20+2-16	2-20+2-16	3-12	3-10
RB along X	2-20+2-16	4-16	2-20+2-16	4-16	3-12	3-10
RB along Y	2-20+2-16	4-16	4-16	2-16+2-12	2-12+1-10	3-10
Beam stirrups	8@100mmC/C		8@100mmC/C		6@150mmC/C	
(b) Column reinforcement						
Column C1	8-20 + 4-16		8-20		4-16	
Column C2	12-20		4-25+4-20		8-12	
Column C3	4-25+8-20					
Column ties	10@90mmC/C		8@100mmC/C		6@150mmC/C	
(c) Dimensions						
Beams along X	300mm x 450mm		300mm x 400mm		250mm x 350mm	
Beams along Y	300mm x 400mm		300mm x 400mm		250mm x 300mm	
Columns C1 & C2	450mm x 450mm		400mm x 400mm		250mm x 250mm	
Columns C3	500mm x 500mm					
Slab depth	150mmm		150mmm		100mmm	

6.3.3 Numerical Modelling of buildings for nonlinear analysis

The nonlinear analysis and performance assessment program, Perform 3D (CSI, 2006) is employed for the estimation of the structural responses of the selected buildings. The RC beams and columns are modelled using the chord rotation model which consists of the plastic hinge and an elastic segment with stiff end zones. The plastic hinge and an elastic segment are together called as FEMA beam or FEMA column component depending on whether the beam or column is modelled. A tri-linear force-deformation (F-D) relationship implemented in Perform 3D (CSI, 2006) is used in this study. It is defined by stiffness, strength and deformation parameters of the RC members. As shown in Figure 6-5 (a), at least five parameters namely effective stiffness, K_e, yield moment, M_y, ultimate or capping moment, M_c, pre-capping rotation, θ_p and post-capping rotation, θ_{pc} are required to completely define the F-D relationship. Effective stiffness, K_e is obtained from the expression given by Elwood and Eberhard (2009) which is expressed as a fraction of the gross flexural stiffness, EI_g. Depending on the axial load, it varies from $0.2EI_g$ to $0.7EI_g$, where E is the modulus of elasticity and I_g is the moment of inertia of the gross section. Other studies and guidelines such as ACI-318-14 (2014), FEMA-356 (2000) and Panagiotakos and Fardis (2001) have also provided effective stiffness as some percentage of the gross flexural stiffness. The yield moment, M_y is estimated from the expression given by Panagiotakos and Fardis (2001) and the capping moment, M_c is taken as $1.13M_y$ as derived by Haselton et al. (2008) from the number of experimental tests. The pre-capping rotation, θ_p and post-capping rotation, θ_{pc} are obtained from the expressions given by Haselton et al. (2008). The residual moment, M_r is taken as $0.001M_c$ as recommended in the user guide of Perform 3D (CSI, 2006). To incorporate the contribution of the slab to the stiffness of structure, the exterior and interior beams are respectively approximated as L and T-beams with the original beam as web and part of the slab as the flange. The effective flange width is estimated from the expressions given in ACI-318-14 (2014). The P-delta effect is included in the analyses to account for the geometrical nonlinearity.

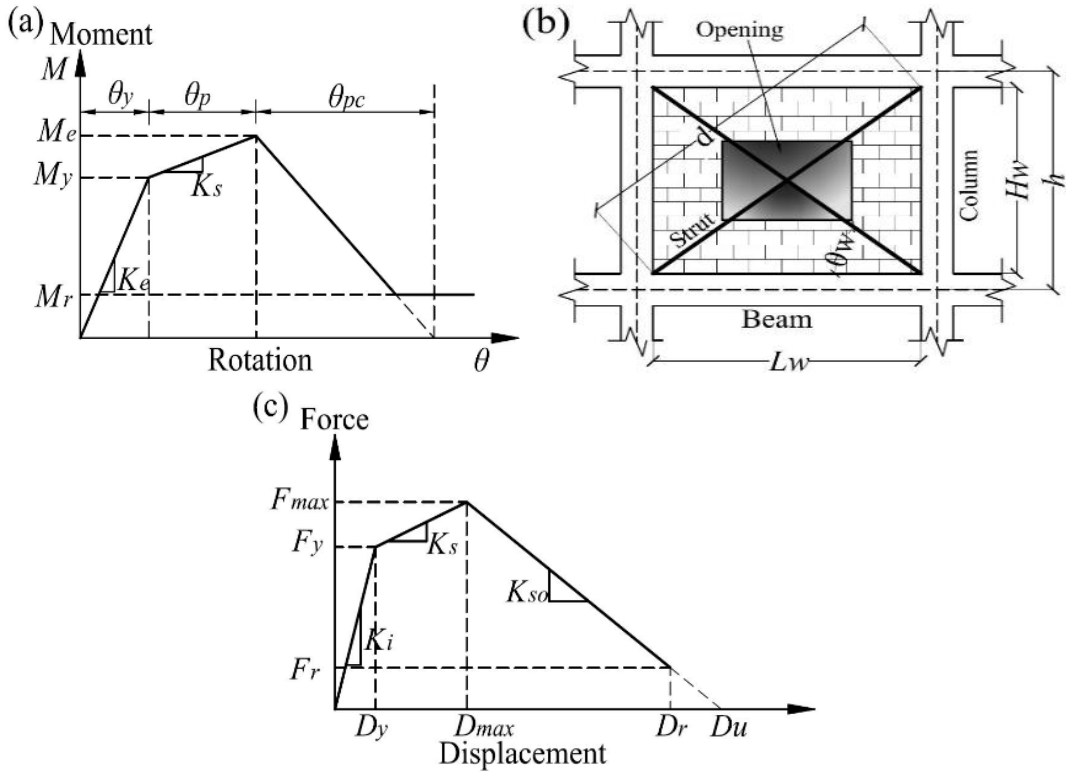

Figure 6-5 (a) F-D relationship of RC member; (b) equivalent strut representation of masonry wall and (c) F-D relationship of the equivalent strut.

On the other hand, masonry infill wall is modelled using a pair of equivalent struts in two diagonal directions as shown in Figure 6-5 (b). Similar to the F-D relationship of the RC members, a minimum of five parameters, namely initial stiffness, K_i, yield strength, F_y, maximum strength, F_{max}, deformation at maximum strength, D_{max} and deformation at zero strength, D_u are required to define the F-D relationship of the masonry wall shown in Figure 6-5 (c). The F-D relationship of the equivalent strut has been proposed by many studies such as Saneinejad and Hobbs (1995), Panagiotakos and Fardis (1996), Dolšek and Fajfar (2008) and more recently by Burton and Deierlein (2013). In this study, initial stiffness, K_i and yield strength, F_y of the masonry wall are estimated from the expression given by Panagiotakos and Fardis (1996) as:

$$K_i = \frac{G_w L_w t_w}{H_w} \tag{6.2}$$

$$F_y = f_{tp} t_w L_w \tag{6.3}$$

where G_w and f_{tp} are the shear modulus and cracking strength of the infill wall respectively. L_w, t_w and H_w are respectively the length, thickness and height of the infill wall. The ratio of yield strength, F_y to maximum strength, F_{max} is taken as 0.6 as proposed by Dolšek and Fajfar (2008). The mean ratio of 0.71 was obtained by Burton and Deierlein (2013) from the 14 test

results. Sattar and Liel (2010) also adopted the ratio of yield to maximum strength as 0.55. The deformation at maximum strength, D_{max} is assumed to occur at the storey drift of 0.20% for short infill wall and 0.15% for the long infill wall with window, while the deformation at zero strength, D_u is taken as 5 times D_{max} as given in Dolšek and Fajfar (2008). Other researchers such as Manzouri (1995) and Shing et al. (2009) also found the occurrence of maximum strength at the storey drift of 0.25%. The residual strength, F_r is taken as 10% of the yield strength as in Panagiotakos and Fardis (1996).

The typical masonry infilled RC buildings considered in this study have window and door openings in the masonry wall. The effect of the opening is considered by appropriately modifying the equivalent strut width by introducing a reduction factor which in turn modifies the initial strength and stiffness of the masonry wall. A number of researchers such as Al-Chaar (2002), Asteris et al. (2011), Dawe and Seah (1988), Decanini et al. (2012), Durrani and Luo (1994), Mondal and Jain (2008) and Smyrou et al. (2011) have proposed reduction factors based on the size and location of the opening. In this study, the reduction factor proposed by Durrani and Luo (1994) is used since it is observed to provide the mean reduction factor amongst others.

In addition, 3% modal damping is specified along with a very small stiffness proportional Rayleigh damping of the order of 0.1% to damp out the higher mode displacements. Using the F-D relationships of RC members and masonry infill wall defined above, the numerical model was previously calibrated with the experimental test results. The details of model calibration can be found in Thinley and Hao (2016) both for the uniformly infilled RC buildings and building with the open ground floor.

6.3.4 Consideration of uncertainties

Fragility analysis involves a number of uncertainties since it is probabilistic in nature. Some of the uncertainties are due to the inherent randomness of a phenomenon referred to as aleatory uncertainties while others are due to the lack of knowledge known as the epistemic uncertainties. In the context of this study, the aleatory uncertainties mainly include randomness in the material, geometrical and ground motion parameters while epistemic uncertainties include variation in damage limit state, analysis method and structural modelling. The evaluation of epistemic uncertainties is very subjective and therefore not considered in this study. Only the effect of random variations in ground motions and the most influential material parameters are considered. Unlike the material parameters which vary significantly due to poor quality control during construction and inevitable deterioration during service life, the variation of geometrical parameters such as beam and column sizes is

small compared to those of material parameters. Hence the structural dimensions are considered as deterministic. The effect of material uncertainty is first studied for '3 storey new' building by considering both ground motion and material uncertainties as described in section 5. The material parameters considered for the study are described below.

6.3.4.1 Material uncertainty

The random fluctuations of the most influential material parameters, namely the compressive strength of concrete, f_c, the yield strength of steel, f_y and the compressive strength of masonry, f_m are considered to study the effect of these parameters on the development of fragility curves. The modulus of elasticity of concrete and masonry are also empirically related to their respective compressive strengths. The mean values of f_m, f_c and f_y used for the analyses of '3 storey new' masonry infilled RC building are 6.07 MPa, 20 MPa and 415 MPa respectively while the corresponding CoV of 0.20, 0.20 and 0.09 are adopted for f_m, f_c and f_y respectively. It is to be noted that the design values of these parameters are taken as mean while the coefficient of variations (CoVs) are assumed according to the relevant studies as discussed below.

Compressive strength of concrete, f_c

The CoV of concrete is taken from the Indian Standards for Plain and Reinforced Concrete, IS 456 (2000). In the absence of sufficient data, the Indian Standard recommends CoV of 0.23 and 0.20 for the design strengths of 15 MPa and 20 MPa respectively. Similar CoVs were also estimated by other researchers such as Barlett and MacGregor (1996), Ellinwood (1978) and Mirza et al. (1976). The CoV of 0.186 was estimated by Barlett and MacGregor (1996) while studying the relationship between cast in place concrete and the specified concrete strength. Ellingwood (1978) estimated CoV of 0.21 and Mirza et al. (1976) suggested CoV of 0.18 and 0.14 for average and excellent quality control during construction respectively. In line with other studies, f_c is assumed to be normally distributed.

Yield strength of steel, fy

The CoV of 0.09 with a normal distribution is assumed in line with the inferences of the other researchers. From the test results of 500 sample rebars, Basu et al. (2004) estimated the mean yield strength and CoV to be 509 MPa and 0.0893 respectively. From the test results of 4000 samples of grades 40 and 60 bars, Mirza and MacGregor (1979) also estimated mean and CoV of 337 MPa and 0.107 respectively for grade 40 bars and 503 MPa and 0.093 respectively for grade 60 bars. The rebar CoV of 0.08 was also assumed by Nielson and DesRoches (2007) while studying the seismic fragility of highway bridges.

Compressive strength of masonry, f_m

Kaushik et al. (2007) conducted a number of prism test on Indian bricks and obtained the mean compressive strengths of 6.07 MPa and 3.77 MPa with respective CoVs of 0.24 and 0.20 for brick masonry with medium and weak cement mortars respectively. Since Indian bricks are used for construction in Bhutan, these details are adopted in this study. Gumaste et al. (2007) and Sarangapani et al. (2005) also estimated similar values for Indian bricks. It is assumed to be normally distributed as in other studies.

6.3.5 Selection of Damage States

Interstorey drift is used as the demand measure (*DM*) since it is more closely correlated to the damages of the buildings. The correlation of interstorey drift with the damages of buildings is given in a number of studies and guidelines such as Ghobarah (2004), Rossetto and Elnashai (2003), ATC-40 (1996), FEMA 356 (2000), Vision-2000 (1995) and ASCE/SEI 41-14 (2014). In this study, the damage states developed by Ghobarah (2004) for the masonry infilled RC buildings are used to define damages of the masonry infilled RC buildings. In the absence of similar damage criteria developed for the masonry infilled RC buildings with the open ground floor or soft storey buildings, the damage criteria specified in the Vision 2000 (1995) are used for defining the damages of the soft storey buildings in this study. The damage criteria of Vision 2000 (1995) are normally used for assessing the damages of the bare frame buildings. It is also reasonable to use it for the soft storey buildings since the response of the soft storey buildings is mainly governed by the open ground storey without infill walls. The correlation of interstorey drift with the corresponding damages of building defined by Ghobarah (2004) and Vision 2000 (1995) are given in Table 6-3.

Table 6-2 Damage states correlated to interstorey drift of building

		Interstorey drift (IDR) limit (%)	
Performance levels	Damage state	Ghobarah (2004)	Vision 2000
Fully Operational (FO)	No Damage	<0.1	<0.2
Operational (O)	Repairable	0.1≤IDR<0.4	<0.5
Life Safety (LS)	Irreparable	0.4≤IDR<0.7	<1.5
Near Collapse (NC)	Severe	0.7≤IDR≤0.8	<2.5
Collapse (C)	Complete	IDR>0.8	>2.5

6.3.6 Incremental Dynamic Analysis (IDA)

The incremental dynamic analysis involves carrying out a number of nonlinear dynamic response simulations of a structural model under a suite of ground motion records, each scaled to a predefined intensity levels to obtain the *IM* of ground motion records corresponding to the *DM* of the structural model. In this section, the general procedure of IDA leading to the derivation of fragility curves for the buildings considered in this study is described. The fragility curves of the masonry infilled and soft storey buildings are developed following the procedure in this section. Initially, Sa (T_1, 5%) is used as intensity measures to generate IDA and fragility curves. It is later renormalised to develop fragility curves in terms of PGA.

With all the components required for the generation of fragility curves described above, IDA is performed for the building model using a suite of ground motion records in Table 6-1, each scaled to a number of intensity levels. The values of S_a (T_1, 5%) corresponding to the first mode period of the building is first estimated for each ground motion. It is then scaled in such a way that S_a (T_1, 5%) ranges from a minimum of 0.05g to a maximum of 2.50g to which a collapse or dynamic instability of building is expected. The S_a (T_1, 5%) value is then increased in steps of 0.05g from 0.05g to 0.50g and then in steps of 0.10g from 0.50g to 2.50g. This results in 30 intensity levels for each ground motion. IDA is performed for the building model using Perform 3D (CSI, 2006) program starting from first intensity level of 0.05g and continued serially up to a particular intensity level when the building becomes dynamically unstable. On average, 15 dynamic nonlinear analyses are required to be run for each ground motion to arrive at the intensity level that causes dynamic instability of the building model. This results in approximately 330 runs for 22 ground motion records for each building model. The stepping algorithm is used to trace the IDA curve here, since it is much simpler and straightforward than the other algorithm such as the hunt and fill method. The maximum interstorey drift corresponding to each intensity level is estimated and the same procedure is repeated for all other ground motions. The IDA curve is plotted from the pairs of S_a (T_1, 5%) and maximum interstorey drift for each ground motion record. Finally, S_a (T_1, 5%) value is estimated corresponding to interstorey drift value of each damage state given in Table 6-3 for each ground motion. This results in 22 S_a (T_1, 5%) values for each damage states from 22 simulations with 22 selected ground motions. Kolmogorov-Smirnov test was carried out for these 22 ln(S_a (T_1, 5%)) values and was found to be normally distributed with a significance level of more than 10% for all building models considered in this study. The mean, μ_{ln} and standard deviation, σ_{ln} of ln (S_a (T_1, 5%)) are then estimated from the 22 S_a (T_1, 5%) values which are then fitted in Equation (6.1) to generate fragility curves of the buildings. The fragility curves developed for the typical masonry infilled and soft storey RC buildings in Bhutan are depicted and discussed in sections 4 and 5 respectively.

6.4 Effect of material uncertainties

Prior to generating the fragility curves of the buildings described in section 2.2, it is imperative to ascertain whether the effect of material uncertainties is significant enough to be considered for the fragility analysis. Many studies have neglected material uncertainties claiming them to be insignificant. To achieve this objective, fragility curves of '3 storey new' masonry infilled buildings are generated for two cases named as case I and case II. In case I, only the design or mean material parameter values are considered, while the most influential material parameters as described in section 2.4 are statistically varied in generating the fragility curves in case II. The fragility curves of various damage states obtained from the two cases are compared to study the effect of material uncertainties.

The case I is quite straightforward wherein the '3 storey new' masonry infilled RC building is numerically modelled in Perform 3D (CSI, 2006) program using only the design values of material parameters. As described in section 2, fragility curves are derived for various damage states using the ground motion suite in Table 6-1.

On the other hand, it is not straightforward to perform IDA and hence to generate fragility curves in case II which involves modelling the statistical variation in material parameters in the numerical simulations. To address this problem, Rosenbluth Point Estimate Method (RPEM) is used to model the statistical variation of material parameters. RPEM greatly reduces the number of simulations as compared to Monte Carlo simulations and is known to provide an accurate estimation of moment of a statistical function for normally distributed variables (Kirke and Hao, 2004). The accuracy of this method was previously verified by Monte Carlo Simulation Method in Thinley and Hao (2017). The method involves considering two point estimates at one standard deviation on either side of the mean value for each variable. The performance function is then estimated for all possible combination of the point estimates. The number of point estimates and the number of possible combinations are given by $2n$ and 2^n respectively, where n is the number of variables considered. The three material variables, f_m, f_c and f_y considered in this study result in 6 point estimates and 8 possible combinations as given in Table 6-4. The notations f_m^+, f_c^+ and f_y^+ denote mean plus one standard deviation and f_m^-, f_c^- and f_y^- denote mean minus one standard deviation. The values of f_m, f_c and f_y in Table 6-4 are calculated from their mean and CoV described in section 2.4. Hence, unlike in case I where there is only one numerical model involved for the mean material parameters, there are 8 numerical models involved in case II to effect the statistical variation of material parameters as given in Table 6-4.

Table 6-3 Application of Rosenbluth Point Estimate Method

Model No.	Combination	f_m (MPa)	f_c (MPa)	f_y (MPa)
1	$f_m^+ f_c^+ f_y^+$	7.29	24.00	452.35
2	$f_m^- f_c^+ f_y^+$	4.86	24.00	452.35
3	$f_m^+ f_c^- f_y^-$	7.29	16.00	377.65
4	$f_m^- f_c^- f_y^-$	4.86	16.00	377.65
5	$f_m^+ f_c^- f_y^+$	7.29	16.00	452.35
6	$f_m^- f_c^- f_y^+$	4.86	16.00	452.35
7	$f_m^+ f_c^+ f_y^-$	7.29	24.00	377.65
8	$f_m^- f_c^+ f_y^-$	4.86	24.00	377.65

For each of these 8 combinations/models, same procedures are followed as in case I for generating IDA curves from the suite of ground motions in Table 6-1. The results are used to estimate the lognormal mean, μ_{ln} and standard deviation, σ_{ln} of *IM* (S_a (T_1, 5%)) corresponding to each *DS*. This required conducting an approximately 330 dynamic nonlinear analyses for each model and a total of 2640 runs for 8 combinations. The μ_{ln} and σ_{ln} of *IM* estimated for each of these 8 combinations are further averaged to obtain the final lognormal mean and standard deviation. This final averaged mean and standard deviation are then fitted in Equation (6.1) to generate fragility curves for the second case. In order to comprehensively study the effect of material uncertainties, fragility curves are generated using both PGA and S_a (T_1, 5%) as intensity measures. The μ_{ln} and σ_{ln} of *IM* estimated for the two cases are given in Table 6-5.

Based on the lognormal mean and standard deviation values in Table 6-5, fragility curves are generated for each damage state based on both the intensity measures. Figures 6-6 and 6-7 depict the comparison of fragility curves obtained from the two cases in terms of PGA and S_a (T_1, 5%) respectively.

Table 6-4 Lognormal mean and standard deviation with and without consideration of random variation of material parameters

	S_a (T_1, 5%) (g)		PGA (g)	
Damage states	μ_{ln}	σ_{ln}	μ_{ln}	σ_{ln}
(a) Case I- Consideration of only mean material parameters				
No Damage	-1.556	0.380	-2.163	0.186
Repairable	-0.210	0.351	-0.816	0.175
Irreparable	0.135	0.355	-0.471	0.205
Severe	0.188	0.357	-0.418	0.205
(b) Case II- With consideration of statistical variation of material parameters				
No Damage	-1.548	0.375	-2.103	0.179
Repairable	-0.204	0.358	-0.759	0.174
Irreparable	0.146	0.361	-0.408	0.204
Severe	0.197	0.363	-0.357	0.206

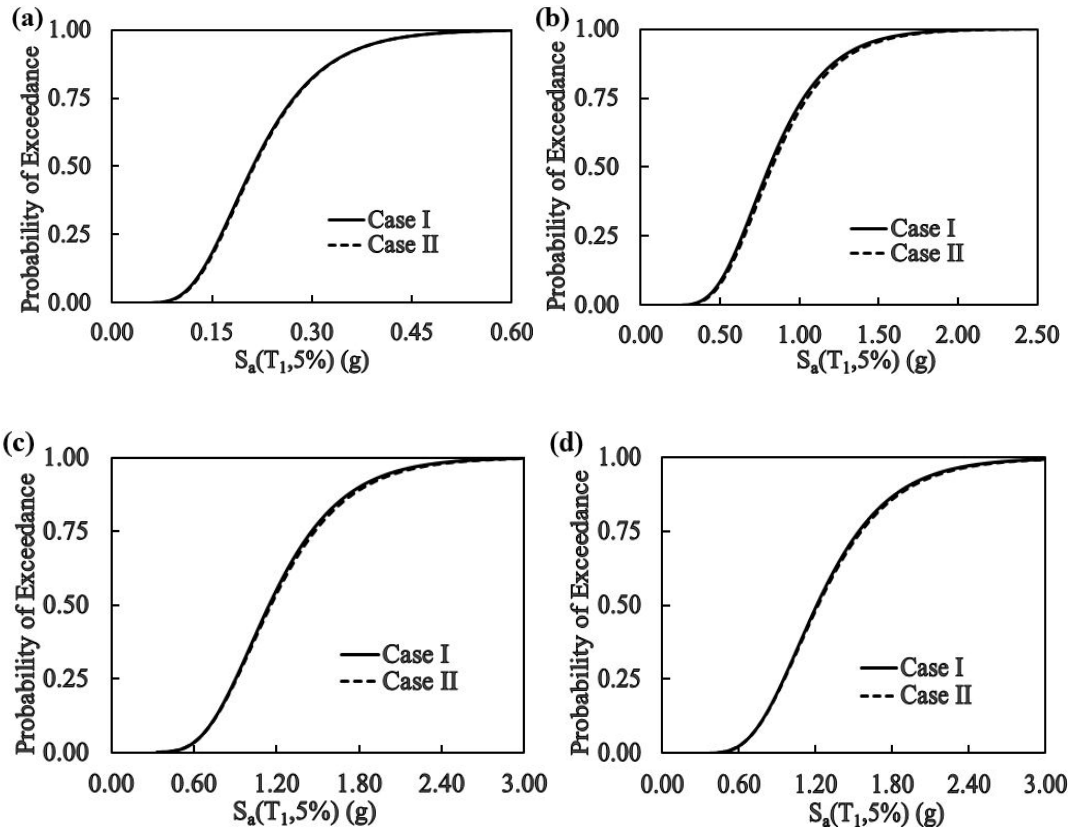

Figure 6-6 Comparison of fragility curves for Case I and Case II in terms of S_a (T_1, 5%) for (a) no damage; (b) repairable; (c) irreparable and (d) severe damages.

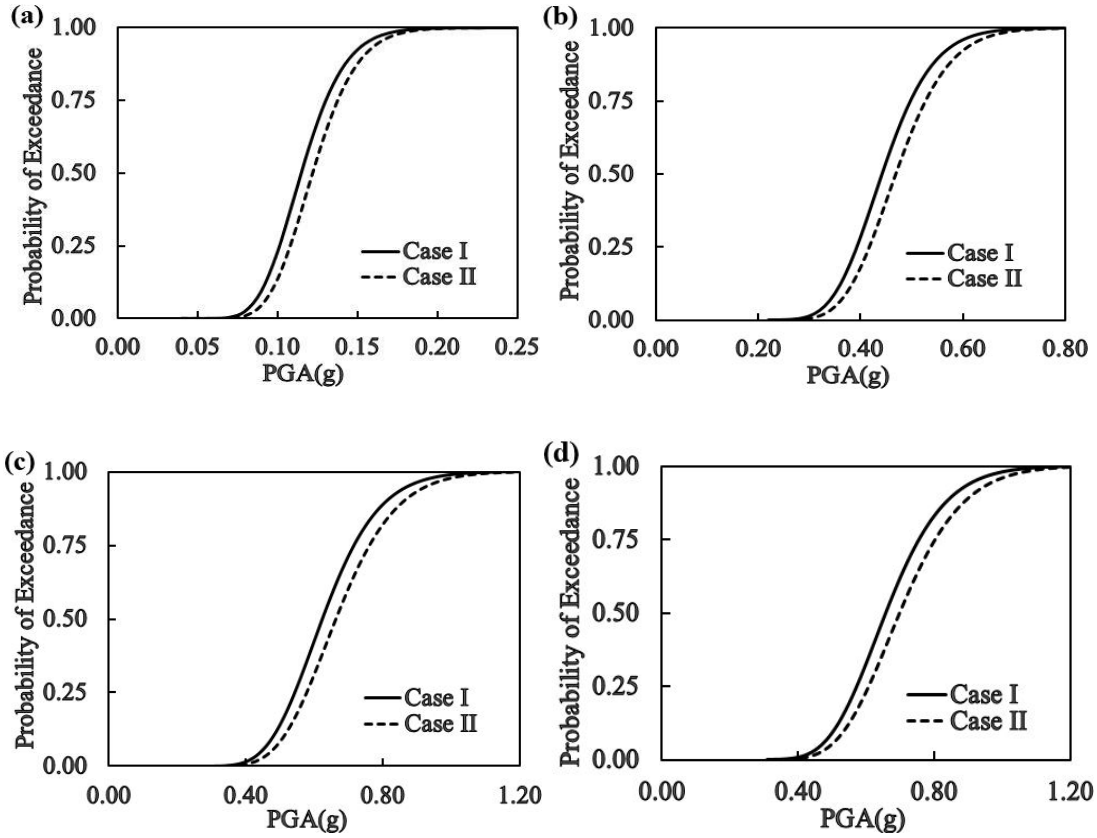

Figure 6-7 Comparison of fragility curves for Case I and Case II in terms of PGA for (a) no damage; (b) repairable; (c) irreparable and (d) severe damages.

It can be observed from Figure 6-6 that there is negligible difference between the fragility curves when S_a (T_1, 5%) is used as *IM*. The closeness in the values is due to a very small difference in the first mode period of the buildings obtained in case I and case II. The first mode period of the building that considers only the design or mean values is T_1 = 0.111 Sec while the average first mode period of the 8 building models that consider the statistical variation of material parameters is 0.104 Sec. On the other hand, when PGA is used as *IM*, some difference in the fragility curves is observed in predicting the damages as shown in Figure 6-7. However, the difference is not substantial with a maximum difference of 11%. For instance, when PGA=0.5g, the probability of the building experiencing repairable damage is predicted to be 75.4% and 64.7% respectively for the case I and Case II as shown in Figure 6-7 (b). In short, neglecting the material uncertainty would have a negligible effect when S_a (T_1, 5%) is used as *IM* and slightly over predicts the damage when PGA is used as *IM*. Hence, considering only the ground motion uncertainty would be sufficient enough to predict the

reliable damages of the buildings. Other researchers such as Jeon et al. (2015), Kwon and Elnashai (2006) and Ji et al. (2009) also observed a very small influence from the randomness of material parameters compared to the randomness in the ground motion parameters. Moreover, S_a (T_1, 5%) was found to be more effective/reliable than PGA for structures with the first mode dominated responses, such as masonry infilled RC buildings in Bhutan with the maximum height of 6 storeys (Shome et al., 1998). Because of the relative insignificant influences of statistical variations of material parameters, only the ground motion uncertainty is considered for the fragility analysis of the other buildings considered in this study hereafter.

6.5 Fragility curves for typical masonry infilled RC buildings

The fragility curves of '6 storey' and '3 storey old' masonry infilled RC buildings are developed following the procedure in section 2.6 and using the ground motion suite in Table 6-1. The lognormal mean, μ_{ln} and standard deviation, σ_{ln} of *IM* in terms of both S_a (T_1, 5%) and PGA corresponding to each damage state of the buildings are given in Table 6-6. For easy comparison, the corresponding values derived above for '3 storey new' building are also listed in the table. The first mode period of '6 storey', '3 storey new' and '3 storey old' of the masonry infilled RC buildings are respectively 0.261 Sec, 0.111 Sec and 0.135 Sec which are actually used for estimating corresponding S_a (T_1, 5%) for each ground motion record.

Table 6-5 Lognormal mean and standard deviation of IM obtained for 3 typical masonry infilled RC buildings

	6 storey		3 Storey New		3 Storey Old	
Damage states	μ_{ln}	σ_{ln}	μ_{ln}	σ_{ln}	μ_{ln}	σ_{ln}
(a) IM in terms of S_a (T_1,5%)						
No Damage	-2.067	0.387	-1.556	0.380	-2.253	0.503
Repairable	-0.622	0.353	-0.210	0.351	-0.815	0.483
Irreparable	-0.077	0.324	0.135	0.355	-0.367	0.483
Severe	0.045	0.322	0.188	0.357	-0.285	0.484
Collapse-IDA	0.322	0.318	0.219	0.361	-0.006	0.483
(b) IM in terms of PGA						
No Damage	-2.976	0.343	-2.163	0.186	-2.937	0.311
Repairable	-1.531	0.350	-0.816	0.175	-1.499	0.300
Irreparable	-0.986	0.341	-0.471	0.205	-1.051	0.302
Severe	-0.864	0.340	-0.418	0.205	-0.969	0.308
Collapse-IDA	-0.587	0.320	-0.388	0.208	-0.689	0.321

The IDA curves generated from the ground motion suite for the three masonry infilled RC buildings are shown in Figure 6-8. The vertical lines from left to right in Figure 6-8 indicate

no damage, repairable, irreparable and severe damages corresponding to the interstorey drift of 0.1%, 0.4%, 0.7% and 0.8% respectively as specified in Table 6-3. The interstorey drift above 0.8% indicates the collapse of the building. However, as shown in Figure 6-8, only '3 storey new' building approximately adheres to the adopted damage limits with the occurrence of collapse at around 0.8% to 0.9% interstorey drift ratio. The collapse of '6 storey' and '3 storey old' buildings approximately occur at the interstorey drift ratio of around 1% and 1.2% respectively. The damage limits specified by Ghobarah (2004) were derived from a number of analytical and experimental studies of the masonry infilled RC building. As such, it is not expected to be directly applicable to the individual masonry infilled RC building. In this study, another limit sate named as 'Collapse-IDA' is defined to indicate the collapse of the buildings. It is estimated from the IDA and corresponds to the particular intensity level of the ground motion record at which the numerical model of the building becomes dynamically unstable indicating the collapse of the building. This corresponds to the point on the IDA curve at which the curve starts to become horizontal as shown in Figure 6-8. The *IM* corresponding to this point is estimated for all the ground motion records and their lognormal mean and standard deviation are given in Table 6-6 as the 'Collapse IDA' limit state. The fragility curve for this limit state is similarly generated as shown in Figures 6-9 and 6-10. This limit state indicates the actual *IM* at which the building collapses. It is more specific and believed to be more accurate than the limit state given by Ghobarah (2004) for the buildings considered in this study.

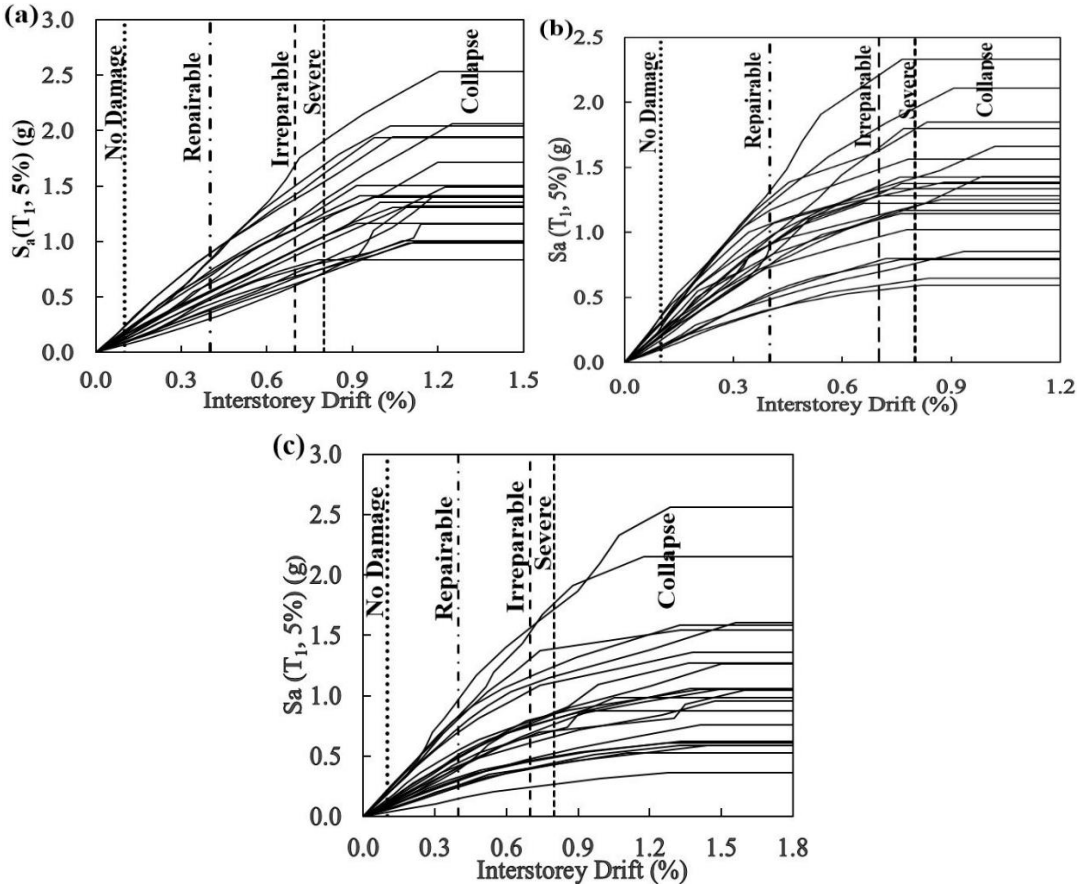

Figure 6-8 IDA curves for (a) 6 storey; (b) 3 storey new and (c) 3 storey old masonry infilled RC buildings.

The fragility curves derived for the various damage states from μ_{ln} and σ_{ln} values in Table 6-6 are shown in Figures 6-9 and 6-10, respectively for $S_a(T_1, 5\%)$ and PGA intensity measures. Only the fragility curves in terms of $S_a(T_1, 5\%)$ are discussed in detail here since $S_a(T_1, 5\%)$ is a more reliable ground motion intensity measure than PGA as discussed above. However, the discussions are also largely applicable to the fragility curves developed in terms of PGA. The fragility curves in terms of PGA are presented since PGA can be directly obtained from ground motion record and therefore these curves allow a quick assessment of building fragility given a seismic ground motion.

Fragility curves are normally evaluated by means of median *IM* which is defined as the *IM* at a 50% probability of exceedance of reaching a specific damage state. As shown in Figure 6-9, 50% probabilities of exceedance of no damage, repairable damage, irreparable damage, severe and collapse-IDA damage states are reached at the $S_a(T_1, 5\%)$ values of 0.13 g, 0.54 g, 0.93 g, 1.04 g and 1.38 g, respectively for '6 storey' masonry infilled RC building. Similarly, at the $S_a(T_1, 5\%)$ values of 0.21 g, 0.81 g, 1.14 g, 1.21 g and 1.24 g, 50% probabilities of exceedance of no damage, repairable damage, irreparable damage, severe damage and

collapse are reached respectively for '3 storey new' masonry infilled RC building, and the corresponding values for the '3 storey old' masonry infilled RC building are 0.11 g, 0.44 g, 0.69 g, 0.75 g and 0.99 g respectively. As noted earlier, it is interesting to observe that the collapse damage limits of Ghobarah (2004) agree well with the one estimated from IDA for '3 storey new' building as shown by the closeness of the severe and collapse-IDA fragility curves in Figure 6-9 (b). However, the damage limits of Ghobarah (2004) over predicts the collapse of '6 storey' and '3 storey old' masonry infilled RC buildings as compared to the collapse fragility curve estimated from IDA.

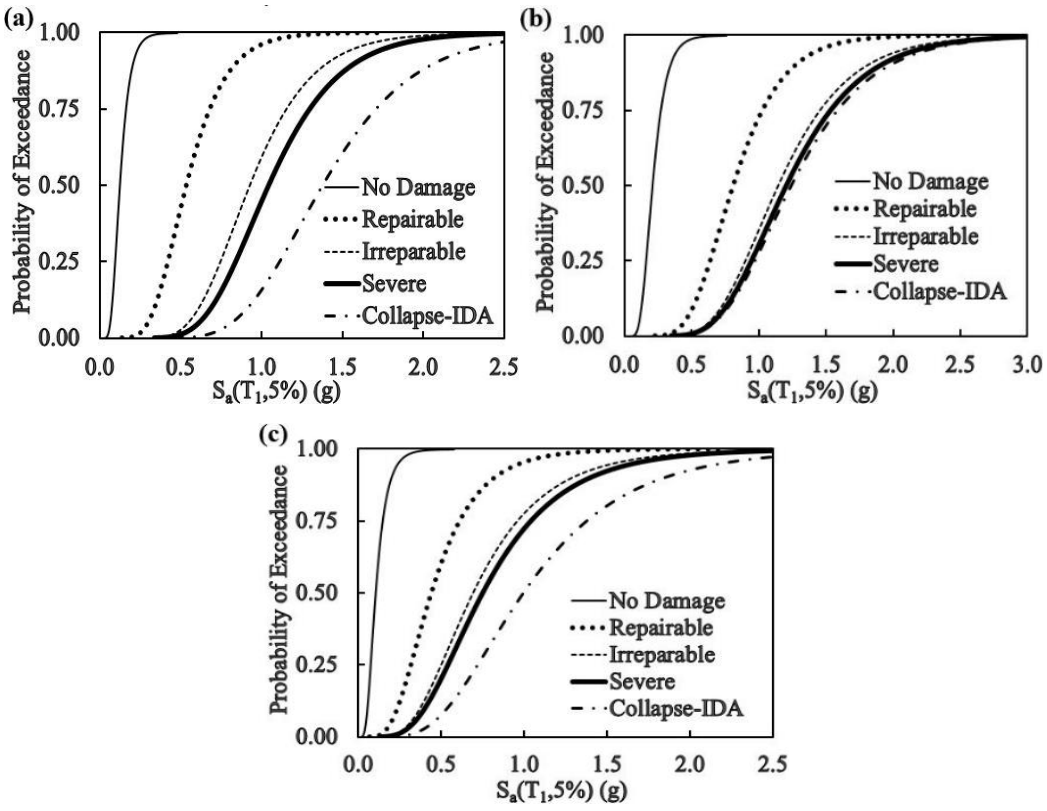

Figure 6-9 Fragility curves for (a) 6 storey; (b) 3 storey new and (c) 3 storey old masonry infilled RC buildings derived in terms of S_a (T_1, 5%) for various damage states.

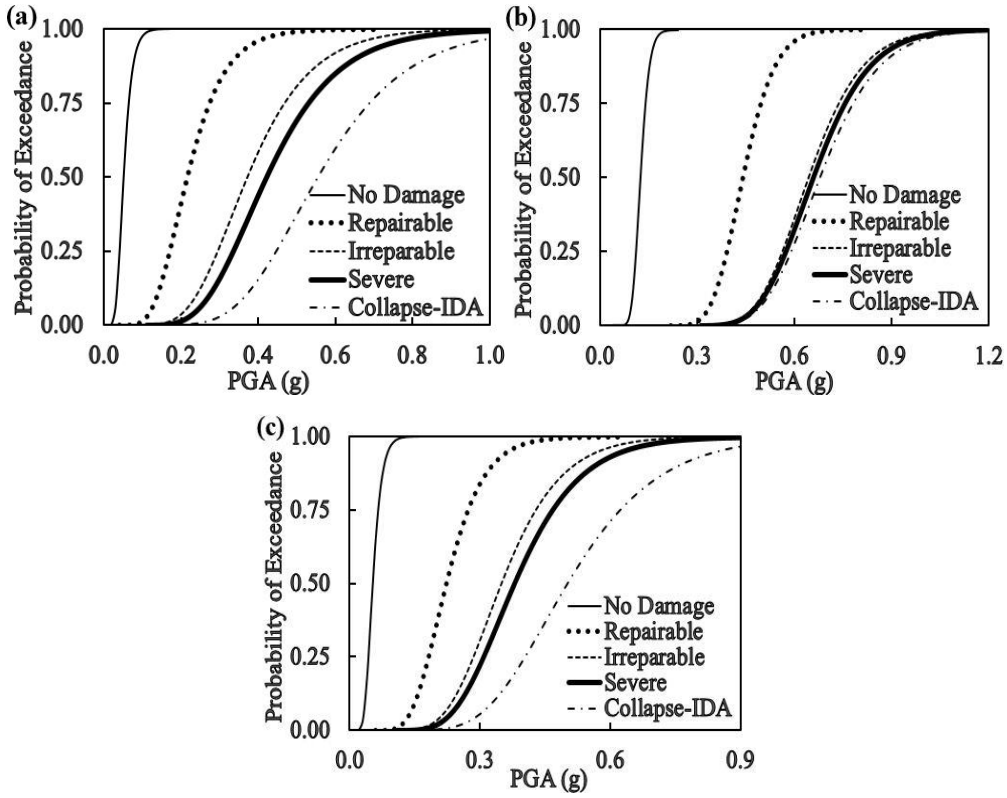

Figure 6-10 Fragility curves for (a) 6 storey; (b) 3 storey new and (c) 3 storey old masonry infilled RC buildings derived in terms of PGA for various damage states.

The comparison of fragility curves of three masonry infilled RC buildings for various damage states are shown in Figure 6-11. It can be noticed from the figure that '3 storey new' building performs much better than the other two buildings in the case of no damage, repairable, irreparable and severe damages with higher S_a (T_1, 5%) values. For instance, for the 50% probability of exceedance of repairable damage, the S_a (T_1, 5%) values of '6 storey' and '3 storey old' buildings are respectively 0.54 g and 0.44 g, while it is 0.81 g for '3 storey new' building. On the other hand, at the collapse-IDA damage state, '6 storey' building performs better than that of 3 storey buildings as shown in Figure 6-11 (e). This could be due to the higher strength and stiffness of the '6 storey' building columns. As the response of masonry infilled RC building enters into the nonlinear range, the inelastic action is gradually being transferred to the columns from the infill walls. Hence columns with larger size, higher material strength and more reinforcement perform better, leading to the '6 storey' building capable of resisting larger seismic ground motions without collapse although its masonry walls suffer more damage than '3 storey new' building at the same ground motion level. This is evident from the fragility curves of '6 storey' buildings in Figure 6-11 which keep moving towards right from no damage state to collapse-IDA limit state. In general, the fragility curves of '3 storey old' building are above the fragility curves of the other buildings at all damage states confirming it the most vulnerable building among the three. This is expected since it

was not designed to any standard but built purely based on some thumb rules by the building owners without involving any technical person. The better performance of the '6 storey' and '3 storey new' masonry infilled RC buildings are expected as they were designed according to the Indian Seismic Code. However, the performance of '6 storey' building is not very satisfactory with respect to the initial damage states which could be due to the larger displacement of the '6 storey' building that resulted in larger damages to the masonry infill walls although the RC frame can sustain a larger excitation than '3 storey new' building before it collapses.

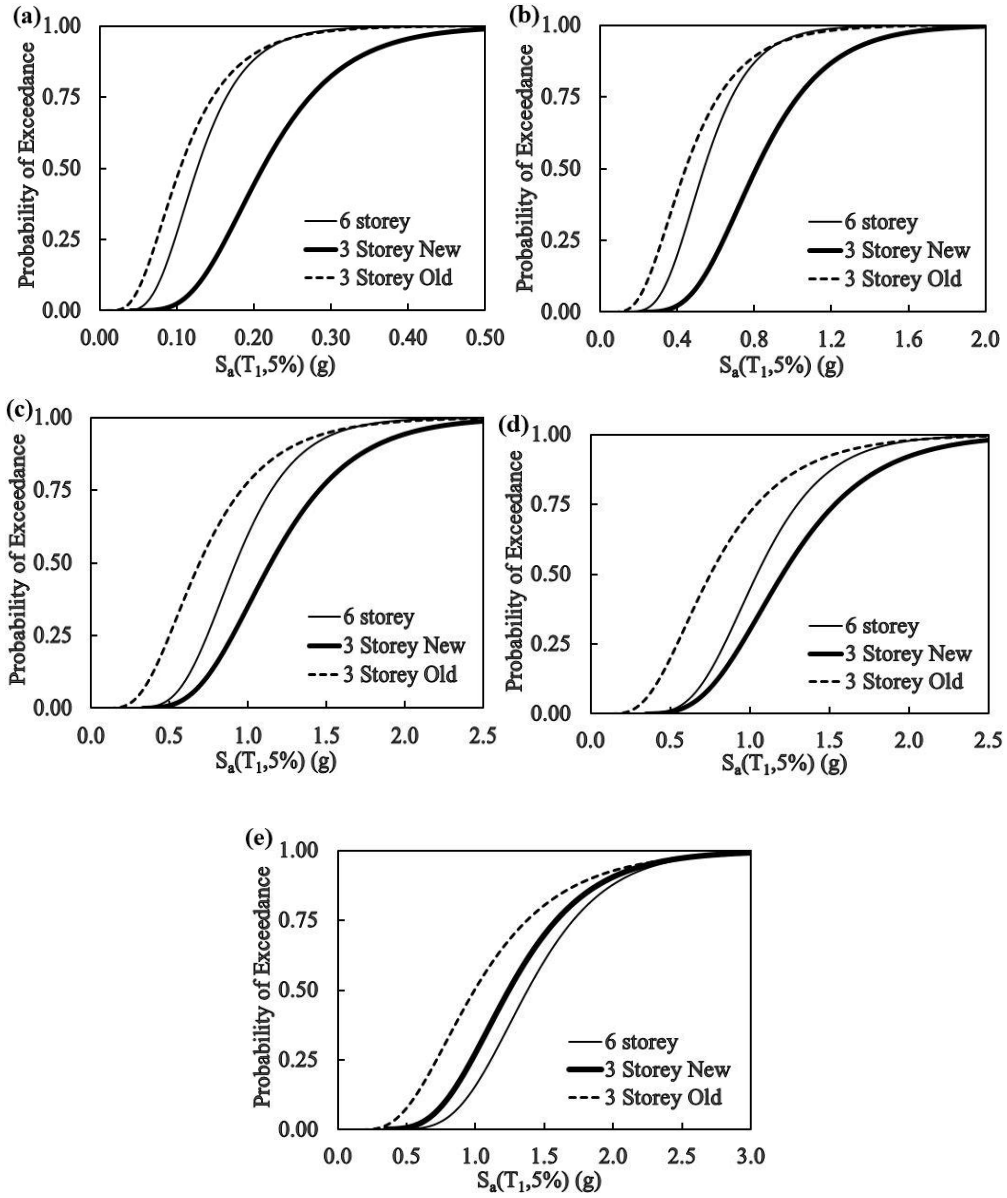

Figure 6-11 Comparison of fragility curves for (a) no damage; (b) repairable; (c) irreparable; (d) severe and (e) collapse-IDA damage states for masonry infilled RC buildings.

6.6 Fragility curves of soft storey buildings

In addition to the masonry infilled RC buildings described in section 2.2, there are a number of masonry infilled RC buildings with the ground floor open for parking and other commercial activities. They are commonly known as the soft storey buildings. These buildings are proven to be more vulnerable to the earthquakes in the past such as 2001 Gujarat, 2008 Wenchuan and 2015 Nepal earthquakes. Hence, it is equally important to predict the performances of these buildings.

In this study, the soft storey buildings considered for the fragility analysis are derived from the masonry infilled RC buildings considered above by removing the infill walls from the ground floor. They are referred to as soft storey '6 storey', '3 storey new' and '3 storey old' RC buildings. Except for the removal of infill walls from the ground floor, all the other details such as member dimensions and reinforcement details are kept unchanged. Although the soft storey buildings considered in this study are derived from the respective masonry infilled RC buildings described in section 2.2, they do truly represent the typical soft storey buildings in Bhutan because both the masonry infilled and soft storey buildings in Bhutan are designed as bare frames neglecting the strength and stiffness of the infill walls.

The fragility curves of the soft storey buildings are similarly derived as that of the masonry infilled RC buildings. The calibrated numerical model of the soft storey building in Thinley and Hao (2016) is employed in this study to perform the nonlinear response simulations. The model is very similar to the one for masonry infilled RC buildings described in section 2.3 except that the stiffness of the ground floor columns is modified to capture its dominant nonlinear response. More detailed descriptions can be found in Thinley and Hao (2016). The lognormal mean, μ_{ln} and standard deviation, σ_{ln} of *IM* in terms of both S_a (T_1, 5%) and PGA corresponding to each damage states of the soft storey buildings are given in Table 6-7. The first mode periods of the soft storey buildings used for the estimation of S_a (T_1, 5%) for each ground motion record are 1.109 Sec, 0.8919 Sec and 2.38 Sec for '6 storey', '3 storey new' and '3 storey old' soft storey buildings respectively. In the absence of the credible damage states for the soft storey buildings, the damage sates recommended by Vision 2000 for bare RC frame are used to define damages of the soft storey buildings in this study, as discussed above.

Table 6-6 Lognormal mean and standard deviation estimated for soft storey buildings at various damage states

	6 storey		3 Storey New		3 Storey Old	
Damage states	μ_{ln}	σ_{ln}	μ_{ln}	σ_{ln}	μ_{ln}	σ_{ln}
(a) IM in terms of S_a (T_1,5%)						
No Damage	-3.116	0.482	-3.267	0.166	-5.255	0.137
Repairable	-2.214	0.460	-2.352	0.166	-4.339	0.137
Irreparable	-1.095	0.461	-1.248	0.168	-3.241	0.137
Severe	-0.544	0.449	-0.712	0.188	-2.730	0.137
Collapse-IDA	-0.269	0.391	-0.040	0.298	-2.350	0.160
(b) IM in terms of PGA						
No Damage	-3.287	0.297	-3.592	0.465	-4.030	0.379
Repairable	-2.366	0.296	-2.677	0.464	-3.114	0.379
Irreparable	-1.235	0.297	-1.573	0.464	-2.015	0.379
Severe	-0.679	0.295	-1.037	0.464	-1.505	0.380
Collapse-IDA	-0.397	0.347	-0.365	0.534	-1.124	0.394

Figures 6-12 and 6-13 show the fragility curves in terms of S_a (T_1, 5%) and PGA, respectively. Similar to the masonry infilled RC buildings, only those curves in terms of S_a (T_1, 5%) are discussed although the fragility curves of soft storey buildings in terms of PGA are shown here. As shown in Figure 6-12, the damage limit of Vision 2000 does not agree well with the actual damages of the soft storey buildings as evident from the large difference in the fragility curves of severe damage and collapse-IDA damage states. From Figure 6-12 (a), the 50% probabilities of exceedance of no damage, repairable damage, irreparable damage, severe damage and collapse-IDA damage states are reached at the S_a (T_1, 5%) values of 0.044 g, 0.109 g, 0.334g, 0.580 g and 0.764 g, respectively for '6 storey' building with soft storey. The corresponding values are 0.038 g, 0.095 g, 0.287 g, 0.491 g and 0.961 g for '3 storey new' and 0.005 g, 0.013 g, 0.039 g, 0.065 g and 0.095 g for '3 storey old' soft storey building as shown in Fig. 12 (b) and 12 (c), respectively. The very small S_a (T_1, 5%) values for '3 storey old' soft storey building indicates it is susceptible to small ground excitations because this building is very soft with the first mode period, T_1=2.38 Sec.

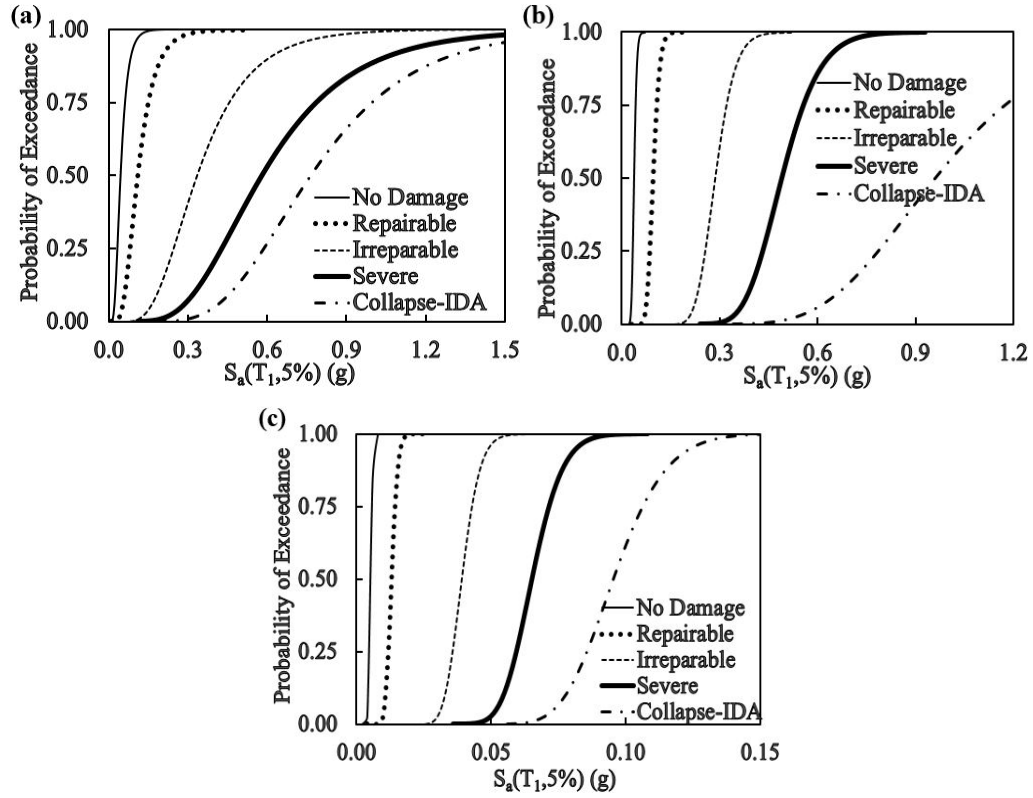

Figure 6-12 Fragility curves for (a) 6 storey; (b) 3 storey new and (c) 3 storey old soft storey buildings derived in terms of S_a (T_1, 5%) for various damages.

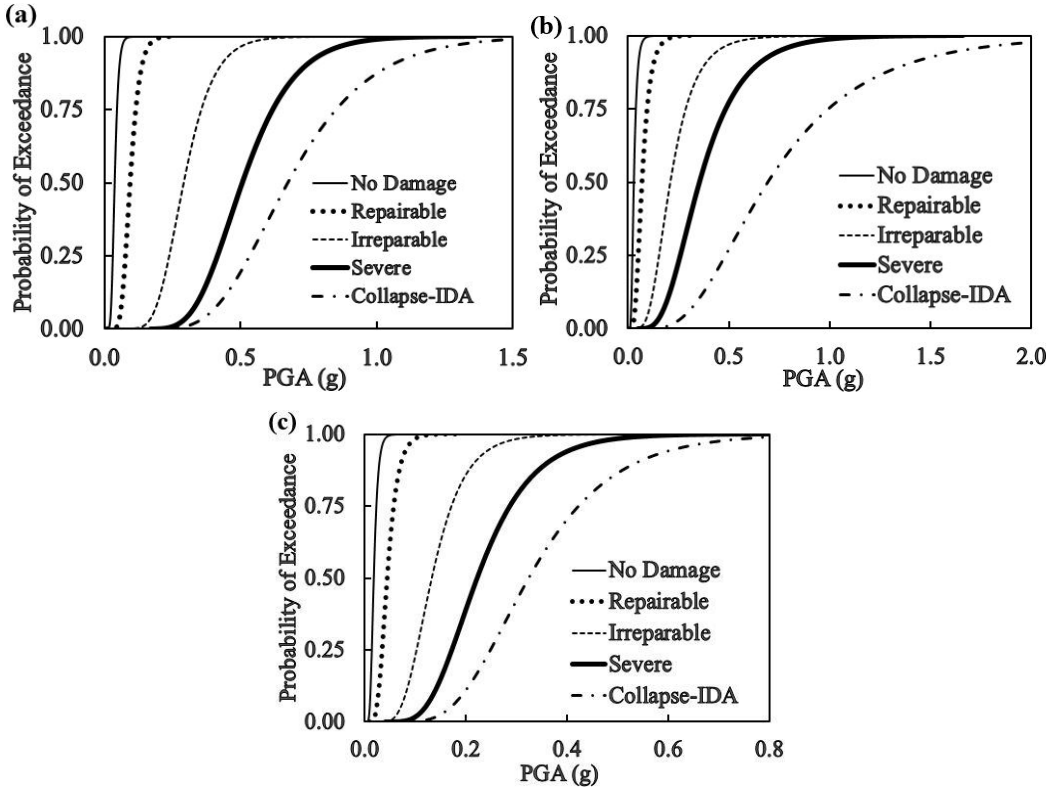

Figure 6-13 Fragility curves for (a) 6 storey; (b) 3 storey new and (c) 3 storey old soft storey buildings derived in terms of PGA for various damage states.

The comparison of fragility curves for various damage states of the three soft storey buildings is shown in Figure 6-14. Only the fragility curves in terms of $S_a(T_1, 5\%)$ are compared here. It is obvious from Figure 6-14 that '3 storey old' building is the most vulnerable soft storey building with 100% probability of collapse at the $S_a(T_1, 5\%)$ value of 0.162g. Since the response of soft storey buildings is mainly governed by the specification of the ground floor columns, the high vulnerability of '3 storey old' building is owing to its very weak columns as evident from Table 6-2. Except for the collapse-IDA damage state, '6 storey' building performs better or suffer less damages as compared to the '3 storey new' soft storey building for the damage probabilities above 30%. This could be due to the higher specification of the '6 storey' building columns as described above, which fully govern the response of soft storey buildings. For the damage probabilities below 30% and for the collapse-IDA damage state, '3 storey new' building performs better than the '6 storey' soft storey building. The higher collapse probability experienced by the '6 storey' building as compared to '3 storey new' soft storey building could be due to the influence of higher axial load from the five storeys above. It is to be noted that apart from the collapse-IDA damage state which was estimated for the respective buildings, the damage states of Vision 2000 for bare RC frame are applied uniformly to all soft storey buildings in deriving the fragility curves.

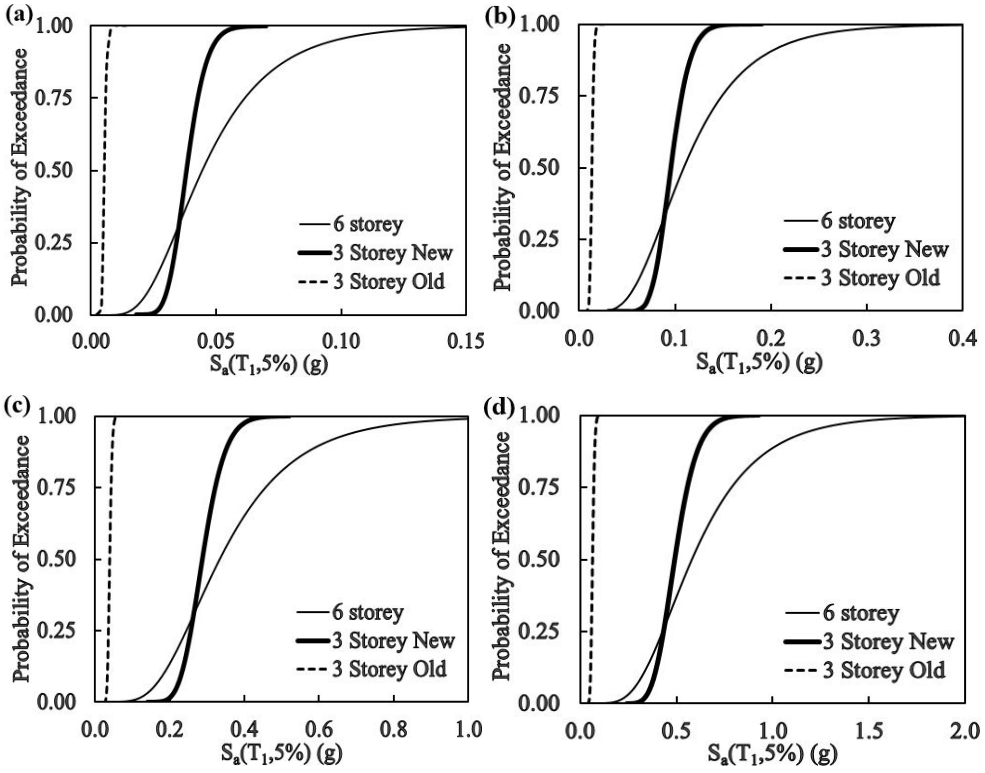

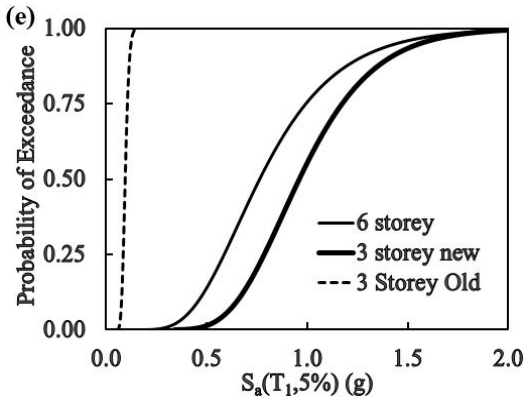

Figure 6-14 Comparison of fragility curves for (a) no damage; (b) repairable; (c) severe and (d) collapse-IDA damage states of soft storey buildings.

6.7 Comparison of Fragility Curves for masonry infilled and soft storey buildings

To study the effect of the soft storey or in other words, the effect of infill walls at the ground floor of buildings, the fragility curves of the masonry infilled and soft storey buildings are compared. Figure 6-15 depicts the comparison of the collapse-IDA damage state. Only the comparison for the collapse-IDA damage state is shown since a very similar trend is observed for all other damage states. It can be clearly observed from Figure 6-15 that the removal of masonry infill walls from the ground floor has a significant effect on the response of the building. In fact, the building is rendered highly vulnerable with the removal of infill wall from the ground floor. For instance, corresponding to the $S_a(T_1, 5\%)$ value of 0.10 g, '6 storey' masonry infilled building has only about 15% probability of exceedance of undergoing collapse, while the probability of exceedance of collapse increases to 75% for the soft storey building. The effect is even more significant for '3 storey old' building wherein the soft storey building shows a 100% probability of exceedance of collapse compared to a 0% probability of exceedance of collapse of the masonry infilled building as shown in Figure 6-15 (c). The soft storey effect is also apparent from the first mode period of the masonry infilled and soft storey buildings which are given in the previous sections. It can be observed that there is a significant increase in the fundamental period when infill wall is removed from the ground floor. The increase in period is very significant especially for the '3 storey old' building because its columns have very low concrete strength, small size and low reinforcement ratio. For this old building type, contributions from infill masonry walls to stiffness and strength are critical for resisting ground excitations.

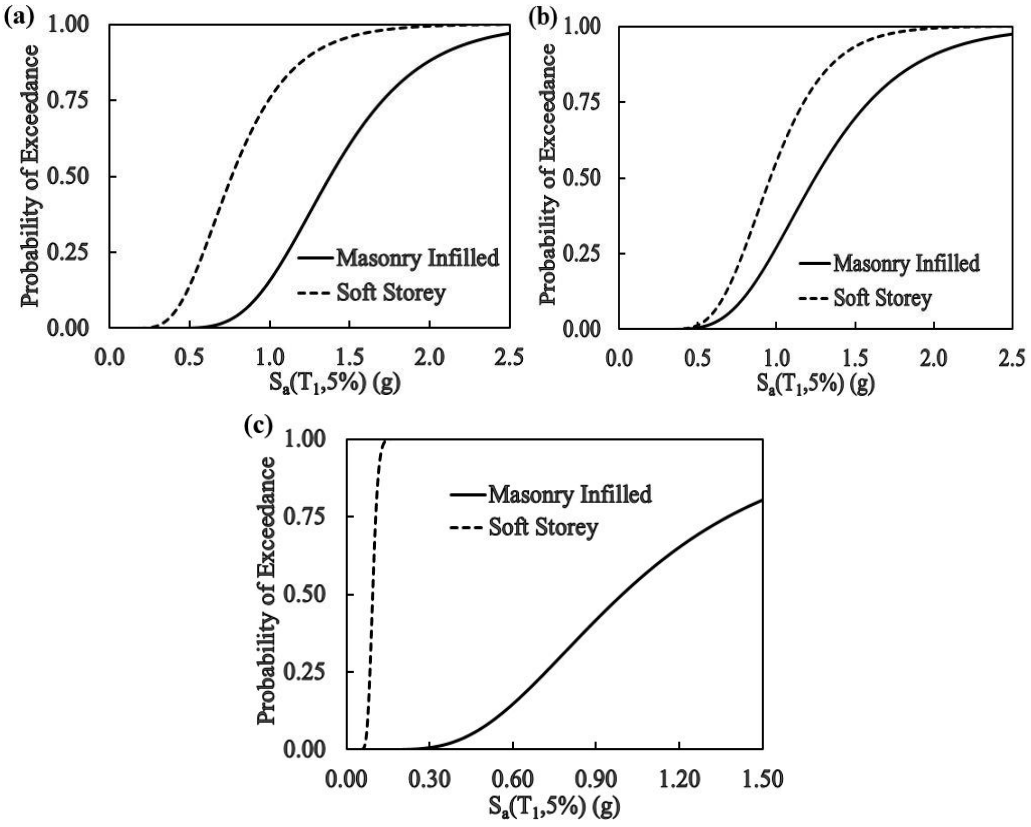

Figure 6-15 Comparison of fragility curves for collapse-IDA damage state for (a) 6 storey; (b) 3 storey new and (d) 3 storey old soft storey buildings.

6.8 Summary and conclusion

This paper presents fragility curves developed for three typical masonry infilled RC buildings in Bhutan. The results indicate that uncertainties in ground motions dominate the uncertainties associated with material property fluctuations. The RC buildings with soft storey are more vulnerable to seismic ground motions compared to the masonry infilled RC frames. The old RC frames with soft storey built without performing proper analysis and design are extremely susceptible to ground excitations. Masonry infill walls of these buildings contribute significantly to structural stiffness and strength for seismic ground motion resistance. Therefore removing masonry infill walls for making open spaces for commercial usage, a common practice in Bhutan, should be prevented for building safety unless other strengthening measures are properly implemented. These fragility curves of building stocks in the high seismicity country are developed for subsequent seismic risk analysis. They represent the first seismic fragility curves ever developed for buildings in Bhutan, a long overdue course for the high seismicity country. The results can also be used in planning the effective and economic strengthening measures of building structures for live and economy protection should a similar earthquake occurred recently in the neighbour country, Nepal, hit Bhutan.

6.9 References

ACI-318-14 (2014). *Building code requirements for structural concrete (ACI 318-02) and commentary (ACI 318R-02).* American Concrete Institute, Detroit, MI.

Al-Chaar, G. (2002). *Evaluating strength and stiffness of unreinforced masonry infill structures*. No. ERDC/CERL-TR-02-1. Engineer Research and Development Centre Champaign, US Army Corps of Engineers.

Ambraseys, N., & Jackson, D. (2003). A note on early earthquakes in northern India and southern Tibet. *Current Science, 84***,** 570-582.

Asteris, P. G., Chrysostomou, C. Z., Giannopoulos, I. P., & Smyrou, E. (2011). Masonry infilled reinforced concrete frames with openings. In: *Proceedings of the 3rd International Conference on Computational Methods in Structural Dynamics and Earthquake Engineering*, Greece.

ATC-40 (1996). *Seismic Evaluation and Retrofit of concrete Buildings volume 1*. Applied Technology Council, Redwood City, California, USA.

Baker, J. W. (2015). Efficient analytical fragility function fitting using dynamic structural analysis. *Earthquake Spectra, 31***,** 579-599.

Barlett, F. M., & MacGregor, J. G. (1996). Statistical analysis of the compressive strength of concrete in structures. *ACI Material, 93* (2), 158-68.

Basu, P. C., Shylamoni, P., & Roshan, A. D. (2004). Characterisation of steel reinforced for RC structures: An overview and related issues. *The Indian Concrete Journal.*

Burton, H., & Deierlein, G. (2013). Simulation of seismic collapse in nonductile reinforced concrete frame buildings with masonry infills. *Journal of Structural Engineering, 140***,** A4014016.

Calvi, G. M., Pinto, R., Magenes, G., Bommer, J. J., Restrepo-Velez, L. F., & Crowley, H. (2006). Development of seismic vulnerability assessment methodologies over the past 30 years. *ISET journal of Earthquake Technology, 43***,** 75-104.

CSI (2006). *Nonlinear Analysis and Performance Assessment for 3-D Structures.* Computers and Structures, Inc., Berkeley.

Dawe, J., & Seah, C. (1989). Lateral load resistance of masonry panels in flexible steelframes. In: *8th Internation Brick and Block Masonry Conference*, Dublin, Ireland, 19-21 September, pp. 606-616.

Decanini, L., Liberatore, L., & Mollaioli, F. (2012). The influence of openings on the seismic behaviour of infilled framed structures. In: *Proceedings of the 15 World Conference on Earthquake Engineering*, Lisbon, Portugal, 24-28 September.

Dolšek, M., & Fajfar, P. (2008). The effect of masonry infills on the seismic response of a four-storey reinforced concrete frame—a deterministic assessment. *Engineering Structures, 30* (7), 1991-2001.

Dorji, J. (2009). *Seismic performance of brick infilled RC frame structures in low and medium rise buildings in Bhutan*. Master degree thesis, Centre for Built Environment and Engineering Research, Queensland University of Technology, Brisbane, Australia.

Drukpa, D., Velasco, A. A., & Doser, D. I. (2006). Seismicity in the Kingdom of Bhutan (1937-2003): Evidence for crustal transcurrent deformation. *Journal of Geophysical Research (Solid Earth), 111***,** 6301.

Dumova-Jovanoska, E. (2000). Fragility curves for reinforced concrete structures in Skopje (Macedonia) region. *Soil Dynamics and Earthquake Engineering, 19***,** 455-466.

Durrani, A. J., & Luo, Y. (1994). *Seismic retrofit of flat-slab buildings with masonry infills.* Technical Report, National Center for Earthquake Engineering Research, San Francisco, CA, pp. 1-8.

Ellingwood, B. (1977). Statistical analysis of RC beam-column interaction. *Journal of the Structural Division, ASCE, 103.*

Elwood, K. J., & Eberhard, M. O. (2009). Effective stiffness of reinforced concrete columns. *ACI Structural Journal, 106*,(4), 476.

FEMA 356 (2002). *Prestandard and Commentary for the Seismic Rehabilitation of Buildings.* Federal Emergency Management Agency, Washington DC, USA.

FEMA 306 (1998). *Evaluation of earthquake damaged concrete masonry wall buildings*. Federal Emergency Management Agency, Washington DC, USA.

Gahalaut, V., Rajput, S., & Kundu, B. (2011). Low seismicity in the Bhutan Himalaya and the stress shadow of the 1897 Shillong Plateau earthquake. *Physics of the Earth and Planetary Interiors, 186***,** 97-102.

Ghobarah, A. (2004). On drift limits associated with different damage levels. In: *Proceedings of the International workshop on performance-based seismic design*, Department of Civil Engineering, McMaster University, Hamilton, ON, Canada, 28 June -1 July.

Gumaste, K., Rao, K. N., Reddy, B. V., & Jagadish, K. (2007). Strength and elasticity of brick masonry prisms and wallettes under compression. *Materials and structures, 40* (2), 241-253.

Haselton, C. B., Goulet, C. A., Mitrani-Reiser, J., Beck, J. L., Deierlein, G. G., Porter, K. A., Stewart, J. P., & Taciroglu, E. (2008). *An assessment to benchmark the seismic performance of a code-conforming reinforced-concrete moment-frame building*. PEER Report 2007/12, Pacific Earthquake Engineering Research Center, University of California, Berkeley, California.

Hetenyi, G., Roux-Mallouf, L., Berthet, T., Cattin, R., Cauzzi, C., Phuntsho, K., & Grolimund, R. (2016). Joint approach combining damage and paleoseismology observations constrains the 1714 AD Bhutan earthquake at magnitude 8±0.5. *Geophysical Research Letters*, *43* (10), 10695-10702.

IS 1893 (2002). *Criteria for Earthquake Resistant Deisgn of Structures*. Bureau of Indian Standards, New Delhi, India.

IS 456 (2000). *Indian Standards for Plain and Reinforced Concrete*. Bureau of Indian Standards, New Delhi, India.

Jeon, J. S., Lowes, L. N., Desroches, R., & Brilakis, I. (2015). Fragility curves for non-ductile reinforced concrete frames that exhibit different component response mechanisms. *Engineering Structures, 85***,** 127-143.

Ji, J., Elnashai, A. S., & Kuchma, D. A. (2009). Seismic fragility relationships of reinforced concrete high-rise buildings. *The Structural Design of Tall and Special Buildings, 18***,** 259-277.

Kaushik, H. B., Rai D. C., & Jain, S. K. (2007). Stress-strain characteristics of clay brick masonry under uniaxial compression. *Journal of materials in Civil Engineering, 19* (9), 728-739.

Kirke, A., & Hao, H. (2004). Estimation of failure probabilities of RC frame structures in Singapore to the simulated largest credible ground motion. *Engineering Structures, 26* (1), 139-150.

Kumar, S., Wesnousky, S. G., Jayangondaperumal, R., Nakata, T., Kumakara, Y., & Singh, V. (2010). Paleoseismological evidence of surface faulting along the northeastern Himalayan

front, India: Timing, size, and spatial extent of great earthquakes. *Journal of Geophysical Research: Solid Earth,* 115.

Kwon, O. S., & Elnashai, , A. (2006). The effect of material and ground motion uncertainty on the seismic vulnerability curves of RC structure. *Engineering structures, 28,* 289-303.

Manzouri, T. (1995). *Nonlinear finite element analysis and experimental evaluation of retrofitting.* PhD Thesis, University of Colorado-Boulder.

Mazzoni, S., Hachem, M., & Sinclair, M. (2012). An Improved Approach for Ground Motion Suite Selection and Modification for Use in Response History Analysis. In: *Proceedings of the 15th World Conference on Earthquake Engineering,* Lisbon, Portugal.

Mirza, S. A., & MacGregor, J. G. (1979). Variability of mechanical properties of reinforcing bars. *Journal of the Structural Division, ASCE, 105,* 751-766.

Mirza, S. A., Hatzinikolas, M., & MacGregor, J. G. (1979). Statistical descriptions of strength of concrete. *Journal of the Structural Division, ASCE, 80,* 167-76.

Mondal, G., & Jain, S. K. (2008). Lateral stiffness of masonry infilled reinforced concrete (RC) frames with central opening. *Earthquake Spectra, 24* (3), 701-723.

Nielson, B. G., & DesRoches, R. (2007). Seismic fragility methodology for highway bridges using a component level approach. *Earthquake Engineering and Structural Dynamics, 36* (6), 823-839.

Panagiotakos, T. B., & Fardis, M. N. (2001). Deformations of reinforced concrete members at yielding and ultimate. *ACI Structural Journal, 98* (2), 135-148.

Panagiotakos, T., & Fardis, M. (1996). Seismic response of infilled RC frames structures. In: *Proceedings of the 11th World Conference on Earthquake Engineering,* Acapulco, Mexico, 23-28 June.

Pejovic, J., & Jankovic, S. (2016). Seismic fragility assessment for reinforced concrete high-rise buildings in Southern Euro-Mediterranean zone. *Bulletin of Earthquake Engineering, 14,* 185-212.

Rosenblueth, E. (1975). Point estimates for probability moments. In: *Proceedings of the National Academy of Sciences, 72* (10), 3812-3814.

Rossetto, T., & Elnashai, A. (2003). Derivation of vulnerability functions for European-type RC structures based on observational data. *Engineering structures, 25,* 1241-1263.

Saneinejad, A., & Hobbs, B. (1995). Inelastic design of infilled frames. *Journal of Structural Engineering, 121,* 634-650.

Sarangapani, G., Venlatarama Reddy, B., & Jagadish, K. (2005). Brick-mortar bond and masonry compressive strength. *Journal of materials in civil engineering, 17,* 229-237.

Sattar, S., & Liel, A. B. (2010). Seismic performance of reinforced concrete frame structures with and without masonry infill walls. In: *Proceedings of the 9th US National and 10th Canadian conference on earthquake engineering,* Toronto, Canada.

Shahi, R., Lam, N. T., Gad, E. F., Saifullah, I., Wilson, J. L., & Watson, K. (2014). Choice of Intensity Measure in Incremental Dynamic Analysis. In: *Proceedings of the Australian Earthquake Engineering Society Conference,* Lorne, Victoria, Australia, 21-23 November.

Shing, P. B., Stavridia, A., Koutromanos, I., William, K., Blackard, B., Kyriakides, M. A., Billington, S., & Arnold, S. (2009). Seismic performance of non-ductile RC frames with brick infill. *ATC/SEI Conference on Improving theSeismic Performanceof Existing Buildings and Other Structures,* 1117-28.

Shome, N. (1999). *Probabilistic seismic demand analysis of nonlinear structures*. PhD Thesis, Stanford University, Stanford, CA, US.

Shome, N., Cornell, C. A., Bazzurro, P., & Carballo, J. E. (1998). Earthquakes, records, and nonlinear responses. *Earthquake Spectra, 14***,** 469-500.

Smyrou, E., Blandon, C., Antoniou, S., Pinho, R., & Crisafulli, F. (2011). Implementation and verification of a masonry panel model for nonlinear dynamic analysis of infilled RC frames. *Bulletin of Earthquake Engineering, 9***,** 1519-1534.

Thinley, K., & Hao, H. (2016). Seismic response analyses and performance assessment of masonry-infilled reinforced concrete frame buildings in Bhutan without and with soft storey. *Advances in Structural Engineering***,** 1369433216661336.

Thinley, K., & Hao, H. (2017). Seismic performane of reinforced concrete frame buildings in Bhutan based on fuzzy probability analysis. *Soil Dynamics and Earthquake Engineering***,** *92*, 604-620.

Thinley, K., Hao, H., & Tashi, C. (2017). Seismic Performance of Reinforced Concrete Buildings in Thimphu, Bhutan. *International Journal of Structural Stability and Dynamics***,** *17* (7), 1750074.

UNDP Report. (2006). *Report on Thimphu Valley Earthquake Risk Management Program*. Standards and Quality Control Authority, Ministry of Works and Human Settlement, Thimphu, Bhutan.

Vamvatsikos, D., & Cornell, C. A. (2002). Incremental dynamic analysis. *Earthquake Engineering & Structural Dynamics, 31***,** 491-514.

Vision 2000 (1995). *Performance Based Seismic Engineering of Buildings; conceptual framework*. Structural Engineers Association of California, Sacramento, CA, US.

CHAPTER 7 EFFECT OF PARTIALLY INFILLED WALL ON THE SEISMIC BEHAVIOR OF REINFORCED CONCRETE FRAME BUILDINGS

7.1 Abstract

The partially infilled reinforced concrete (RC) frames have been one of the major victims of earthquakes in the past. It is normally called as the captive column effect wherein the lower portion of the column is kept captive by the surrounding infill wall while the upper portion is allowed to deform laterally. The upper free portion of the column attracts huge shear force during earthquakes and might get severely damaged and possibly lead to the collapse of the buildings. Although there are a number of studies conducted on the masonry infilled RC frames in general, yet partially infilled frames have not been adequately studied under the dynamic load. In this study, a three storey RC building with partial infill wall on the ground floor is studied under the ground motions of the 475 year return period. The height of the infill wall is varied along the height of the columns and the resulting shear demands are estimated. To study the mitigation measures of the captive column effect, the shear and moment capacities of the ground floor columns are increased by factors of 2.5 and 4 times of the original design strength. It is found that the captive column effect is the maximum when the infill wall height is 75% of the column clear height. Increasing the shear strength of the column is found to be beneficial but providing the infill wall up to the full height of the column to eliminate the short-column effect is the most desirable for structure protection.

7.2 Introduction

The regular masonry infill walls in the reinforced concrete (RC) frame building are considered by many researchers as beneficial to the overall performance of the building. The infill wall increases the stiffness, strength and damping of the RC frame and in turn, reduces the lateral deformation. However, irregular arrangement of masonry infill wall in the RC frame causes a number of detrimental effects such as soft storey effect, captive column effect and torsional effect. The captive columns are the consequence of partially infilling the RC frame with the masonry walls. The lower portion of the column is kept captive by the surrounding infill wall leaving only the upper portion of the column for the potential deformation as shown in Figure 7-1. The total deformation that is designed to be sustained by the full height of the column, H is forced upon to the reduced height of the column, h. This results in the increase in column shear force and hence possibly severe damages to the upper free portion of the column during the earthquakes. In many previous earthquakes such as the 1985 Mexico earthquake, 2001 Gujarat earthquake, 2008 Wenchuan earthquake and 2015 Nepal earthquake, captive columns

induced by the partial infill masonry walls were heavily damaged leading to the collapse of the buildings. The requirement of providing light and ventilation to the buildings inevitably leads to the formation of a number of captive columns as described in Guevara and Garcia (2005). The captive columns are commonly found in almost all masonry infilled RC buildings such as schools, hospitals, residential and commercial buildings and pose a great risk to the lives and properties of the occupants.

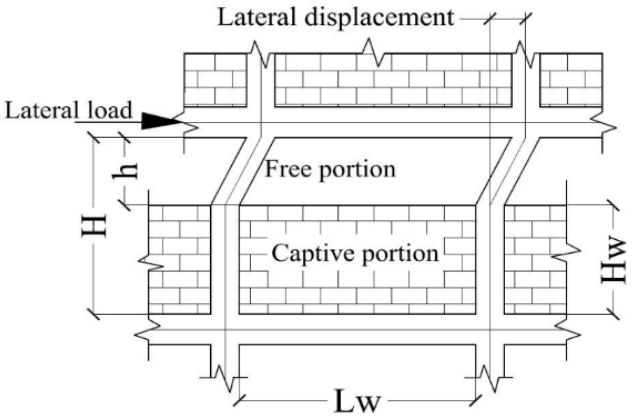

Figure 7-1 Captive column effect induced by the partially infill wall.

In spite of the numerous damages during the earthquakes in the past, partially infilled RC frames have not been adequately studied. There are only a handful of experimental studies and a very few analytical studies currently undertaken on the partially infilled RC frames. Chiou et al. (1999) carried out the full-scale tests on one-bay one-storey fully infilled, partially infilled and bare frames. The partial infill wall was found to induce short column effect leading to the severe damage of columns under the in-plane monotonic loading. To study the mitigation measures of the captive column effect, Babu et al. (2006) conducted tests on two sets of partially infilled RC frames with and without masonry inserts. The performance of partially infilled frame with masonry inserts was reported to be better than without it. Similarly, Huang et al. (2006) tested two sets of one-bay one- storey RC frames consisting of fully infill, partially infill walls and bare frames with and without wrapping the columns with the carbon fiber reinforced polymer (CFRP) sheets under the horizontal cyclic loads. They observed improvement in the lateral load capacity and reduction of captive column effect for the case where CFRP sheet is used. Jayaguru and Subramanian (2012) also tested two sets of two-bay two-storey non-ductile RC frame with partial infill wall on the ground floor. The first set was tested under the lateral load without reinforcing the columns while the second set was tested by wrapping the ground floor columns and portion of the first floor beams by glass fiber reinforced polymer (GFRP) composites. It was observed that the RC frame retrofitted with GFRP was able to overcome the captive column effect to some extent but its effectiveness

was limited by the bond between the column and GFRP sheet. Taher and Afefy (2008) investigated the seismic response of low, medium and high-rise buildings with partial infill walls and with various percentages of openings. They reported the increase in stiffness, strength and frequency of the buildings depending on the location and percentage of openings. They also observed the higher contribution to stiffness and strength by infill walls in the lower floors than those located on the upper floors. Pradhan et al. (2014) studied the effect of the partial infill wall using two sets of masonry strengths and also varying the height of the partial infill wall in the frame. They observed the increase in the shear force of columns by 1.5 times and recommended the full wall to be provided in the frame.

All these experimental and analytical studies exposed the vulnerability of columns of frames with the partial infill walls. However, they were all studied under the static loading which may not capture the realistic dynamic response characteristics under earthquake ground motions. Moreover, no design recommendations are provided although an improvement in the performance using the masonry inserts and FRPs were shown. Paulay and Priestley (1992) provided two design options, one of which involves isolating the infill wall from the RC frame and the other one involving the design of both infill wall and RC frame to the given seismic force. Similar options are also provided by Fardis (2009) such as isolation of the infill wall, reduction of the opening size by locating the openings away from the columns and proper design of the infill wall and RC frame for the captive column effect. Indian ductile detailing code, IS-13920 (1993) and Eurocode-8 (2002) recommend the provision of confining ties throughout the column height with partial infill walls. However, the effectiveness of these recommendations in mitigating the captive column effect is not well understood yet until now.

This study is aimed at investigating the effect of partially infilled RC frame found in Bhutan with different infill wall heights under the earthquake ground motion and also to study the effectiveness of increasing the shear capacity of the columns of RC frame with partial infill walls for overcoming the captive column effect. A typical three storey masonry infilled RC building currently existing in Thimphu, Bhutan and designed according to Indian Seismic Code, IS-1893 (2002) is considered for the study. The exterior ground floor RC frames are provided with partial infill walls of varying heights, while the top two floors are kept as originally designed with full masonry infill. The ground motions predicted from the Probabilistic Seismic Hazard Analysis at the generic soil sites in Thimphu, Bhutan are used for the analyses. The nonlinear analysis and performance assessment program, Perform 3D (CSI, 2006) is used for the numerical simulation. From this study, it was observed that captive column effect becomes the most significant when the infill wall height is 75% of the clear height of the column. Increasing the shear and moment capacities of ground floor columns

does lower the deformation of the columns and in turn, improves the overall performance of the building.

7.3 Description of an example building

A typical 3 storey masonry infilled RC building designed according to Indian Seismic Code is considered as an example building in this study. The building is a real existing building in Thimphu, Bhutan wherein the architectural and structural details of the building are obtained from the Thimphu municipal corporation office. The column and masonry infill wall layout plan of the building is shown in Figure 7-2(a). To study the captive column effect, the exterior RC frames of the ground floor is partially infilled with the brick masonry walls, while the infill walls in the internal and the top storey RC frames are kept unchanged. Five cases of the partially infilled frame with infill wall heights of 0.0H, 0.25H, 0.5H, 0.75H and 1.0H are considered for the analyses as shown in Figure 7-2(b). The partially infilled frames are considered on the ground floor only since they are more commonly found in the existing buildings. Moreover, as observed by Taher and Afefy (2008), the overall response of the building is more prominently influenced by the infill walls located on the lower floors than those located on the upper floors.

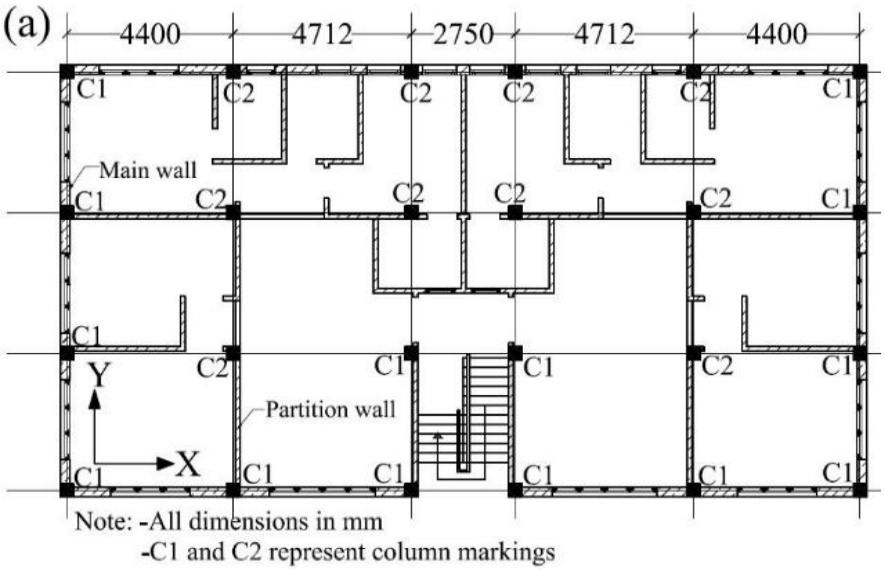

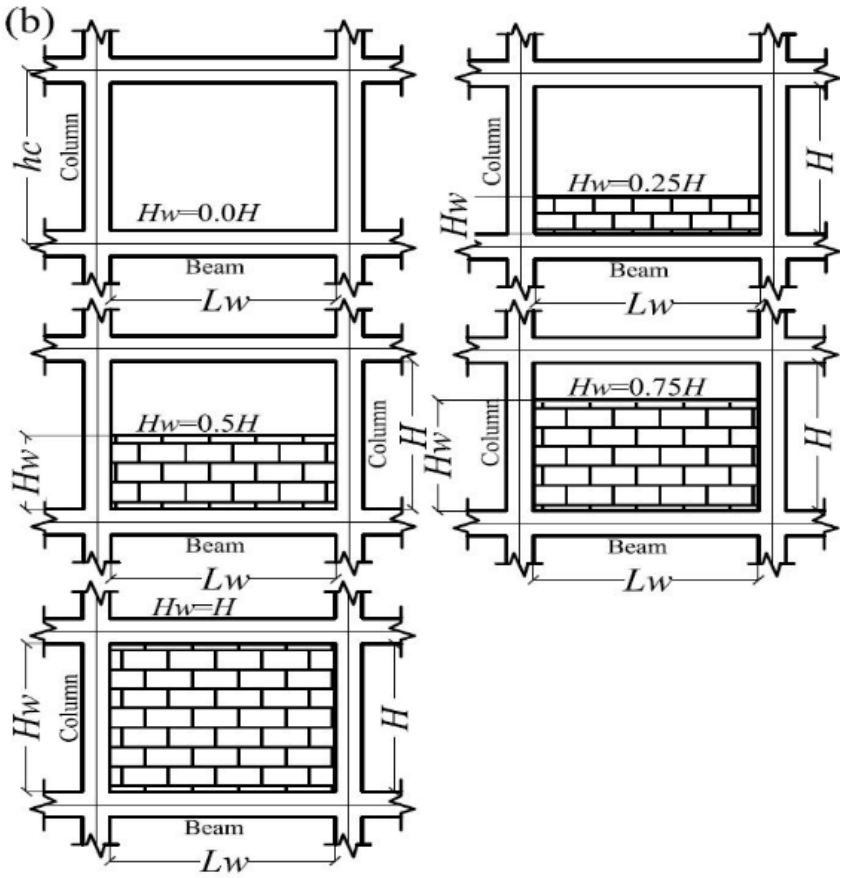

Figure 7-2 (a) Masonry infill wall layout plan of 3 storey building and (b) various heights of infill wall considered for analyses.

The reinforcement and member dimension details of the building are given in Table 7-1. The compressive strength and the unit weight of concrete used are respectively 20 MPa and 25 kN/m^3. Similarly, the compressive strength and unit weight of brick masonry wall used are respectively 6.07 MPa and19.6 kN/m^3, corresponding to the medium mortar mix with cement to sand ratio of 1:4. The yield strength of reinforcement used is 415 MPa. The live load of 2 kN/m^2 and 0.75 kN/m^2 are respectively applied on the floors and roofs of the buildings. The superimposed dead load of 1kN/m^2 is also applied on all the floors. The clear cover of 40 mm and 25 mm are respectively specified for columns and beams of these buildings.

Table 7-1 Reinforcement and member dimension details of the example building

	Dimension	Reinforcement (Bar dia.	
(a) Floor Beams (FB) and Roof Beams(RB)			
		Top bar	Bottom bar
FB along X	300x400	4-20	2-20+2-16
FB along Y	300x400	2-20+2-16	4-16
RB along X	300x400	2-20+2-16	4-16
RB along Y	300x400	4-16	2-16+2-12
Beam stirrups	8@100mmC/C near column face and 8@150C/C at the centre		
(b) Column			
Column C1	400x400	8-20	
Column C2	400x400	4-25+4-20	
Column ties	8@100mmC/C throughout		
(c)Slab	150mmm	10@150mmC/C both	

To study the effectiveness of increasing the capacity of the columns in mitigating the captive column effect, shear and moment capacities of the ground floor columns estimated from the design values are increased by the factors of 2.5 and 4. These are achieved by increasing the size of columns, decreasing the spacing of ties and increasing the longitudinal area of the column reinforcements. Indian Seismic Code recommends the columns of the soft storey floors be designed for 2.5 times the moments and shears estimated for the bare frame columns. The same principle is assumed here by adopting the factor of 2.5 to study the captive column effect. Factor 4 is also used to study the effectiveness of further increasing the shear capacity of the columns in mitigating the captive column effect.

7.4 Ground motions

The ground motions predicted from PSHA by Thinley et al. (2017) for the generic soil sites in Thimphu, Bhutan in Chapter 2 of this thesis for the return period of 475 years are used for the analyses. Since the building considered for the analysis is adopted from one of the real existing buildings in Bhutan, the use of these ground motions and realistic building model could provide realistic results. The acceleration time histories of the ground motions at the generic soil sites are shown in Figure 7-3.

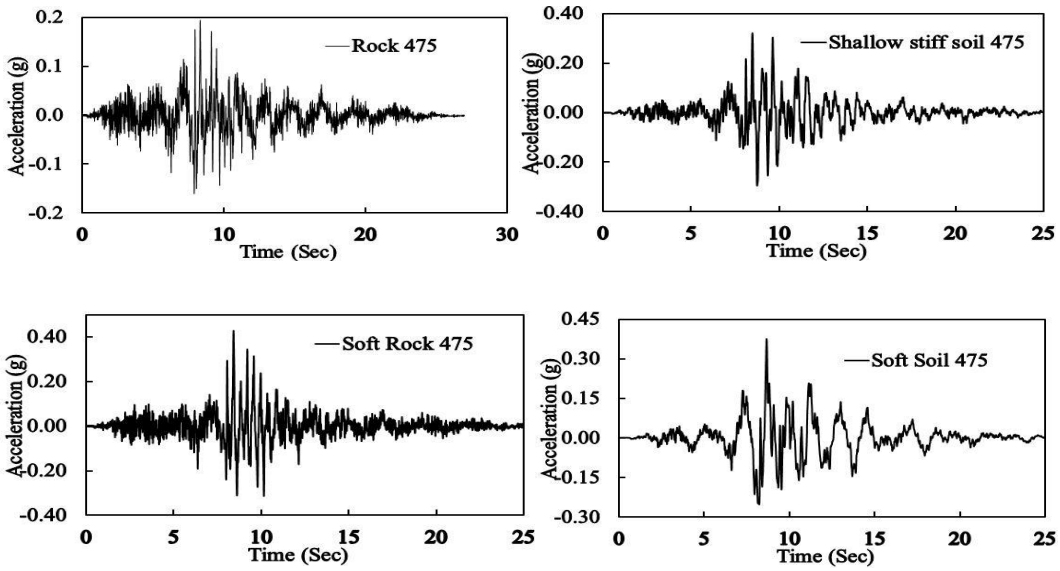

Figure 7-3 Acceleration time histories of ground motions at the generic soil sites for 475 year return period.

7.5 Numerical modelling of partially infilled RC frame

Simulating the nonlinear response of the masonry infilled RC frames has been a challenge owing to the interaction of infill wall with the RC frame. However, persistent research in the area led to the development of various numerical models capable of simulating the nonlinear response with varying degree of accuracies. These models are however developed mostly for the fully infilled frame and only a handful of researchers have considered openings in the model. On the other hand, there is very limited literature dealing with the numerical modelling of the partially infilled frame.

The numerical modelling of fully infilled frames and the infilled frames with openings were carried out in the earlier study in Thinley and Hao (2016) and the same have been employed in this study. This section is focused on modelling the partially infilled frame. Similar to the fully infilled frame, the numerical modelling of the partially infilled frame consists of modelling the partial infill wall and the surrounding RC frame.

7.5.1 Modelling of partial infill wall

Unlike the full infill wall, only a couple of researchers have given some information on the numerical modelling of the partial infill wall using the equivalent strut model. Al-Chaar (2002) proposed the use of equivalent strut to model the partial infill wall wherein the estimation of the strut width is recommended to be made from the expression given in Mainstone (1971) using the reduced height of the wall. The equivalent strut is placed as shown in the Figure 7-4(a) to represent the partial infill wall and recommended the exclusion of reduction for the

opening. Pradhan (2012) also developed an expression to estimate the equivalent strut width of the partial infill wall based on the contact length between the masonry wall and the frame. The expression of strut width given by Mainstone (1971) and Pradhan (2012) are respectively given in Equations (7.1) and (7.2).

$$w = 0.175 d\lambda^{-0.4} \tag{7.1}$$

$$w = k_x \frac{L_w}{\sqrt{L_w^2 + (H_w - k_x)^2}} \tag{7.2}$$

where $\lambda = \sqrt[4]{\left[\frac{(E_w t_w sin2\theta)}{4E_c I_c H_w}\right]}$ and $k_x = 2.29\frac{\pi}{2}\left[\frac{E_c I_c H_w}{E_w t_w h_c}\right]^{\frac{1}{3}}$.

E_w, H_w, L_w, t_w and d are respectively the modulus of elasticity, height, length, thickness and the diagonal length of the partial infill wall. E_c, I_c, and h_c are the modulus of elasticity, the moment of inertia and centre to centre height of the column respectively. The angle between the diagonal strut and the horizontal is represented by θ. In this study, Equation (7.1) recommend by Al-Chaar (2002) is used to estimate the width of equivalent strut using the reduced height of the wall, H_w. However, Equation (7.2) also provides the similar results. As in the case of the full infill wall, the F-D relationship of an equivalent strut developed by Panagiotakos and Fardis (1996) is used in this study which is as shown in the Figure 7-4(b). The stand out difference in the case of partial infill wall is the estimation of the strut width using the reduced height of the wall which is central to the estimation of stiffness, strength and deformation parameters. The initial stiffness, K_i and secant stiffness, K_s are estimated from

$$K_i = \frac{G_w L_w t_w}{H_w} \tag{7.3}$$

$$K_s = \frac{E_w w t_w}{d} \tag{7.4}$$

where G_w is the shear modulus of the wall. The negative stiffness of the softening branch K_{so} is taken as 10% of the initial stiffness. The force corresponding to yield point is estimated from the expression

$$F_y = f_{tp} t_w L_w \tag{7.5}$$

where f_{tp}= cracking strength of the infill wall. The maximum strength, F_{max} and the residual strength, F_r are taken as $1.67F_y$ and $0.1F_y$ respectively as per Dolšek and Fajfar (2008). The displacements corresponding to the yield point D_y, maximum strength D_{max} and at residual strength D_r are estimated from the following expression.

$$D_y = \frac{F_y}{K_i} \tag{7.6}$$

$$D_{max} = D_y + \frac{F_{max} - F_y}{K_s} \tag{7.7}$$

$$D_r = \frac{F_{max} - F_r}{K_{so}} \tag{7.8}$$

The displacement at collapse, D_u is taken as $5D_{max}$ as given in Dolšek and Fajfar (2008).

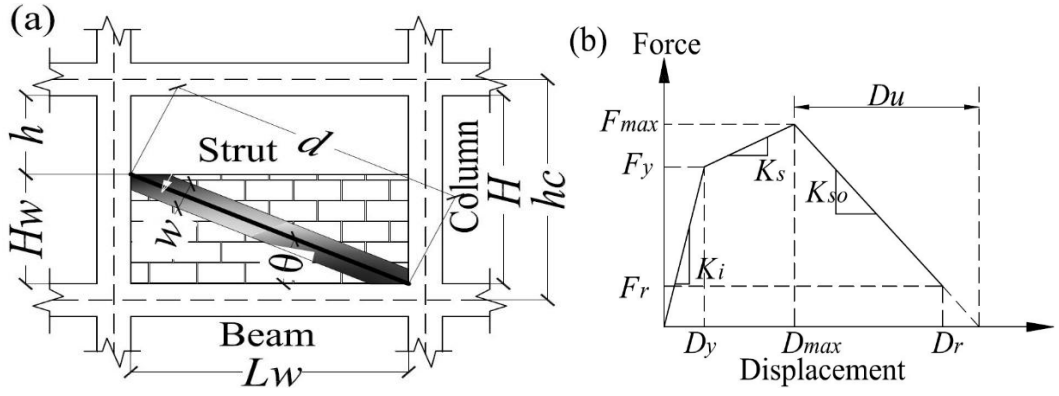

Figure 7-4 (a) Representation of partial infill wall by an equivalent strut and (b) F-D relationship of an equivalent strut.

7.5.2 Modelling of surrounding RC frame

The numerical modelling RC beams is done as in the earlier study in Thinley and Hao (2016) using the chord rotation model and employing the F-D relationship given in the Perform 3D (CSI, 2006) program. However, the modelling of columns surrounding the partial infill wall needs special attention. As discussed in the previous section, reduction in the effective column height due to the presence of partial infill wall results in the huge concentration of shear force in the upper free portion of the column during the seismic excitation. The shear force is concentrated especially at the point of column where the infill wall terminates. Hence, in order to capture this localized shear concentration in the numerical analysis, a zero-length shear hinge is placed at the point where the infill wall terminates as shown in Figure 7-5(a) and 7-5(b). The flexural response is simulated using the FEMA column component which consists of plastic hinge and an elastic segment as shown in Figure 7-5(b). The force-deformation (F-D) relationship of the FEMA column component is defined as in Thinley and Hao (2016). To define the shear force-deformation relationship of shear hinge, it is first determined whether the column would undergo shear, flexure-shear and flexure failures by comparing the plastic shear capacity, V_p to the shear strength, V_n of the column. The column is said to undergo shear, flexure-shear and flexure failures if the ratio of V_p/V_n is greater than one, between 1.0 and 0.6 and less than 0.6 respectively (Elwood, 2004). The ratio of V_p/V_n is found to be more than 1.0

for columns with infill wall height of 0.75 times the clear column height indicating the shear failure. The ratio is found to be in between 1.0 and 0.6 for columns with wall heights of 0.5 and 0.25 times the clear column height indicating the flexure-shear failure. The force-deformation (F-D) relationship for shear and flexure-shear failures are adopted from Elwood and Moehle (2004) and are shown in Figure 7-5(c) and 7-5(b) respectively. As shown in the figure, the F-D curve is activated once the column shear demand surpasses the column shear capacity and thereby initiating the shear failure. Burton and Deierlein (2014) and Jeon et al. (2015) used the similar model to model the concentration of shear in column ends due to infill wall.

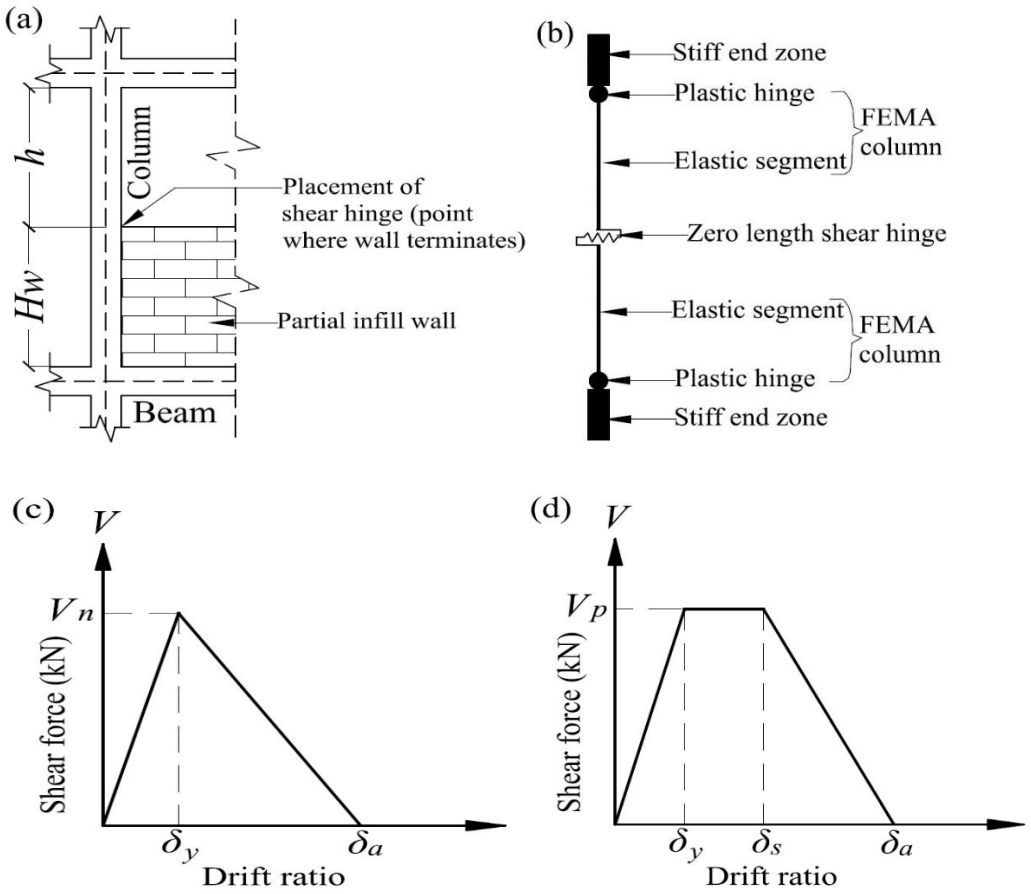

Figure 7-5 Numerical modelling of column with partial infill wall, (a) column with partial infill wall, (b) chord rotation model with shear hinge, (c) F-D relationship of shear hinge for shear failure and (d) F-D relationship of shear hinge for flexure-shear failure.

The F-D relationship for shear and flexure-shear failures requires the estimation of shear strength, V_n, plastic shear capacity, V_p, yield drift ratio, δ_y, drift ratio at shear failure, δ_s and drift ratio at axial load failure, δ_a. The shear strength is estimated from the expression given by Sezen and Moehle (2004) which is as given below.

$$V_n = k\frac{A_v f_y d}{s} + k\left(\frac{0.5\sqrt{f_c}}{a/d}\sqrt{1+\frac{P}{0.5A_g\sqrt{f_c}}}\right)0.8A_g \quad (7.9)$$

where k is taken as 1 assuming displacement ductility of less than 2. A_v, f_y, a, d, s, fc, P and A_g are the area of transverse reinforcement, yield strength of steel, shear span of column, effective depth of column cross section, spacing of column ties, compressive strength of concrete, axial load and gross cross sectional area of column respectively. The plastic shear capacity of column is estimated from Equation (7.10) considering the fixed boundary condition.

$$V_p = \frac{2M_p}{L} \quad (7.10)$$

where M_p is the plastic moment capacity which is estimated from the standard section analysis and L is the height of the column. The yield drift ratio of longitudinal reinforcement, δ_y is estimated from the expressions given in Elwood and Moehle (2004) as in Equation (7.11). It is calculated as the sum of drifts due to flexure, bar slip and shear.

$$\delta_y = \delta_{flex} + \delta_{slip} + \delta_{shear} = \frac{L}{6}\phi_y + \frac{d_b f_y \phi_y}{4\sqrt{f_c}} + \frac{2M_p}{(5/6)A_g GL} \quad (7.11)$$

where ϕ_y, d_b and G are curvature at yielding, diameter of longitudinal reinforcement and shear modulus of column respectively. The drift ratios at shear failure, δ_s and at axial load failure, δ_a are estimated from the expressions developed by Elwood and Moehle (2005a) and Elwood and Moehle (2005b) respectively which are as given below.

$$\delta_s = \frac{3}{100} + 4\rho^{"} - \frac{v}{40\sqrt{f_c}} - \frac{P}{40A_g f_c} \geq \frac{1}{100} \quad (7.12)$$

$$\delta_a = \frac{4}{100}\frac{1+tan^2\theta}{tan\theta + P\left(\frac{s}{A_{st}f_{yt}d_c tan\theta}\right)} \quad (7.13)$$

where ρ'', v, A_{st}, f_{yt}, d_c and θ are respectively the transverse steel ratio, nominal shear stress, area of transverse reinforcement parallel to the applied shear, yield strength of transverse reinforcement, depth of column core parallel to the applied shear and critical crack angle which is assumed as 65 degrees. The other denotations are same as described in the preceding equations.

7.6 Numerical results and discussion

With the use of numerical models as discussed above and the ground motions described in section 3, the nonlinear analyses are carried out using Perform 3D (CSI, 2006) program for the masonry infilled 3 storey building with partial infill walls at the ground floor. The analyses

are repeated for the various heights of the partial infill wall and also for the cases where the moment and shear capacities of the ground floor columns are increased by 2.5 and 4 times. The fundamental periods of the buildings with various heights of infill wall at the ground floor for the normally designed RC frames are given in Table 7-2. It can be observed from the table that the period of the building decreases as the wall height increases. This indicates the contribution of infill walls to increasing the stiffness of the building and thereby likely increasing the seismic forces.

Table 7-2 Periods of building with various wall heights

Wall height	Periods (Sec)		
	1st mode	2nd mode	3rd mode
0.00H	0.1541	0.0363	0.0233
0.25H	0.1527	0.0362	0.0232
0.50H	0.1472	0.0358	0.0232
0.75H	0.1298	0.0346	0.0230
1.00H	0.0975	0.0291	0.0218

The response quantity of great interest is the shear demand of the ground floor columns since a large shear force is expected at the point of the columns where the masonry infill wall terminates. Another response quantity of interest is the interstorey drift which indicates the overall performance of the building. The shear forces estimated for the ground floor columns at the various soil sites and under the 475 year return period ground motions are given in Figure 7-6. It is to be noted that the shear force is estimated for the ground floor corner columns since it is found to be more critical than the other middle columns. The interstorey drifts of the building estimated at the shallow stiff soil site for various heights of infill wall are shown in Figure 7-7.

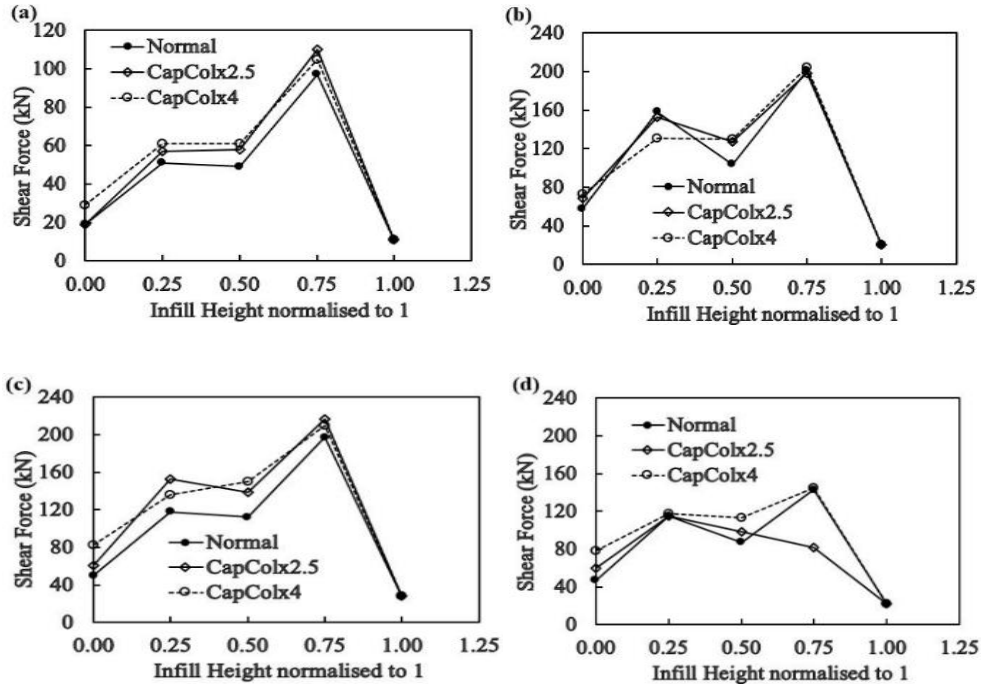

Figure 7-6 Column shear force corresponding to the various heights of infill wall at (a) rock; (b) shallow stiff soil; (c) soft rock and (d) soft soil sites under the 475 year return period ground motion.

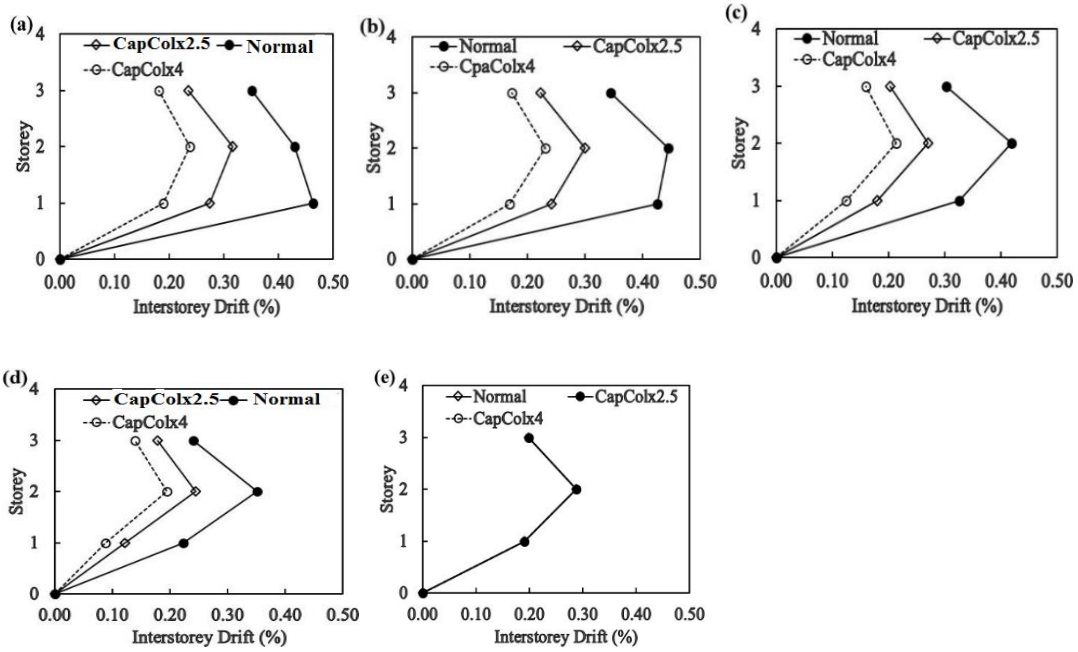

Figure 7-7 Interstorey drift of building with increased strength of ground floor columns at shallow stiff soil under the 475 year return period ground motion for infill wall height of (a) 0.0H; (b) 0.25H; (c) 0.5H; (d) 0.75H and (e) 1.0H.

Figure 7-6 shows the plot of the shear force estimated for the ground floor column when the infill wall height is 0%, 25%, 50%, 75% and 100% of the clear column height as shown in Figure 7-2(b) at the various soil sites under the 475 year return period ground motions. The

term ‘Normal’ denotes the building whose ground floor columns are normally designed while the terms ‘CapColx2.5’ and ‘CapColx4’ denote the building whose ground floor columns are increased by factors 2.5 and 4 from the original design respectively. As shown in the figure, the shear force increases slightly with the increase in the strength of the column. Since seismic forces are attracted in proportion to the element stiffness, increasing the strength of the columns and the stiffness attracts larger horizontal shear forces. The figure also reveals that the increase in the shear strength of the column has no measurable effect in reducing the shear demand in the column or overcoming the captive column effect. However, looking from the perspective of the demand-capacity ratio, the columns with higher strength have lower demand capacity ratios indicating the lower deformation. It can also be observed from the figure that the captive column effect is more significant at the stiffer soil site than at the flexible soil site. There is a considerable increase in the shear force at the stiffer site such as rock than at the flexible soft soil site.

Another important observation that can be deduced from Figure 7-6 is the occurrence of the maximum shear force when the wall height is 75% of the clear height of the column. This is expected since the lower 75% of the column height is effectively held captive by the surrounding infill wall leaving only the upper 25% of the column height for lateral deformation. The shear force decreases as the height of the column for lateral deformation increases by reducing the height of the infill wall. However, as observed in the figure, the shear force estimated at the ground floor columns with the infill wall heights of 25% and 50% are close to each other although much lower shear force is expected for the 25% wall height with larger column height available for deformation. In this regard, it was observed that the larger shear force is attracted by the lower portion of the column instead of the upper free portion of the column when the infill wall height is 25% of the clear column height. This indicates that the shorter wall height is not able to effectively hold the lower portion of the column. Moreover, the lower portion of the column being shorter and stiffer than the upper portion attracts more shear force. In the case of the partially infilled frame with 50% wall height, the lower portion of the column is effectively held captive by the infill wall and the shear force is attracted by the upper free portion of the column similar to the 75% infill wall. The shear force estimated for the ground floor column without infill wall is lower than the case of 25%, 50% and 75% infill wall owing to the full column height available for deformation. Similarly, minimum shear force is observed in the case of the fully infilled frame or 100% infill wall since captive column effect is out of the question in this case.

From Figure 7-7, the reduction in the interstorey drift is observed when the capacity of the column is increased by factors of 2.5 and 4. Referring to Figure 7-7(b) for the 25% wall height,

the maximum interstorey drift estimated for the building whose ground floor columns are normally designed is 0.44%, while the interstorey drifts of 0.30% and 0.23% are respectively observed for the building whose ground floor columns with partial infill walls are increased by the factors of 2.5 and 4 respectively. This shows an overall improvement in the performance of the building with the increase in the capacity of columns notwithstanding the height of the infill wall. It is interesting to note that there is no effect in increasing the capacity of the columns for the full height of the infill wall as shown in Figure 7-7(e). It is because the column stiffness is significantly smaller than the wall stiffness and therefore increasing the column stiffness has minimum effect. Similar observations are observed at the rock, soft rock and soft soil sites which are not shown here.

The effect of the captive column could be similar if partial infill walls are similarly considered in the ground floor of the 6 storey RC building as considered in the previous chapters. However, the effect could differ if the structural details of the columns encasing the partial infill wall, the strength of the partial infill wall that give rise to the captive column, the height of the partial infill wall relative to the height of surrounding columns and the nature of ground motion are different.

7.7 Conclusion

Following conclusions can be drawn from this study:

1) The captive column effect becomes the most prominent when the wall height is 75% of the clear height of the column. When the wall height is reduced to 25% of the clear column height, larger shear force is attracted by the lower portion of the column in contact with infill wall due to the increase in stiffness.

2) The effect of the captive column is more significant for the buildings located on the stiffer soil sites than that on the flexible soil site.

3) Increasing the capacity of the columns leads to a slight increase in the shear demand of the column, but with lower demand-capacity ratio, the columns with increased capacity are expected to undergo lesser deformation.

4) Increasing the capacity of the columns results in the reduction of the interstorey drift irrespective of the height of the infill wall, confirming the overall reduction in lateral deformation.

5) Increasing the capacity of columns has no effect on the fully infilled frame.

7.8 References

Al-Chaar, G. (2002). *Evaluating strength and stiffness of unreinforced masonry infill structures*. No. ERDC/CERL-TR-02-1. Engineer Research and Development Centre Champaign, US Army Corps of Engineers.

Babu, R. S., Venkatasubramani, R., & Venkatasubramani, G. (2006). Seismic strengthening of partially infill RC buildings using brick inserts-experimental investigation on 3D model structure. *Structure*, 3600, 1430.

Burton, H., & Deierlein, G. (2013). Simulation of seismic collapse in nonductile reinforced concrete frame buildings with masonry infills. *Journal of Structural Engineering, 140,* A4014016.

Chiou, Y. J., Tzeng, J. C., & Liou, Y. W. (1999). Experimental and analytical study of masonry infilled frames. *Journal of Structural Engineering, 125*, 1109-1117.

CSI (2006). *Nonlinear Analysis and Performance Assessment for 3-D Structures.* Computers and Structures, Inc., Berkeley.

Elwood, K. J. (2004). Modelling failures in existing reinforced concrete columns. *Canadian Journal of Civil Engineering, 31*, 846-859.

Elwood, K. J., & Moehle, J. P. (2004). Evaluation of existing reinforced concrete columns. *Proceedings of the 13th world conference on earthquake engineering, August 1-6, Vancouver, Canada.*

Elwood, K. J., & Moehle, J. P. (2005a). Drift capacity of reinforced concrete columns with light transverse reinforcement. *Earthquake Spectra, 21*, 71-89.

Elwood, K. J., & Moehle, J. P. (2005b). Axial capacity model for shear-damaged columns. *ACI Structural Journal*, 102(4), 578-587.

Eurocode 8 (2002). *Design of Structures for earthquake resistance–Part 1: General rules, seismic actions and rules for buildings*. European Standard, NF EN, 1, Brussels.

Fardis, M. (2009). *Seismic Design, Assessment and Retrofitting of Concrete Buildings*. London New York, Springer Dordrecht Heidelberg.

Guevra, L. T., & Garcia, L. E. (2005). The captive-and short-column effects. *Earthquake Spectra, 21*, 141-160.

Huang, C. H., Tuan, Y. A., & Hsu, R. Y. (2006). Nonlinear pushover analysis of infilled concrete frames. *Earthquake Engineering and Engineering Vibration, 5*, 245-255.

IS 1893 2002. *Criteria for Earthquake Resistant Design of Structures*. Bureau of Indian Standards, New Delhi, India.

IS 13920 1993. *Ductile Detailing of Reinforced Concrete Structures subjected to seismic forces-Code of Practice*. Bureau of Indian Standard, New Delhi, India.

Jayaguru, C., & Subraminian, K. 2012. Retrofit of RC frames with captive-column defects. *KSCE Journal of Civil Engineering, 16*, 1202-1208.

Jeon, J. S., Lowes, L. N., Desroches, R., & Brilakis, I. (2015). Fragility curves for non-ductile reinforced concrete frames that exhibit different component response mechanisms. *Engineering Structures, 85,* 127-143.

Paulay, T., & Priestley, M. (1992). *Seismic Design of Reinforced Concrete and Masonry Buildings.* John Wily and Sons Inc., New York.

Pradhan, P., Maskey, R., & Pradhan, P. (2014). Stiffness Behaviour and Shear Effect in Partially Infilled Reinforced Concrete Frames. *Journal of Earthquake Engineering, 18*, 580-588.

Pradhan, P. M. (2012). Equivalent strut width for partial infilled frames. *Journal of Civil Engineering Research*, 2, 42-48.

Sezen, H., & Moehle, J. P. (2004). Shear strength model for lightly reinforced concrete columns. *Journal of Structural Engineering*, *130*, 1692-1703.

Taher, S. E., & Afefy, H. M. (2008). Role of masonry infill in seismic resistance of RC structures. *The Arabian Journal for Science and Engineering*, *33*.

Thinley, K., & Hao, H. (2016). Seismic response analyses and performance assessment of masonry-infilled reinforced concrete frame buildings in Bhutan without and with soft storey. *Advances in Structural Engineering***,** 1369433216661336.

Thinley, K., Hao, H., & Tashi, C. (2017). Seismic Performance of Reinforced Concrete Buildings in Thimphu, Bhutan. *International Journal of Structural Stability and Dynamics***,** *17* (7), 1750074.

CHAPTER 8 CONCLUSION AND RECOMMENDATIONS

8.1 Main Contributions

This study is carried out with the main objective of assessing the seismic performance of existing RC buildings with or without infill walls in Bhutan and in other parts of the world in general. The presence of a number of existing RC buildings which were built with or without any kind of design compounded with the high seismicity of the country makes it extremely necessary to assess the seismic performance of these buildings in Bhutan. To realistically assess the performance of the buildings, a number of issues associated with the incorporation of openings and soil structure interaction and consideration of soft storey and partially infilled wall are addressed. The three typical existing masonry infilled RC buildings in Bhutan which were built with or without seismic design are considered for the study. In view of understanding and providing the most comprehensive idea on the performance of RC building structures in Bhutan, seismic assessment is conducted for RC frame buildings with or without masonry infill wall and RC frame buildings with the open ground floor. Numerous dynamic nonlinear analyses are conducted employing the nonlinear analysis and performance assessment software, Perform 3D. Following are the summary and main contributions/conclusions transpired from this study.

Prediction of earthquake ground motions in Bhutan

Bhutan still has no seismic design code of its own. Moreover, there is no record of ground motions available in Bhutan in spite of the occurrence of a number of earthquakes in the past. For the realistic seismic assessment of building structures in Bhutan, it is paramount to employ ground motions that characterize the seismicity and site conditions of the country. In this study, probabilistic seismic hazard analysis (PSHA) is carried out using the area sources within a radius of 400 km from Thimphu, Bhutan. From PSHA, earthquake ground motions at the rock, shallow stiff soil, soft rock and soft soil sites are predicted for the 475 and 2475 year return periods. These ground motions are employed for the seismic assessment of building structures in Bhutan in this study. They are predicted for the first time and could immensely help engineers and researchers in Bhutan for the design and assessment of buildings and other structures.

Seismic performance assessment of RC buildings without infill walls in Bhutan

Masonry infilled RC buildings are normally designed as bare frames neglecting the infill walls. There are also some RC buildings without infill walls in Bhutan or in other parts of the world where glass façades are used. It is important to assess the seismic performance of these buildings since RC frames are the main lateral load resisting elements. Unlike many studies

in the past where distinct damage boundaries were used to define the damages of the buildings, fuzziness in the damage boundaries is used in this study. In addition, inevitable random fluctuations of the material and geometrical parameters are considered for assessing the building performances more realistically. From the study, it is observed that the RC buildings designed and built according to Indian Seismic Code could experience, with the high probability,the irreparable and severe damages under the 475 year return period ground motion and high probability of collapse under the 2475 year return period ground motion. The old RC buildings which were built without any kind of design could undergo with high probability the severe damage under the 475 year return period ground motion and high probability of complete collapse under the 2475 year ground motion.

Seismic assessment of RC buildings with masonry infill walls

Masonry infilled RC frame buildings are the most common building structures in Bhutan. Assessing the seismic performance of these buildings is highly necessary since the scale of destruction and loss of lives during earthquakes would certainly depend on the safety of these buildings. The masonry infilled RC buildings built by the local technicians without design and those designed according to the Indian Seismic Code are probabilistically assessed for seismic performance. Similar to the RC buildings without masonry infill wall, fuzziness in the damage boundaries and randomness in the material and geometrical parameter uncertainties are considered for the assessment. In contrast to many other studies where openings are neglected, the presence of the opening in the infill walls is duly considered. The study suggests that the existing masonry infilled RC buildings designed and built according to the Indian Seismic Code have the high probability of experiencing repairable damage under the 475 year return period ground motion and high probability of experiencing irreparable to severe damages under the 2475 year return period ground motion. On the other hand, the old masonry infilled RC buildings that were not designed to any standard have the high probability of experiencing repairable to irreparable damages under 475 year return period ground motion and high probability of experiencing irreparable to complete collapse under the 2475 year return period ground motion. Compared to the performance of RC buildings without infill walls, these buildings exhibit improved performance.

Seismic assessment of RC buildings with open ground floor

The RC buildings with the open ground floor or popularly known as the soft storey buildings are very common in Bhutan and in other parts of the world. They are known to be more vulnerable to earthquakes and need special attention. The seismic performance of these buildings is also probabilistically assessed. The study reveals that the recently built soft storey buildings have the high probability of undergoing irreparable to severe damages under the 475

year return period ground motion and severe to complete collapse under the 2475 year return period ground motion. The old soft storey buildings built by the local technicians have the high probability of undergoing irreparable to severe damages under the 475 year return period ground motion and complete collapse under the 2475 year return period ground motion. Soft storey buildings are indeed more vulnerable to earthquakes than the masonry infilled RC buildings. It was observed that seismic performance of soft storey buildings is highly dependent on the strength and stiffness of the ground floor columns. Infill walls on the upper storeys play little or no role in the energy dissipation.

Adequacy of using Indian Seismic Code for building structures in Bhutan

Indian Seismic Code is being used for the design of buildings in Bhutan since 1997. The adequacy of its use for the building structures and site conditions in Bhutan has not been investigated before. In this study, it is studied by analyzing the typical RC buildings in Bhutan using the Indian Seismic Code response spectrum matched ground motion. The structural responses obtained from this analysis are compared with the corresponding responses obtained from the analysis of the same buildings using the predicted ground motions in Bhutan. It is observed that Indian Seismic Code underestimates the structural responses and its direct application for the design of buildings in Bhutan should be dealt with caution. In addition, the adequacy of the design provision of Indian Seismic Code for the soft storey buildings is investigated for the soft storey buildings in Bhutan. It is observed that increasing the capacity of the soft storey columns and beams according to the Indian Seismic Code enhances the performance of the building. However, the structures are still more vulnerable to earthquake ground motions than masonry infilled buildings. It is also observed that increasing the capacity of only the columns results in almost the same performance indicating the unnecessity of increasing the capacity of beams.

Effect of soil-structure interaction on the seismic performance of the buildings

The effect of soil-structure interaction (SSI) is considered for the seismic performance of existing RC buildings with or without masonry infill walls and soft storey buildings in Bhutan using the uncoupled spring support. It was observed that SSI has no significant effect on the performance of the buildings founded on the soft rock site and has slightly detrimental or beneficial effect for those on the shallow stiff soil sites under the return periods of both 475 and 2475 years. At the soft soil site, SSI is found to have a considerable and often detrimental effect on the performance of the buildings. In general, it is observed that beneficial or detrimental effect of SSI is highly influenced by the fundamental period of the building and site natural period of the soil. However, it is always advisable to include SSI in the design and performance assessment of the buildings founded on the soft soil site.

Fragility analysis of masonry infilled RC buildings with and without soft storey in Bhutan

The fragility curve is an important statistical tool for evaluating the vulnerability of buildings. The fragility curves are developed for the first time in the country for the existing masonry infilled RC buildings with and without soft storey by incorporating both the ground motion and material uncertainties. They can be used for planning the effective and economic strengthening measures of building structures so as to mitigate the loss of lives and properties. The masonry infilled RC buildings with soft storey are found to be more vulnerable than the buildings without it. In fact, the old masonry infilled RC buildings with soft storey are found to be extremely vulnerable to ground excitations. Masonry infill walls significantly contribute to the structural stiffness and strength in resisting the seismic action for soft storey buildings. Construction of soft storey buildings should be avoided where ever possible unless they are properly designed.

Effect of partial infill wall on the seismic behavior of RC buildings

The effect of the partial infill wall is studied in terms of shear demand and interstorey drift by varying the height of the infill wall along the column height. The effect is also investigated by increasing the capacity of the columns through increased dimension and reinforcements. It was observed that captive column effect becomes highly prominent when the wall height is 75% of the clear height of the column. When the wall height is reduced to 25% of the clear column height, larger shear force is attracted by the lower portion of the column in contact with the infill wall owing to the increase in stiffness. Increasing the capacity of the columns slightly helps in reducing the captive column effect, but has no effect on the fully infilled frame. The effect is found to be more significant at the stiff soil sites than at the soft soil site.

8.2 Recommendations for future works

An extensive effort has been made in this research to estimate the damage probabilities of the RC buildings with or without masonry infill walls as realistically practical as possible. However, there are some areas that could not be covered in this study but could definitely improve the outcome of this research. The following are the research areas that could help improve the outcome of this research.

1. The earthquake ground motions are predicted in this study by assuming the generic soil sites in Bhutan as done in many other studies. Carrying out the real soil site investigation in Bhutan and using the real soil data could make the prediction of ground motion more realistic. This, in turn, would result in more realistic damage probabilities of the buildings.

2. The irregular arrangement of masonry infill walls in plan and elevation respectively give rise to torsional and soft storey effects which are detrimental to the safety of the buildings. While the soft storey effect is sufficiently covered in this research, the torsional effect could not be covered in this study. Considering the irregular arrangement of infill walls in plan and hence the torsional effect would provide more insights on the seismic performance of the masonry infilled RC buildings.

3. The seismic performance assessment of the RC buildings with or without masonry infill walls considered in this study is conducted for the in-plane loadings. Since earthquakes can occur from any direction, considering the out of plane loading in addition to the in-plane loading would result in more realistic damage probabilities of the buildings.

4. In the absence of the interstorey drift limits available for the building structures in Bhutan, the interstorey drift limits associated with the various damage limits recommended by other researchers are used in this study. The interstorey drift limits specifically developed for the buildings in Bhutan would make the outcome of this research more reliable. For this, an experimental test can be conducted on columns whose geometry, reinforcement and concrete strength details are adhered to the existing columns in Bhutan.

5. While the study showed the high vulnerability of RC buildings with the open ground floor and those that were built without adhering to any design standard, recommendation on the retrofitting options for the same is not provided. Study on some retrofitting options and at the same time recommending some options could add to the completeness of this research.

BIBLIOGRAPHY DISCLAIMER

Every reasonable effort has been made to acknowledge the owners of copyright material. I would be pleased to hear from any copyright owner who has been omitted or incorrectly acknowledged.

APPENDIX I

STATEMENTS OF THE CO-AUTHORS

To whom it may concern

I, Kinzang Thinley conducted literature review, numerical investigation, analysis of numerical results and written manuscripts of the paper titled "Seismic performance of reinforced concrete buildings in Thimphu, Bhutan" which was revised and edited by the second co-author. The third co-author help in performing the Probabilistic Seismic Hazard Analysis.

(.....)

I, as a Co-author, endorse that this level of contribution by the candidate indicated above is appropriate.

(Professor Hong Hao) (.....)

(Mr. Choki Tashi) (.....)

To whom it may concern

I, Kinzang Thinley conducted literature review, numerical investigation, analysis of numerical results and written manuscripts of the following papers which were all revised and edited by the co-author.

1) Seismic performance of reinforced concrete frame buildings in Bhutan based on fuzzy probability analysis.
2) Seismic response analysis and performance assessment of masonry infilled RC buildings in Bhutan without and with soft storey.
3) Seismic damage prediction of masonry infilled RC buildings without and with soft storey in Bhutan based on fuzzy probability analysis.
4) Seismic fragility analysis of masonry infilled reinforced concrete frame buildings in Bhutan.
5) Effect of partially infill wall on the seismic behaviour of reinforced concrete frame buildings.

(.....)

I, as a Co-author, endorse that this level of contribution by the candidate indicated above is appropriate.

(Professor Hong Hao) (.....)